

LABORATORY PETROPHYSICAL TESTING FOR CORE FROM BOREHOLES IG_BH04, IG_BH05, AND IG_BH06

APM-REP-01332-0447

November 2024

Richard Chalaturnyk
GeoREF
Reservoir Geomechanics Research Group
University of Alberta

nwmo

NUCLEAR WASTE
MANAGEMENT
ORGANIZATION

SOCIÉTÉ DE GESTION
DES DÉCHETS
NUCLÉAIRES



This report has been prepared under contract to NWMO. The report has been reviewed by NWMO, but the views and conclusions are those of the authors and do not necessarily represent those of the NWMO.

All copyright and intellectual property rights belong to NWMO.

Nuclear Waste Management Organization
22 St. Clair Avenue East, 4th Floor
Toronto, Ontario
M4T 2S3
Canada

Tel: 416-934-9814
Web: www.nwmo.ca

DOCUMENT HISTORY

Title:	Laboratory Petrophysical Testing for Core from Boreholes IG_BH04, IG_BH05 and IG_BH06		
Report Number:	APM-REP-01332-0447		
Revision:	R000	Date:	2024-11-04
Authored by:	Richard Chalaturnyk GeoREF, University of Alberta		

Revision Summary		
Revision Number	Date	Description of Changes/Improvements
R000	2024-11-04	Initial issue

SIGNATURES

Prepared by:		Richard Chalaturnyk, Ph.D., P.Eng., Fellow EIC, Professor
Reviewed by:		Francy Guerrero Zabala, M.Sc.
Approved by:		Richard Chalaturnyk, Ph.D., P.Eng., Fellow EIC, Professor

EXECUTIVE SUMMARY

As a part of NWMO's Adaptive Phased Management (APM) Site Selection phase, the Geomechanical Reservoir Experimental Facility (GeoREF) laboratory at the University of Alberta was contracted by NWMO to carry out petrophysical testing of samples from inclined boreholes IG_BH04, IG_BH05, and IG_BH06 drilled in the Wabigoon Lake Ojibway Nation (WLON)-Ignace Area, Ontario. Work described in this technical report was completed with data generated from testing conducted in accordance with the test plan prepared and accepted by NWMO for this project.

This report summarizes the results of the petrophysical testing of axial and radial sub-cores (relative to axis of the boreholes), prepared from crystalline rock, 61 mm diameter (HQ3) core samples obtained from boreholes IG_BH04, IG_BH05, and IG_BH06, to determine: the hydraulic conductivity, the potential for hydraulic conductivity anisotropy, and the petrophysical properties, such as water content, density, helium porosity, etc. Eight rock core samples from borehole IG_BH04, eight rock core samples from borehole IG_BH05, and eight rock core samples from borehole IG_BH06 were provided by NWMO for testing. Specimens were prepared by cutting along the axis of the core (axial direction) or the specimen was cut perpendicular to the axis of the core (radial direction) in any arbitrary orientation. The following three types of test specimens were cut from the samples with a diamond core barrel: 1) one 61 mm diameter by 61 mm length (axial direction), which was used only for hydraulic testing, 2) one 25 mm diameter by 25 mm length (axial direction), which was used for index testing and subsequently for hydraulic testing, and 3) one 25 mm diameter by 25 mm length, (radial direction) for hydraulic testing. End trimmings from the 25 mm test specimen preparation process were used for grain density testing. Tests for petrophysical index properties included: (as-received) bulk density, water content by mass (%), water content by volume (%), dry density (g/cm^3), water saturated bulk density (g/cm^3), grain density (g/cm^3), water loss porosity (%), helium porosity (%), and total porosity from grain density (%).

Transient pulse decay testing conducted in nine GeoREF specialized triaxial cells was used to measure the hydraulic conductivity and specific storage of the test specimens under isotropic stresses. Hydraulic conductivity testing was conducted under as close as possible to fully water-saturated conditions. The analysis of all transient pulse decay hydraulic conductivity test results was completed by fitting the theoretical model curve provided by Hsieh et al. (1981) to the recorded laboratory data.

Additionally, steady-state gas permeability testing under isotropic stress conditions was also employed. This testing was conducted using the specialized IsoTHM systems located within the GeoREF facility at the University of Alberta. The steady-state gas permeability of the specimens was assessed under various isotropic stresses. Additionally, the testing adhered to the ASTM D4525-13e2 *Standard Test Method for Permeability of Rocks by Flowing Air*, ensuring both the rigor and validity of GeoREF's testing protocols.

The average grain density for the biotite granodiorite-tonalite rocks was $2.671 \text{ g}/\text{cm}^3$ and the average grain density for the amphibolite rocks was $3.072 \text{ g}/\text{cm}^3$, whereas the as-received bulk density of all rock types varied between $2.586 \text{ g}/\text{cm}^3$ and $2.670 \text{ g}/\text{cm}^3$ with a mean of $2.635 \text{ g}/\text{cm}^3$. In general, it was difficult to differentiate between IG_BH05 and IG_BH06 specimens, but the IG_BH04 specimens showed a slightly higher as-received bulk density than the IG_BH05 and IG_BH06 specimens. Due to the low water content of the specimens, the variation in the density parameters (i.e., dry density and water saturated bulk density) reflects the same trends as the as-received bulk density. The dry density varied between $2.584 \text{ g}/\text{cm}^3$ and $2.669 \text{ g}/\text{cm}^3$.

with a mean of 2.633 g/cm³. The water saturated bulk density varied between 2.586 g/cm³ and 2.671 g/cm³ with a mean of 2.636 g/cm³. For water content (by mass percent), the range of values is from 0.030% to 0.190% with a mean value of 0.091%. Water loss porosity ranged from 0.02% to 0.53% with a mean value of 0.24%. Water loss porosity exhibits significant variability between the specimens because it is directly related to saturated, connected pore volume and the ability to move water out of the pore volume of the specimen. Water loss porosity is much less than helium porosity or grain density-calculated total porosity. Total porosity based on grain density ranged from 0.26% to 2.49% with a mean value of 1.42%, which is of the same order as the porosity measured using the helium porosimeter. Helium porosity measurements provide a valuable assessment of connected pore volume within each test specimen. Helium porosity varied from 0.58% to 3.05% with a mean value of 1.47%. While no formal cluster analysis (i.e., k-means) was completed on a crossplot between total porosity and helium porosity, the results suggest that the petrophysical data from borehole IG_BH04 is different than that of the boreholes IG_BH05 / IG_BH06 dataset.

The analysis of steady-state gas permeability was conducted following the methodology proposed by Moghadam (2016). Steady state gas testing was successful for test specimens. The effective confining stresses for tests conducted on all three borehole specimens ranged from 13.6 MPa to 26.9 MPa. Within the variability of the measured permeability, all test specimens show a decrease in permeability with an increase in effective confining stress, generally showing a one order of magnitude decrease in permeability for a 10 MPa increase in effective confining stress. For the complete dataset of 61mm diameter specimen results, the average permeability at low effective stress (15.0 MPa) was 2.46e-19 m², at medium effective stress (20.5 MPa) was 6.29e-20 m², and at high effective stress (25.2 MPa) was 1.51e-20 m².

Hydraulic conductivity testing was successful for most of the biotite granodiorite-tonalite rock test specimens. The effective confining stresses for tests conducted on all three borehole specimens ranged from 6.7 MPa to 28.6 MPa. Pulse decay tests conducted on the amphibolite rocks were not run to full equilibration due to prohibitive test times resulting from the extremely low hydraulic conductivity of these specimens. For these amphibolite specimens, tests were terminated after a fixed time period of 10 days. Within the variability of the measured hydraulic conductivities, all test specimens show a decrease in hydraulic conductivity with an increase in effective confining stress, generally showing a one order of magnitude decrease in hydraulic conductivity for a 10 MPa increase in effective confining stress, irrespective of specimen diameter or specimen orientation (axial or radial). The ratio of axial to radial hydraulic conductivity, defined as an anisotropy factor, was found to increase by a factor of two with an increase in effective confining stress from 10 MPa to 20 MPa. Given that the orientation of the core samples in inclined boreholes IG_BH04, IG_BH05, and IG_BH06 was not provided, the reader is cautioned that these anisotropy values should be considered approximate and likely do not reflect the actual in-situ anisotropy for any of the boreholes sampled.

The testing program also provided results that allows the sensitivity of hydraulic conductivity with respect to the specimen size to be examined. For borehole IG_BH04, 25 mm specimens display higher hydraulic conductivities than those of 61 mm specimens. For borehole IG_BH05, there appears to be no apparent difference between 61 mm and 25 mm specimens, and for borehole IG_BH06, 61 mm specimens show higher hydraulic conductivities, which is opposite to the trend seen in specimens from borehole IG_BH04.

The analysis of the pulse decay hydraulic conductivity test results using Hsieh et al. (1981), provided not only a solution for hydraulic conductivity but also a determination of the specific storage, S_s , of the specimens tested. GeoREF adopted this approach because the additional

constraint of matching the pulse decay response to both hydraulic conductivity and specific storage provides a better estimate of hydraulic conductivity. However, due to the influence from test system parameters such as compressibility or upstream and downstream reservoir storage volumes, GeoREF refers to the specific storage determined in the tests carried out here as an “apparent” specific storage, AS_s. For the complete dataset of 61 mm diameter specimen results, the average AS_s = 2.4e-08 ± 0.9e-08 m⁻¹. For the complete dataset of 25 mm diameter axial specimen results, the average AS_s = 3.6e-07 ± 0.5e-07 m⁻¹ and for the complete dataset of 25 mm diameter radial specimen results, the average AS_s = 4.6e-07 ± 1.2e-07 m⁻¹.

The report documents the experimental challenges and associated uncertainty with determining index parameters on test specimens whose pore volume and water content are extremely low. These petrophysical characteristics also create challenging conditions for accurate and repeatable hydraulic conductivity testing using the transient pulse decay technique. For the current program, the most difficult conditions to control during the hydraulic conductivity testing, and the ones which had the greatest impact on executing a successful test, were leaks through fittings and/or the membrane and very small changes in ambient test temperature, on the order of ± 0.01 °C.

TABLE OF CONTENTS

EXECUTIVE SUMMARY	iv
1. Introduction.....	1
2. Background Information	1
2.1 Geological Setting	1
2.2 Technical Objectives	3
2.3 Sample Depth Corrections	3
3. Description of Testing Procedures.....	3
3.1 Test Specimens.....	3
3.2 Index Testing.....	6
3.2.1 As-received Water Content, Re-saturated Water Content, As-Received Bulk Wet Density, Re-saturated Bulk Density, Bulk Dry Density, Porosity	7
3.2.2 As-Received Bulk Wet Density.....	7
3.2.2.1 Dimension Measurements	7
3.2.3 Re-saturated Bulk Density, Bulk Dry Density, As-received Water Content, Re-saturated Water Content, As-received Water Loss Porosity, and Re-saturated Water Loss Porosity	7
3.2.4 Helium Porosity.....	9
3.2.5 Grain Density and Total Porosity.....	9
3.3 Steady-State Gas Permeability Testing.....	9
3.3.1 Saturation Process for Steady-State Gas Permeability Testing.....	9
3.3.2 Steady-State Gas Permeability Testing.....	10
3.3.3 Analysis of Steady-State Gas Permeability Test Results.....	11
3.4 Hydraulic Conductivity Testing	11
3.4.1 Saturation Process for Hydraulic Conductivity Testing	12
3.4.2 Pulse Decay Testing	12
3.4.3 Analysis of Pulse Decay Hydraulic Conductivity Test Results	13
4. Laboratory results	15
4.1 Index Property Testing Results	16

4.2	Steady-State Gas Permeability Testing Results	29
4.3	Hydraulic Conductivity Testing Results.....	34
4.3.1	Influence of specimen diameter on hydraulic conductivity	47
4.3.2	Anisotropy in hydraulic conductivities.....	49
4.4	Specific Storage Obtained from Hydraulic Conductivity Testing.....	54
5.	Data Quality- Uncertainties and Limitations	58
5.1	Introduction.....	58
5.2	Index Testing.....	58
5.2.1	General Specimen Preparation	58
5.2.2	Specimen orientation	58
5.2.3	Uncertainty in As-Received (Natural Conditions) Density.....	58
5.2.4	Uncertainty in Dimension Measurements	58
5.2.5	Uncertainty in Water Content and Dry Bulk Density	59
5.2.6	Uncertainty in Water Saturated Bulk Density and Water Loss Porosity	60
5.2.7	Uncertainties in Total Porosity (from Grain Density).....	60
5.2.8	Uncertainties in Helium Porosimetry	61
5.2.9	Total porosity vs. He porosity	61
5.2.10	Sensitivity of porosity measurements based on grain density	62
5.3	Hydraulic Conductivity Testing Results.....	64
5.3.1	Anisotropy Limitations	65
5.3.2	Errors or uncertainties in the fitting of the solution.....	66
5.3.2.1	The measurement of the upstream and downstream pressure response	66
5.3.2.2	Identification of the pulse initiation	66
5.3.2.3	Water Properties (density and viscosity)	66
5.3.2.4	Specimen Area and Length.....	67
5.3.2.5	Measurement of the Upstream and Downstream Reservoir Storage.....	67
5.3.3	Specific Storage Determination.....	67

References	69
Appendix A: List of original and corrected sample depths along borehole.	71
Appendix B: Hydraulic Conductivity and Steady State Gas Permeability Test Summaries – IG_BH04	72
Appendix C: Hydraulic Conductivity and Steady State Gas Permeability Test Summaries – IG_BH05	120
Appendix D: Hydraulic Conductivity and Steady State Gas Permeability Test Summaries – IG_BH06	163

LIST OF TABLES

	Page
Table 1. Naming convention labels used for IGBH04, IGBH05, and IGBH06 specimens.	6
Table 2. List of index properties measured / calculated.....	6
Table 3. Pulse decay procedure for a single 25mm and 61mm diameter specimen.	12
Table 4 Depth and Lithology of Core Samples for IG_BH04, IG_BH05, and IG_BH06.....	17
Table 5 Summary of Grain Density Results.....	18
Table 6 Summary of Index Properties Measured on 25 mm diameter Specimens per borehole from IG_BH04.	21
Table 7 Summary of Index Properties Measured on 25 mm diameter Specimens per borehole from IG_BH05.	22
Table 8 Summary of Index Properties Measured on 25 mm diameter Specimens per borehole from IG_BH06.	23
Table 9. Statistical summary of Petrophysical Properties of Samples from IG_BH04.....	26
Table 10. Statistical summary of Petrophysical Properties of Samples from IG_BH05.....	27
Table 11. Statistical summary of Petrophysical Properties of Samples from IG_BH06.....	27
Table 12. Summary of Petrophysical Properties of All Samples from IG_BH04, IG_BH05, and IG_BH06	28
Table 13. Summary of Steady State Gas Permeability Testing for IG_BH04, IG_BH05, and IG_BH06.	30
Table 14 Summary of Hydraulic Conductivity Testing for Test Run #1 on IG_BH04.....	35
Table 15 Summary of Hydraulic Conductivity Testing for Test Run #2 on IG_BH04.....	36
Table 16 Summary of Hydraulic Conductivity Testing for Test Run #3 on IG_BH04.....	37
Table 17 Summary of Hydraulic Conductivity Testing for Test Run #1 on IG_BH05.....	38
Table 18 Summary of Hydraulic Conductivity Testing for Test Run #2 on IG_BH05.....	39
Table 19 Summary of Hydraulic Conductivity Testing for Test Run #3 on IG_BH05.....	40
Table 20 Summary of Hydraulic Conductivity Testing for Test Run #1 on IG_BH06.....	41
Table 21 Summary of Hydraulic Conductivity Testing for Test Run #2 on IG_BH06.....	42

Table 22 Summary of Hydraulic Conductivity Testing for Test Run #3 on IG_BH06.....	43
Table 23. Hydraulic Conductivity Anisotropy for 25 mm Feldspar-phyric tonalite Specimens from All Boreholes.	50
Table 24. Hydraulic Conductivity Anisotropy for 25 mm Biotite granodiorite-tonalite Specimens from IG_BH04.....	50
Table 25 Hydraulic Conductivity Anisotropy for 25 mm Biotite granodiorite-tonalite Specimens from IG_BH05.....	50
Table 26 Hydraulic Conductivity Anisotropy for 25 mm Biotite granodiorite-tonalite Specimens from IG_BH06.....	51

LIST OF FIGURES

	Page
Figure 1: Orientation of test specimens cut from core samples.....	5
Figure 2: Expected upstream and downstream pore pressure response in a pulse decay test where a positive pulse is applied in the upstream reservoir. In the current testing program, a combination of positive or negative pulse was applied in either upstream or downstream reservoir.....	13
Figure 3: Variation in grain density for each major rock type.....	19
Figure 4: Variation in a) As received bulk density and b) water content (by mass) with specimen depth.....	24
Figure 5: Variation in water content by mass.....	24
Figure 6: Variation in helium porosity.....	25
Figure 7 Cross plot of total porosity and helium porosity.....	26
Figure 8. Variation of permeability with applied effective isotropic (confining) stress for biotite granodiorite-tonalite specimens.....	31
Figure 9. Variation of permeability with applied effective isotropic (confining) stress for feldspar-phyric tonalite specimens.....	32
Figure 10. Variation of permeability with applied effective isotropic (confining) stress for amphibolite specimens.....	33
Figure 11. Variation of hydraulic conductivity of feldspar-phyric tonalite with effective confining stress for 25 mm axial specimens – all boreholes.....	44
Figure 12. Variation of hydraulic conductivity of feldspar-phyric tonalite with effective confining stress for 25 mm radial specimens – all boreholes.....	45
Figure 13. Variation of hydraulic conductivity of feldspar-phyric tonalite with effective confining stress for 61 mm axial specimens – all boreholes.....	45
Figure 14. Variation of hydraulic conductivity of biotite granodiorite-tonalite with effective confining stress for 25 mm axial specimens – all boreholes.....	46
Figure 15. Variation of hydraulic conductivity of biotite granodiorite-tonalite with effective confining stress for 25 mm radial specimens – all boreholes.....	46
Figure 16. Variation of hydraulic conductivity of biotite granodiorite-tonalite with effective confining stress for 61 mm axial specimens – all boreholes.....	47
Figure 17: Specimen diameter influence on hydraulic conductivity of biotite granodiorite-tonalite for axial test specimens from borehole IG_BH04.....	48

Figure 18: Specimen diameter influence on hydraulic conductivity of biotite granodiorite-tonalite for axial test specimens from borehole IG_BH05.....	48
Figure 19: Specimen diameter influence on hydraulic conductivity of biotite granodiorite-tonalite for axial test specimens from IG_BH06.....	49
Figure 20: Hydraulic conductivity anisotropy of feldspar-phyric tonalite for 25 mm test specimens from borehole IG_BH04 and IG_BH06.....	52
Figure 21: Hydraulic conductivity anisotropy of biotite granodiorite-tonalite for 25 mm test specimens from borehole IG_BH04.....	52
Figure 22: Hydraulic conductivity anisotropy of biotite granodiorite-tonalite for 25 mm test specimens from borehole IG_BH05.....	53
Figure 23: Hydraulic conductivity anisotropy of biotite granodiorite-tonalite for 25 mm test specimens from IG_BH06.....	53
Figure 24. Variation of apparent specific storage of feldspar-phyric tonalite with effective stress for 25 mm axial specimens – all boreholes.....	54
Figure 25. Variation of apparent specific storage of feldspar-phyric tonalite with effective stress for 25 mm radial specimens – all boreholes.....	55
Figure 26. Variation of apparent specific storage of feldspar-phyric tonalite with effective stress for 61 mm axial specimens – all boreholes.....	55
Figure 27. Variation of apparent specific storage of biotite granodiorite-tonalite with effective stress for 25 mm axial specimens – all boreholes.....	56
Figure 28. Variation of apparent specific storage of biotite granodiorite-tonalite with effective stress for 25 mm radial specimens – all boreholes.....	56
Figure 29. Variation of apparent specific storage of biotite granodiorite-tonalite with effective stress for 61 mm axial specimens – all boreholes.....	57
Figure 30. Total porosity from grain density versus He porosity.....	62
Figure 31. Comparison of He and water loss porosity.....	63

1. Introduction

The Initial Borehole Drilling and Testing project in the Wabigoon Lake Ojibway Nation (WLON)-Ignace Area, Ontario, is part of the Phase 2 Geoscientific Preliminary Field Investigations of the NWMO's Adaptive Phased Management (APM) Site Selection Phase.

This project comprises the drilling and testing of six deep boreholes within the northern portion of the Revell batholith, including boreholes IG_BH04, IG_BH05, and IG_BH06. The boreholes are located a direct distance of 43 km northwest of the Town of Ignace.

The Geomechanical Reservoir Experimental Facility (GeoREF) laboratory at the University of Alberta was contracted by NWMO to carry out the petrophysical testing of samples from boreholes IG_BH04, IG_BH05, and IG_BH06. This report summarizes the results of the petrophysical testing of axial and radial sub-cores (relative to axis of the boreholes) from these three boreholes.

Work described in this technical report was completed with data generated from testing conducted in accordance with the test plan document prepared and accepted by the NWMO for this project.

2. Background Information

2.1 Geological Setting

The approximately 2.7-billion-year-old Revell batholith is in the western part of the Wabigoon Subprovince of the Archean Superior Province. The batholith is roughly elliptical in shape trending northwest, is approximately 40 km in length, 15 km in width, and covers an area of approximately 455 km². Based on geophysical modelling, the batholith is approximately 2 km to 3 km thick through the center of the northern portion (SGL 2015). The batholith is surrounded by supracrustal rocks of the Raleigh Lake (to the north and east) and Bending Lake (to the southwest) greenstone belts (Stone, 2010b).

Boreholes IG_BH04, IG_BH05, and IG_BH06 are located within an investigation area of approximately 19 km² in size, situated in the northern portion of the Revell batholith. Bedrock exposure in the area is generally very good due to minimal overburden, few water bodies, and relatively recent logging activities. Ground elevations generally range from 400 to 450 m above sea level. The ground surface broadly slopes towards the northwest as indicated by the flow direction of the main rivers in the area. Local water courses tend to flow to the southwest towards Mennin Lake.

Four main rock units are identified in the supracrustal rock group: mafic metavolcanic rocks, intermediate to felsic metavolcanic rocks, metasedimentary rocks, and mafic intrusive rocks. Sedimentation within the supracrustal rock assemblage was largely synvolcanic, although sediment deposition in the Bending Lake area may have continued past the volcanic period (Stone 2009; Stone 2010a; Stone 2010b). All supracrustal rocks are affected, to varying degrees, by penetrative brittle-ductile to ductile deformation under greenschist- to amphibolite-facies metamorphic conditions (Blackburn and Hinz 1996; Stone et al. 1998). In some locations, primary features, such as pillow basalt or bedding in sedimentary rocks are preserved, in other locations, primary relationships are completely masked by penetrative deformation. Uranium-lead (U-Pb) geochronological analysis of the supracrustal rocks produced ages that range between 2734.6 +/- 1.1 Ma and 2725 +/- 5 Ma (Stone et al. 2010).

Three main suites of plutonic rock are recognized in the Revell batholith, including, from oldest to youngest: a biotite tonalite to granodiorite suite, a hornblende tonalite to granodiorite suite, and a biotite granite to granodiorite suite (Stone, 2009; Stone et al., 2010). Plutonic rocks of the biotite tonalite to granodiorite suite occur along the southwestern and northeastern margins of the Revell batholith. The principal type of rock within this suite is a white to grey, medium-grained, variably massive to foliated or weakly gneissic, biotite tonalite to granodiorite. One sample of foliated and medium-grained biotite tonalite produced a U-Pb age of 2734.2 ± 0.8 Ma (Stone et al. 2010). The hornblende tonalite to granodiorite suite occurs in two irregularly-shaped zones surrounding the central core of the Revell batholith. Rocks of the hornblende tonalite to granodiorite suite range compositionally from tonalite through granodiorite to granite and include significant proportions of quartz diorite and quartz monzodiorite. One sample of coarse-grained grey mesocratic hornblende tonalite produced a U-Pb age of 2732.3 ± 0.8 Ma (Stone et al. 2010). Rocks of the biotite granite to granodiorite suite underlie most of the northern, central and southern portions of the Revell batholith. Rocks of this suite are typically coarse-grained, massive to weakly foliated, and white to pink in colour. The biotite granite to granodiorite suite ranges compositionally from granite through granodiorite to tonalite. A distinct potassium (K)-feldspar megacrystic granite phase of the biotite granite to granodiorite suite occurs as an oval-shaped body in the central portion of the Revell batholith (Golder and PGW 2017). One sample of coarse-grained, pink, massive K-feldspar megacrystic biotite granite produced a U-Pb age of 2694.0 ± 0.9 Ma (Stone et al. 2010).

The bedrock surrounding boreholes IG_BH04, IG_BH05, and IG_BH06 is composed mainly of massive to weakly foliated felsic intrusive rocks that vary in composition between granodiorite and tonalite, and together form a relatively homogeneous intrusive complex. Bedrock identified as tonalite transitions gradationally into granodiorite and no distinct contact relationships between these two rock types are typically observed (SRK and Golder 2015; Golder and PGW 2017). Massive to weakly foliated granite is identified at the ground surface to the northwest of the feldspar-megacrystic granite. The granite is observed to intrude into the granodiorite-Tonalite bedrock, indicating it is distinct from, and younger than, the intrusive complex (Golder and PGW 2017).

West-northwest trending mafic dykes interpreted from aeromagnetic data extend across the northern portion of the Revell batholith and into the surrounding greenstone belts. One mafic dyke occurrence, located to the west of the area, is approximately 18-30 m wide (Golder and PGW 2017). All these mafic dykes have a similar character and are interpreted to be part of the Wabigoon dyke swarm. One sample from the same Wabigoon swarm produced a U-Pb age of 1887 ± 13 Ma (Stone et al. 2010), indicating that these mafic dykes are Proterozoic in age. It is assumed based on surface measurements that these mafic dykes are sub-vertical (Golder and PGW 2017).

Long, narrow valleys are located along the western and southern limits of the investigation area. These local valleys host creeks and small lakes that drain to the southwest and may represent the surface expression of structural features that extend into the bedrock. A broad valley is located along the eastern limits of the investigation area and hosts a more continuous, unnamed water body that flows to the south. The linear and segmented nature of this waterbody's shorelines may also represent the surface expression of structural features that extend into the bedrock. Regional observations from mapping have indicated that structural features are widely spaced (typical 30 to 500 cm spacing range) and dominantly comprised of sub-vertical joints with two dominant orientations, northeast and northwest trending (Golder and PGW 2017). Interpreted bedrock lineaments generally follow these same dominant orientations in the northern portion of the Revell batholith (DesRoches et al. 2018). Minor sub-horizontal joints

have been observed with minimal alteration, suggesting they are younger and perhaps related to glacial unloading. One mapped regional-scale fault, the Washeibemaga Lake fault, trends east and is located to the west of the Revell batholith. Ductile lineaments, also shown on Figure 2, follow the trend of foliation mapped in the surrounding greenstone belts. Additional details of the lithological units and structures found at surface within the investigation area are reported in Golder and PGW (2017).

2.2 Technical Objectives

The technical objectives of the petrophysical laboratory testing program were to determine:

- a) the hydraulic conductivity;
- b) the anisotropy of the hydraulic conductivity, and if so, how strong it is;
- c) the steady state permeability to gas; and
- d) the petrophysical properties, such as water content, density, helium porosity, etc.,

of the crystalline rock core samples from boreholes IG_BH04, IG_BH05, and IG_BH06 which were provided by NWMO.

2.3 Sample Depth Corrections

During the core logging of borehole IG_BH05 and IG_BH06, the logged depths were not reconciled with the depths obtained by the drilling supervisor calculated from measurement of the drill string and drill rod stick-up. This resulted in the core logging depths and thereby the collected petrophysical sample depths being artificially deeper than the drilled borehole depths. Therefore, an action was implemented to reconcile the core logging depths with the drilled depths. This resulted in an updated dataset with corrected core logging and sample depths. All depths referred to in the text of this report are corrected core logging sample depths in meters below ground surface along borehole. Appendix A of this report provide a list with the original logged and the corrected core sample depths. Refer to the respective reports *Geological and Geotechnical Core Logging, Photography and Sampling for IG_BH05 and for IG_BH06* (WSP, 2023a; WSP, 2023b) for details of the correction applied to the core logging data.

3. Description of Testing Procedures

The petrophysical testing program was carried out by the Reservoir Geomechanics Research Group [RG]² at the University of Alberta in the Geomechanical Reservoir Experimental Research Facility (GeoREF). Eight rock core samples from IG_BH04, eight rock core samples from borehole IG_BH05, and eight rock core samples from borehole IG_BH06 were provided by NWMO for testing. All core samples were stored in the Natural Resources Engineering Facility (NREF) moisture- and temperature-controlled storage facility prior to and after the experiments.

3.1 Test Specimens

All received rock core samples had a diameter of 61 mm (HQ3). As shown schematically in Figure 1, the following four types of test specimens were cut from the samples with a diamond core barrel following *GeoREF Standard Operating Procedure (SOP)-0011 (Preparation of Rock Specimens)*:

- a) one 61 mm diameter by 61 mm length along the axis of the core (axial direction), which was used only for hydraulic conductivity testing,

- b) one 61 mm diameter by 61 mm length along the axis of the core (axial direction), which was used only for steady state gas permeability testing,
- c) one 25 mm diameter by 25 mm length specimen along the axis (axial direction) of the core, which was used for index testing, and subsequently for hydraulic conductivity testing, and
- d) one 25 mm diameter by 25 mm length specimen cut perpendicular to the axis of the core (radial direction) in any arbitrary orientation, which was used for hydraulic conductivity testing.

End trimmings from the 25 mm test specimen preparation process were used for grain density testing. In all cases, test specimen location selection was completed to avoid sampling any large phenocrysts of feldspars crosscutting the whole specimen.

GeoREF received samples directly from NWMO with a Chain of Custody Form labelled with the following format:

CommunityName_BoreholeNumber_TestTypeTestNumber

Specifications for each section of the label are:

- Community Name: IG.
- Bore Hole Number: BH04, BH05, or BH06.
- Test Type: Petrophysical Suite (PS or AR).

Examples of this labeling convention are:

“IG_BH04_PS003” - sample for Petrophysical Suite tests from IG_BH04.

“IG_BH05_AR044” - sample for Petrophysical Suite tests using an archive (AR) sample from IG_BH05.

“IG_BH06_PS006” - sample for Petrophysical Suite test from IG_BH06.

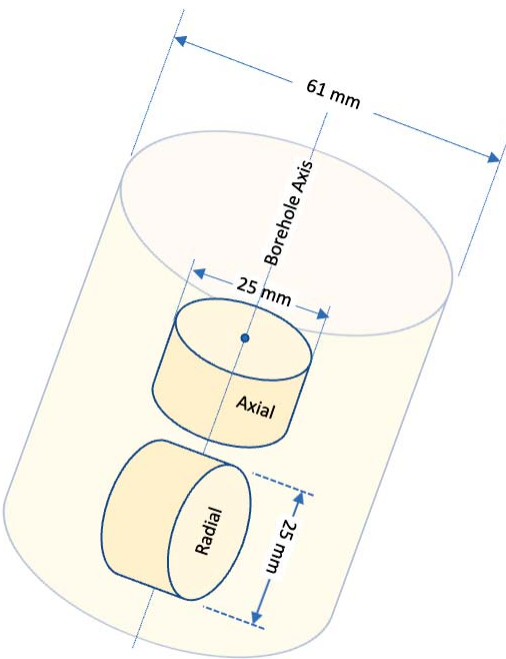


Figure 1: Orientation of test specimens cut from core samples.

GeoREF subsampled the cores to create specimens. The required testing suite and specimen dimensions for each sample were provided and used as part of the suffix labeling convention. These testing suites were hydraulic conductivity testing (HC) and steady state gas permeability testing (SSG). Index testing was completed on all HC25a specimens; therefore, a specific suffix was not created for index testing. The index testing included:

- (as-received) bulk density,
- (as-received) water content by mass (%),
- (as-received) water content by volume (%),
- (vacuum oven dried) dry density (g/cm^3),
- (re-saturated) water saturated bulk density (g/cm^3),
- grain density (g/cm^3),
- (re-saturated) water loss porosity (%),
- helium porosity (%), and
- total porosity from grain density (%).

Boreholes IG_BH04, IG_BH05, and IG_BH06 were inclined; therefore, test specimens cut along the axis and perpendicular to the core would be sub-vertical and sub-horizontal, respectively.

The specimen orientation relative to the core sample ('a' for axial, 'r' for radial) and the diameter (61 mm or 25 mm) were also included in the naming convention. Table 1 provides the definition for each suffix added to NWMO's labeling convention of provided sample. The full Laboratory Tracking Number naming convention format used was:

CommunityName_BoreholeNumber_TestTypeTestNumber_TestingSuite_Orientation_Diameter.
For example:

- "IG_BH04_PS003_HC25a" was Index testing on 25mm diameter axial specimen and hydraulic conductivity testing from sample IG_BH04_PS003.
- "IG_BH05_PS003_HC25r" was Hydraulic Conductivity testing on 25mm diameter radial specimen from sample IG_BH05_PS003.
- "IG_BH05_PS005_HC61a" was Hydraulic Conductivity testing on 61mm diameter axial specimen from sample IG_BH05_PS005.
- "IG_BH06_PS004_SSG61a" was Steady State Gas Permeability testing on 61mm diameter axial specimen from sample IG_BH06_PS004.

Table 1. Naming convention labels used for IG_BH04, IG_BH05, and IG_BH06 specimens.

Codes	Definition
(25a) *no specific suffix assigned for index testing, see text above	(as-received) bulk density, water content by mass (%), water content by volume (%), dry density (g/cm ³), water saturated bulk density (g/cm ³), water loss porosity (%), helium porosity (%) and total porosity from grain density (%).
HC	Hydraulic Conductivity
SSG	Steady State Gas Permeability
61	diameter and length of specimen, in mm
25	diameter and length of specimen, in mm
a	parallel to core sample axis
r	perpendicular to core sample axis in any arbitrary orientation

3.2 Index Testing

Index testing on the rock specimens was completed on the 25mm diameter axial cut specimens only (HC25a specimens) and comprised density, water content, and porosity measurements, following ASTM standards and ISRM suggested methods. The complete list of index properties that were measured / calculated are shown in Table 2.

Table 2. List of index properties measured / calculated.

As-received Bulk Wet Density (g/cm ³)	As-received Water Content (wt.%)	As-received Water Loss Porosity (%)
As-received Water Content (vol.%)	Re-saturated Water Loss Porosity (%)	Re-saturated Bulk Density (g/cm ³)
Helium Porosity (%)	Bulk Dry Density (g/cm ³)	Re-saturated Water Content (wt. %)
Total Porosity from Grain Density (%)	Grain Density (g/cm ³)	Re-saturated Water Content (vol. %)

The following subsections describe the procedures that were used to measure water content, total porosity, and connected porosity measured as water-loss porosity and helium porosity.

3.2.1 As-received Water Content, Re-saturated Water Content, As-Received Bulk Wet Density, Re-saturated Bulk Density, Bulk Dry Density, Porosity

Determination of as-received, re-saturated, and dry densities was completed according to ASTM D7263-21 *Standard Test Methods for Laboratory Determination of Density and Unit Weight of Soil*. The TorBal AGCN120 balance capable of determining mass up to 120 g with an accuracy of 0.1 mg was used to measure the mass.

3.2.2 As-Received Bulk Wet Density

Immediately after sample cutting, the mass of the specimen was measured to determine the mass as close to the as-received natural state as possible, M_{ar} (M). The mass was measured 10 times at 30 second intervals to obtain an average, consistent reading.

3.2.2.1 Dimension Measurements

The sample dimensions were measured after their mass had been recorded to minimize water loss to atmosphere. The regular cylindric specimens were measured with a high precision Mitutoyo IP65 Outside Micrometer accurate to 0.001mm (1 μ m). The specimen volume, V (L^3), was calculated from an average of 10 caliper readings for diameter (d) and length (L).

$$V = \frac{\pi d^2 L}{4}$$

The as-received (natural condition) bulk wet density, $\rho_{bulk,ar}$ (M/L³), was calculated by:

$$\rho_{bulk,ar} = \frac{M_{ar}}{V}$$

3.2.3 Re-saturated Bulk Density, Bulk Dry Density, As-received Water Content, Re-saturated Water Content, As-received Water Loss Porosity, and Re-saturated Water Loss Porosity

Determination of the as-received water content was completed according to ASTM D2216-19 - *Standard Test Methods for Laboratory Determination of Water (Moisture) Content of Soil and Rock by Mass*. It was expected that the crystalline rock from these boreholes had less than 1% water content. Therefore, water content of the samples was calculated to the nearest 0.01%. The water removal (drying) procedure deviated from ASTM D2216-19 by applying a vacuum pressure (~ -80 kPa) to the specimens while being oven-dried at a temperature of 110°C for 3 to 4 weeks.

The specimens were saturated by water immersion in a vacuum with an absolute pressure of < 0.8 kPa for a period of at least 72 hours. Each specimen was then surface-dried using a moist cloth to carefully remove excess surface water and to ensure that no fragments were lost. The mass was measured 10 times at 30 second intervals and averaged to obtain the mass of specimen in the re-saturated condition, M_{rs} (M). The saturation procedure deviated from ASTM D2216-19 by repeating the saturation/weighing procedure two times per week (e.g., Monday and Thursday) for a minimum of 4 weeks. The specimen was considered fully saturated once

the change in M_{rs} to the next was less than 0.5 mg (five times the accuracy of the instrument) and had been saturated for at least 4 weeks.

Previous testing data shows that specimens from IG_BH02 and IG_BH03 reached a dry state between 12 and 25 days. Therefore, the drying procedure deviated from ASTM D2216-19 by repeating the drying and weighing procedure two times per week (e.g. Monday and Thursday) for a minimum of 4 weeks. The specimen was considered dry once the change in M_{dry} from one measurement to the next was less than 0.25 mg and had been under drying conditions for at least 4 weeks. Since the TorBal AGCN120 has an accuracy of 0.1 mg; the 0.25 mg threshold was considered to be within the accuracy of the instrument and is <0.001% of the index specimen mass of ~30g. Consequently, the 0.25 mg threshold specification met the ASTM D2216-19 requirements.

The re-saturated bulk density, $\rho_{bulk,rs}$ (M/L^3), was calculated by:

$$\rho_{bulk,rs} = \frac{M_{rs}}{V}$$

The dry density, $\rho_{bulk,dry}$ (M/L^3), was calculated by:

$$\rho_{bulk,dry} = \frac{M_{dry}}{V}$$

The as-received water content by mass ($\omega_{mass,ar}$) (or gravimetric method) was calculated by:

$$\omega_{mass,ar} = \frac{M_{ar} - M_{dry}}{M_{dry}} (100\%)$$

The as-received water content by volume ($\omega_{vol,ar}$) were calculated by:

$$\omega_{vol,ar} = \frac{M_{ar} - M_{dry}}{\rho_{water}} \frac{1}{V} (100\%)$$

where ρ_{water} was assumed as 1 g/cm³. The re-saturated water content by mass ($\omega_{mass,rs}$) (or gravimetric method) was calculated by:

$$\omega_{mass,rs} = \frac{M_{rs} - M_{dry}}{M_{dry}} (100\%)$$

The re-saturated water content by volume ($\omega_{vol,rs}$) were calculated by:

$$\omega_{vol,rs} = \frac{M_{rs} - M_{dry}}{\rho_{water}} \frac{1}{V} (100\%)$$

The as-received water loss porosity ($\phi_{WL,ar}$) was calculated by:

$$\phi_{WL,ar} = \frac{M_{ar} - M_{dry}}{\rho_{water}} \frac{1}{V} (100\%)$$

The connected, re-saturated water loss porosity ($\phi_{WL,rs}$) was calculated by:

$$\phi_{WL,rs} = \frac{M_{rs} - M_{dry}}{\rho_{water}} \frac{1}{V} (100\%)$$

3.2.4 Helium Porosity

Helium porosity (ϕ_{He}) was measured using Helium Porosimeter testing guided by ASTM D6226-21 *Standard Test Methods for Open Cell Contents of Rigid Cellular Plastics* and SOP 014b *Pore volume measurements* using the Anton Parr Ultrapyc 5000. The measurement was completed on dry samples, based on Boyle's law of gas expansion using helium gas. Ten measurements per specimen were executed and averaged. The porosimeter device measures solid volume (V_s) based on connected pore volume, thereby the connected Helium porosity (ϕ_{He}) is calculated by:

$$\phi_{He} = \frac{V - V_s}{V} (100\%)$$

3.2.5 Grain Density and Total Porosity

Determination of grain density via Water Pycnometer, $\rho_{grain, pyc}$ (M/L³), was done according to ASTM D854-14 – *Standard Tests Methods for Specific Gravity of Soil Solids by Water Pycnometer*. The total porosity (ϕ_{tot}) is calculated from:

$$\phi_{tot} = 1 - \frac{\rho_{bulk, dry}}{\rho_{grain, pyc}} (100\%)$$

3.3 Steady-State Gas Permeability Testing

To measure the permeability of the test specimens, steady-state gas permeability testing under isotropic stress conditions was employed. This testing was conducted using the specialized IsoTHM systems located within the GeoREF facility at the University of Alberta. The steady-state gas permeability of the specimens was assessed under various isotropic stresses at a testing temperature of 33.5 °C. Each specimen, with a diameter of 61mm, was securely mounted in the isotropic triaxial cell, model NMC6500-61. These cells adhere to the ASTM D7012-14e1 standards, but with modifications that include additional pore pressure lines to the top and bottom platens. Moreover, they are uniquely designed for applying isotropic stresses exclusively. The NMC6500-61 cell, specifically chosen for its compatibility with 61mm diameter specimens, facilitated accurate and reliable testing. To replicate conditions as close to fully saturated gas as possible, nitrogen gas was used in the permeability measurements, which ensures negligible gas diffusion into the sample membrane during testing. For procedural guidance and alignment with industry standards, GeoREF incorporated several methodologies outlined in Moghadam (2016). Additionally, the testing adhered to the ASTM D4525-13e2 *Standard Test Method for Permeability of Rocks by Flowing Air*, ensuring both the rigor and validity of GeoREF's testing protocols.

3.3.1 Saturation Process for Steady-State Gas Permeability Testing

The procedure for saturating the specimens closely followed the guidelines established in SOP 016 for the Vacuum Saturation System, commonly used in the transient pulse decay approach. Initially, the system was evacuated using a vacuum of 2 kPa. The evacuation process varied depending on the specimens but, in general, evacuation took less than 24 hours to be

completed, ensuring that none of the pore lines came into contact with water during this stage. Following the evacuation, the specimen was methodically flooded with nitrogen gas, introduced from the upstream end (top platen). This process continued until the nitrogen gas had flowed through the specimen, confirmed by its emergence at the downstream end (bottom platen). Upon achieving this state, the pressure was maintained up to 12 hours to ensure complete saturation. The effectiveness and precision of the saturation process were verified through repeated tests. In these tests, the pore pressure was closely monitored; a consistent pressure reading indicated that the porous media was fully saturated. This saturation meant that the nitrogen gas had successfully occupied all interconnected pores, with no evidence of gas pressure decay due to potential compartmentalization within the media.

3.3.2 Steady-State Gas Permeability Testing

For all tests, the procedure involved injecting gas into the specimen from the upstream end (top platen) to the downstream end (bottom platen). The steady-state gas tests were executed by establishing a constant differential pressure across the specimen. This was achieved by lowering the bottom reservoir pump pressure and increasing the top reservoir pump pressure. Additionally, the flow rate was adjusted to reach steady-state conditions more rapidly. High-precision pressure transducers were used to record the top and bottom pressures. The flow rate was monitored through the injected flow rate data obtained from the top reservoir pump (Quixiz pump) and by monitoring the cumulative delivered gas volume (L^3) as a function of time (T). The flow rate was determined by the slope of the L^3/T relationship.

Permeability was calculated when both the differential pressure across the specimen and the flow rate remained constant for over an hour at a specific gas pressure step. During each steady-state test, the average pore pressure was maintained constant, ensuring the average effective stress within the specimen remained unchanged. The confining and pore pressures were incrementally increased four times, while maintaining the same effective stress, to allow steady-state gas permeability measurements at four gas pressures.

Once the permeability measurements were completed at a low effective stress, the procedure involved incremental increase of the effective stress to medium and then to high effective stress conditions. At each effective stress level, the process was repeated for a minimum of four mean gas pressures to establish the permeability and reciprocal mean pressure relationship.

The steady-state gas permeability procedure is summarized as follows:

1. **Preparation and Mounting:** Prepare and mount the specimen in the testing cell.
2. **Initial Confining Stress:** Increase the confining stress using a pump to a nominal level (500 kPa) to facilitate saturation.
3. **Saturation Process:** Execute the specimen evacuation saturation procedure in accordance with the GeoREF Vacuum Procedure.

4. **Setting Stress Conditions:** Increase the stress conditions and stabilize them at the lowest effective stress level.
5. **Low Effective Stress Testing:** Conduct four steady-state gas permeability measurements (at four mean gas pressures) under low effective stress conditions.
6. **Incremental Stress Adjustments:** Adjust the cell pressure and pore pressure incrementally to both the medium and the highest effective stress levels, following the desired effective stress path. Conduct the permeability tests at each of these stress levels respectively.
7. **Completion of Testing:** If testing for the specimen is complete, proceed to the next step. If not, repeat the necessary steps.
8. **Specimen Removal:** Decrease the pressures and carefully remove the specimen from the cell.

3.3.3 Analysis of Steady-State Gas Permeability Test Results

The analysis of steady-state gas permeability was conducted following the methodology proposed by Moghadam (2016). The permeability to gas (k) is calculated using the mass flow rate (\dot{m}) according to Darcy's equation for gases:

$$\dot{m} = \frac{kAM}{2RTLz\mu} (P_{up}^2 - P_{down}^2) \quad 1$$

In this equation, (μ) represents the gas viscosity, which is calculated at the average gas pressure. Similarly, the gas compressibility factor, denoted as (z), is also determined at this average pressure. Both the gas viscosity and the compressibility factor are calculated using PyFluids, an open-source Python library developed under an MIT license (available at <https://pypi.org/project/pyfluids/>). (R) is the universal gas constant, (T) is the absolute temperature, and (M) is the molecular weight of the gas. P_{up} and P_{down} denote the upstream and downstream pressures across the sample, respectively.

The mass flow rate (\dot{m}) is determined using the following relation:

$$\dot{m} = \frac{P_{up}QM}{zRT} \quad 2$$

Here, (Q) is the volumetric flow rate. These equations provide the foundation for analyzing the gas permeability of the specimens, taking into account the key variables such as pressure, temperature, and flow rate, and ensuring a rigorous and precise calculation of permeability.

3.4 Hydraulic Conductivity Testing

The transient pulse decay testing used to measure the hydraulic conductivity of the test specimens under isotropic stresses at a nominal test temperature of 40°C were conducted in two types of GeoREF specialized triaxial cells, the IPT-61 and the IPT-25. These cells were designed conforming to ASTM D7012-14e1 but include enhancements of pore pressure lines to

the top and bottom platens as well as the application of isotropic stresses only. The IPT-61 was used specifically for 61 mm diameter specimen tests and the IPT-25 was for 25 mm diameter specimen tests. Experimental system configurations followed Brace et al. (1968) and the data analysis procedure followed Hsieh et al (1980). The effective isotropic stresses applied to the test specimens were computed based on the specimen depth and the following stress-depth trendline equations for the Canadian Shield as reported in Yong and Maloney (2015) and communicated to NWMO in APM-CORR-01332-48674:

$$\sigma_m = 0.030 z + 4.86 \text{ [MPa]}$$

where σ_m = mean total stress [MPa] and z = specimen depth (m).

Effective stresses were determined assuming a hydrostatic pore pressure gradient computed by the following equation (as outlined in the accepted Test Plan):

$$\text{Pore Pressure} = 9.804 \text{ Depth} - 164.4 \text{ [kPa]},$$

and by following Terzaghi's effective stress definition (i.e., Biot's coefficient of 1).

Over the range of sample depths tested, the pore pressure magnitudes ranged from 2.5 to 8.5 MPa. Hydraulic conductivity testing was conducted under as close as possible to fully water-saturated conditions and followed the SOP 022 GeoREF Vacuum Procedure.

3.4.1 Saturation Process for Hydraulic Conductivity Testing

Saturation of the test specimen in the isotropic cell was achieved under a high vacuum of 2 kPa (much lower than the ambient water saturation pressure) at a nominal test temperature of 40°C. The sample was periodically loaded with a gas (nitrogen) pressure from one end while the pressure response at the other end was monitored. Initially, pressure does not propagate through the specimen, but as drying occurs, a continuous non-aqueous phase starts developing within the specimen that allows pressure to propagate. This continuous vapor source provides an efficient drive to sweep any remaining gas from the sample. The sample storage (the volume of water required to induce a unit increase in pressure) was also monitored during the re-saturation stage of the test. Based on initial due diligence testing by GeoREF, it was found that the sample storage was constant after a pore pressure of approximately 6 MPa was applied to the system. Consequently, a nominal pore pressure of 9 MPa was used for all the hydraulic conductivity tests.

3.4.2 Pulse Decay Testing

The pulse decay test was executed at three confining stress conditions. The procedure for setting up the hydraulic conductivity measured at low, medium, and high effective stress conditions following the technique proposed by Brace et al. (1968) and outlined in SOP-015 Absolute Perm are as follows (Table 3):

Table 3. Pulse decay procedure for a single 25 mm and 61 mm diameter specimen.

Step	Description
1	Mount specimen in cell.
2	Increase confining stress with pump isolated inside of environmental chamber to a nominal amount (500 kPa) for saturation;

3	Execute flow line and specimen evacuation saturation procedure (GeoREF Vacuum Procedure);
4	Start with the lowest effective stress condition.
5	Adjust cell pressure and pore pressure incrementally to required effective stress condition, following the desired effective stress path;
6	Hold cell pressure and pore pressure for specimen saturation while periodically measuring saturation using desired technique (see above);
7	Execute transient pulse decay test;
8a	If pulse has not decayed within 10 days or the specimen has been in the system for 14 days, the test is considered complete. Collected data will be used for analysis (see below). Move to Step 9.
8b	Move to medium effective stress condition, go back to step 5.
8c	If medium effective stress condition test is completed, move to highest effective stress condition, go back to step 5.
8d	If testing completed for specimen, move to step 9.
9	Decrease pressures; and
10	Remove specimen.

NOTE: If the specimen had reached the end of the scheduled testing period the specimen was removed from the testing system, regardless of the state of the test. The available collected data was used to perform the required analysis in Section 3.4.3.

3.4.3 Analysis of Pulse Decay Hydraulic Conductivity Test Results

The procedure for setting up the hydraulic conductivity test followed the technique proposed by Brace et al. (1968) and the analysis of all transient pulse decay hydraulic conductivity test results was completed by fitting the theoretical model provided by Hsieh et al. (1981) to the recorded laboratory data. The background to the Hsieh et al. (1981) method is described below.

A schematic drawing of the expected pressure response is shown in Figure 2.

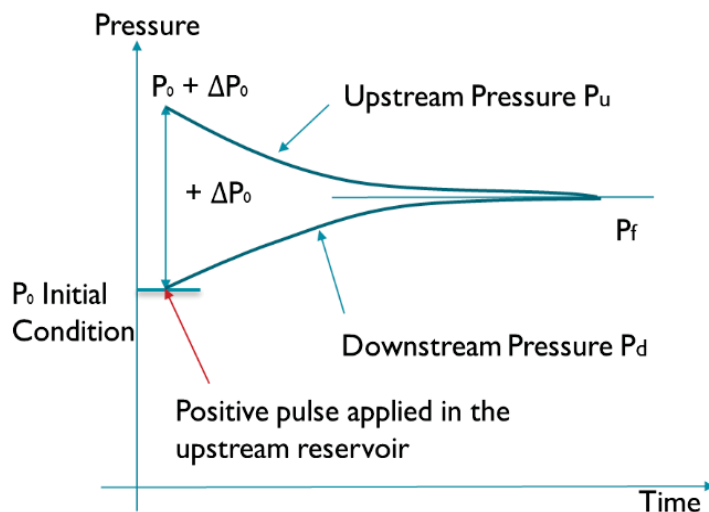


Figure 2: Expected upstream and downstream pore pressure response in a pulse decay test where a positive pulse is applied in the upstream reservoir. In the current

testing program, a combination of positive or negative pulse was applied in either upstream or downstream reservoir.

One-dimensional transient flow of a compressible fluid through a saturated porous and compressible medium can be described by the following equation, which combines the principle of conservation of fluid mass in a deformable matrix and Darcy's law for laminar flow through a hydraulically isotropic matrix:

$$\frac{\partial^2 h}{\partial x^2} - \frac{S_s}{K} \frac{\partial h}{\partial t} = 0, \text{ for } 0 < x < l \text{ and } t > 0$$

$$h(0, t) = h_d(t), \text{ for } t \geq 0$$

$$h(l, t) = h_u(t), \text{ for } t \geq 0$$

$$h_u(0) = H$$

where,

$h(x, t)$	is the hydraulic head in the specimen (dimension L),
h_d and h_u	are the hydraulic heads in the downstream and upstream reservoirs (L),
x	is the distance along the specimen axis referenced from the downstream end (L),
t	is the time from the onset of the experiment (T),
H	is the instantaneous step increase in hydraulic head (L) in the upstream or downstream reservoir at $t = 0$,
A	is the cross-sectional area of the specimen (L^2),
l	is the total length of the specimen (L),
S_d and S_u	are the compressive storages of the downstream and upstream reservoirs, respectively (L^2), defined as the changes in fluid volume in the reservoirs per unit change in hydraulic head in the reservoirs, and
K and S_s	are the hydraulic conductivity (L/T) and the specific storage (L^{-1}) of the specimen, respectively.

An analytic solution of the transient-pulse test incorporating both a constant specific storage and the hydraulic conductivity was derived by Hsieh et al. (1981) using a Laplace transform technique. Their approach allows both the permeability and the specific storage of a specimen to be determined. The specific storage S_s , is defined as the volume of water that a unit volume of saturated aquifer releases from storage when exposed to a unit decline in average head (Hantush 1964). This parameter (dimension L^{-1}) is dependent on the compressibility of the pore fluid, and both the bulk and matrix compressibility's of the solid, as well as the interconnected porosity of the specimen:

$$S_s = \gamma_w [nC_w + C_{eff} - (1 + n)C_s]$$

where

γ_w and C_w are the unit weight (M/L^3) and compressibility of the water (LT^2/M), respectively,

C_{eff} is the effective or bulk compressibility of the sample (LT^2/M),
 C_s is the compressibility of the minerals in the sample (LT^2/M), and
 n is the porosity of the sample.

The solution is:

$$\frac{P(x,t)}{\Delta P_0} = \frac{1}{1 + \beta + \gamma} + 2 \sum_{m=0}^{\infty} \frac{\exp \exp (-\alpha \phi_m^2) \left[\cos \phi_m \xi - \left(\frac{\gamma \phi_m}{\beta} \right) \sin \phi_m \xi \right]}{\left(1 + \beta + \gamma - \frac{\gamma \phi_m^2}{\beta} \right) \cos \phi_m - \phi_m \left(1 + \gamma + \frac{2\gamma}{\beta} \right) \sin \phi_m}$$

where ξ and α are dimensionless variables, are β and γ are dimensionless parameters defined by:

$$\xi = \frac{x}{l}, \quad \alpha = \frac{Kt}{l^2 S_s}, \quad \beta = \frac{S_s A l}{S_u}, \quad \gamma = \frac{S_d}{S_u}.$$

Furthermore, ϕ_m are the roots of:

$$\tan \phi = \frac{(\gamma + 1)\phi}{\frac{\gamma \phi^2}{\beta} - \beta}$$

The solutions for dimensionless hydraulic heads at the specimen ends, $x = 0$ and l , were used by Hsieh et al. (1981) to evaluate the response characteristics of the hydraulic heads at upstream and downstream reservoirs in various simulated cases.

The relationship between hydraulic conductivity K and permeability k is described in following equation:

$$K = \frac{\gamma_w}{\mu_w} k$$

where μ_w is the dynamic viscosity of water (M/LT). The viscosity of de-ionized (DI) water was calculated using the NIST Chemistry workbook (<https://webbook.nist.gov/chemistry/fluid/>).

4. Laboratory results

A total of 24 rock core samples, eight each from borehole IG_BH04, IG_BH05, and IG_BH06, were provided by NWMO for testing. Table 4 provides the depth intervals and NWMO-interpreted lithological classification of the 24 core samples received by GeoREF.

From IG_BH04, IG_BH05, and IG_BH06 (all inclined boreholes), each borehole had:

- eight 25 mm diameter axial specimens that were tested for index properties and hydraulic conductivity,
- eight 25 mm diameter radial specimens that were tested for hydraulic conductivity, and
- eight 61 mm diameter axial specimens that were tested for hydraulic conductivity.

Also, from:

- IG_BH04, three 61 mm diameter axial specimens were tested for steady state gas permeability,
- IG_BH05, two 61 mm diameter axial specimens were tested for steady state gas permeability,
- IG_BH06, three 61 mm diameter axial specimens were tested for steady state gas permeability.

4.1 Index Property Testing Results

Grain density determined from water pycnometry tests is a fundamental component in the calculation of the index properties of the test specimens. Table 5 lists the grain density determined from pycnometer tests on cuttings taken during the preparation of test specimens. As well, Figure 3 illustrates the grain density variation for each rock type. The grain densities associated with each sample are applied to each test specimen prepared from that sample to calculate total porosity from grain density. The average grain densities of the samples were: Amphibolite = 2.900 g/cm³ from 2 tests, Diabase = 3.069 g/cm³ from 1 test, Feldspar-phyric Tonalite = 2.709 g/cm³ from 4 tests, and for Biotite granodiorite-tonalite = 2.716 g/cm³ from 17 tests (Table 12).

Table 4 Depth and Lithology of Core Samples for IG_BH04, IG_BH05, and IG_BH06.

Sample ID	Depth along borehole From (m)	Depth along borehole To (m)	Length (m)	Lithology
IG_BH04_PS003	398.71	399.08	0.37	Biotite granodiorite-tonalite
IG_BH04_PS005	506.81	507.19	0.38	Biotite granodiorite-tonalite
IG_BH04_PS006	559.34	559.70	0.36	Biotite granodiorite-tonalite
IG_BH04_PS007	621.64	622.00	0.36	Biotite granodiorite-tonalite
IG_BH04_PS008	714.14	714.53	0.39	Biotite granodiorite-tonalite
IG_BH04_PS009	828.14	828.51	0.37	Biotite granodiorite-tonalite
IG_BH04_PS010	888.64	889.01	0.37	Feldspar-phyric Tonalite
IG_BH04_PS011	934.39	934.84	0.45	Feldspar-phyric Tonalite
IG_BH05_PS001	294.39	294.73	0.34	Diabase
IG_BH05_PS002	433.83	434.10	0.27	Biotite granodiorite-tonalite
IG_BH05_PS003	527.39	527.70	0.31	Biotite granodiorite-tonalite
IG_BH05_PS004	641.19	641.46	0.27	Biotite granodiorite-tonalite
IG_BH05_PS005	752.25	752.56	0.31	Biotite granodiorite-tonalite
IG_BH05_AR044	787.98	788.25	0.27	Amphibolite
IG_BH05_PS006	852.24	852.48	0.24	Biotite granodiorite-tonalite
IG_BH05_AR051	855.15	855.37	0.22	Amphibolite
IG_BH06_PS001	371.70	371.99	0.29	Biotite granodiorite-tonalite
IG_BH06_AR011	398.91	399.33	0.42	Feldspar-phyric-Tonalite
IG_BH06_PS002	565.20	565.47	0.27	Biotite granodiorite-tonalite
IG_BH06_PS003	668.56	668.84	0.28	Biotite granodiorite-tonalite
IG_BH06_PS004	731.35	731.61	0.26	Biotite granodiorite-tonalite
IG_BH06_PS006	833.89	833.29	0.4	Biotite granodiorite-tonalite
IG_BH06_AR056	908.58	908.96	0.38	Feldspar-phyric Tonalite
IG_BH06_PS007	932.63	932.89	0.26	Biotite granodiorite-tonalite

Table 5 Summary of grain density results.

Specimen ID	Avg. depth along borehole	Lithology	Grain Density
	m		g/cm ³
IG_BH04_PS003_HC25a	398.746	Biotite granodiorite-tonalite	2.653
IG_BH04_PS005_HC25a	506.833	Biotite granodiorite-tonalite	2.660
IG_BH04_PS006_HC25a	559.460	Biotite granodiorite-tonalite	2.622
IG_BH04_PS007_HC25a	621.263	Biotite granodiorite-tonalite	2.652
IG_BH04_PS008_HC25a	714.163	Biotite granodiorite-tonalite	2.677
IG_BH04_PS009_HC25a	828.163	Biotite granodiorite-tonalite	2.669
IG_BH04_PS010_HC25a	888.688	Feldspar-phyric Tonalite	2.697
IG_BH04_PS011_HC25a	934.615	Feldspar-phyric Tonalite	2.709
IG_BH05_PS001_HC25a	294.558	Diabase	3.069
IG_BH05_PS002_HC25a	433.853	Biotite granodiorite-tonalite	2.682
IG_BH05_PS003_HC25a	527.417	Biotite granodiorite-tonalite	2.716
IG_BH05_PS004_HC25a	641.243	Biotite granodiorite-tonalite	2.674
IG_BH05_PS005_HC25a	752.273	Biotite granodiorite-tonalite	2.684
IG_BH05_AR044_HC25a	788.023	Amphibolite	2.902
IG_BH05_PS006_HC25a	852.278	Biotite granodiorite-tonalite	2.692
IG_BH05_AR051_HC25a	855.178	Amphibolite	2.898
IG_BH06_PS001_HC25a	371.723	Biotite granodiorite-tonalite	2.655
IG_BH06_AR011_HC25a	398.948	Feldspar-phyric-Tonalite	2.709
IG_BH06_PS002_HC25a	565.223	Biotite granodiorite-tonalite	2.673
IG_BH06_PS003_HC25a	669.580	Biotite granodiorite-tonalite	2.679
IG_BH06_PS004_HC25a	731.960	Biotite granodiorite-tonalite	2.702
IG_BH06_PS006_HC25a	832.915	Biotite granodiorite-tonalite	2.647
IG_BH06_AR056_HC25a	908.603	Amphibolite	2.722
IG_BH06_PS007_HC25a	932.650	Biotite granodiorite-tonalite	2.691

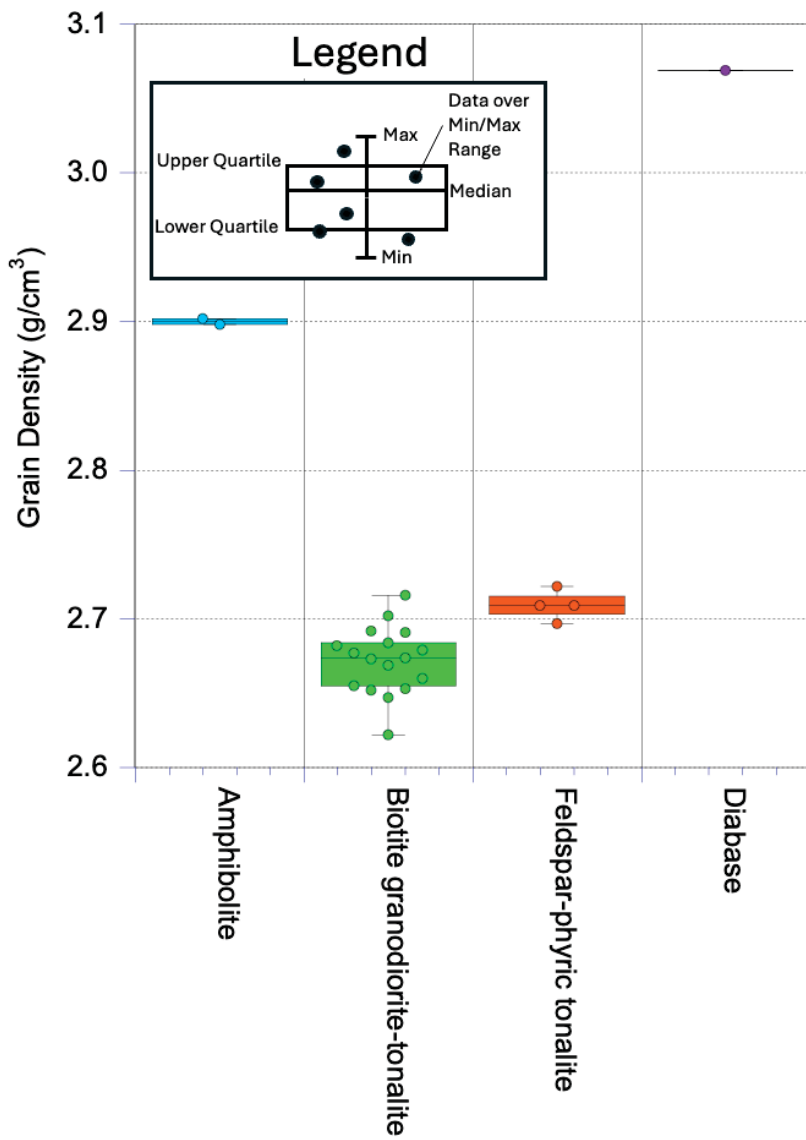


Figure 3: Variation in grain density for each major rock type.

An individual summary of all the petrophysical index test results for 25 mm diameter specimens prepared from core samples from boreholes IG_BH04, IG_BH05, and IG_BH06 are found in Table 6, Table 7, and Table 8 respectively.

Table 9, Table 10, and Table 11 provide the mean and standard deviation for each of the petrophysical properties provided in Table 6, Table 7, and Table 8 for boreholes IG_BH04, IG_BH05, and IG_BH06, respectively. For the complete dataset from all boreholes, Table 12 provides the mean and standard deviation for each of the petrophysical properties for the diabase, amphibolite, feldspar-phyric tonalite, and biotite granodiorite-tonalite rock types. Only one diabase specimen, 2 amphibolite, and 4 feldspar-phyric tonalite rock types were tested; therefore, assessing the statistical variability of their petrophysical properties within this program is not possible. Conversely, 17 tests (between all three boreholes) conducted for the biotite granodiorite-tonalite rock type allow statistical variability to be assessed.

The as-received bulk density of all samples varied between 2.609 g/cm³ and 3.005 g/cm³ with a mean of 2.696 g/cm³. The variability as a function of borehole and specimen depth is illustrated in Figure 4. In general, it was difficult to differentiate as-received bulk density between the boreholes, but three IG_BH05 specimens—Diabase (3.005 g/cm³) and two Amphibolites (2.868 and 2.935 g/cm³)—showed higher values than the other IG_BH04, IG_BH05, and IG_BH06 specimens and rock types.

Due to the low water content of the specimens, the variation in the density parameters (i.e., dry density, water saturated bulk density) reflects the same trends as the as-received bulk density. The dry density of all samples varied between 2.604 g/cm³ and 2.999 g/cm³ with a mean of 2.692 g/cm³. The vacuum saturated bulk density varied between 2.613 g/cm³ and 3.007 g/cm³ with a mean of 2.699 g/cm³.

For water content (by mass), the range of values is from 0.11% to 0.26% with a mean value of 0.183%. The variability with depth is illustrated in Figure 4 and the variability between each individual test specimen is shown in Figure 5.

Re-saturated water loss porosity of all samples ranged from 0.36% to 1.06% with a mean value of 0.738%. Water loss porosity exhibits significant variability between the specimens because it is directly related to saturated, connected pore volume and the ability to move water out of the pore volume of the specimen. On average, re-saturated water loss porosity (0.738%) is much less than helium porosity (0.955%) or grain density-calculated total porosity (1.086%).

Total porosity based on grain density of all samples ranged from 0.02% to 2.62% with a mean value of 1.086%, which is of the same order as the porosity measured using the helium porosimeter. Helium porosity measurements provide a valuable assessment of connected pore volume within each test specimen. Helium porosity of all samples varied from 0.06% to 2.62% with a mean value of 0.955%. A histogram for the variability of helium porosity is shown in Figure 6.

Figure 7 provides a cross plot between total porosity and helium porosity to better understand whether a difference may exist between boreholes. While no formal cluster analysis (i.e., k-means) was completed on this dataset, the results shown in Figure 7 appear to suggest that based on the separation of the centroids of each borehole dataset, there may be some difference between boreholes, but given the scatter in the data this remains inconclusive.

Table 6 Summary of index properties measured on 25 mm diameter specimens per borehole from IG BH04.

Specimen ID	Lithology	Avg Depth along borehole	(Bulk Density as received)	Dry Density	Water Sat. Bulk Density	Grain Density	Water Content by Vol.	Helium Porosity	Re-saturated Porosity	Water Loss from Grain Density
		m	g/cm³	g/cm³	g/cm³	g/cm³	%	%	%	%
IG_BH04_PS003_HC25a	Biotite granodiorite-tonalite	398.746	2.654	2.650	2.657	2.653	0.16	0.41	1.30	0.65
IG_BH04_PS005_HC25a	Biotite granodiorite-tonalite	506.833	2.665	2.660	2.669	2.660	0.17	0.46	0.94	0.88
IG_BH04_PS006_HC25a	Biotite granodiorite-tonalite	559.460	2.670	2.666	2.673	2.622	0.17	0.46	0.78	0.77
IG_BH04_PS007_HC25a	Biotite granodiorite-tonalite	621.263	2.668	2.664	2.673	2.652	0.18	0.47	0.06	0.92
IG_BH04_PS008_HC25a	Biotite granodiorite-tonalite	714.163	2.662	2.657	2.666	2.677	0.20	0.53	1.12	0.93
IG_BH04_PS009_HC25a	Biotite granodiorite-tonalite	828.163	2.628	2.624	2.632	2.669	0.17	0.46	1.30	0.84
IG_BH04_PS010_HC25a	Feldspar-phryic Tonalite	888.688	2.653	2.649	2.655	2.697	0.14	0.38	0.89	0.63
IG_BH04_PS011_HC25a	Feldspar-phryic Tonalite	934.615	2.680	2.673	2.683	2.709	0.26	0.69	0.93	1.06

Table 7 Summary of index properties measured on 25 mm diameter specimens per borehole from IG_BH05.

Specimen ID	Lithology	Avg. Depth along borehole	Dry Density (as received)	Water Sat. Bulk Density	Grain Density	Water Content by Mass	Water Content by Vol.	Heilum Porosity	Re-saturated Water Loss	Total Porosity	From Grain Density
IG_BH05_PS001_HC25a	Diabase	294.558	3.005	2.999	3.007	3.069	0.19	0.57	1.52	0.79	2.29
IG_BH05_PS002_HC25a	Biotite granodiorite-tonalite	433.853	2.644	2.639	2.646	2.682	0.20	0.52	1.73	0.67	1.61
IG_BH05_PS003_HC25a	Biotite granodiorite-tonalite	527.417	2.651	2.646	2.655	2.716	0.19	0.51	1.77	0.94	2.60
IG_BH05_PS004_HC25a	Biotite granodiorite-tonalite	641.243	2.609	2.604	2.613	2.674	0.19	0.49	2.62	0.84	2.62
IG_BH05_PS005_HC25a	Biotite granodiorite-tonalite	752.273	2.659	2.654	2.665	2.684	0.20	0.52	1.14	1.05	1.10
IG_BH05_AR044_HC25a	Amphibolite	788.023	2.868	2.861	2.869	2.902	0.26	0.74	1.08	0.86	1.41
IG_BH05_PS006_HC25a	Biotite granodiorite-tonalite	852.278	2.691	2.687	2.692	2.692	0.14	0.39	0.50	0.46	0.17
IG_BH05_AR051_HC25a	Amphibolite	855.178	2.935	2.932	2.936	2.898	0.12	0.36	0.48	0.42	NA

Table 8 Summary of index properties measured on 25 mm diameter specimens per borehole from IG BH06.

Specimen ID	Lithology	Avg. Depth along borehole	Bulk Density (as received)	Dry Density	Water Sat. Bulk Density	Grain Density	Water Content by Mass	Water Content by Vol.	Heilium Porosity	Re-saturated Water Loss Porosity	Total Porosity from Grain Density
IG_BH06_PS001_HC25a	Biotite granodiorite-tonalite	371.723	2.653	2.648	2.656	2.655	0.21	0.56	0.51	0.77	0.26
IG_BH06_AR011_HC25a	Feldspar-phyric-Tonalite	398.948	2.701	2.698	2.701	2.709	0.14	0.37	0.39	0.36	0.43
IG_BH06_PS002_HC25a	Biotite granodiorite-tonalite	565.223	2.664	2.658	2.665	2.673	0.22	0.59	0.51	0.75	0.56
IG_BH06_PS003_HC25a	Biotite granodiorite-tonalite	669.100	2.666	2.661	2.668	2.679	0.19	0.50	0.43	0.69	0.66
IG_BH06_PS004_HC25a	Biotite granodiorite-tonalite	731.370	2.677	2.672	2.679	2.702	0.19	0.51	0.79	0.71	1.13
IG_BH06_PS006_HC25a	Biotite granodiorite-tonalite	833.915	2.645	2.640	2.646	2.647	0.19	0.51	0.86	0.60	0.27
IG_BH06_AR056_HC25a	Feldspar-phyric tonalite	908.603	2.704	2.701	2.705	2.722	0.11	0.30	0.23	0.41	0.74
IG_BH06_PS007_HC25a	Biotite granodiorite-tonalite	932.650	2.663	2.658	2.665	2.691	0.19	0.52	1.05	0.72	1.26

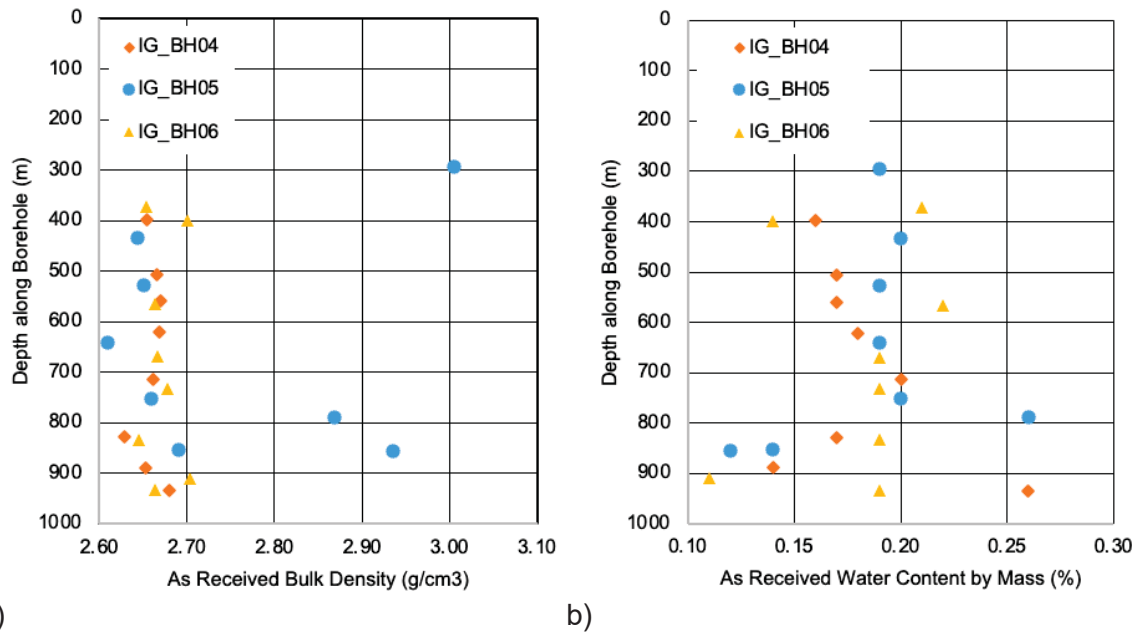


Figure 4: Variation in a) As received bulk density and b) water content (by mass) with specimen depth.

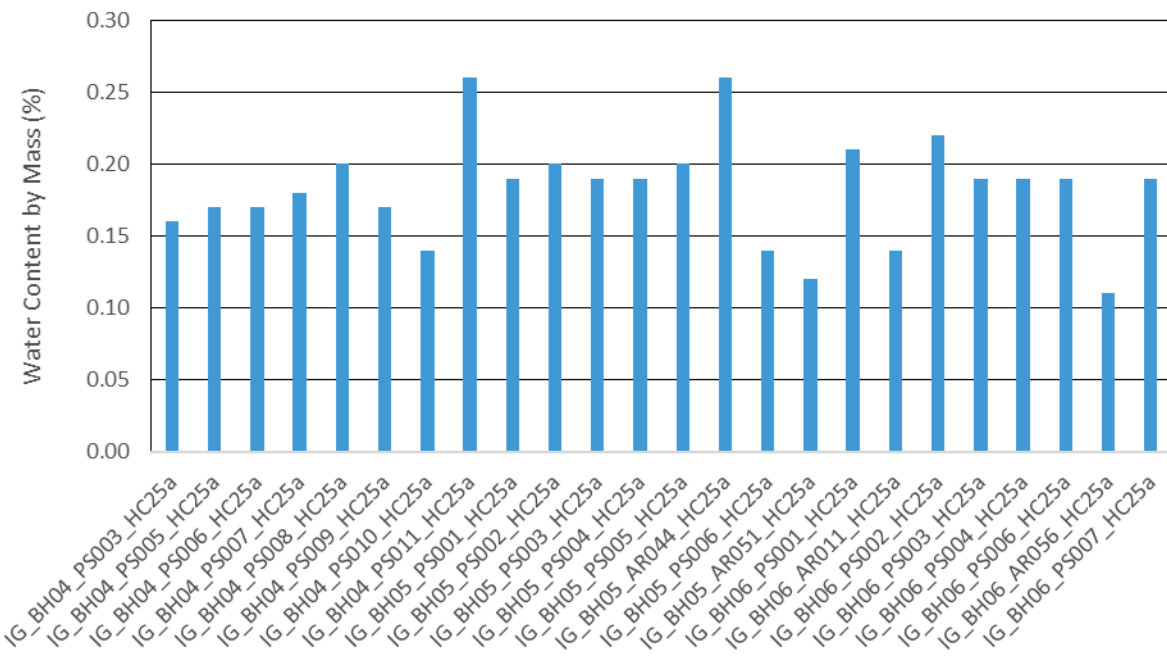


Figure 5: Variation in water content by mass.

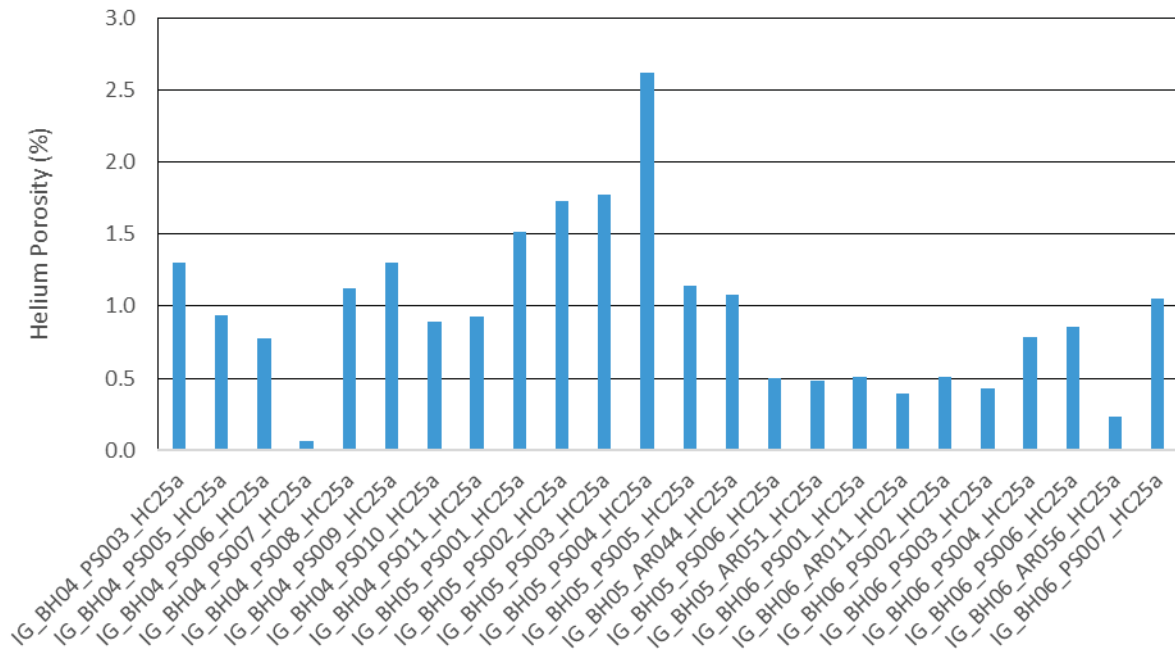


Figure 6: Variation in helium porosity.

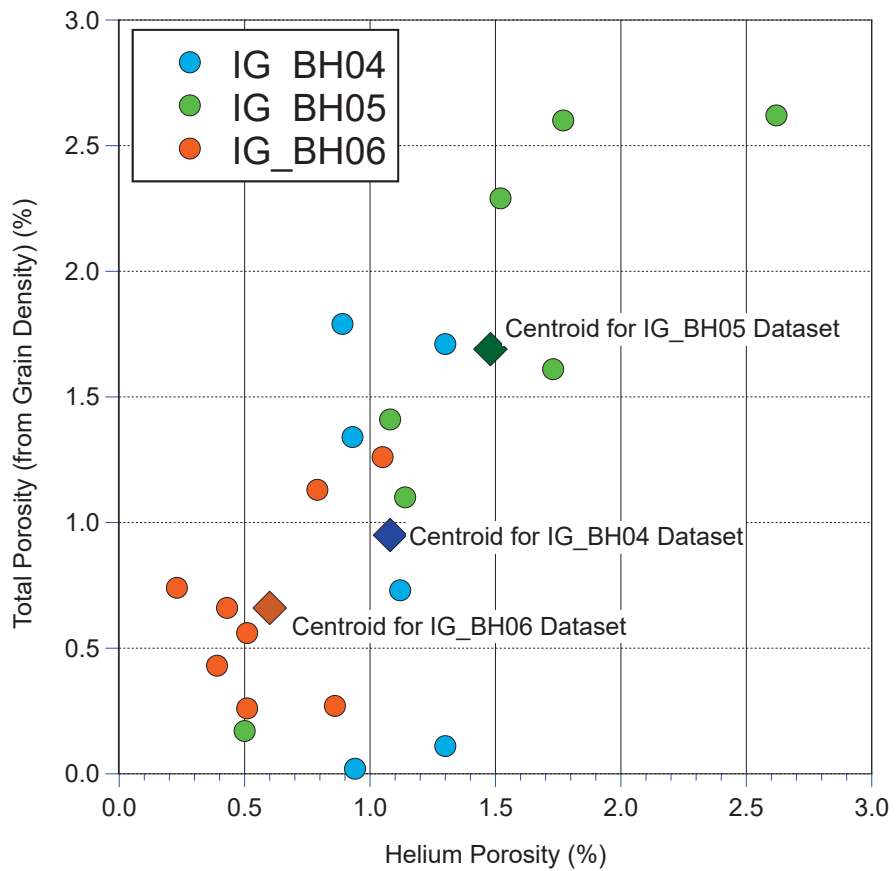


Figure 7 Cross plot of total porosity and helium porosity.

Table 9. Statistical summary of petrophysical properties of samples from IG_BH04.

Petrophysical Property	Units	Biotite granodiorite-tonalite		Feldspar-phyric Tonalite	
		Mean	Std. Dev.	Min.	Max.
(as received) Bulk Density	g/cm ³	2.658	0.014	2.653	2.680
Dry Density	g/cm ³	2.654	0.014	2.649	2.673
Water Saturated Bulk Density	g/cm ³	2.662	0.014	2.655	2.683
Grain Density	g/cm ³	2.656	0.017	2.697	2.709
Water Content by Mass	%	0.175	0.013	0.140	0.260
Water Content by Volume	%	0.465	0.035	0.380	0.690
Helium Porosity	%	0.917	0.426	0.890	0.930
Water Loss Porosity	%	0.832	0.097	0.630	1.060
Total Porosity from Grain Density	%	0.643	0.097	1.340	1.790

Table 10. Statistical summary of petrophysical properties of samples from IG_BH05.

Petrophysical Property	Units	Diabase	Biotite granodiorite-tonalite		Amphibolite	
			Value	Mean	Std. Dev.	Min.
(as received) Bulk Density	g/cm ³	3.005	2.651	0.026	2.868	2.935
Dry Density	g/cm ³	2.999	2.646	0.027	2.861	2.932
Water Saturated Bulk Density	g/cm ³	3.007	2.654	0.026	2.869	2.936
Grain Density	g/cm ³	3.069	2.690	0.014	2.898	2.902
Water Content by Mass	%	0.190	0.184	0.022	0.120	0.260
Water Content by Volume	%	0.570	0.486	0.049	0.360	0.740
Helium Porosity	%	1.520	1.552	0.707	0.480	1.080
Water Loss Porosity	%	0.790	0.792	0.208	0.420	0.860
Total Porosity from Grain Density	%	2.290	1.620	0.931	1.410	1.410

Table 11. Statistical summary of petrophysical properties of samples from IG_BH06.

Petrophysical Property	Units	Biotite granodiorite-tonalite		Feldspar-phyric Tonalite	
		Mean	Std. Dev.	Mean	Std. Dev.
(as received) Bulk Density	g/cm ³	2.661	0.010	2.703	0.002
Dry Density	g/cm ³	2.656	0.010	2.700	0.002
Water Saturated Bulk Density	g/cm ³	2.663	0.010	2.703	0.003
Grain Density	g/cm ³	2.675	0.019	2.716	0.009
Water Content by Mass	%	0.198	0.012	0.125	0.021
Water Content by Volume	%	0.532	0.032	0.335	0.049
Helium Porosity	%	0.692	0.224	0.310	0.113
Water Loss Porosity	%	0.707	0.054	0.385	0.035
Total Porosity from Grain Density	%	0.690	0.387	0.585	0.219

Table 12. Summary of petrophysical properties of all samples from IG_BH04, IG_BH05, and IG_BH06.

Lithology	Diabase				Amphibolite				Feldspar-phyric Tonalite				Biotite granodiorite-tonalite			
Property	Units	Count	Value	Count	Mean	Std. Dev	Count	Mean	Std. Dev	Count	Mean	Std. Dev	Count	Mean	Std. Dev	Count
(as received) Bulk Density	g/cm ³	1	3.005	2	2.902	0.034	4	2.685	0.020	17	2.657	0.018				
Dry Density	g/cm ³	1	2.999	2	2.897	0.035	4	2.680	0.021	17	2.652	0.018				
Water Sat. Bulk Density	g/cm ³	1	3.007	2	2.903	0.033	4	2.686	0.020	17	2.660	0.018				
Grain Density	g/cm ³	1	3.069	2	2.900	0.002	4	2.709	0.009	17	2.672	0.022				
Water Content by Mass	%	1	0.190	2	0.190	0.070	4	0.163	0.058	17	0.186	0.019				
Water Content by Volume	%	1	0.570	2	0.550	0.190	4	0.435	0.150	17	0.495	0.048				
Helium Porosity	%	1	1.520	2	0.780	0.300	4	0.610	0.306	17	1.024	0.595				
Water Loss Porosity	%	1	0.790	2	0.640	0.220	4	0.615	0.276	17	0.776	0.141				
Total Porosity (Grain Density)	%	1	2.290	1	1.410	0.000	4	1.075	0.527	15	0.987	0.819				

4.2 Steady-State Gas Permeability Testing Results

The laboratory program also measured steady state gas permeability on dried specimens under a range of effective confining stresses. Appendices A, B, and C provide the detailed testing summaries of each successful test conducted for IG_BH04, IG_BH05, and IG_BH06, respectively.

Table 13 provides the key test specimen identifier and for each specimen and the results from successful steady state gas permeability tests conducted over a series of effective confining stresses.

Steady state gas (SSG) permeability testing for specimens in borehole IG_BH04 tests were conducted over three ranges of effective confining stress, depending on core sample depth:

Low range:	13.6MPa to 16.9MPa
Medium range:	18.6MPa to 21.9MPa
High range:	23.6MPa to 26.9MPa

For borehole IG_BH05, SSG tests were conducted over three ranges of effective confining stress:

Low range:	14.3 MPa to 15.0 MPa
Medium range:	19.4 MPa to 20.0 MPa
High range:	24.3 MPa to 25.0 MPa

For borehole IG_BH06, SSG tests were conducted over three ranges of effective confining stress:

Low range:	13.9 MPa to 17.3 MPa
Medium range:	18.9 MPa to 22.3 MPa
High range:	23.9 MPa to 26.8 MPa

Figure 8 (biotite granodiorite-tonalite), Figure 9 (feldspar-phyric tonalite), and Figure 10 (amphibolite) provide summary illustrations of how permeability varies with effective stress. Within the variability of the measured permeability, all test specimens show a decrease in permeability with an increase in effective confining stress. These generally show a one order of magnitude decreases in permeability for a 10 MPa increase in effective confining stress, irrespective of borehole orientation.

Table 13. Summary of steady state gas permeability testing for IG_BH04, IG_BH05, and IG_BH06.

Test ID	Lithology	Specimen Orientation	(as received) Bulk Density (g/cm ³)	Helium Porosity (%)	Effective Confining Stress 1 (MPa)	Permeability 1 (m ²)	Effective Confining Stress 2 (MPa)	Permeability 2 (m ²)	Effective Confining Stress 3 (MPa)	Permeability 3 (m ²)
IG_BH04_PS008_SSG61a	Biotite grandiorite-tonalite	Axial	2.662	1.12	13.6	2.03E-19	18.6	4.57E-20	23.6	1.28E-20
IG_BH04_PS009_SSG61a	Biotite grandiorite-tonalite	Axial	2.628	1.30	15.5	1.74E-19	20.8	5.69E-20	25.7	2.74E-20
IG_BH04_PS010_SSG61a	Feldspar-phyric tonalite	Axial	2.653	0.89	16.9	1.53E-19	21.9	2.96E-20	26.9	6.90E-21
IG_BH05_AR044_SSG61a	Amphibolite	Axial	2.868	1.08	15.0	5.60E-21	20.0	7.34E-22	25.0	3.92E-22
IG_BH05_PS005_SSG61a	Biotite grandiorite-tonalite	Axial	2.659	1.14	14.3	4.27E-19	19.4	5.27E-20	24.3	4.05E-21
IG_BH06_AR056_SSG61a	Feldspar-phyric tonalite	Axial	2.704	0.23	17.3	1.96E-19	22.3	7.47E-20	NA	NA
IG_BH06_PS004_SSG61a	Biotite grandiorite-tonalite	Axial	2.677	0.79	13.9	3.67E-19	18.9	1.14E-19	23.9	1.47E-20
IG_BH06_PS006_SSG61a	Biotite grandiorite-tonalite	Axial	2.645	0.86	16.8	4.30E-19	21.8	1.26E-19	28.0	3.84E-20

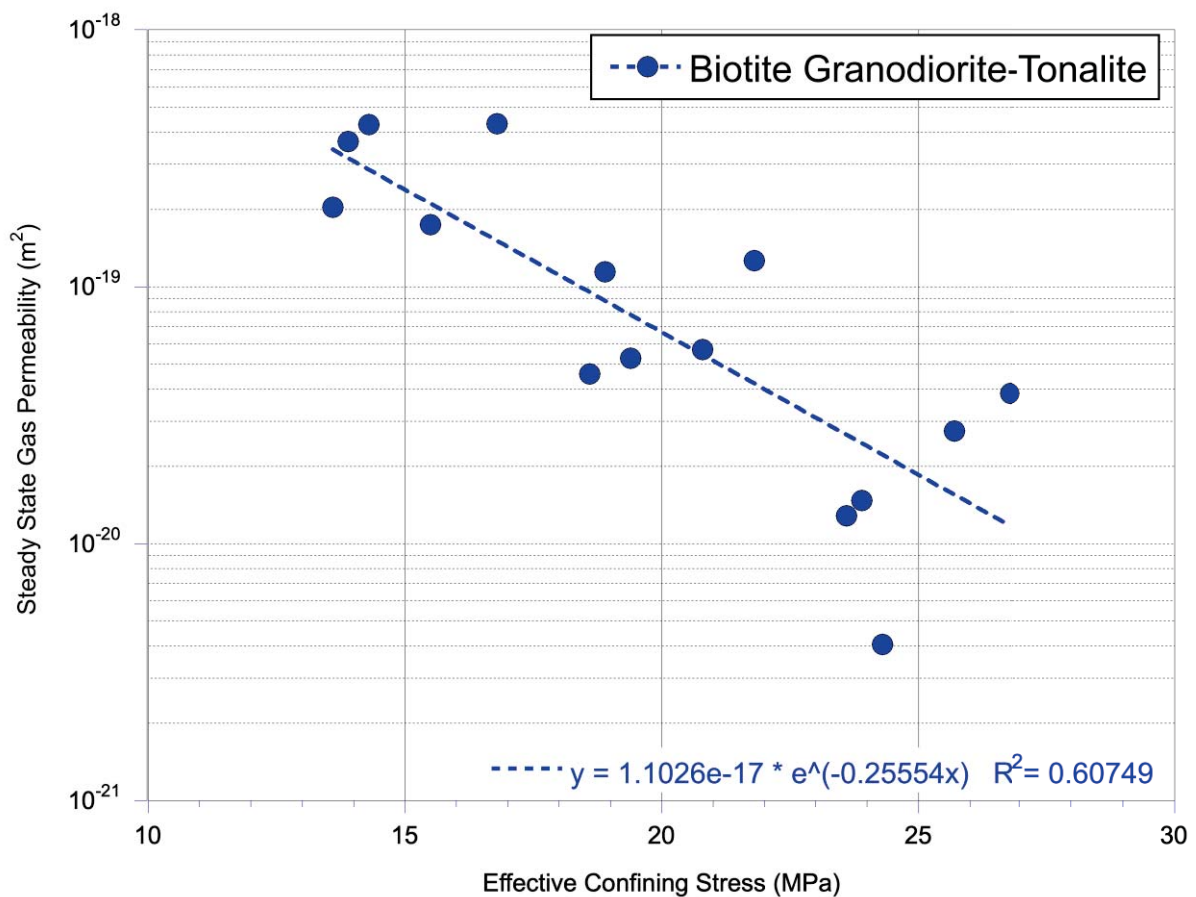


Figure 8. Variation of permeability with applied effective isotropic (confining) stress for biotite granodiorite-tonalite specimens.

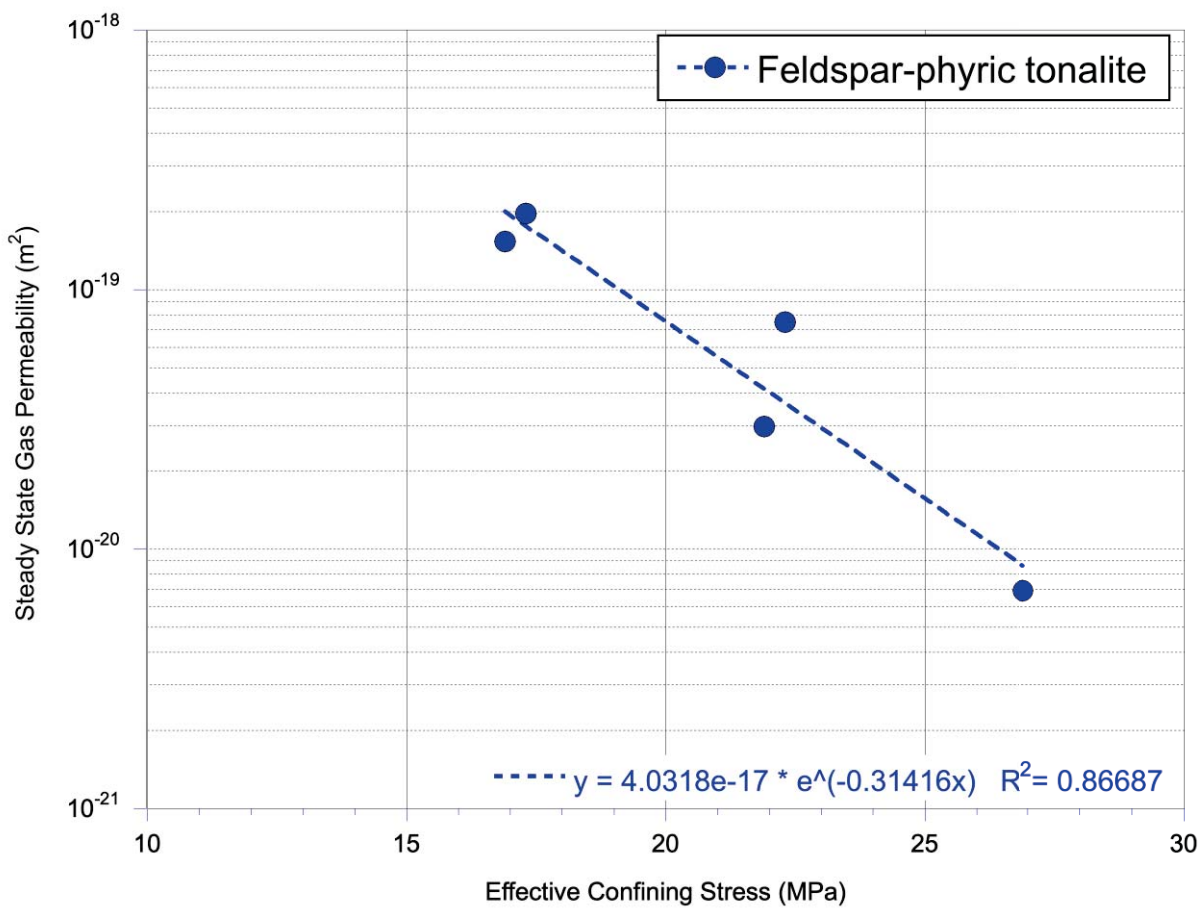


Figure 9. Variation of permeability with applied effective isotropic (confining) stress for feldspar-phyric tonalite specimens.

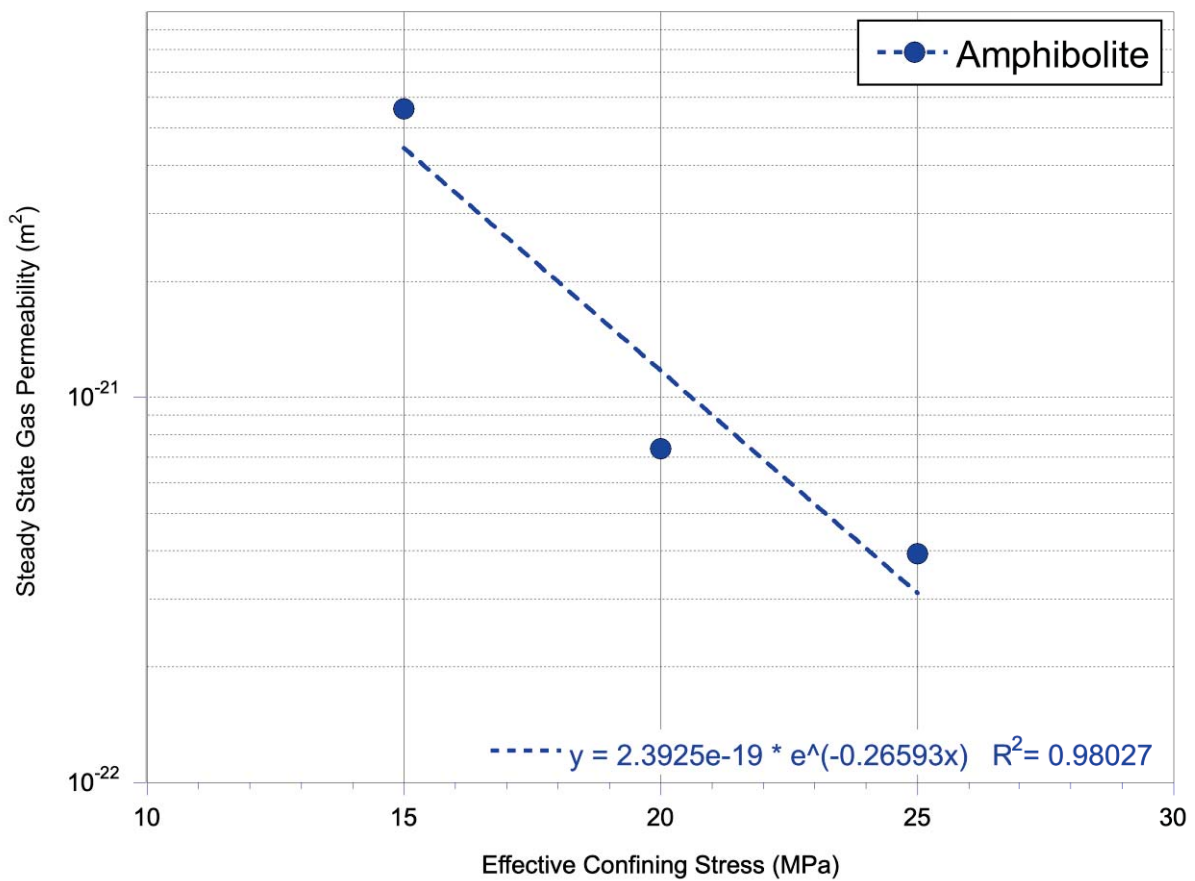


Figure 10. Variation of permeability with applied effective isotropic (confining) stress for amphibolite specimens.

4.3 Hydraulic Conductivity Testing Results

The laboratory program also measured the saturated hydraulic conductivity under a range of effective confining stresses. The tables below provide a summary of results from the hydraulic conductivity testing. Results for borehole IG_BH04 for testing runs #1, #2, and #3 are provided in Table 14, Table 15, and Table 16, respectively. Results for borehole IG_BH05 for testing runs #1, #2, and #3 are provided in Table 17, Table 18, and Table 19, respectively. Results for borehole IG_BH06 for testing runs #1, #2, and #3 are provided in Table 20, Table 21, and Table 22, respectively. Appendices A, B, and C provide the detailed testing summaries of each successful test conducted for boreholes IG_BH04, IG_BH05, and IG_BH06, respectively.

These comprehensive tables (14 to 22) provide key test specimen identifiers, including lithology, specimen orientation relative to borehole axis and as-received bulk density. For each specimen, successful hydraulic conductivity test results for tests conducted over a series of effective confining stresses are provided. In several cases, the initial permeability was so low that, for the time allocated for the test, which was 10 days, no pulse was transmitted across the specimen. These instances have been identified as “NPP” in the table and then no subsequent tests at higher effective confining stresses were conducted on these specimens.

The tables include results for hydraulic conductivity tests conducted on 61 mm and 25 mm diameter specimens: test ID's that end in “_61” are for 61 mm specimens and those ending in “_25” are for 25 mm specimens. Hydraulic conductivity tests conducted on the amphibolite and diabase rock types were not fully completed and were terminated early due to the extremely low permeability of these specimens. Similarly, only a limited number of tests on feldspar-phyric tonalite were also not fully completed due to very low permeability. Hydraulic conductivity testing was successfully completed for most of the biotite granodiorite-tonalite test specimens.

For borehole IG_BH04, hydraulic conductivity tests were conducted over three ranges of effective confining stress:

Low range:	6.7MPa to 10.6MPa
Medium range:	14.8MPa to 16.1MPa
High range:	19.9MPa to 28.6MPa

For borehole IG_BH05, hydraulic conductivity tests were conducted over three ranges of effective confining stress:

Low range:	8.6MPa to 11.5MPa
Medium range:	12.9MPa to 17.0MPa
High range:	18.0MPa to 19.4MPa

For borehole IG_BH06, hydraulic conductivity tests were conducted over three ranges of effective confining stress:

Low range:	7.6MPa to 12.1MPa
Medium range:	12.4MPa to 16.4MPa
High range:	17.3MPa to 21.4MPa

Table 14 Summary of hydraulic conductivity testing for test run #1 on IG_BH04.

Test ID	Lithology	Specimen Orientation	(as received) Bulk Density (g/cm ³)	Confining Stress (MPa)	Pore Pressure (MPa)	Effective Confining Stress (MPa)	Permeability (m ²)	Apparent Specific Storage (l/m)	Hydraulic Conductivity (m/s)
IG_BH04_PS003_HC25a	Biotite granodiorite-tonalite	axial	16.5	9.33	7.18	1.42E-19	1.30E-07	2.11E-12	
IG_BH04_PS003_HC25r	Biotite granodiorite-tonalite	radial	2.654	16.4	9.42	6.94	1.70E-19	7.62E-08	2.53E-12
IG_BH04_PS003_HC61a	Biotite granodiorite-tonalite	axial		16.7	9.44	7.22	6.17E-20	3.99E-08	9.29E-13
IG_BH04_PS005_HC25a	Biotite granodiorite-tonalite	axial		18.6	9.15	9.42	5.51E-19	5.76E-08	8.22E-12
IG_BH04_PS005_HC25r	Biotite granodiorite-tonalite	radial	2.665	18.4	9.16	9.25	8.33E-19	1.83E-08	1.24E-11
IG_BH04_PS005_HC61a	Biotite granodiorite-tonalite	axial		18.5	9.14	9.38	5.16E-19	9.66E-08	7.70E-12
IG_BH04_PS006_HC25a	Biotite granodiorite-tonalite	axial		19.7	9.22	10.5	1.59E-19	2.13E-07	2.40E-12
IG_BH04_PS006_HC25r	Biotite granodiorite-tonalite	radial	2.670	19.5	9.31	10.2	9.73E-20	1.72E-07	1.45E-12
IG_BH04_PS006_HC61a	Biotite granodiorite-tonalite	axial		19.6	9.28	10.3	4.70E-20	4.80E-08	7.06E-13
IG_BH04_PS007_HC25a	Biotite granodiorite-tonalite	axial					NPP	NPP	
IG_BH04_PS007_HC25r	Biotite granodiorite-tonalite	radial	2.668				NPP	NPP	
IG_BH04_PS007_HC61a	Biotite granodiorite-tonalite	axial					NPP	NPP	
IG_BH04_PS008_HC25a	Biotite granodiorite-tonalite	axial		22.6	9.21	13.4	4.35E-20	9.51E-08	6.54E-13
IG_BH04_PS008_HC25r	Biotite granodiorite-tonalite	radial	2.662				NPP	NPP	
IG_BH04_PS008_HC61a	Biotite granodiorite-tonalite	axial			22.6	9.36	13.2	5.23E-20	8.64E-08
IG_BH04_PS009_HC25a	Biotite granodiorite-tonalite	axial		24.7	8.86	15.9	1.96E-19	7.79E-08	2.94E-12
IG_BH04_PS009_HC25r	Biotite granodiorite-tonalite	radial		2.628			NPP	NPP	
IG_BH04_PS009_HC61a	Biotite granodiorite-tonalite	axial					NPP	NPP	
IG_BH04_PS010_HC25a	Feldspar-phryic tonalite	axial							
IG_BH04_PS010_HC25r	Feldspar-phryic tonalite	radial	2.653	25.6	9.32	16.2	4.91E-21	1.87E-07	7.30E-14
IG_BH04_PS010_HC61a	Feldspar-phryic tonalite	axial					NPP	NPP	
IG_BH04_PS011_HC25a	Feldspar-phryic tonalite	axial					NPP	NPP	
IG_BH04_PS011_HC25r	Feldspar-phryic tonalite	radial		2.680			NPP	NPP	
IG_BH04_PS011_HC61a	Feldspar-phryic tonalite	axial							

Table 15 Summary of hydraulic conductivity testing for test run #2 on IG_BH04.

Test ID	Lithology	Specimen Orientation	(as received) Bulk Density (g/cm^3)	Confining Stress (MPa)	Pore Pressure (MPa)	Effective Confining Stress (MPa)	Permeability (m^2)	Apparent Specific Storage ($1/\text{m}$)	Hydraulic Conductivity (m/s)
IG_BH04_PS003_HC25a	Biotite granodiorite-tonalite	axial	21.5	8.74	12.7	5.40E-20	1.06E-07	8.05E-13	
IG_BH04_PS003_HC25r	Biotite granodiorite-tonalite	radial	2.654	21.3	9.76	11.5	8.13E-20	1.29E-09	1.21E-12
IG_BH04_PS003_HC61a	Biotite granodiorite-tonalite	axial		21.6	8.81	12.8	8.57E-20	1.19E-07	1.28E-12
IG_BH04_PS005_HC25a	Biotite granodiorite-tonalite	axial		23.5	9.43	14.1	2.55E-19	1.54E-07	3.81E-12
IG_BH04_PS005_HC25r	Biotite granodiorite-tonalite	radial	2.665	18.3	10.5	7.8	1.00E-18	4.30E-08	1.49E-11
IG_BH04_PS005_HC61a	Biotite granodiorite-tonalite	axial		23.5	9.40	14.1	3.45E-19	1.80E-07	5.16E-12
IG_BH04_PS006_HC25a	Biotite granodiorite-tonalite	axial		24.7	9.20	15.5	4.71E-20	1.22E-07	7.10E-13
IG_BH04_PS006_HC25r	Biotite granodiorite-tonalite	radial	2.670	24.5	9.17	15.3	3.24E-20	7.82E-08	4.83E-13
IG_BH04_PS006_HC61a	Biotite granodiorite-tonalite	axial		24.6	9.13	15.4	2.11E-20	6.27E-08	3.18E-13
IG_BH04_PS007_HC25a	Biotite granodiorite-tonalite	axial			NPP				
IG_BH04_PS007_HC25r	Biotite granodiorite-tonalite	radial	2.668		NPP				
IG_BH04_PS007_HC61a	Biotite granodiorite-tonalite	axial			NPP				
IG_BH04_PS008_HC25a	Biotite granodiorite-tonalite	axial		27.6	9.39	18.2	1.53E-20	5.83E-08	2.30E-13
IG_BH04_PS008_HC25r	Biotite granodiorite-tonalite	radial	2.662				NPP		
IG_BH04_PS008_HC61a	Biotite granodiorite-tonalite	axial		27.6	9.28	18.3	2.14E-20	8.24E-08	3.21E-13
IG_BH04_PS009_HC25a	Biotite granodiorite-tonalite	axial		29.8	8.56	21.2	8.38E-20	4.87E-08	1.26E-12
IG_BH04_PS009_HC25r	Biotite granodiorite-tonalite	radial	2.628				NPP		
IG_BH04_PS009_HC61a	Biotite granodiorite-tonalite	axial					NPP		
IG_BH04_PS010_HC25a	Feldspar-phryic tonalite	axial					NPP		
IG_BH04_PS010_HC25r	Feldspar-phryic tonalite	radial	2.653				NPP		
IG_BH04_PS010_HC61a	Feldspar-phryic tonalite	axial					NPP		
IG_BH04_PS011_HC25a	Feldspar-phryic tonalite	axial		31.8	9.13	22.7	2.39E-20	2.52E-07	3.59E-13
IG_BH04_PS011_HC25r	Feldspar-phryic tonalite	radial	2.680	31.7	9.15	22.6	2.33E-20	1.76E-07	3.48E-13
IG_BH04_PS011_HC61a	Feldspar-phryic tonalite	axial		31.8	9.12	22.7	3.05E-19	1.07E-07	4.57E-12

Table 16 Summary of hydraulic conductivity testing for test run #3 on IG_BH04.

Test ID	Lithology	Specimen Orientation	(as received) Bulk Density (g/cm ³)	Confining Stress (MPa)	Pore Pressure (MPa)	Effective Confining Stress (MPa)	Permeability (m ²)	Apparent Specific Storage (l/m)	Hydraulic Conductivity (m/s)
IG_BH04_PS003_HC25a	Biotite granodiorite-tonalite	axial	24.9	9.41	15.5	1.96E-20	9.90E-08	2.93E-13	
IG_BH04_PS003_HC25r	Biotite granodiorite-tonalite	radial	2.654	25.4	9.43	16.0	1.88E-20	9.59E-08	2.79E-13
IG_BH04_PS003_HC61a	Biotite granodiorite-tonalite	axial		26.6	9.11	17.5	4.92E-20	1.04E-07	7.36E-13
IG_BH04_PS005_HC25a	Biotite granodiorite-tonalite	axial		24.9	9.12	15.8	9.18E-20	8.58E-08	1.37E-12
IG_BH04_PS005_HC25r	Biotite granodiorite-tonalite	radial	2.665	25.4	9.11	16.3	1.18E-19	3.44E-08	1.75E-12
IG_BH04_PS005_HC61a	Biotite granodiorite-tonalite	axial		25.1	9.10	16.0	1.36E-19	1.15E-07	2.04E-12
IG_BH04_PS006_HC25a	Biotite granodiorite-tonalite	axial		26.6	9.09	17.5	3.85E-20	5.66E-08	5.80E-13
IG_BH04_PS006_HC25r	Biotite granodiorite-tonalite	radial	2.670	25.1	9.84	15.3	1.29E-20	7.00E-08	1.93E-13
IG_BH04_PS006_HC61a	Biotite granodiorite-tonalite	axial		25.2	9.43	15.8	9.13E-21	3.23E-08	1.37E-13
IG_BH04_PS007_HC25a	Biotite granodiorite-tonalite	axial					NPP		
IG_BH04_PS007_HC25r	Biotite granodiorite-tonalite	radial		2.668			NPP		
IG_BH04_PS007_HC61a	Biotite granodiorite-tonalite	axial					NPP		
IG_BH04_PS008_HC25a	Biotite granodiorite-tonalite	axial							
IG_BH04_PS008_HC25r	Biotite granodiorite-tonalite	radial		2.662					
IG_BH04_PS008_HC61a	Biotite granodiorite-tonalite	axial							
IG_BH04_PS009_HC25a	Biotite granodiorite-tonalite	axial							
IG_BH04_PS009_HC25r	Biotite granodiorite-tonalite	radial		2.628					
IG_BH04_PS009_HC61a	Biotite granodiorite-tonalite	axial							
IG_BH04_PS010_HC25a	Feldspar-phryic tonalite	axial							
IG_BH04_PS010_HC25r	Feldspar-phryic tonalite	radial		2.653					
IG_BH04_PS010_HC61a	Feldspar-phryic tonalite	axial							
IG_BH04_PS011_HC25a	Feldspar-phryic tonalite	axial		36.7	9.14	27.6	1.32E-20	1.06E-07	1.99E-13
IG_BH04_PS011_HC25r	Feldspar-phryic tonalite	radial	2.680	36.7	9.19	27.5	1.26E-20	2.10E-07	1.88E-13
IG_BH04_PS011_HC61a	Feldspar-phryic tonalite	axial		36.7	9.41	27.3	1.69E-19	9.13E-08	2.54E-12

Table 17 Summary of hydraulic conductivity testing for test run #1 on IG_BH05.

Test ID	Lithology	Specimen Orientation	(as received) Bulk Density (g/cm ³)	Confining Stress (MPa)	Pore Pressure (MPa)	Effective Confining Stress (MPa)	Permeability (m ²)	Apparent Specific Storage (1/m)	Hydraulic Conductivity (m/s)
IG_BH05_AR044_HC25a	Amphibolite	axial							NPP
IG_BH05_AR044_HC25r	Amphibolite	radial	2.868						NPP
IG_BH05_AR044_HC61a	Amphibolite	axial							NPP
IG_BH05_AR051_HC25a	Amphibolite	axial							NPP
IG_BH05_AR051_HC25r	Amphibolite	radial	2.935						NPP
IG_BH05_AR051_HC61a	Amphibolite	axial							NPP
IG_BH05_PS001_HC25a	Diabase	axial							NPP
IG_BH05_PS001_HC25r	Diabase	radial	3.005						NPP
IG_BH05_PS001_HC61a	Diabase	axial							NPP
IG_BH05_PS002_HC25a	Biotite granodiorite-tonalite	axial		17.3	9.25	8.05			2.85E-12
IG_BH05_PS002_HC25r	Biotite granodiorite-tonalite	radial	2.644	17.2	9.23	7.97	1.13E-19	1.39E-07	1.68E-12
IG_BH05_PS002_HC61a	Biotite granodiorite-tonalite	axial		17.3	9.26	8.04			1.32E-12
IG_BH05_PS003_HC25a	Biotite granodiorite-tonalite	axial		18.9	8.86	10.0	4.26E-20	1.37E-07	6.36E-13
IG_BH05_PS003_HC25r	Biotite granodiorite-tonalite	radial	2.651	18.8	8.81	10.0	6.23E-20	1.43E-07	9.25E-13
IG_BH05_PS003_HC61a	Biotite granodiorite-tonalite	axial		19.0	9.25	9.75	5.13E-20	1.19E-07	7.64E-13
IG_BH05_PS004_HC25a	Biotite granodiorite-tonalite	axial		21.2	9.55	11.7	1.45E-19	8.18E-08	2.18E-12
IG_BH05_PS004_HC25r	Biotite granodiorite-tonalite	radial	2.609	21.2	9.54	11.7	1.53E-19	5.56E-08	2.26E-12
IG_BH05_PS004_HC61a	Biotite granodiorite-tonalite	axial		21.2	9.55	11.7	1.07E-19	8.53E-08	1.60E-12
IG_BH05_PS005_HC25a	Biotite granodiorite-tonalite	axial		23.2	8.68	14.5		3.32E-20	4.94E-13
IG_BH05_PS005_HC25r	Biotite granodiorite-tonalite	radial	2.659	23.0	8.64	14.4	3.61E-20	1.29E-07	5.35E-13
IG_BH05_PS005_HC61a	Biotite granodiorite-tonalite	axial		23.3	8.70	14.6	2.75E-20	8.43E-08	4.09E-13
IG_BH05_PS006_HC25a	Biotite granodiorite-tonalite	axial		25.1	9.55	15.6	2.27E-20	2.10E-07	3.39E-13
IG_BH05_PS006_HC25r	Biotite granodiorite-tonalite	radial	2.691	24.9	9.77	15.1	1.84E-20	2.25E-07	2.73E-13
IG_BH05_PS006_HC61a	Biotite granodiorite-tonalite	axial		25.2	9.81	15.4	2.13E-20	8.14E-08	3.17E-13

Table 18 Summary of hydraulic conductivity testing for test Run #2 on IG_BH05.

Test ID	Lithology	Specimen Orientation	(as received) Bulk Density (g/cm ³)	Confining Stress (MPa)	Pore Pressure (MPa)	Effective Confining Stress (MPa)	Permeability (m ²)	Apparent Specific Storage (1/m)	Hydraulic Conductivity (m/s)
IG_BH05_AR044_HC25a	Amphibolite	axial							NPP
IG_BH05_AR044_HC25r	Amphibolite	radial	2.868						NPP
IG_BH05_AR044_HC61a	Amphibolite	axial							NPP
IG_BH05_AR051_HC25a	Amphibolite	axial							NPP
IG_BH05_AR051_HC25r	Amphibolite	radial	2.935						NPP
IG_BH05_AR051_HC61a	Amphibolite	axial							NPP
IG_BH05_PS001_HC25a	Diabase	axial							NPP
IG_BH05_PS001_HC25r	Diabase	radial	3.005						NPP
IG_BH05_PS001_HC61a	Diabase	axial							NPP
IG_BH05_PS002_HC25a	Biotite granodiorite-tonalite	axial		22.3	8.73	13.6	5.60E-20	1.23E-07	8.28E-13
IG_BH05_PS002_HC25r	Biotite granodiorite-tonalite	radial	2.644	22.2	8.71	13.5	3.15E-20	1.07E-07	4.69E-13
IG_BH05_PS002_HC61a	Biotite granodiorite-tonalite	axial		22.3	8.72	13.6	4.01E-20	1.79E-07	6.00E-13
IG_BH05_PS003_HC25a	Biotite granodiorite-tonalite	axial		23.9	9.10	14.8	1.95E-20	9.06E-08	2.90E-13
IG_BH05_PS003_HC25r	Biotite granodiorite-tonalite	radial	2.651	23.7	9.18	14.5	2.65E-20	1.43E-07	3.93E-13
IG_BH05_PS003_HC61a	Biotite granodiorite-tonalite	axial							NPP
IG_BH05_PS004_HC25a	Biotite granodiorite-tonalite	axial		26.2	9.40	16.8	5.42E-20	9.10E-08	8.16E-13
IG_BH05_PS004_HC25r	Biotite granodiorite-tonalite	radial	2.609	26.1	9.52	16.6	4.58E-20	1.00E-07	6.82E-13
IG_BH05_PS004_HC61a	Biotite granodiorite-tonalite	axial		26.2	9.40	16.8	4.67E-20	7.40E-08	7.00E-13
IG_BH05_PS005_HC25a	Biotite granodiorite-tonalite	axial		28.1	9.37	18.7	1.62E-20	9.69E-08	2.41E-13
IG_BH05_PS005_HC25r	Biotite granodiorite-tonalite	radial	2.659	27.9	9.34	18.6	1.37E-20	1.08E-07	2.03E-13
IG_BH05_PS005_HC61a	Biotite granodiorite-tonalite	axial		28.3	9.39	18.9	1.23E-20	6.96E-08	1.83E-13
IG_BH05_PS006_HC25a	Biotite granodiorite-tonalite	axial		30.0	9.34	20.7	9.09E-21	1.38E-07	1.36E-13
IG_BH05_PS006_HC25r	Biotite granodiorite-tonalite	radial	2.691	29.8	9.34	20.5	7.43E-21	1.22E-07	1.10E-13
IG_BH05_PS006_HC61a	Biotite granodiorite-tonalite	axial		30.2	9.40	20.8	9.63E-21	8.14E-08	1.44E-13

Table 19 Summary of hydraulic conductivity testing for test run #3 on IG_BH05.

Test ID	Lithology	Specimen Orientation	(as received) Bulk Density (g/cm ³)	Confining Stress (MPa)	Pore Pressure (MPa)	Effective Confining Stress (MPa)	Permeability (m ²)	Apparent Specific Storage (1/m)	Hydraulic Conductivity (m/s)
IG_BH05_AR044_HC25a	Amphibolite	axial							NPP
IG_BH05_AR044_HC25r	Amphibolite	radial	2.868						NPP
IG_BH05_AR044_HC61a	Amphibolite	axial							NPP
IG_BH05_AR051_HC25a	Amphibolite	axial							NPP
IG_BH05_AR051_HC25r	Amphibolite	radial	2.935						NPP
IG_BH05_AR051_HC61a	Amphibolite	axial							NPP
IG_BH05_PS001_HC25a	Diabase	axial							NPP
IG_BH05_PS001_HC25r	Diabase	radial	3.005						NPP
IG_BH05_PS001_HC61a	Diabase	axial							NPP
IG_BH05_PS002_HC25a	Biotite granodiorite-tonalite	axial		27.2	8.99	18.2		1.95E-20	5.03E-08
IG_BH05_PS002_HC25r	Biotite granodiorite-tonalite	radial	2.644						NPP
IG_BH05_PS002_HC61a	Biotite granodiorite-tonalite	axial							NPP
IG_BH05_PS003_HC25a	Biotite granodiorite-tonalite	axial		28.9	9.15	19.8		6.39E-21	1.15E-07
IG_BH05_PS003_HC25r	Biotite granodiorite-tonalite	radial	2.651	28.7	9.10	19.6		1.01E-20	1.32E-07
IG_BH05_PS003_HC61a	Biotite granodiorite-tonalite	axial							1.50E-13
IG_BH05_PS004_HC25a	Biotite granodiorite-tonalite	axial		31.2	9.36	21.8		4.30E-20	6.57E-08
IG_BH05_PS004_HC25r	Biotite granodiorite-tonalite	radial	2.609	31.1	8.81	22.3		1.38E-20	8.72E-08
IG_BH05_PS004_HC61a	Biotite granodiorite-tonalite	axial							NPP
IG_BH05_PS005_HC25a	Biotite granodiorite-tonalite	axial		33.1	9.45	23.7		5.17E-21	1.70E-07
IG_BH05_PS005_HC25r	Biotite granodiorite-tonalite	radial	2.659	32.9	9.42	23.5		5.38E-21	7.82E-08
IG_BH05_PS005_HC61a	Biotite granodiorite-tonalite	axial		33.3	9.48	23.8		6.17E-21	8.69E-08
IG_BH05_PS006_HC25a	Biotite granodiorite-tonalite	axial							NPP
IG_BH05_PS006_HC25r	Biotite granodiorite-tonalite	radial	2.691	34.7	10.4	24.3		2.01E-21	4.06E-08
IG_BH05_PS006_HC61a	Biotite granodiorite-tonalite	axial		35.2	10.5	24.7		4.18E-21	3.92E-08

Table 20 Summary of hydraulic conductivity testing for test run #1 on IG_BH06.

Test ID	Lithology	Specimen Orientation	(as received) Bulk Density (g/cm ³)	Confining Stress (MPa)	Pore Pressure (MPa)	Effective Confining Stress (MPa)	Permeability (m ²)	Apparent Specific Storage (1/m)	Hydraulic Conductivity (m/s)
IG_BH06_AR011_HC25a	Feldspar-phyric tonalite	axial	17.1	9.25	7.82	6.39E-21	2.36E-07	9.64E-14	
IG_BH06_AR011_HC25r	Feldspar-phyric tonalite	radial	2.701	17.1	8.86	8.22	7.30E-21	2.02E-07	1.09E-13
IG_BH06_AR011_HC61a	Feldspar-phyric tonalite	axial	17.1	8.86	8.25	5.20E-21	9.42E-08	7.81E-14	
IG_BH06_AR056_HC25a	Feldspar-phyric tonalite	axial	26.2	9.41	16.7	1.44E-21	8.96E-08	2.14E-14	
IG_BH06_AR056_HC25r	Feldspar-phyric tonalite	radial	2.704		NPP				
IG_BH06_AR056_HC61a	Feldspar-phyric tonalite	axial	26.3	8.81	17.5	1.29E-21	8.30E-08	1.92E-14	
IG_BH06_PS001_HC25a	Biotite granodiorite-tonalite	axial	16.0	9.17	6.86	5.39E-20	1.39E-07	8.02E-13	
IG_BH06_PS001_HC25r	Biotite granodiorite-tonalite	radial	2.653	15.9	8.82	7.09	5.06E-20	2.28E-07	7.51E-13
IG_BH06_PS001_HC61a	Biotite granodiorite-tonalite	axial	16.1	8.88	7.23	3.82E-20	1.22E-07	5.69E-13	
IG_BH06_PS002_HC25a	Biotite granodiorite-tonalite	axial	19.6	9.18	10.4	4.02E-20	6.73E-08	5.99E-13	
IG_BH06_PS002_HC25r	Biotite granodiorite-tonalite	radial	2.664	19.5	8.79	10.7	6.03E-20	1.16E-07	8.96E-13
IG_BH06_PS002_HC61a	Biotite granodiorite-tonalite	axial	19.7	8.83	10.9	3.52E-20	7.95E-08	5.24E-13	
IG_BH06_PS003_HC25a	Biotite granodiorite-tonalite	axial	21.6	9.12	12.5	8.84E-20	6.57E-08	1.32E-12	
IG_BH06_PS003_HC25r	Biotite granodiorite-tonalite	radial	2.666	21.4	9.06	12.3	7.39E-20	7.54E-08	1.10E-12
IG_BH06_PS003_HC61a	Biotite granodiorite-tonalite	axial	21.7	9.10	12.6	6.45E-20	9.27E-08	9.61E-13	
IG_BH06_PS004_HC25a	Biotite granodiorite-tonalite	axial	22.9	9.57	13.3	1.16E-20	3.24E-08	1.73E-13	
IG_BH06_PS004_HC25r	Biotite granodiorite-tonalite	radial	2.677	22.9	9.60	13.4	1.43E-20	1.52E-07	2.15E-13
IG_BH06_PS004_HC61a	Biotite granodiorite-tonalite	axial	22.9	9.58	13.4	1.75E-20	1.15E-07	2.63E-13	
IG_BH06_PS006_HC25a	Biotite granodiorite-tonalite	axial	24.9	8.78	16.1	2.53E-19	6.08E-08	3.80E-12	
IG_BH06_PS006_HC25r	Biotite granodiorite-tonalite	radial	2.645	24.8	8.63	16.2	1.04E-19	1.04E-07	1.55E-12
IG_BH06_PS006_HC61a	Biotite granodiorite-tonalite	axial			NPP				
IG_BH06_PS007_HC25a	Biotite granodiorite-tonalite	axial	26.6	8.89	17.7	1.81E-19	1.42E-07	2.70E-12	
IG_BH06_PS007_HC25r	Biotite granodiorite-tonalite	radial	2.663	26.4	8.87	17.5	1.93E-19	1.41E-07	2.87E-12
IG_BH06_PS007_HC61a	Biotite granodiorite-tonalite	axial	26.7	8.89	17.8	9.24E-20	1.26E-07	1.38E-12	

Table 21 Summary of hydraulic conductivity testing for test run #2 on IG_BH06.

Test ID	Lithology	Specimen Orientation	(as received) Bulk Density (g/cm ³)	Confining Stress (MPa)	Pore Pressure (MPa)	Effective Confining Stress (MPa)	Permeability (m ²)	Apparent Specific Storage (1/m)	Hydraulic Conductivity (m/s)
IG_BH06_AR011_HC25a	Feldspar-phyric tonalite	axial	22.1	9.36	12.75	4.88E-21	1.45E-07	7.37E-14	
IG_BH06_AR011_HC25r	Feldspar-phyric tonalite	radial	2.701	22.1	9.30	12.77	4.10E-21	1.50E-07	6.13E-14
IG_BH06_AR011_HC61a	Feldspar-phyric tonalite	axial	22.1	9.31	12.79	3.41E-21	1.12E-07	5.12E-14	
IG_BH06_AR056_HC25a	Feldspar-phyric tonalite	axial	2.704				NPP		
IG_BH06_AR056_HC25r	Feldspar-phyric tonalite	radial					NPP		
IG_BH06_AR056_HC61a	Feldspar-phyric tonalite	axial					NPP		
IG_BH06_PS001_HC25a	Biotite granodiorite-tonalite	axial	21.0	9.08	11.91	2.63E-20	1.30E-07	3.92E-13	
IG_BH06_PS001_HC25r	Biotite granodiorite-tonalite	radial	2.653	20.8	9.01	11.82	2.39E-20	9.35E-08	3.54E-13
IG_BH06_PS001_HC61a	Biotite granodiorite-tonalite	axial	21.1	9.08	12.02	2.09E-20	6.45E-08	3.11E-13	
IG_BH06_PS002_HC25a	Biotite granodiorite-tonalite	axial	24.6	9.08	15.51	2.08E-20	9.54E-08	3.11E-13	
IG_BH06_PS002_HC25r	Biotite granodiorite-tonalite	radial	2.664	24.4	8.65	15.76	2.93E-20	8.17E-08	4.35E-13
IG_BH06_PS002_HC61a	Biotite granodiorite-tonalite	axial	24.7	8.68	16.03	9.45E-21	2.90E-08	1.41E-13	
IG_BH06_PS003_HC25a	Biotite granodiorite-tonalite	axial	26.6	8.91	17.64	3.89E-20	1.79E-08	5.80E-13	
IG_BH06_PS003_HC25r	Biotite granodiorite-tonalite	radial	2.666	26.4	8.85	17.50	3.71E-20	8.06E-08	5.51E-13
IG_BH06_PS003_HC61a	Biotite granodiorite-tonalite	axial	26.7	8.89	17.79	3.71E-20	7.08E-08	5.53E-13	
IG_BH06_PS004_HC25a	Biotite granodiorite-tonalite	axial	27.9	9.46	18.43	4.66E-21	7.05E-09	6.94E-14	
IG_BH06_PS004_HC25r	Biotite granodiorite-tonalite	radial	2.677	27.9	9.58	18.37	8.06E-21	1.37E-07	1.24E-13
IG_BH06_PS004_HC61a	Biotite granodiorite-tonalite	axial	27.9	9.58	18.36	8.76E-21	9.00E-08	1.31E-13	
IG_BH06_PS006_HC25a	Biotite granodiorite-tonalite	axial	29.9	8.80	21.07	8.98E-20	6.08E-08	1.35E-12	
IG_BH06_PS006_HC25r	Biotite granodiorite-tonalite	radial	2.645	29.8	8.82	20.98	4.06E-20	6.69E-08	6.04E-13
IG_BH06_PS006_HC61a	Biotite granodiorite-tonalite	axial					NPP		
IG_BH06_PS007_HC25a	Biotite granodiorite-tonalite	axial	31.6	9.31	22.26	8.15E-20	1.37E-07	1.21E-12	
IG_BH06_PS007_HC25r	Biotite granodiorite-tonalite	radial	31.3	9.30	22.04	8.30E-20	6.13E-08	1.23E-12	
IG_BH06_PS007_HC61a	Biotite granodiorite-tonalite	axial					NPP		

Table 22 Summary of hydraulic conductivity testing for test run #3 on IG_BH06.

Test ID	Lithology	Specimen Orientation	(as received) Bulk Density (g/cm ³)	Confining Stress (MPa)	Pore Pressure (MPa)	Effective Confining Stress (MPa)	Permeability (m ²)	Apparent Specific Storage (1/m)	Hydraulic Conductivity (m/s)
IG_BH06_AR011_HC25a	Feldspar-phyric tonalite	axial	2.701				NPP	NPP	NPP
IG_BH06_AR011_HC25r	Feldspar-phyric tonalite	radial					NPP	NPP	NPP
IG_BH06_AR011_HC61a	Feldspar-phyric tonalite	axial		27.1	10.2	16.9	2.30E-21	1.26E-07	3.46E-14
IG_BH06_AR056_HC25a	Feldspar-phyric tonalite	axial	2.704				NPP	NPP	NPP
IG_BH06_AR056_HC25r	Feldspar-phyric tonalite	radial					NPP	NPP	NPP
IG_BH06_AR056_HC61a	Feldspar-phyric tonalite	axial					NPP	NPP	NPP
IG_BH06_PS001_HC25a	Biotite granodiorite-tonalite	axial	2.653	25.1	9.57	15.5	2.02E-20	1.29E-07	3.02E-13
IG_BH06_PS001_HC25r	Biotite granodiorite-tonalite	radial		24.9	9.51	15.4	1.69E-20	1.11E-07	2.50E-13
IG_BH06_PS001_HC61a	Biotite granodiorite-tonalite	axial		25.2	9.61	15.6	1.41E-20	4.18E-08	2.09E-13
IG_BH06_PS002_HC25a	Biotite granodiorite-tonalite	axial	2.664	29.6	8.67	20.9	1.04E-20	7.97E-08	1.55E-13
IG_BH06_PS002_HC25r	Biotite granodiorite-tonalite	radial		29.4	8.64	20.7	6.37E-21	4.73E-09	9.46E-14
IG_BH06_PS002_HC61a	Biotite granodiorite-tonalite	axial		29.7	8.67	21.0	1.30E-20	4.75E-08	1.94E-13
IG_BH06_PS003_HC25a	Biotite granodiorite-tonalite	axial	2.666	31.5	9.30	22.2	2.65E-20	1.19E-07	3.95E-13
IG_BH06_PS003_HC25r	Biotite granodiorite-tonalite	radial		31.3	9.30	22.0	2.44E-20	1.18E-07	3.63E-13
IG_BH06_PS003_HC61a	Biotite granodiorite-tonalite	axial		31.7	9.28	22.4	2.58E-20	7.15E-08	3.84E-13
IG_BH06_PS004_HC25a	Biotite granodiorite-tonalite	axial	2.677	32.9	9.36	23.5	2.60E-21	1.04E-07	3.88E-14
IG_BH06_PS004_HC25r	Biotite granodiorite-tonalite	radial		32.9	9.23	23.7	3.35E-21	9.13E-08	5.03E-14
IG_BH06_PS004_HC61a	Biotite granodiorite-tonalite	axial		32.9	9.22	23.7	3.78E-21	8.31E-08	5.66E-14
IG_BH06_PS006_HC25a	Biotite granodiorite-tonalite	axial	2.645	34.9	8.73	26.1	3.93E-20	3.65E-08	5.91E-13
IG_BH06_PS006_HC25r	Biotite granodiorite-tonalite	radial		34.8	8.81	26.0	1.59E-20	6.60E-08	2.36E-13
IG_BH06_PS006_HC61a	Biotite granodiorite-tonalite	axial					NPP	NPP	NPP
IG_BH06_PS007_HC25a	Biotite granodiorite-tonalite	axial	2.663	36.5	9.28	27.3	3.25E-20	1.78E-07	4.85E-13
IG_BH06_PS007_HC25r	Biotite granodiorite-tonalite	radial		36.3	9.23	27.0	3.86E-20	1.13E-07	5.74E-13
IG_BH06_PS007_HC61a	Biotite granodiorite-tonalite	axial					NPP	NPP	NPP

Figure 11 to Figure 16 provide summary illustrations of how hydraulic conductivity (HC) varies between specimen size, effective confining stress, and specific borehole specimens. Within the variability of the measured hydraulic conductivities, all test specimens show a decrease in hydraulic conductivity with an increase in effective confining stress irrespective of specimen diameter or specimen orientation (axial or radial). In particular, the first hydraulic conductivity test at 15.1 MPa for the feldspar-phyric tonalite rock type is lower than the subsequent tests at higher confinement (see Figure 12), very likely due to the test specimens coming from different depths in IG_BH04 and, as noted in Figure 12, show different index properties (see also Table 6).

For tests conducted on amphibolite and feldspar-phyric tonalite, there were insufficient successful test results to indicate an overall trend regarding similarities for hydraulic conductivities. For tests conducted on biotite granodiorite-tonalite, which are the largest number of 25mm axial, 25mm radial, and 61mm axial specimens, Figure 14, Figure 15, and Figure 16 all suggest that the hydraulic conductivities of boreholes IG_BH04, IG_BH05 and IG_BH06 specimens are similar. In all cases, there is a large amount of scatter, and fitting a trend line with a good correlation coefficient per borehole or in general were not possible.

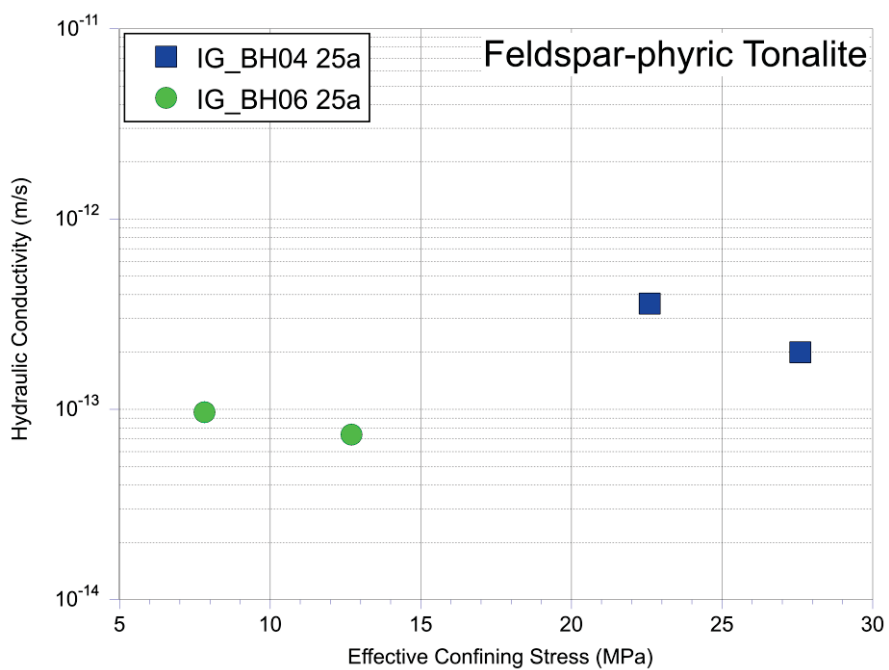


Figure 11. Variation of hydraulic conductivity of feldspar-phyric tonalite with effective confining stress for 25 mm axial specimens – all boreholes.

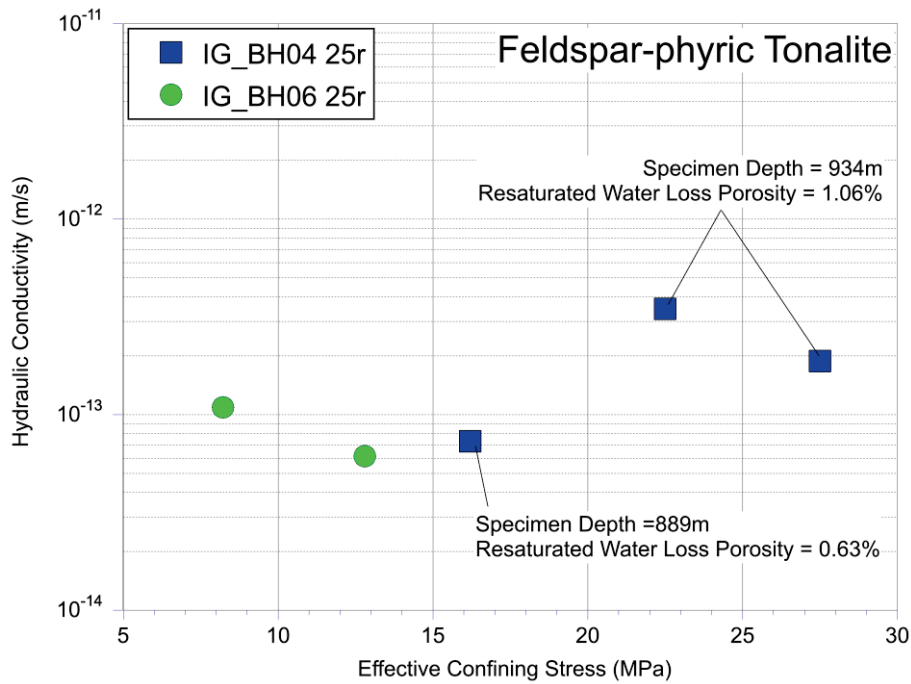


Figure 12. Variation of hydraulic conductivity of feldspar-phyric tonalite with effective confining stress for 25 mm radial specimens – all boreholes.

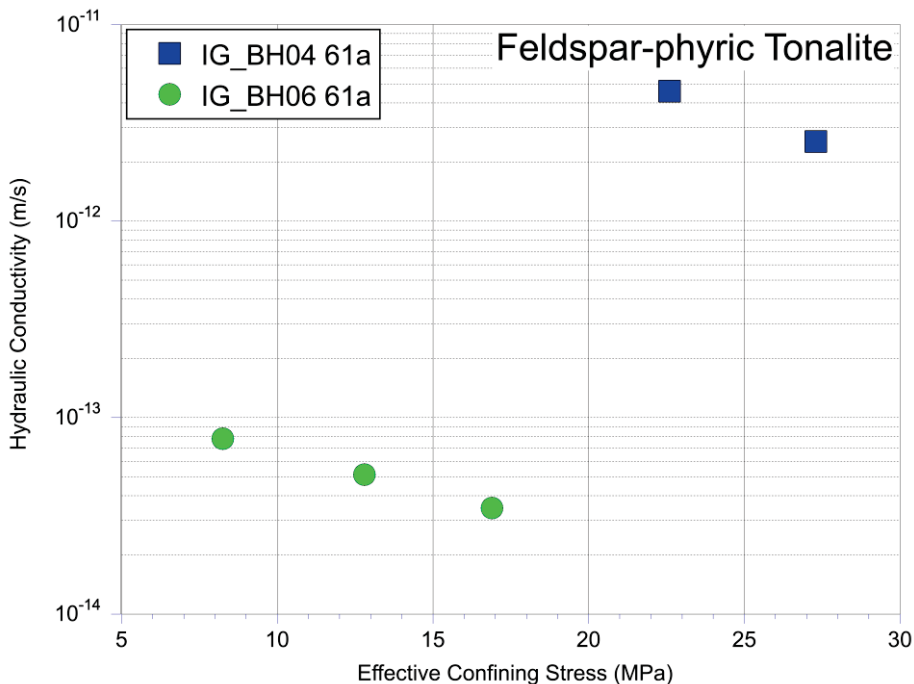


Figure 13. Variation of hydraulic conductivity of feldspar-phyric tonalite with effective confining stress for 61 mm axial specimens – all boreholes.

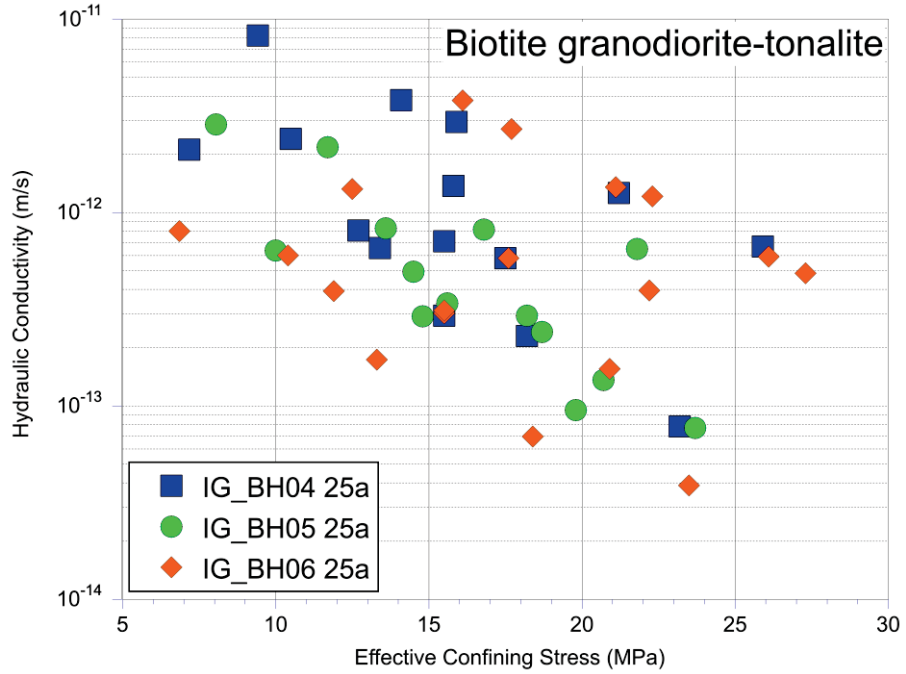


Figure 14. Variation of hydraulic conductivity of biotite granodiorite-tonalite with effective confining stress for 25 mm axial specimens – all boreholes.

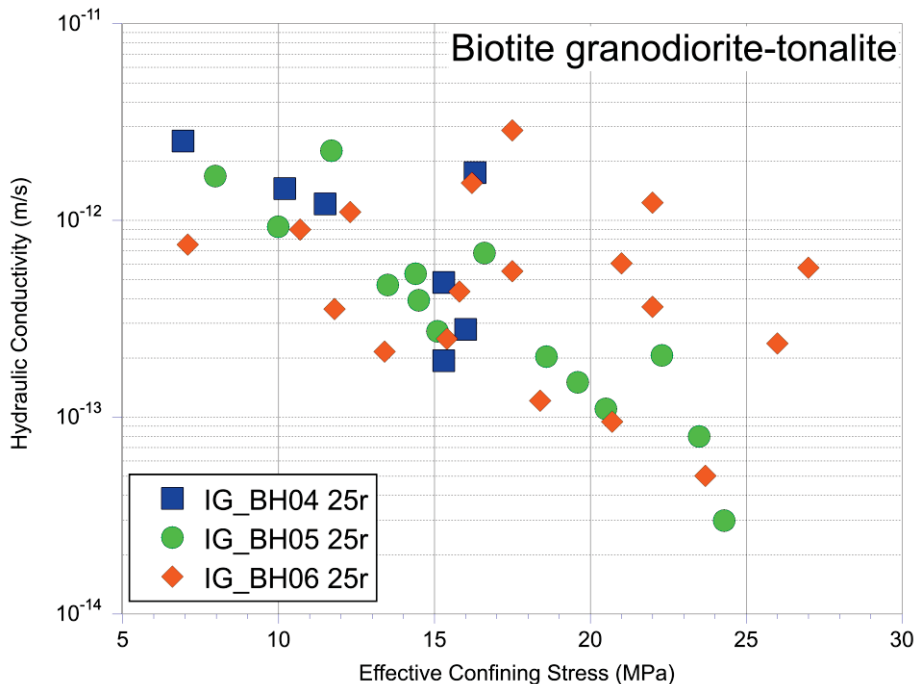


Figure 15. Variation of hydraulic conductivity of biotite granodiorite-tonalite with effective confining stress for 25 mm radial specimens – all boreholes.

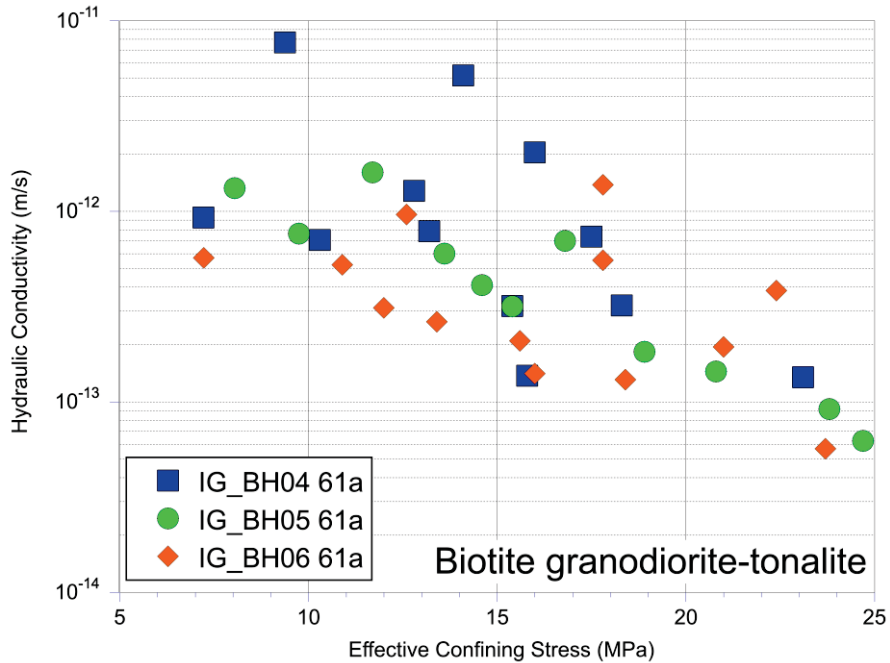


Figure 16. Variation of hydraulic conductivity of biotite granodiorite-tonalite with effective confining stress for 61 mm axial specimens – all boreholes.

4.3.1 Influence of specimen diameter on hydraulic conductivity

Figures 17, 18 and 19 illustrate the variation of hydraulic conductivity with effective confining stress for axially oriented 25mm and 61mm diameter specimens from IG_BH04, IG_BH05 and IG_BH06, respectively. Based on this data, it is reasonable to assume that specimen diameter has not significantly influenced the hydraulic conductivity measurements. The clustering that appears in the IG_BH06 results shown in Figure 19 appear to correlate with the helium porosity magnitudes measured on those specimens (see Table 8) whereby low helium porosity corresponds to a lower hydraulic conductivity. For sample group PS001, PS002 and PS004, the average helium porosity was 0.6% while for the sample group PS006 and PS007, the average helium porosity was 0.96%. Interestingly, these porosity values are inverse to depth, with the shallower (depth range from 371m to 731m) PS001, PS002 and PS004 specimens having a lower helium porosity than the deeper (depth range from 834m to 933m) PS006 and PS007 specimens.

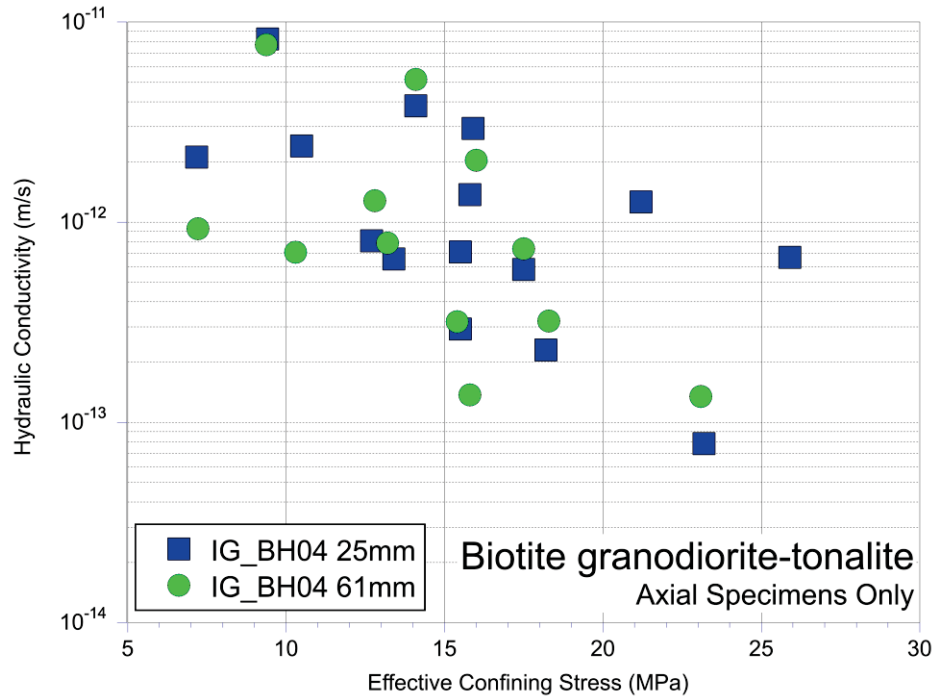


Figure 17: Specimen diameter influence on hydraulic conductivity of biotite granodiorite-tonalite for axial test specimens from borehole IG_BH04.

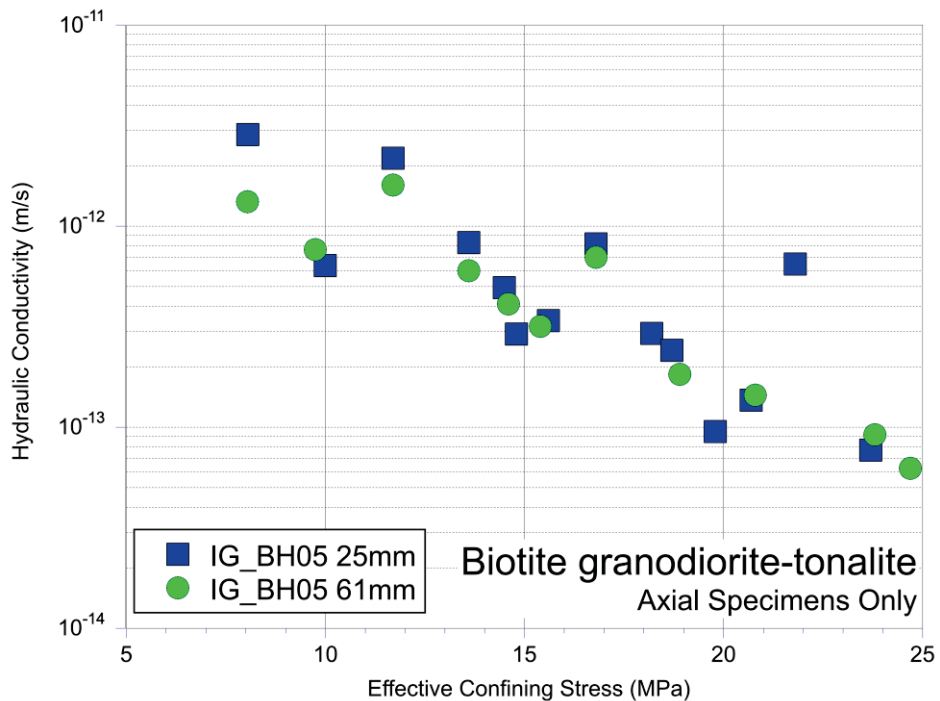


Figure 18: Specimen diameter influence on hydraulic conductivity of biotite granodiorite-tonalite for axial test specimens from borehole IG_BH05.

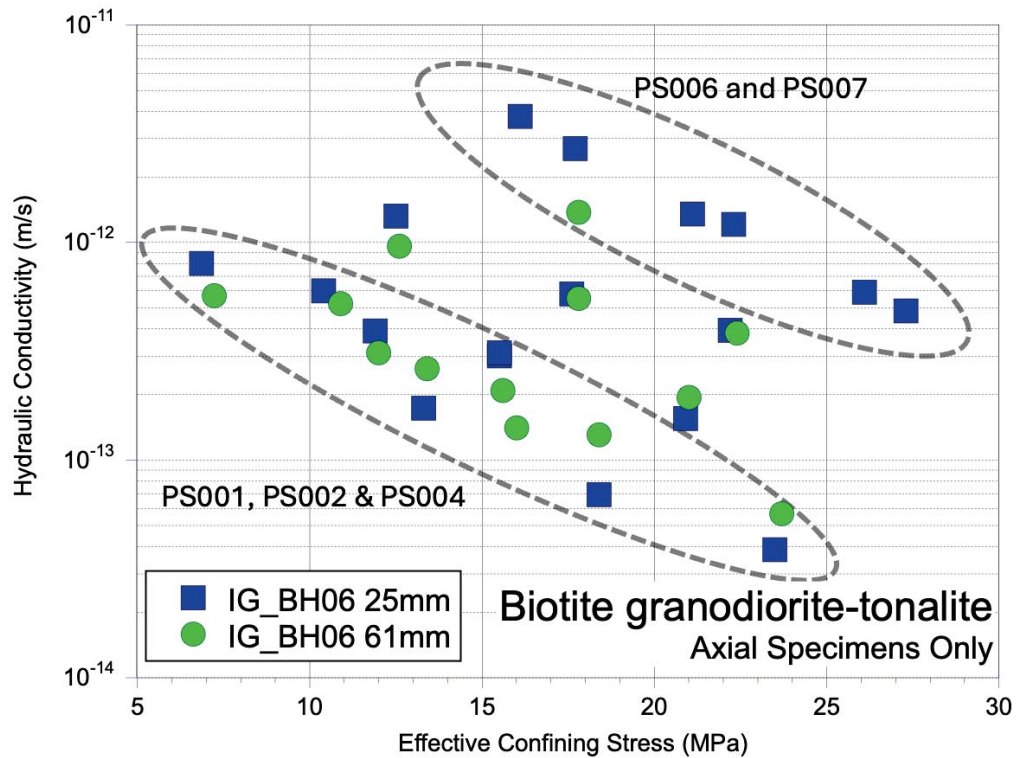


Figure 19: Specimen diameter influence on hydraulic conductivity of biotite granodiorite-tonalite for axial test specimens from IG_BH06.

4.3.2 Anisotropy in hydraulic conductivities.

Extracting the axial and radial hydraulic conductivity results for a specific sample and common effective confining stress from Tables 14 to 22 allows the potential anisotropy in hydraulic conductivity to be assessed. Note that for the inclined boreholes IG_BH04, IG_BH05, and IG_BH06, this anisotropy would be parallel and perpendicular (in no particular normal direction) to the borehole axis and not “vertical” and “horizontal” orientations.

The results for feldspar-phyric tonalite specimen anisotropy are shown in Table 23 for effective stress ranges from 8.02 to 27.5 MPa and with an anisotropy ratio ranging from 0.88 to 1.20.

Table 24 provides the anisotropy ratio for biotite granodiorite-tonalite from IG_BH04 for effective stress ranges from 7.06 to 16.43 MPa and with an anisotropy ratio ranging from 0.55 to 3.68.

Table 25 provides the anisotropy ratio for biotite granodiorite-tonalite from IG_BH05 for effective stress ranges from 8.01 to 23.57 MPa and with an anisotropy ratio ranging from 0.64 to 3.15.

Table 26 provides the anisotropy ratio for biotite granodiorite-tonalite from IG_BH06 for effective stress ranges from 6.97 to 27.15 MPa and with an anisotropy ratio ranging from 0.57 to 2.50.

Table 23. Hydraulic conductivity anisotropy for 25 mm feldspar-phyric tonalite specimens from all boreholes.

Sample	Average Effective Stress (MPa)	Hydraulic Conductivity Anisotropy Ratio (axial/radial)
IG_BH04_PS011	22.6	1.03
IG_BH04_PS011	27.5	1.06
IG_BH06_AR011	8.02	0.88
IG_BH06_AR011	12.8	1.20

Table 24. Hydraulic conductivity anisotropy for 25 mm biotite granodiorite-tonalite specimens from IG_BH04.

Sample	Average Effective Stress (MPa)	Hydraulic Conductivity Anisotropy Ratio (axial/radial)
IG_BH04_PS003	7.06	0.83
IG_BH04_PS003	12.14	0.67
IG_BH04_PS003	15.77	1.05
IG_BH04_PS005	8.60	0.55
IG_BH04_PS005	11.68	0.31
IG_BH04_PS005	16.07	0.78
IG_BH04_PS006	10.34	1.66
IG_BH04_PS006	15.37	3.68
IG_BH04_PS006	16.43	1.20

Table 25 Hydraulic conductivity anisotropy for 25 mm biotite granodiorite-tonalite specimens from IG_BH05.

Sample	Average Effective Stress (MPa)	Hydraulic Conductivity Anisotropy Ratio (axial/radial)
IG_BH05_PS002	8.01	1.70
IG_BH05_PS002	13.53	1.77
IG_BH05_PS003	10.02	0.69
IG_BH05_PS003	14.66	0.74
IG_BH05_PS003	19.68	0.64
IG_BH05_PS004	11.66	0.96
IG_BH05_PS004	16.69	1.20
IG_BH05_PS004	22.07	3.15
IG_BH05_PS005	14.44	0.92
IG_BH05_PS005	18.65	1.19
IG_BH05_PS005	23.57	0.96
IG_BH05_PS006	15.34	1.24
IG_BH05_PS006	20.56	1.24

Table 26 Hydraulic conductivity anisotropy for 25 mm biotite granodiorite-tonalite specimens from IG_BH06.

Sample	Average Effective Stress (MPa)	Hydraulic Conductivity Anisotropy Ratio (axial/radial)
IG_BH06_PS001	6.97	1.07
IG_BH06_PS001	11.87	1.11
IG_BH06_PS001	15.45	1.21
IG_BH06_PS002	10.55	0.67
IG_BH06_PS002	15.64	0.71
IG_BH06_PS002	20.81	1.64
IG_BH06_PS003	12.40	1.20
IG_BH06_PS003	17.57	1.05
IG_BH06_PS003	22.12	1.09
IG_BH06_PS004	13.34	0.80
IG_BH06_PS004	18.40	0.57
IG_BH06_PS004	23.61	0.77
IG_BH06_PS006	16.13	2.45
IG_BH06_PS006	21.02	2.24
IG_BH06_PS006	26.05	2.50
IG_BH06_PS007	17.61	0.94
IG_BH06_PS007	22.15	0.98
IG_BH06_PS007	27.15	0.84

Figure 20 shows that the hydraulic conductivity anisotropy ratio for 25 mm feldspar-phyric tonalite specimens from boreholes IG_BH04 and IG_BH06 is approximately unity, suggesting a relatively uniform permeability tensor. Figure 21, Figure 22, and Figure 23 show the hydraulic conductivity anisotropy ratio for 25 mm biotite granodiorite-tonalite specimens from boreholes IG_BH04, IG_BH05, and IG_BH06, respectively. The anisotropy ratio does seem to remain relatively consistent with varying effective confining stress even though the magnitude of hydraulic conductivity decreases with an increase in effective confining stress on the specimens. This would tend to indicate that the mechanism leading to a reduction in hydraulic conductivity may be related more to pore volume reduction rather than to fracture aperture reduction, where crack closure would likely respond more anisotropically to changes in effective confining stress. No specific testing was conducted to support this hypothesis.

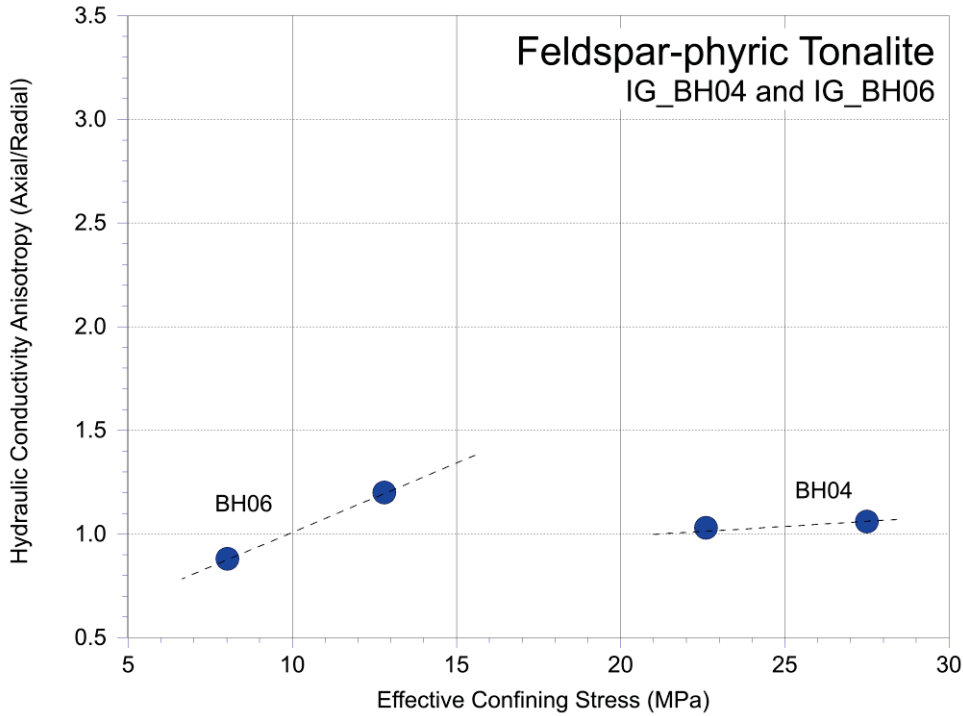


Figure 20: Hydraulic conductivity anisotropy of feldspar-phyric tonalite for 25 mm test specimens from borehole IG_BH04 and IG_BH06.

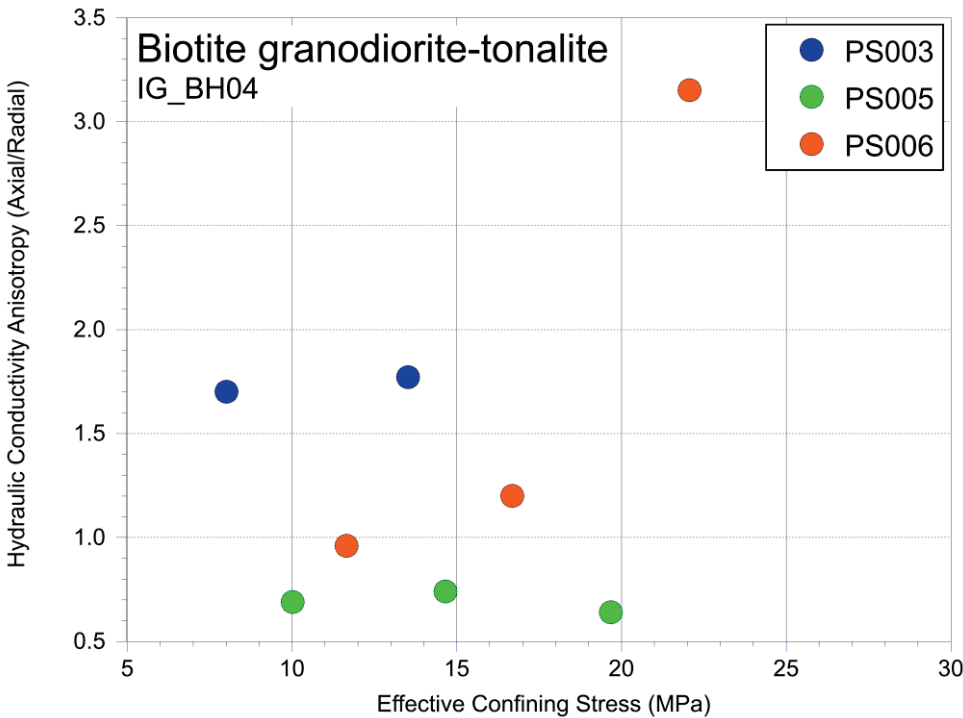


Figure 21: Hydraulic conductivity anisotropy of biotite granodiorite-tonalite for 25 mm test specimens from borehole IG_BH04.

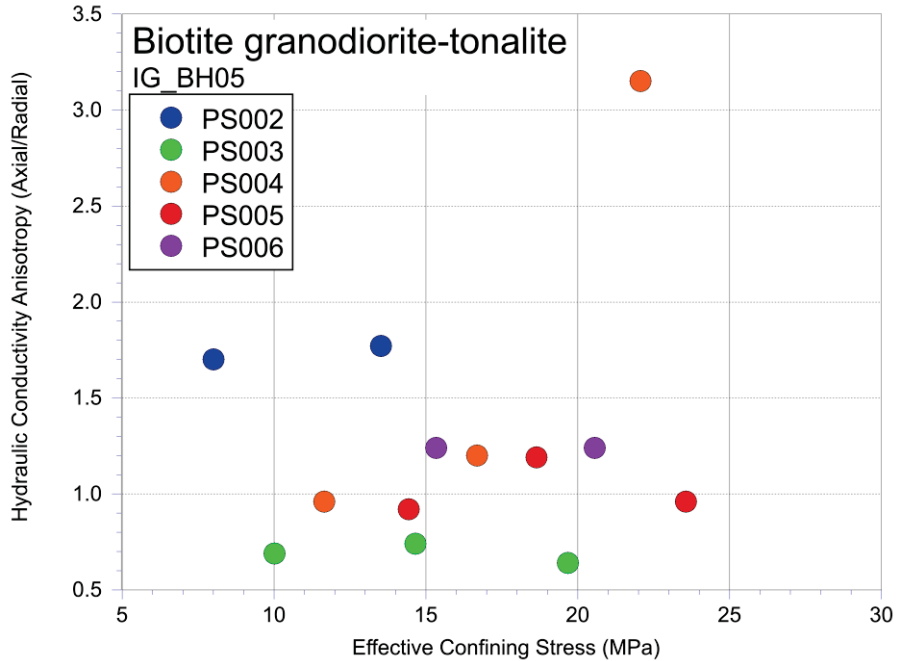


Figure 22: Hydraulic conductivity anisotropy of biotite granodiorite-tonalite for 25 mm test specimens from borehole IG_BH05.

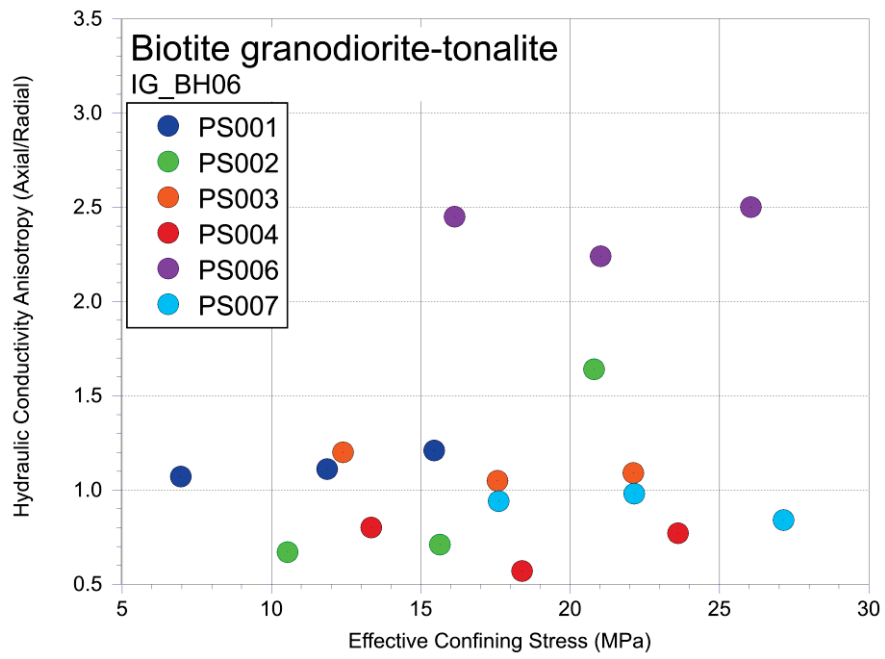


Figure 23: Hydraulic conductivity anisotropy of biotite granodiorite-tonalite for 25 mm test specimens from IG_BH06.

4.4 Specific Storage Obtained from Hydraulic Conductivity Testing

The analysis of the pulse decay hydraulic conductivity test results using Hsieh et al. (1981) method, as discussed in § 3.4.3, provides not only a solution for hydraulic conductivity but also a determination of the specific storage, S_s , of the specimen. GeoREF adopted this approach because the additional constraint of matching the pulse decay response to both hydraulic conductivity and specific storage provides a better estimate of hydraulic conductivity. However, there is less certainty around the value of specific storage determined for the test specimen because of several factors that can affect this parameter, such as test system compressibility and the upstream and downstream reservoir storage volumes. These factors are discussed in more detail in § 5.3.3, but due to these factors, GeoREF will refer to the specific storage determined through the hydraulic testing as an “apparent” specific storage, AS_s , in this report to ensure the reader is aware of the limitations noted in § 5.3.3.

The AS_s variability for feldspar-phyric tonalite from the 25 mm axial, 25 mm radial, and 61 mm axial specimens are shown in Figure 24, Figure 25, and Figure 26, respectively. The AS_s variability for biotite granodiorite-tonalite from the 25 mm axial, 25 mm radial, and 61 mm axial specimens are shown in Figure 27, Figure 28, and Figure 29, respectively.

In spite of the very limited data for the feldspar-phyric tonalite rock type, results from this program suggest a uniform apparent specific storage value in the range of $1 \times 10^{-7} \text{ m}^{-1}$ to $2 \times 10^{-7} \text{ m}^{-1}$. Results from the biotite granodiorite-tonalite lithology suggests a mild sensitivity to effective confining stress, but given the scatter of the data, it is not possible to establish a robust relationship. The results from this program suggest a uniform apparent specific storage value in the range of $8 \times 10^{-8} \text{ m}^{-1}$ to $9 \times 10^{-8} \text{ m}^{-1}$.

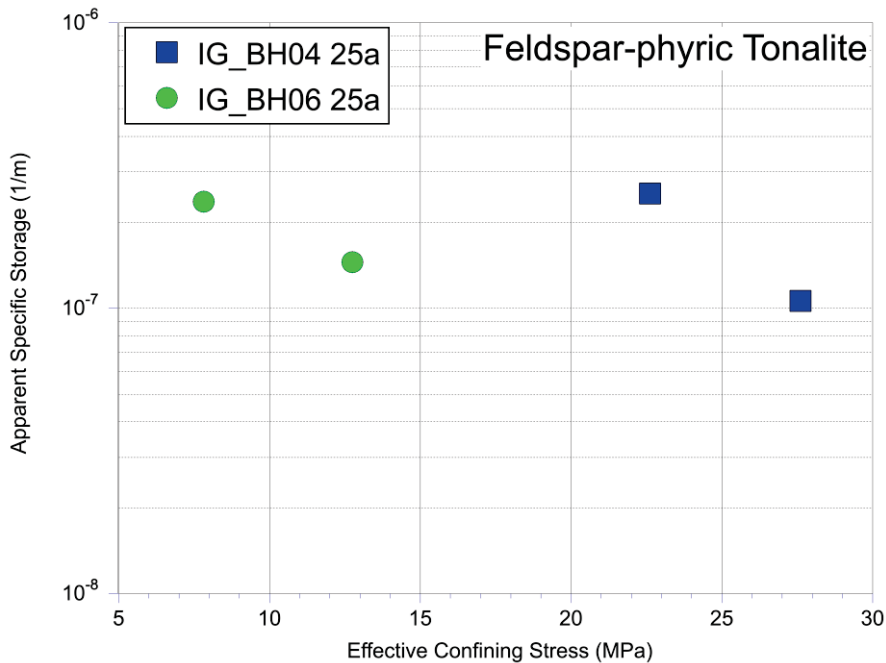


Figure 24. Variation of apparent specific storage of feldspar-phyric tonalite with effective stress for 25 mm axial specimens – all boreholes.

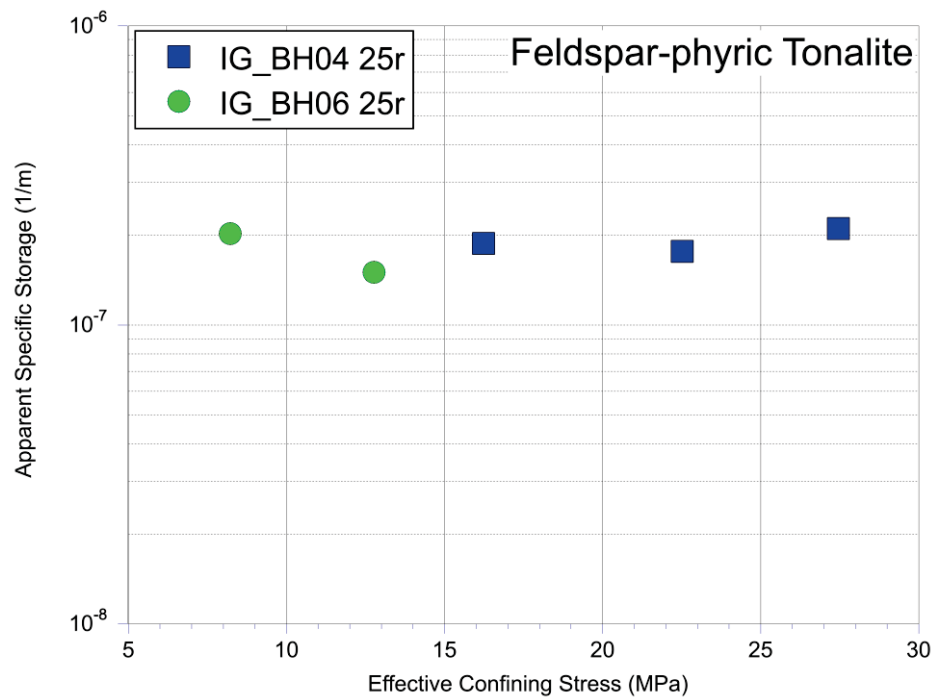


Figure 25. Variation of apparent specific storage of feldspar-phyric tonalite with effective stress for 25 mm radial specimens – all boreholes.

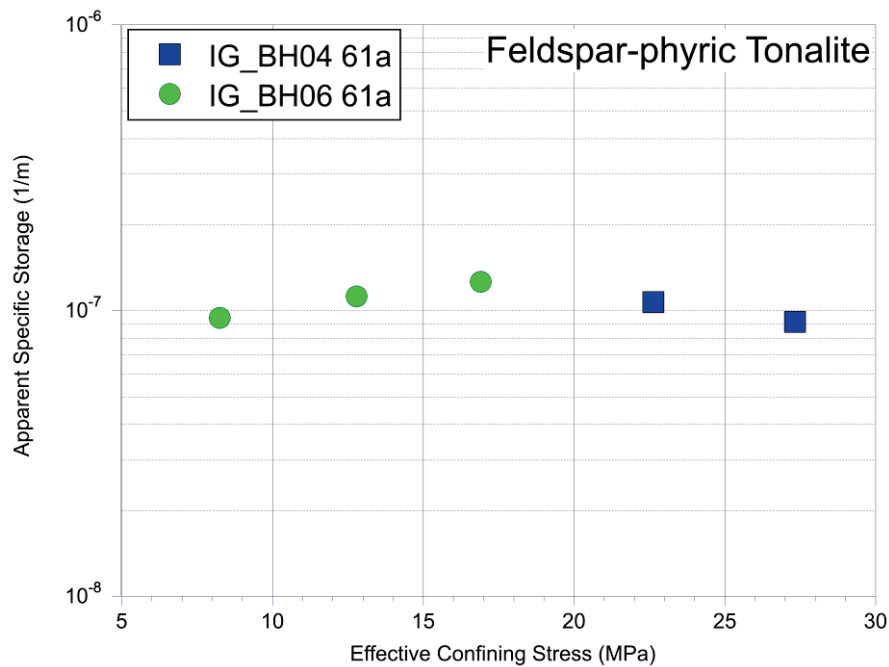


Figure 26. Variation of apparent specific storage of feldspar-phyric tonalite with effective stress for 61 mm axial specimens – all boreholes.

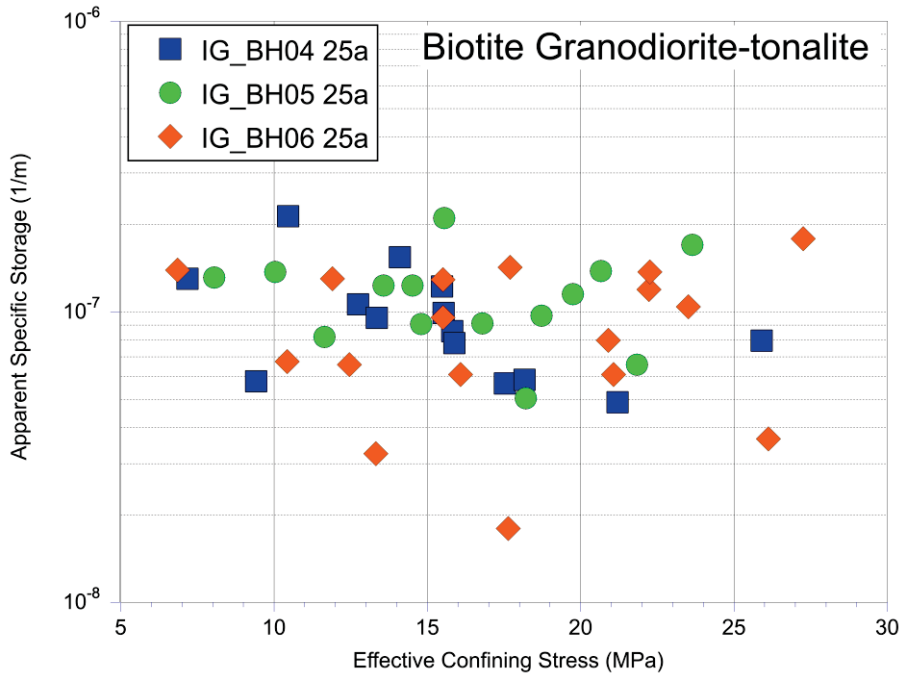


Figure 27. Variation of apparent specific storage of biotite granodiorite-tonalite with effective stress for 25 mm axial specimens – all boreholes.

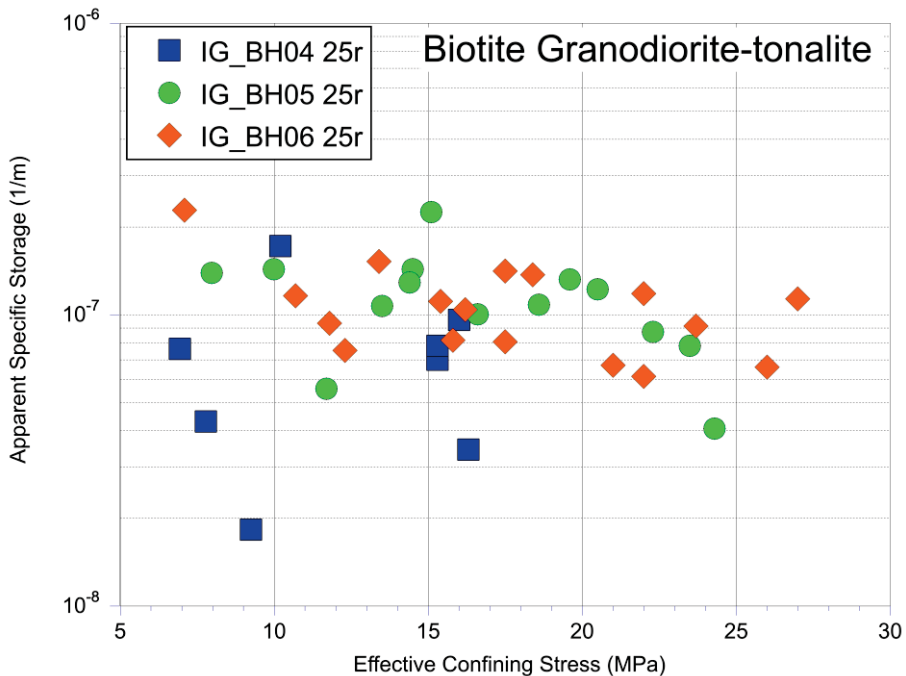


Figure 28. Variation of apparent specific storage of biotite granodiorite-tonalite with effective stress for 25 mm radial specimens – all boreholes.

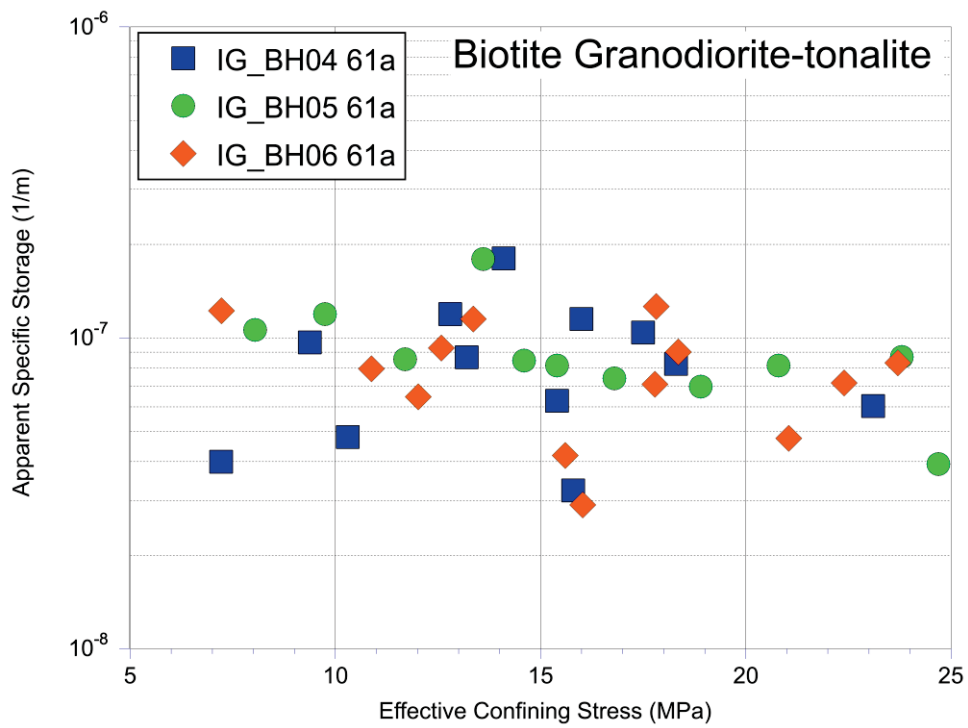


Figure 29. Variation of apparent specific storage of biotite granodiorite-tonalite with effective stress for 61 mm axial specimens – all boreholes.

5. Data Quality- Uncertainties and Limitations

5.1 Introduction

The pore volume and water content of the specimens tested in this program were extremely low. As a result, there are several experimental challenges that may impact the uncertainty of the measured parameters.

5.2 Index Testing

5.2.1 General Specimen Preparation

The order of specimen preparation may impact each specimen's quality. For example, if the axial specimen was cut first, it may induce stress relief in the radial specimen, potentially causing additional porosity /permeability changes (i.e., core disturbance). Additionally, if coring rates were increased during the specimen preparation process, micro damage due to heating may cause an increase in porosity / permeability, which may not occur in other specimens. Each of these items would not be systematic errors. Additional permeability alterations may occur when the wet (water) saw was used to cut the ends of the specimens. This process may produce fine particles that could invade the pore spaces at the ends of the specimen as well as induce localized microfracturing along the face of the cut surface. Given the extremely small pore spaces of the crystalline rocks and the continual flushing during cutting, it is likely that fines plugging will not have a large impact on HC or SSG test results.

5.2.2 Specimen orientation

Since all three boreholes (IG_BH04, IG_05, and IG_06) were inclined and specimen orientations were not identified, it is very likely that radially oriented specimens (relative to axis of borehole) would have been prepared in highly variable directions. Consequently, the results presented in §4.3.2 regarding hydraulic conductivity anisotropy should be interpreted with caution.

5.2.3 Uncertainty in As-Received (Natural Conditions) Density

The uncertainties in the measurement of the natural state mass (M_{nat}) occurred due to challenges maintaining specimen moisture content during preparation. All specimens were prepared using water to cool the core barrel and diamond saw. In general, a 25 mm diameter specimen took approximately 90 mins to create a cylinder and 10 min to cut the ends to be parallel. Over this time interval, there is the potential that a very small amount of water may be added to the specimen, through imbibition or direct injection processes, increasing the M_{nat} . Because the specimens were of very low permeability and porosity, it is likely the volume of water would be extremely low and for the equipment utilized in this resting program would be nearly unquantifiable.

5.2.4 Uncertainty in Dimension Measurements

Dimensions were measured with a high precision Mitutoyo caliper, accurate to 0.01 mm. The uncertainty around the length and diameter measurements are minimal; however, the assumption that the specimen is a perfect right cylinder is not valid. The specimen volume (V) was calculated from an average of 10 caliper readings for each dimension using the following relationship:

$$V = \frac{\pi d^2 L}{4}$$

The specimen preparation procedure may have led to several conditions which impact the perfect volume assumption, including:

- Small chipping of the top or bottom edges of the cylinder
- Small grains falling off the side of the specimen
- Ends may not be perfectly parallel

In each case, the true total volume of the specimen would be less than the calculated perfect volume. This less than perfect volume would lead to a lower mass (M), therefore, the as-received, natural state bulk density would be lower than expected (calculated by):

$$\rho_{\text{bulk,nat}} = \frac{M_{\text{nat}}}{V}$$

This error would hold true for any measurement or calculation that relies on the volume (V) of the specimen (e.g., porosity).

5.2.5 Uncertainty in Water Content and Dry Bulk Density

The measurement of the as-received water content of the specimens were recorded to the nearest 0.01%. Drying to a constant mass (M_{dry}) was achieved by measurement of the sample mass twice a week for 4 weeks until the change in mass from one measurement to the next was less than 0.01% of the initial sample mass. This water content measurement relies only on the mass of the specimens and on removing all of the water from the specimen to get a constant dry mass. Uncertainties or errors that may occur in the measurement include:

- Even though the drying meets the procedural requirements of change in mass from one measurement to the next, all water may not be removed due to the ultra-low permeability / porosity of the specimens, thus increasing M_{dry} .

And while GeoREF minimized the following impacts through the careful storage of specimens, additional dry mass measurement errors may occur if:

- a specimen is left in the atmosphere prior to measuring, it may collect enough moisture to impact the measurement, increasing M_{dry} , or
- a specimen is not allowed to cool to atmospheric conditions, convection from the specimen to atmosphere will create a buoyancy effect, decreasing M_{dry} .

Therefore, the water content by mass (ω_{mass}) (or gravimetric method) and the water content by volume (ω_{vol}) may be incorrect / biased in an increasing or a decreasing manner, as calculated by:

$$\omega_{mass} = \frac{M_{nat} - M_{dry}}{M_{dry}} (100\%)$$

and

$$\omega_{vol} = \frac{M_{nat} - M_{dry}}{\rho_{water} V} (100\%)$$

The dry density was calculate using M_{dry} and V ; therefore, the uncertainty in V as listed above and M_{dry} would create uncertainty in the $\rho_{bulk,dry}$ measurement (increasing or decreasing).

5.2.6 Uncertainty in Water Saturated Bulk Density and Water Loss Porosity

For the procedures outlined in §3.2.3, the uncertainties in this saturation procedure are similar to those associated with the dry mass measurement, including:

- If the specimen is left in the atmosphere prior to measuring, it may lose enough moisture to impact the measurement, decreasing M_{sat} .
- The surface drying of the specimen is arbitrary and difficult to recreate the same specimen surface conditions from one measurement or specimen to the next. When dealing with small specimens this would impact results more than larger specimens, increasing M_{sat} .
- Even though the saturation methods meet the procedural requirements of change in mass from one measurement to the next, all the connected pore spaces may not be saturated due to the ultra-low permeability / porosity of the specimens, decreasing M_{sat} .

The connected water loss porosity (ϕ_{WL}) and saturated bulk density ($\rho_{bulk,sat}$) were calculated with M_{sat} , M_{dry} , and V . Therefore, the calculated value will not have systematic uncertainties, that is, it will be always higher or always lower than the ideal value.

5.2.7 Uncertainties in Total Porosity (from Grain Density)

The total porosity is obtained by means of the results of grain density obtained from water pycnometry. In the grain density measurement (ASTM D485-14), a portion of the specimen is crushed and particles that pass the 4.75-mm (No. 4) sieve are dried to get a mass measurement, then corrected for temperature. In each step, additional mass may be imbibed in the specimen from the atmosphere. For example, the crushed grains may not have been completely dry when the mass was measured. Incomplete drying may result from crushed grains imbibing moisture from the air if they are left for a very short period (even as short as 10 seconds) in the atmosphere. Temperature correction values if not computed for the right temperature (variations as small as 0.1°C) cause a small change in the mass.

The total porosity from grain density is also a function of the dry density, which will undergo similar issues during measurement. For example, the specimen may not be a perfect right cylinder; therefore, the volume measurement may not be as precise. The specimen may have lost a small grain from the edge, which would alter the dry mass. The specimen may also have collected moisture in the same fashion as the crushed grain simply by sitting in the atmosphere after drying and before being weighed. As well, even after oven-drying to the specification set

out in this testing program which exceeds the ASTM requirements, small amounts of water may still be present, not giving the true dry mass.

5.2.8 Uncertainties in Helium Porosimetry

Helium porosity (ϕ_{He}) was measured on dry samples based on Boyle's law of gas expansion using helium gas. The specimens were assumed to be completely dry prior to measurement; however, the same issues surrounding a completely dry specimen discussed above persist here. Therefore, if the specimen was not completely dry, pore space access may be taken up or blocked by water, thereby, helium would not penetrate all the connected pores. Additionally, while the device measures the solid volume (V_s) based on connected pore volume, the connected Helium porosity (ϕ_{He}) is calculated by:

$$\phi_{He} = \frac{V - V_s}{V} (100\%)$$

Therefore, the assumption of a perfect volume (V) may not be true (as discussed above).

5.2.9 Total porosity vs. He porosity

When comparing the results from each method, total porosity is expected to be higher than He porosity, given that the former comprises the measurement of both connected and unconnected pore spaces. However, many uncontrollable errors may occur when dealing with small values and with calculations that rely on the full precision of the instruments but fall within the requirements of the device calibrations/precision required by the ASTM standards.

For the He porosity measurement, the main source of error could be the measurement of the specimen volume used to calculate He porosity, as noted above. Additionally, He porosity measurement are ideally completed on dry specimens, but if the specimens were exposed to ambient conditions in the lab the specimens may collect moisture which could impede helium penetration into the specimen.

A third, more general explanation for differences between the results, is that the He porosity and grain density measurements (used to compute total porosity) were completed on specimens from different locations (i.e., top or bottom) of the same core sample. These slight changes in location could account for differences that could be higher or lower between the two measurement types, as illustrated in Figure 30.

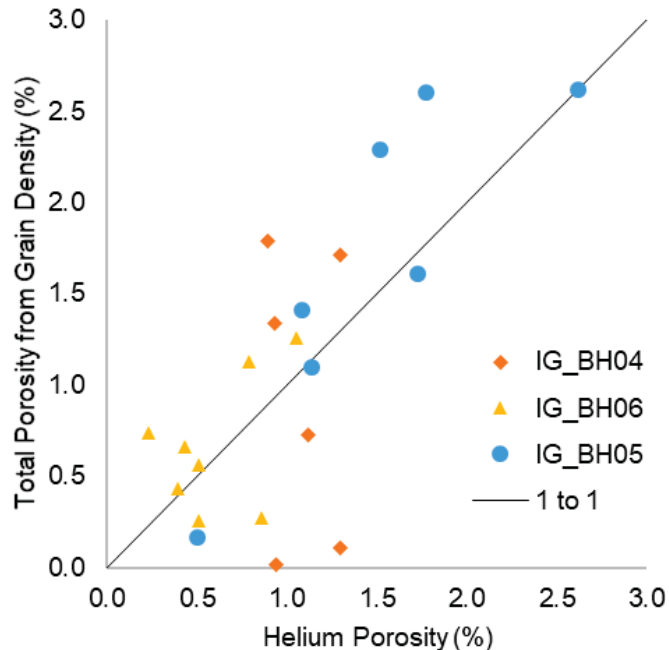


Figure 30. Total porosity from grain density versus He porosity.

5.2.10 Sensitivity of porosity measurements based on grain density

The accepted Test Plan document outlines the procedures for determining specimen dimensions, re-saturated bulk density, bulk dry density, as-received water content, re-saturated water content, as-received water loss porosity, re-saturated water loss porosity, grain density, helium porosity, and total porosity. Over the course of the test program, water loss porosity, computed using the test plan procedures, was larger than the helium porosity for some specimens (see Figure 31), which is unexpected since water loss porosity should reflect some volume of water remaining in the pore spaces.

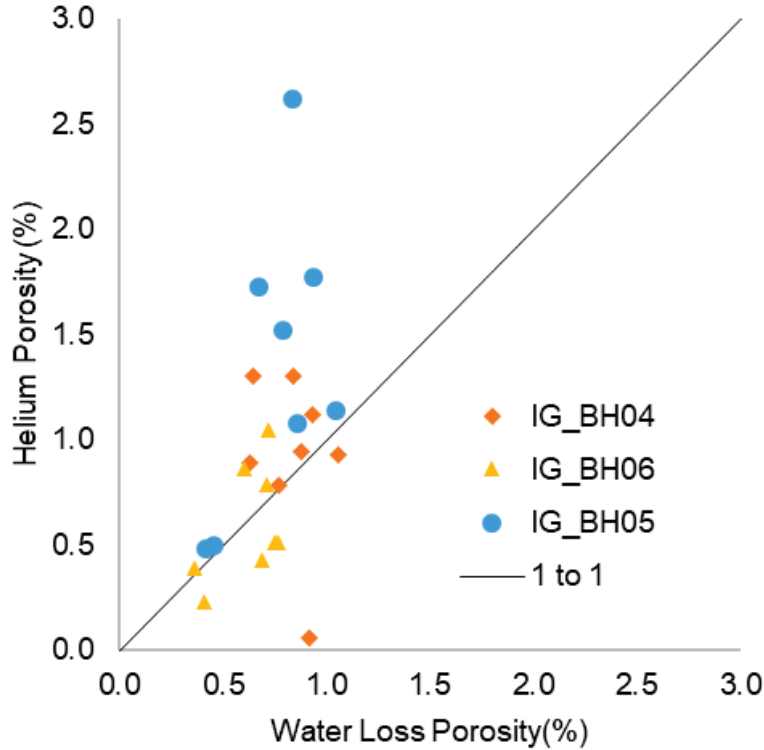


Figure 31. Comparison of He and water loss porosity.

To better understand the potential reasons for this discrepancy, the calculation procedure for water loss porosity was reviewed. The following provides an example calculation of the volume of water required to create a 0.001 change in water loss porosity.

Recall from §3.2.4 that water loss porosity is computed by:

$$\phi_{WL,rs} = \frac{M_{rs} - M_{dry}}{\rho_{water}} \frac{1}{V} (100\%)$$

Rearranging this equation provides the following expression for the change in the mass of water:

$$M_{rs} - M_{dry} = (\rho_{water}) \frac{\pi d^2 L}{4} (\phi_{WL,rs}) = \Delta M$$

Each of the test specimens had the following dimensions:

$$D = 2.5 \text{ cm}$$

$$L = 2.5 \text{ cm.}$$

Assuming a water density of 1 g/cm³ with a unit conversion of 1mL/g, the following volume of water needed to shift the water loss porosity by 0.001 units (or 0.1%) can be computed.

$$\Delta M = (\rho_{water}) \frac{\pi d^2 L}{4} (\phi_{WL,rs})$$

$$= \left(1 \frac{g}{cm^3}\right) \frac{\pi (2.5cm)(2.5cm)(2.5cm)}{4} (0.001)(1mL/g)$$

$$= 0.001227mL \text{ or } 1.23 \mu L$$

1.23 μL of water is a very small volume and, consequently, for a specimen which already has very low porosity, it may be difficult to ensure the specimen was consistently dried removing only surface water. If the specimen was left in the air for too long during the saturation mass measurement step, water may have evaporated prior to measurement. Therefore, for specimens with very low porosity, the error in water loss porosity and porosity derived from grain density is more susceptible to error as each of these techniques require the drying and mass measurement of the rock or rock particles.

5.3 Hydraulic Conductivity Testing Results

The transient pulse decay technique under confined conditions was used to measure hydraulic conductivity. The test required several conditions to be met to complete a successful test, which included:

- Adiabatic conditions during the application and decay of the pulse,
- No leaks in the upstream and downstream reservoir through fittings,
- No leaks between the specimen and confining fluid through the membrane,
- An elastic response of the specimen (i.e., no time dependent deformation),
- No chemical reactions between the specimen and pore fluid,
- The pressure in the specimen is in equilibrium prior to application of the pulse (no residual transients),
- A homogenous specimen, and
- 100% water saturation.

In all cases, the pulse decay test was valid until the integrity of the experimental conditions violated the requirements of for the analytical Hsieh solution (Figure 2).

The most difficult conditions to control in GeoREF laboratory during the hydraulic conductivity (HC) testing, and the ones which had the greatest impact on executing a successful test, were leaks through fittings or the membrane and temperature. For each of these conditions, the impact of leaks and temperature were easily identified and resulted in two scenarios:

- The test was stopped, and sufficient collected data was used for analysis, or
- The test was repeated by disassembly of the system and remounting and testing.

During the execution of the test, very small changes in ambient temperature that may occur - on the order of $\pm 0.01 ^\circ C$ - would cause changes in the upstream and downstream reservoir pressures due to undrained thermal volume changes in the upstream and downstream

reservoirs. These temperature changes can also impact specimen pore volumes, but this is less significant than the pressure changes in the fluid lines of the experimental system.

A signature of the impact of temperature was the upstream and downstream pressure fluctuating/shifting in the same directions and could be caused by as little as 0.01°C change in conditions. This usually occurred for pulse tests that lasted longer than ~ 12 hrs and was a product of the ambient laboratory conditions.

Leaks in the test were identified by one of the following:

- The upstream pulse pressure increasing away from the ideal equilibrium position.
- The downstream pulse pressure increasing away from the ideal equilibrium position.
- Both upstream and downstream pulse pressure increasing away from the equilibrium position. This appears similar to a temperature change; however, only increases occur and do not fluctuate.

The following remaining requirements/conditions of the test can have an impact on the pulse making it difficult to identify:

- If there were time-dependent responses (i.e., creep), the pore structure may be changing generating an additionally transient inside of the specimen.
- A chemical reaction between the specimen and the pore fluid may cause an additional transient in the specimen.
- When moving from one effective stress to the next effective stress testing condition, the increase in stress may cause transients in the specimen (poro-elastic effects) which may not fully dissipate prior to the application of the next pulse.
- The requirement of specimen homogeneity is almost always violated as it is a purely theoretical condition, and it is difficult to understand how it would impact the applied pulse.
- 100% water saturation is required for the theoretical analysis and every effort was used to achieve this; however, if the specimen was not 100% saturated the response would be a component of the specific storage of the solution.

During the testing program, there were discussions concerning running the pulse decay test for significantly longer testing times than what had been adopted in the testing program. Practically, without consideration to testing schedules, this would be possible if very tight controls could be maintained on temperature and if elevated pressures over long periods did not lead to leaks. Modifications to the testing environment following the completion of the current IG_BH04-06 testing program has provided significant improvements for temperature control, but the occurrence of very small leaks over very long test times remains a challenge. For example, for this class of materials (i.e., granitic rocks), the membrane permeability can be on the same order as the specimen permeability, thus distinguishing specimen hydraulic conductivity during the pulse decay in this situation is challenging.

5.3.1 Anisotropy Limitations

One objective of the testing program was the assessment of axial to radial anisotropy of hydraulic conductivity. Unfortunately, the orientation of the core samples in the inclined

boreholes was not provided. This orientation would have provided an opportunity to transform the measured hydraulic conductivities to similar orientations between all the boreholes. The reader is cautioned that anisotropy values presented in this report are approximate and likely do not reflect the actual in-situ anisotropy for any of the boreholes sampled.

5.3.2 Errors or uncertainties in the fitting of the solution

The analysis of the specimen pulse decay response used the fitting of the analytical Hsieh et al. (1981) solution to simultaneously fit the specific storage and the hydraulic conductivity. The requirements of the solution fitting were:

- Measurement of the upstream and downstream pressure response through calibrated pressure transducers.
- Identification of the pulse initiation in the logged data.
- Calculation/look up of the water properties (density and viscosity).
- Specimen area and length.
- Measurements of upstream and downstream reservoir storage.

5.3.2.1 The measurement of the upstream and downstream pressure response

The measurement of the upstream and downstream reservoir pressures used precision-calibrated pressure transducers, capable of measuring over the full range of the pressures in the pulse test from 0 to 10,000 kPa. The full range of these transducers were 30,000 kPa and the precision was $\pm 0.08\%$, therefore there will always be an error associated with the precision of the instrument and the exact value. However, prior to application of the transient pulse, the top and bottom reservoirs were connected to each other through a bypass. This allowed the pressure transducers to be zeroed to each other for the pulse application. This zeroing to each other allowed for the final pressure equilibrium to be within ~ 1 kPa for all the testing.

5.3.2.2 Identification of the pulse initiation

The logging system used in the pulse decay system was set to record data at 5 second intervals. Every effort was made to initiate the pulse at the exact moment the pulse was initiated; however, this was not always possible. Therefore, the pulse may have partially decayed in the 5 second interval prior to the logger capturing the data. This would adjust the start time of the pulse analysis. An offset condition was added to the fitting of the Hsieh solution Excel implementation to account for this case; however, this small timing issue had nearly no impact on the solution.

5.3.2.3 Water Properties (density and viscosity)

The DI water properties were calculated based on the pressure and temperature measured in the system at the start of the pulse test. These properties are accurate and precise, thereby they did not contribute to errors in the pulse decay solution.

5.3.2.4 Specimen Area and Length

For the solution, the length and area of the specimen were precise. The issues surrounding the volume of the specimen discussed above (minor chips from the edges of the specimen) have no impact on the solution of the pulse decay equation.

5.3.2.5 Measurement of the Upstream and Downstream Reservoir Storage

The measurement of the upstream and downstream reservoir storage was the most difficult component of the solution to determine. The procedure for such measurement followed the procedure outlined by Brace et al (1968), which is required for the Hsieh solution to fit the Specific Storage and Hydraulic conductivity theoretical solutions. The components of the upstream and downstream reservoir storage were:

- upstream and downstream valve ball.
- upstream and downstream transducer diaphragm.
- bypass valve ball.
- upstream and downstream porous stones.
- the membrane around specimen.
- pore fluid lines between platens and valves.
- The overall upstream and downstream dead volumes.

Each of these items deform as the pulse is applied, and the deformation is dependent on the size of the pulse and the pore pressure at the time of testing. Additionally, if a new porous stone is added, it will not deform in a similar manner to the previous pore stone. Therefore, the stress history of the porous stone may impact the reservoir storages.

The closer the dead volumes are to the pore volumes of the specimens, the faster the pulse will decay, and thereby less chances of leaks or temperature impacting the testing. In the experimental configuration used here, the dead volumes were ~10-20 mL.

5.3.3 Specific Storage Determination

From above, the biggest uncertainty is the impact of the uncertainty in the upstream and downstream reservoir storage values. These values are used directly to simultaneously fit the permeability and the specific storage solution to the pulse data from the specimen. Therefore, both the specific storage of the specimen and the upstream and downstream reservoir storage are treated as a system in the solution, and it is very difficult to confidently separate the specimen specific storage from the upstream and downstream reservoir storage (S_s appears in α and β).

$$\frac{P(x,t)}{\Delta P_0} = \frac{1}{1 + \beta + \gamma} + 2 \sum_{m=0}^{\infty} \frac{\exp \exp (-\alpha \phi_m^2) \left[\cos \phi_m \xi - \left(\frac{\gamma \phi_m}{\beta} \right) \sin \phi_m \xi \right]}{\left(1 + \beta + \gamma - \frac{\gamma \phi_m^2}{\beta} \right) \cos \phi_m - \phi_m \left(1 + \gamma + \frac{2\gamma}{\beta} \right) \sin \phi_m}$$

where ξ and α are dimensionless variables, and β and γ are dimensionless parameters defined by:

$$\xi = \frac{x}{l}, \quad \alpha = \frac{Kt}{l^2 S_s}, \quad \beta = \frac{S_s A l}{S_u}, \quad \gamma = \frac{S_d}{S_u}.$$

S_s is dependent on the compressibility of the pore fluid, and both the bulk and matrix compressibility's of the solid, as well as the interconnected porosity of the specimen and is defined by the following equation:

$$S_s = \gamma_w [n C_w + C_{eff} - (1 + n) C_s]$$

where S_s is the specific storage ($1/L$), C_w is the compressibility of the fluid (LT^2/M), C_{eff} is the effective or bulk compressibility of the sample (LT^2/M), C_s is the compressibility of the minerals in the sample (LT^2/M), and n is the porosity of the sample.

Identifying the storage effects in the data is straightforward. The specimen storage manifests itself in the early times as the delay in response in the downstream or upstream reservoir after a pulse is applied in the opposing reservoir. If the specific storage was 0, the pulse would be immediately observed in the opposing reservoir. The delay is the impact of the specific storage and the upstream and downstream reservoirs. Therefore, due to the inability in this testing configuration to confidently separate the specimen specific storage from the upstream and downstream specific storage, the resulting specimen specific storage should be viewed as a "fitting" parameter, and not as an absolute value.

References

- Blackburn, C.E. and Hinz, P., 1996. Gold and base metal potential of the northwest part of the Raleigh Lake greenstone belt, northwestern Ontario-Kenora Resident Geologist's District; in Summary of Field Work and Other Activities 1996, Ontario Geological Survey, Miscellaneous Paper 166, p.113-115.
- DesRoches, A., Sykes, M., Parmenter, A. and Sykes, E., 2018. Lineament Interpretation of the Revell Batholith and Surrounding Greenstone Belts (Nuclear Waste Management Organization. No. NWMO-TR-2018-19).
- Golder and PGW (Paterson Grant and Watson Ltd.), 2017. Phase 2 Geoscientific Preliminary Assessment, Geological Mapping, Township of Ignace and Area, Ontario: APM-REP-01332-0225.
- Hantush, M., 1964. Hydraulics of Wells. Advances in Hydroscience, 1, 281-432.
- Moghadam, A.A., 2016. Analytical and Experimental Study of Gas Flow Regime in the Matrix and Fractures of Shale Gas Reservoirs. PhD Thesis, University of Alberta, 215 p.
- SGL (Sander Geophysics Limited), 2015. Phase 2 Geoscientific Preliminary Assessment, Acquisition, Processing and Interpretation of High-Resolution Airborne Geophysical Data, Township of Ignace, Ontario. Prepared for Nuclear Waste Management Organization (NWMO). NWMO Report Number: APM-REP-06145-0002.
- SRK (SRK Consulting, Inc.) and Golder, 2015. Phase 2 Geoscientific Preliminary Assessment, Observation of General Geological Features, Township of Ignace, Ontario. Prepared for Nuclear Waste Management Organization. NWMO Report Number: APM-REP-06145-0004.
- Stone, D., 2009. Geology of the Bending Lake Area, Northwestern Ontario; in Summary of Field Work and Other Activities 2009. Ontario Geological Survey. Open File Report 6240.
- Stone, D., 2010a. Geology of the Stormy Lake Area, Northwestern Ontario; in Summary of Field Work and Other Activities 2010. Ontario Geological Survey, Open File Report 6260.
- Stone, D., 2010b. Precambrian geology of the central Wabigoon Subprovince area, northwestern Ontario. Ontario Geological Survey, Open File Report 5422.
- Stone, D., Halle, J. and Chaloux, E., 1998. Geology of the Ignace and Pekagoning Lake Areas, Central Wabigoon Subprovince; in Summary of Field Work and Other Activities 1998, Ontario Geological Survey, Misc. Paper 169.
- Stone, D., Davis, D.W., Hamilton, M.A. and Falcon, A., 2010. Interpretation of 2009 Geochronology in the Central Wabigoon Subprovince and Bending Lake Areas, Northwestern Ontario, in Summary of Field Work and Other Activities 2010, Ontario Geological Survey, Open File Report 6260.
- WSP, 2023a. Phase 2 Initial Borehole Drilling and Testing, Ignace Area – WP03 Data Report – Geological and Geotechnical Core Logging, Photography and Sampling for IG_BH05. NWMO Report Number: APM-REP-01332-0382.

WSP, 2023b. Phase 2 Initial Borehole Drilling and Testing, Ignace Area – WP03 Data Report – Geological and Geotechnical Core Logging, Photography and Sampling for IG_BH06. NWMO Report Number: APM-REP-01332-0383.

Yonge, S. and Maloney, S., 2015. An update to the Canadian Shield Stress Database. NWMO-TR-2015-18.

Appendix A: List of original and corrected sample depths along borehole.

Refer to Section 2.3 for explanation of depth corrections.

BOREHOLE ID	SAMPLE ID	ORIGINAL - FROM	ORIGINAL - TO	CORRECTED - FROM	CORRECTED - TO
IG_BH05	IG_BH05_PS001	294.59	294.93	294.39	294.73
IG_BH05	IG_BH05_PS002	434.04	434.31	433.83	434.10
IG_BH05	IG_BH05_PS003	527.63	527.94	527.39	527.70
IG_BH05	IG_BH05_PS004	641.46	641.73	641.19	641.46
IG_BH05	IG_BH05_PS005	752.55	752.86	752.25	752.56
IG_BH05	IG_BH05_AR044	788.29	788.56	787.98	788.25
IG_BH05	IG_BH05_PS006	852.55	852.79	852.24	852.48
IG_BH05	IG_BH05_AR051	855.46	855.68	855.15	855.37
IG_BH06	IG_BH06_PS001	371.70	371.99	371.70	371.99
IG_BH06	IG_BH06_AR011	398.91	399.33	398.91	399.33
IG_BH06	IG_BH06_PS002	565.44	565.71	565.20	565.47
IG_BH06	IG_BH06_PS003	668.95	669.23	668.56	668.84
IG_BH06	IG_BH06_PS004	731.83	732.09	731.35	731.61
IG_BH06	IG_BH06_PS005	775.40	775.66	774.86	775.12
IG_BH06	IG_BH06_PS006	833.52	833.92	832.89	833.29
IG_BH06	IG_BH06_AR056	909.32	909.70	908.58	908.96
IG_BH06	IG_BH06_PS007	933.40	933.66	932.63	932.89

Notes:

- a) no changes on depths of borehole IG_BH04.
- b) first two depths of borehole IG_BH06 were not impacted.
- c) All depths are in meters along borehole.

**Appendix B: Hydraulic Conductivity and Steady State Gas Permeability Test Summaries
– IG_BH04**

CONTENTS

	Page
Figure 32 IG_BH04_PS003_HC25a: Effective Confining Stress = 7.18 MPa	74
Figure 33 IG_BH04_PS003_HC25a: Effective Confining Stress = 12.74 MPa	75
Figure 34 IG_BH04_PS003_HC25a: Effective Confining Stress = 15.53 MPa	76
Figure 35 IG_BH04_PS003_HC25r: Effective Confining Stress = 6.94 MPa	77
Figure 36 IG_BH04_PS003_HC25r: Effective Confining Stress = 11.54 MPa	78
Figure 37 IG_BH04_PS003_HC25r: Effective Confining Stress = 16.0 MPa	79
Figure 38 IG_BH04_PS003_HC61a: Effective Confining Stress = 7.22 MPa	80
Figure 39 IG_BH04_PS003_HC61a: Effective Confining Stress = 12.81 MPa	81
Figure 40 IG_BH04_PS003_HC61a: Effective Confining Stress = 17.51 MPa	82
Figure 41 IG_BH04_PS005_HC25a: Effective Confining Stress = 9.42 MPa	83
Figure 42 IG_BH04_PS005_HC25a: Effective Confining Stress = 14.11 MPa	84
Figure 43 IG_BH04_PS005_HC25a: Effective Confining Stress = 15.82 MPa	85
Figure 44 IG_BH04_PS005_HC25r: Effective Confining Stress = 9.25 MPa	86
Figure 45 IG_BH04_PS005_HC25r: Effective Confining Stress = 7.77 MPa	87
Figure 46 IG_BH04_PS005_HC25r: Effective Confining Stress = 16.31 MPa	88
Figure 47 IG_BH04_PS005_HC61a: Effective Confining Stress = 9.38 MPa	89
Figure 48 IG_BH04_PS005_HC61a: Effective Confining Stress = 14.07 MPa	90
Figure 49 IG_BH04_PS005_HC61a: Effective Confining Stress = 15.97 MPa	91
Figure 50 IG_BH04_PS006_HC25a: Effective Confining Stress = 10.46 MPa	92
Figure 51 IG_BH04_PS006_HC25a: Effective Confining Stress = 15.48 MPa	93
Figure 52 IG_BH04_PS006_HC25a: Effective Confining Stress = 17.53 MPa	94
Figure 53 IG_BH04_PS006_HC25r: Effective Confining Stress = 10.22 MPa	95
Figure 54 IG_BH04_PS006_HC25r: Effective Confining Stress = 15.33 MPa	96
Figure 55 IG_BH04_PS006_HC25r: Effective Confining Stress = 15.25 MPa	97
Figure 56 IG_BH04_PS006_HC61a: Effective Confining Stress = 10.29 MPa	98
Figure 57 IG_BH04_PS006_HC61a: Effective Confining Stress = 15.43 MPa	99
Figure 58 IG_BH04_PS006_HC61a: Effective Confining Stress = 15.77 MPa	100
Figure 59 IG_BH04_PS008_HC25a: Effective Confining Stress = 13.36 MPa	101
Figure 60 IG_BH04_PS008_HC25a: Effective Confining Stress = 18.18 MPa	102
Figure 61 IG_BH04_PS008_HC25a: Effective Confining Stress = 23.19 MPa	103

Figure 62	IG_BH04_PS008_HC61a: Effective Confining Stress = 13.21 MPa	104
Figure 63	IG_BH04_PS008_HC61a: Effective Confining Stress = 18.28 MPa	105
Figure 64	IG_BH04_PS008_HC61a: Effective Confining Stress = 23.12 MPa	106
Figure 65	IG_BH04_PS008_SSG61a: Effective Confining Stresses of 13.6MPa, 18.6MPa and 23.6MPa.....	107
Figure 66	IG_BH04_PS009_HC25a: Effective Confining Stress = 15.88 MPa	108
Figure 67	IG_BH04_PS009_HC25a: Effective Confining Stress = 21.20 MPa	109
Figure 68	IG_BH04_PS009_HC25a: Effective Confining Stress = 25.9 MPa	110
Figure 69	IG_BH04_PS009_SSG61a: Effective Confining Stresses of 15.5MPa, 20.8MPa and 25.7MPa.....	111
Figure 70	IG_BH04_PS010_HC25r: Effective Confining Stress = 16.24 MPa	112
Figure 71	IG_BH04_PS010_SSG61a: Effective Confining Stresses of 16.9MPa, 21.9MPa and 26.9MPa.....	113
Figure 72	IG_BH04_PS011_HC25a: Effective Confining Stress = 22.62 MPa	114
Figure 73	IG_BH04_PS011_HC25a: Effective Confining Stress = 27.61 MPa	115
Figure 74	IG_BH04_PS011_HC25r: Effective Confining Stress = 22.52 MPa	116
Figure 75	IG_BH04_PS011_HC25r: Effective Confining Stress = 27.46 MPa	117
Figure 76	IG_BH04_PS011_HC61a: Effective Confining Stress = 22.63 MPa	118
Figure 77	IG_BH04_PS011_HC61a: Effective Confining Stress = 27.33 MPa	119

	Sample Name		IG_BH04_PS003
	Specimen Name		IG_BH04_PS003_HC25a
	Specimen Top Depth		398.715
	Specimen Bottom Depth		398.740
	Test No		ES1
	Test Name		IG_BH04_PS003_HC25a_ES1
	Operator		StephenTalman/FrancyGuerrero
Dimensions	Length	mm	24.210
	Diameter	mm	25.390
	Length	m	0.02421
	Diameter	m	0.02539
Test Data Location	Raw Data File Name		IG_BH04_PS003_HC25a-001-C.dat
	Date & Time		2022-10-27 08:49:52
	Start Row		76
	End Row		622
Test Conditions	Avg Cell Temp	C	39.85
	Avg Confining Pressure	kPa	16506
	Pre Pulse Avg Pore Pressure	kPa	9327
	Pulse Pressure	kPa	-466
	Effective Stress	kPa	7179
	Post Pulse Avg Pore Pressure	kPa	9132
Pore Fluid & Conditions	Type		Water
	Salt	ppm	0
	Density	kg/m3	996.28
	Viscosity	kg.s/m	6.558E-04
	Compressibility	1/Pa	4.36E-10
Solution	Test System		System2-CELL1
Brace	Nominal Decay Time	s	821
	Brace Permeability	m2	1.34E-19
Hsieh	Permeability	m2	1.42E-19
	Specific Storage	1/m	1.30E-07
	Permeability	nD	143.4
	Hydraulic Conductivity	m/s	2.11E-12
	Pearson Coeff	()	0.9997700

IG_BH04_PS003_HC25a Eff Stress:7.18 MPa, HC=2.11e-12 m/s, SS=1.30e-7 1/m

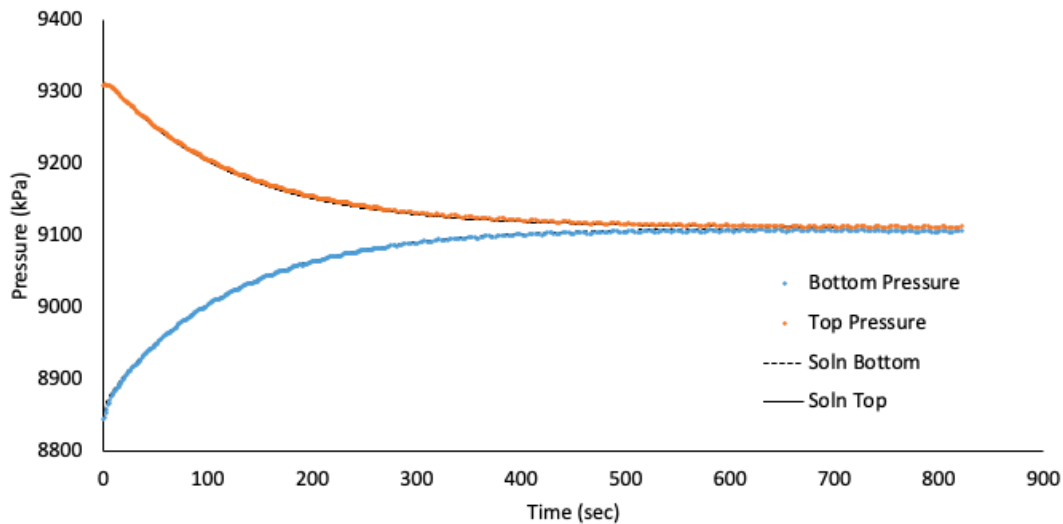


Figure 32 IG_BH04_PS003_HC25a: Effective Confining Stress = 7.18 MPa

	Sample Name		IG_BH04_PS003
	Specimen Name		IG_BH04_PS003_HC25a
	Specimen Top Depth		398.715
	Specimen Bottom Depth		398.740
	Test No		ES2
	Test Name		IG_BH04_PS003_HC25a_ES2
	Operator		Stephen Talman/Francy Guerrero
Dimensions	Length	mm	24.210
	Diameter	mm	25.390
	Length	m	0.02421
	Diameter	m	0.02539
Test Data Location	Raw Data File Name		IG_BH04_PS003_HC25a-001-A.dat
	Date & Time		2022-10-27 08:49:52
	Start Row		68
	End Row		1622
Test Conditions	Avg Cell Temp	C	39.88
	Avg Confining Pressure	kPa	21482
	Pre Pulse Avg Pore Pressure	kPa	8743
	Pulse Pressure	kPa	500
	Effective Stress	kPa	12738
	Post Pulse Avg Pore Pressure	kPa	9029
Pore Fluid & Conditions	Type		Water
	Salt	ppm	0
	Density	kg/m3	996.02
	Viscosity	kg.s/m	6.553E-04
	Compressibility	1/Pa	4.36E-10
Solution	Test System		System2-CELL1
Brace	Nominal Decay Time	s	4929
	Brace Permeability	m2	5.10E-20
Hsieh	Permeability	m2	5.40E-20
	Specific Storage	1/m	1.06E-07
	Permeability	nD	54.7
	Hydraulic Conductivity	m/s	8.05E-13
	Pearson Coeff	()	0.9999225

IG_BH04_PS003_HC25a
Eff Stress:12.74 MPa, HC=8.05e-13 m/s, SS=1.06e-7 1/m

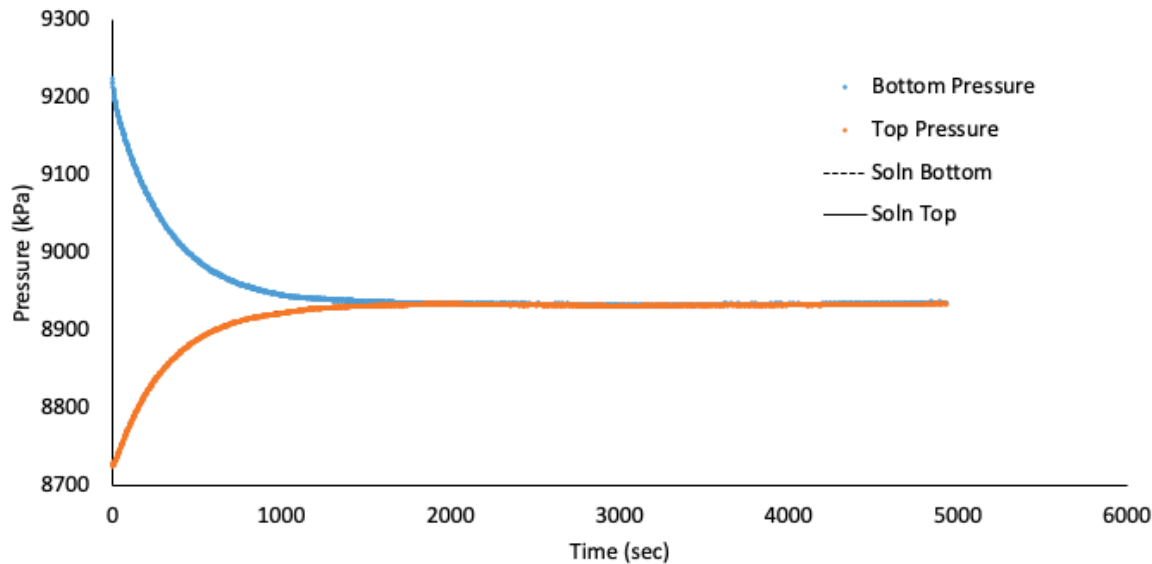


Figure 33 IG_BH04_PS003_HC25a: Effective Confining Stress = 12.74 MPa

	Sample Name		IG_BH04_PS003
	Specimen Name		IG_BH04_PS003_HC25a
	Specimen Top Depth		398.715
	Specimen Bottom Depth		398.740
	Test No		ES3
	Test Name		IG_BH04_PS003_HC25a_ES3
	Operator		StephenTalman/FrancyGuerrero
Dimensions	Length	mm	24.210
	Diameter	mm	25.390
	Length	m	0.02421
	Diameter	m	0.02539
Test Data Location	Raw Data File Name		IG_BH04_PS003_HC25a-002-F.dat
	Date & Time		2022-10-31 08:56:08
	Start Row		70
	End Row		1487
Test Conditions	Avg Cell Temp	C	39.93
	Avg Confining Pressure	kPa	24943
	Pre Pulse Avg Pore Pressure	kPa	9412
	Pulse Pressure	kPa	-489
	Effective Stress	kPa	15532
	Post Pulse Avg Pore Pressure	kPa	9289
Pore Fluid & Conditions	Type		Water
	Salt	ppm	0
	Density	kg/m3	996.29
	Viscosity	kg.s/m	6.548E-04
	Compressibility	1/Pa	4.36E-10
Solution	Test System		System2-CELL1
Brace	Nominal Decay Time	s	4177
	Brace Permeability	m2	1.97E-20
Hsieh	Permeability	m2	1.96E-20
	Specific Storage	1/m	9.90E-08
	Permeability	nD	19.9
	Hydraulic Conductivity	m/s	2.93E-13
	Pearson Coeff	()	0.9996962

IG_BH04_PS003_HC25a Eff Stress:15.53 MPa, HC=2.93e-13 m/s, SS=9.90e-8 1/m

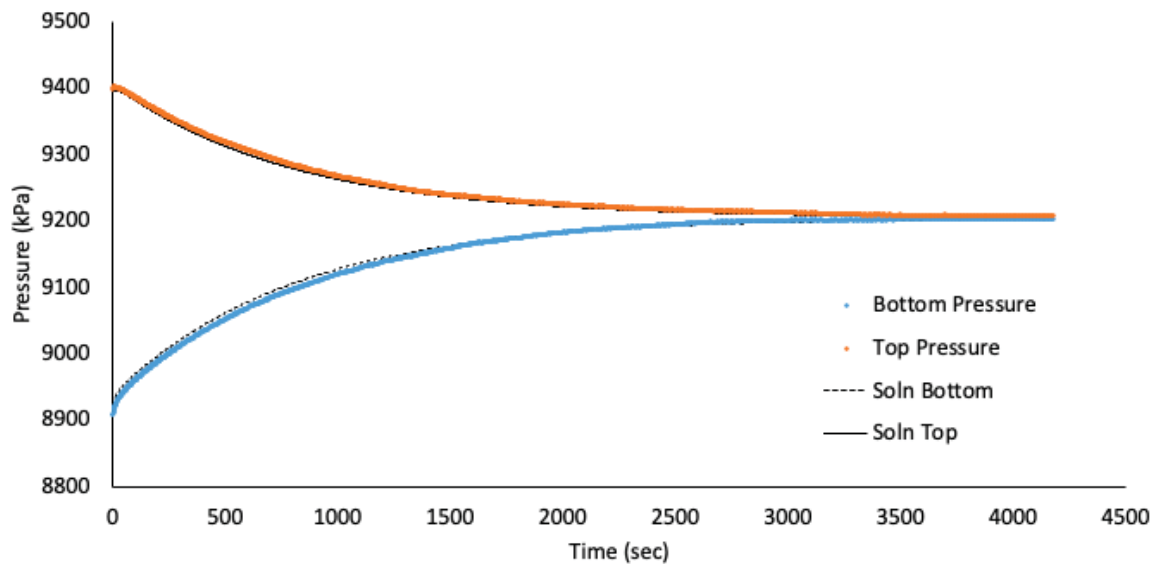


Figure 34 IG_BH04_PS003_HC25a: Effective Confining Stress = 15.53 MPa

	Sample Name		IG_BH04_PS003
	Specimen Name		IG_BH04_PS003_HC25r
	Specimen Top Depth		398.715
	Specimen Bottom Depth		398.740
	Test No		ES1
	Test Name		IG_BH04_PS003_HC25r_ES1
	Operator		StephenTalman/FrancyGuerrero
Dimensions	Length	mm	22.990
	Diameter	mm	25.310
	Length	m	0.02299
	Diameter	m	0.02531
Test Data Location	Raw Data File Name		IG_BH04_PS003_HC25r-001-E.dat
	Date & Time		2022-10-27 08:53:11
	Start Row		71
	End Row		622
Test Conditions	Avg Cell Temp	C	39.65
	Avg Confining Pressure	kPa	16361
	Pre Pulse Avg Pore Pressure	kPa	9421
	Pulse Pressure	kPa	-562
	Effective Stress	kPa	6940
	Post Pulse Avg Pore Pressure	kPa	9189
Pore Fluid & Conditions	Type		Water
	Salt	ppm	0
	Density	kg/m3	996.4
	Viscosity	kg.s/m	6.582E-04
	Compressibility	1/Pa	4.36E-10
Solution	Test System		System2-CELL3
Brace	Nominal Decay Time	s	826
	Brace Permeability	m2	1.58E-19
Hsieh	Permeability	m2	1.70E-19
	Specific Storage	1/m	7.62E-08
	Permeability	nD	172.4
	Hydraulic Conductivity	m/s	2.53E-12
	Pearson Coeff	()	0.9997669

IG_BH04_PS003_HC25r Eff Stress:6.94 MPa, HC=2.53e-12 m/s, SS=7.62e-8 1/m

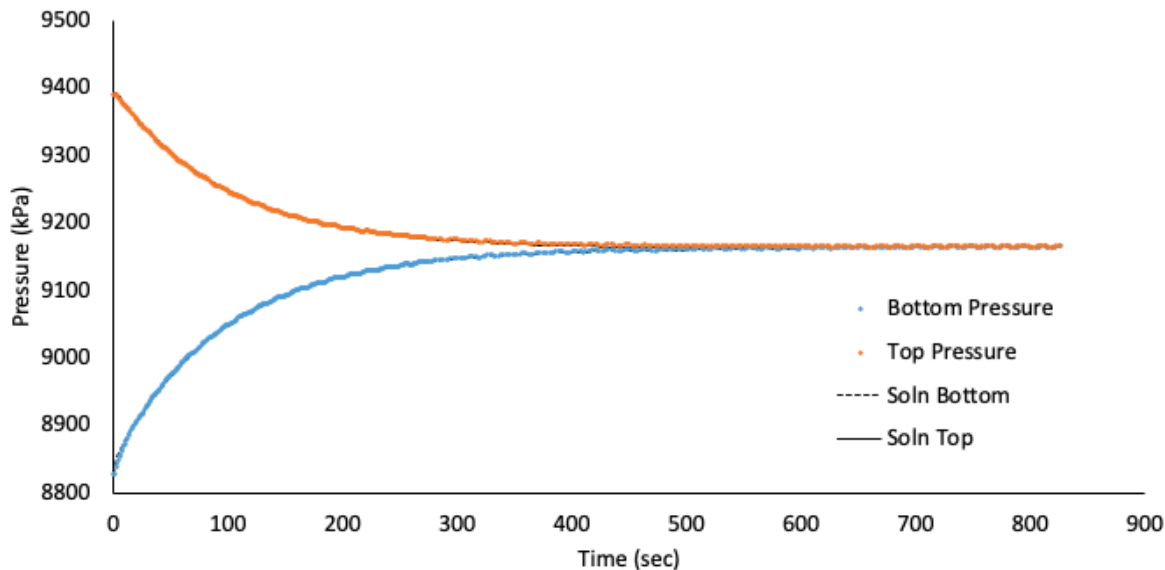


Figure 35 IG_BH04_PS003_HC25r: Effective Confining Stress = 6.94 MPa

	Sample Name		IG_BH04_PS003
	Specimen Name		IG_BH04_PS003_HC25r
	Specimen Top Depth		398.715
	Specimen Bottom Depth		398.740
	Test No		ES2
	Test Name		IG_BH04_PS003_HC25r_ES2
	Operator		StephenTalman/FrancyGuerrero
Dimensions	Length	mm	22.990
	Diameter	mm	25.310
	Length	m	0.02299
	Diameter	m	0.02531
Test Data Location	Raw Data File Name		IG_BH04_PS003_HC25r-001-A.dat
	Date & Time		2022-10-27 08:53:11
	Start Row		90
	End Row		1000
Test Conditions	Avg Cell Temp	C	39.70
	Avg Confining Pressure	kPa	21299
	Pre Pulse Avg Pore Pressure	kPa	9763
	Pulse Pressure	kPa	-242
	Effective Stress	kPa	11536
	Post Pulse Avg Pore Pressure	kPa	9800
Pore Fluid & Conditions	Type		Water
	Salt	ppm	0
	Density	kg/m3	996.53
	Viscosity	kg.s/m	6.577E-04
	Compressibility	1/Pa	4.36E-10
Solution	Test System		System2-CELL3
Brace	Nominal Decay Time	s	1969
	Brace Permeability	m2	8.84E-20
Hsieh	Permeability	m2	8.13E-20
	Specific Storage	1/m	1.29E-09
	Permeability	nD	82.4
	Hydraulic Conductivity	m/s	1.21E-12
	Pearson Coeff	()	0.9966889

IG_BH04_PS003_HC25r Eff Stress:11.54 MPa, HC=1.21e-12 m/s, SS=1.29e-9 1/m

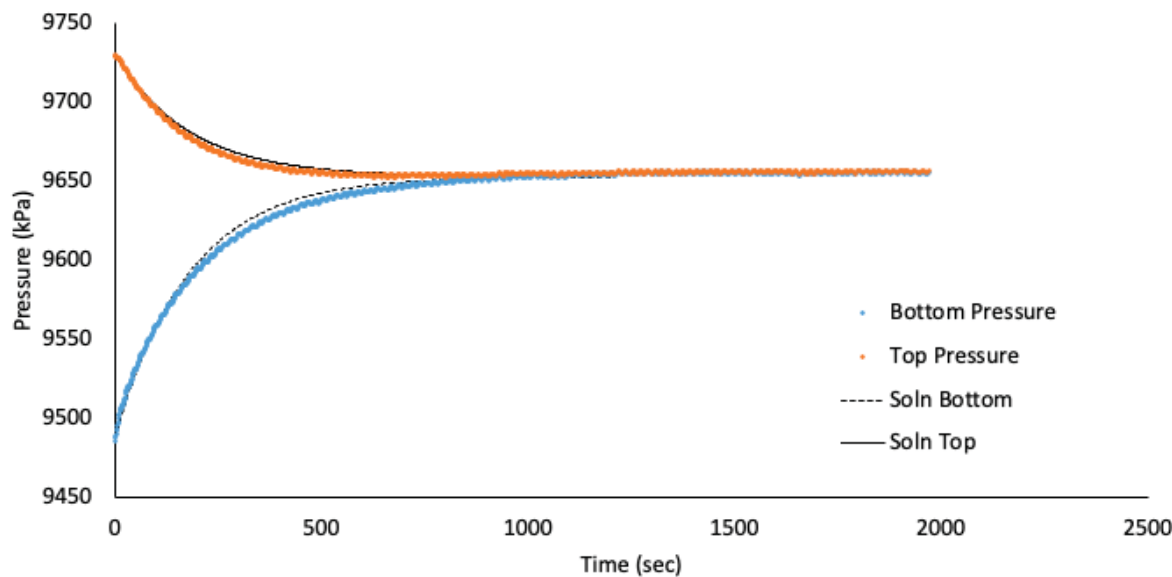


Figure 36 IG_BH04_PS003_HC25r: Effective Confining Stress = 11.54 MPa

	Sample Name		IG_BH04_PS003
	Specimen Name		IG_BH04_PS003_HC25r
	Specimen Top Depth		398.715
	Specimen Bottom Depth		398.740
	Test No		ES3
	Test Name		IG_BH04_PS003_HC25r_ES3
	Operator		StephenTalman/FrancyGuerrero
Dimensions	Length	mm	22.990
	Diameter	mm	25.310
	Length	m	0.02299
	Diameter	m	0.02531
Test Data Location	Raw Data File Name		IG_BH04_PS003_HC25r-001-A.dat
	Date & Time		2022-10-31 08:57:53
	Start Row		70
	End Row		1490
Test Conditions	Avg Cell Temp	C	39.74
	Avg Confining Pressure	kPa	25425
	Pre Pulse Avg Pore Pressure	kPa	9425
	Pulse Pressure	kPa	-527
	Effective Stress	kPa	16000
	Post Pulse Avg Pore Pressure	kPa	9297
Pore Fluid & Conditions	Type		Water
	Salt	ppm	0
	Density	kg/m3	996.37
	Viscosity	kg.s/m	6.571E-04
	Compressibility	1/Pa	4.36E-10
Solution	Test System		System2-CELL3
Brace	Nominal Decay Time	s	4192
	Brace Permeability	m2	1.92E-20
Hsieh	Permeability	m2	1.88E-20
	Specific Storage	1/m	9.59E-08
	Permeability	nD	19.0
	Hydraulic Conductivity	m/s	2.79E-13
	Pearson Coeff	()	0.9996069

IG_BH04_PS003_HC25r Eff Stress:16 MPa, HC=2.79e-13 m/s, SS=9.59e-8 1/m

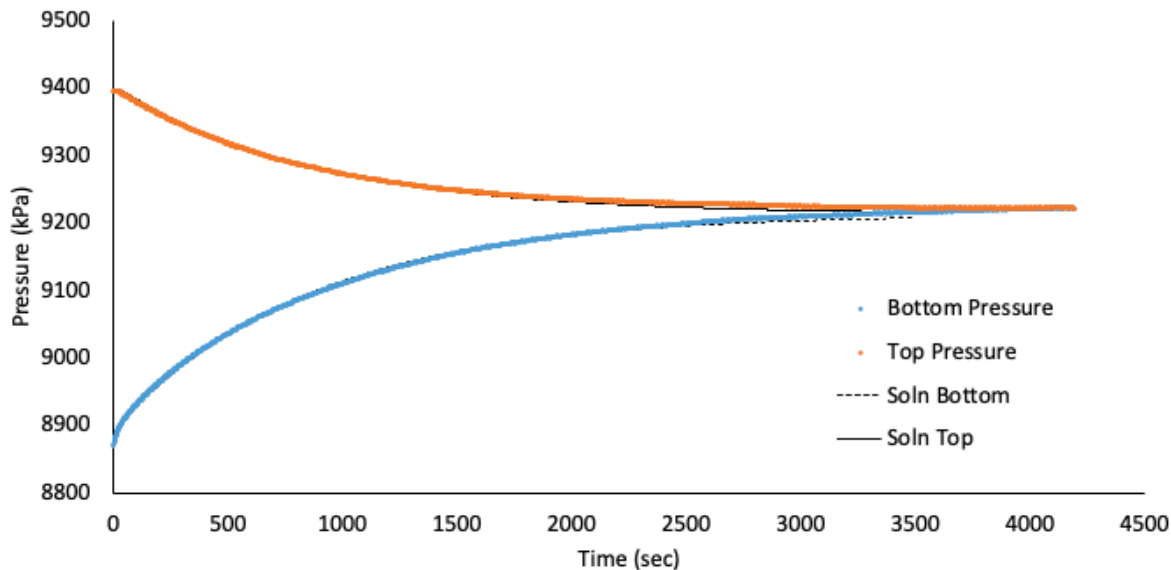


Figure 37 IG_BH04_PS003_HC25r: Effective Confining Stress = 16.0 MPa

	Sample Name		IG_BH04_PS003
	Specimen Name		IG_BH04_PS003_HC61a
	Specimen Top Depth		398.777
	Specimen Bottom Depth		398.840
	Test No		ES1
	Test Name		IG_BH04_PS003_HC61a_ES1
	Operator		StephenTalman/FrancyGuerrero
Dimensions	Length	mm	63.290
	Diameter	mm	61.280
	Length	m	0.06329
	Diameter	m	0.06128
Test Data Location	Raw Data File Name		IG-BH04-PS003-HC61a-003-A.dat
	Date & Time		2023-02-28 13:19:34
	Start Row		69
	End Row		650
Test Conditions	Avg Cell Temp	C	40.08
	Avg Confining Pressure	kPa	16653
	Pre Pulse Avg Pore Pressure	kPa	9436
	Pulse Pressure	kPa	-508
	Effective Stress	kPa	7217
	Post Pulse Avg Pore Pressure	kPa	9337
Pore Fluid & Conditions	Type		Water
	Salt	ppm	0
	Density	kg/m3	996.15
	Viscosity	kg.s/m	6.497E-04
Solution	Compressibility	1/Pa	4.36E-10
	Test System		System3-Cell2
Brace	Nominal Decay Time	s	887
	Brace Permeability	m2	6.17E-20
Hsieh	Permeability	m2	6.17E-20
	Specific Storage	1/m	3.99E-08
	Permeability	nD	62.5
	Hydraulic Conductivity	m/s	9.29E-13
	Pearson Coeff	()	0.9985554

IG_BH04_PS003_HC61a Eff Stress:7.22 MPa, HC=9.29e-13 m/s, SS=3.99e-8 1/m

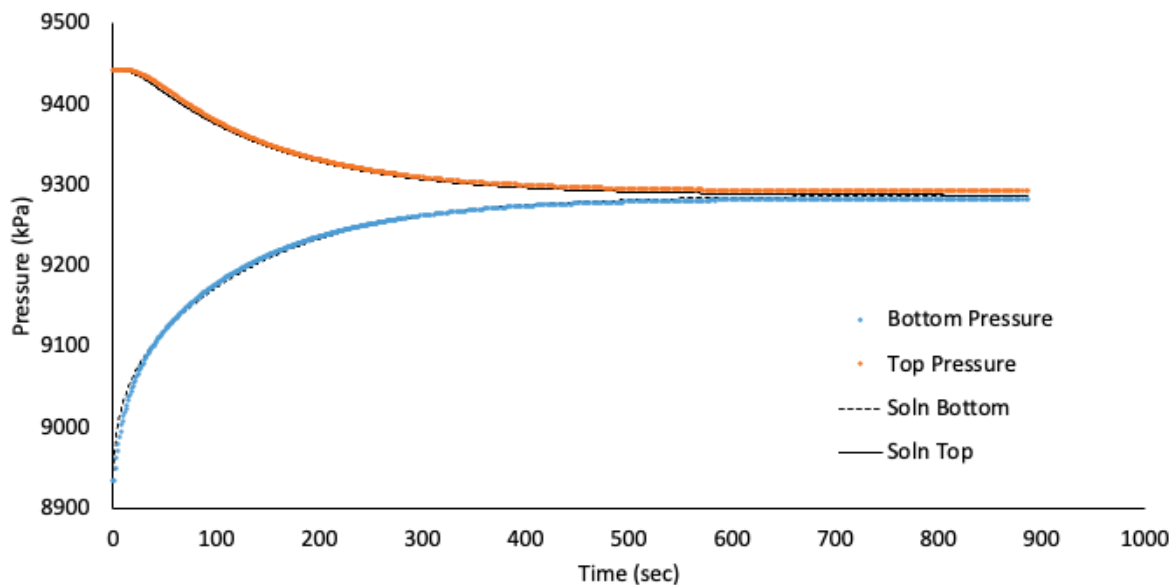


Figure 38 IG_BH04_PS003_HC61a: Effective Confining Stress = 7.22 MPa

	Sample Name		IG_BH04_PS003
	Specimen Name		IG_BH04_PS003_HC61a
	Specimen Top Depth		398.777
	Specimen Bottom Depth		398.840
	Test No		ES2
	Test Name		IG_BH04_PS003_HC61a_ES2
	Operator		StephenTalman/FrancyGuerrero
Dimensions	Length	mm	63.290
	Diameter	mm	61.280
	Length	m	0.06329
	Diameter	m	0.06128
Test Data Location	Raw Data File Name		IG-BH04-PS006-HC61a-004-A.dat
	Date & Time		2023-03-01 08:35:03
	Start Row		77
	End Row		1085
Test Conditions	Avg Cell Temp	C	40.08
	Avg Confining Pressure	kPa	21618
	Pre Pulse Avg Pore Pressure	kPa	8812
	Pulse Pressure	kPa	502
	Effective Stress	kPa	12805
	Post Pulse Avg Pore Pressure	kPa	9043
Pore Fluid & Conditions	Type		Water
	Salt	ppm	0
	Density	kg/m3	995.97
	Viscosity	kg.s/m	6.529E-04
	Compressibility	1/Pa	4.36E-10
Solution	Test System		System3-Cell2
Brace	Nominal Decay Time	s	2322
	Brace Permeability	m2	7.79E-20
Hsieh	Permeability	m2	8.57E-20
	Specific Storage	1/m	1.19E-07
	Permeability	nD	86.9
	Hydraulic Conductivity	m/s	1.28E-12
	Pearson Coeff	()	0.9990932

IG_BH04_PS003_HC61a Eff Stress:12.81 MPa, HC=1.28e-12 m/s, SS=1.19e-7 1/m

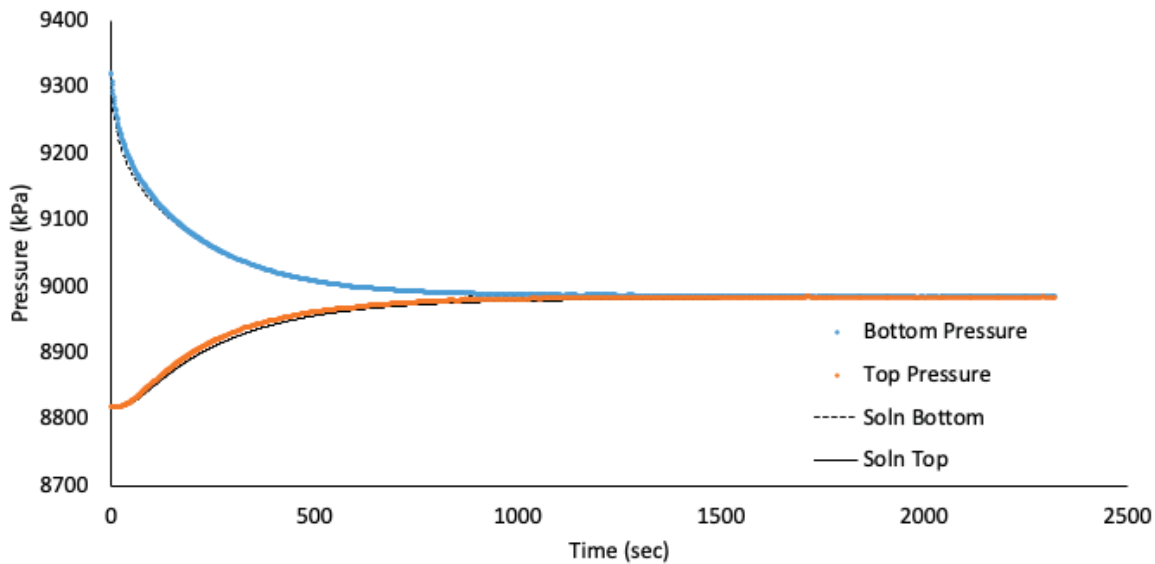


Figure 39 IG_BH04_PS003_HC61a: Effective Confining Stress = 12.81 MPa

	Sample Name		IG_BH04_PS003
	Specimen Name		IG_BH04_PS003_HC61a
	Specimen Top Depth		398.777
	Specimen Bottom Depth		398.840
	Test No		ES3
	Test Name		IG_BH04_PS003_HC61a_ES3
	Operator		StephenTalman/FrancyGuerrero
Dimensions	Length	mm	63.290
	Diameter	mm	61.280
	Length	m	0.06329
	Diameter	m	0.06128
Test Data Location	Raw Data File Name		IG-BH04-PS006-HC61a-004-H.dat
	Date & Time		2023-03-01 08:35:03
	Start Row		87
	End Row		1317
Test Conditions	Avg Cell Temp	C	40.09
	Avg Confining Pressure	kPa	26611
	Pre Pulse Avg Pore Pressure	kPa	9106
	Pulse Pressure	kPa	496
	Effective Stress	kPa	17505
	Post Pulse Avg Pore Pressure	kPa	9004
Pore Fluid & Conditions	Type		Water
	Salt	ppm	0
	Density	kg/m3	996.1
	Viscosity	kg.s/m	6.528E-04
	Compressibility	1/Pa	4.36E-10
Solution	Test System		System3-Cell2
Brace	Nominal Decay Time	s	3310
	Brace Permeability	m2	4.16E-20
Hsieh	Permeability	m2	4.92E-20
	Specific Storage	1/m	1.04E-07
	Permeability	nD	49.8
	Hydraulic Conductivity	m/s	7.36E-13
	Pearson Coeff	()	0.9998175

IG_BH04_PS003_HC61a Eff Stress:17.51 MPa, HC=7.36e-13 m/s, SS=1.04e-7 1/m

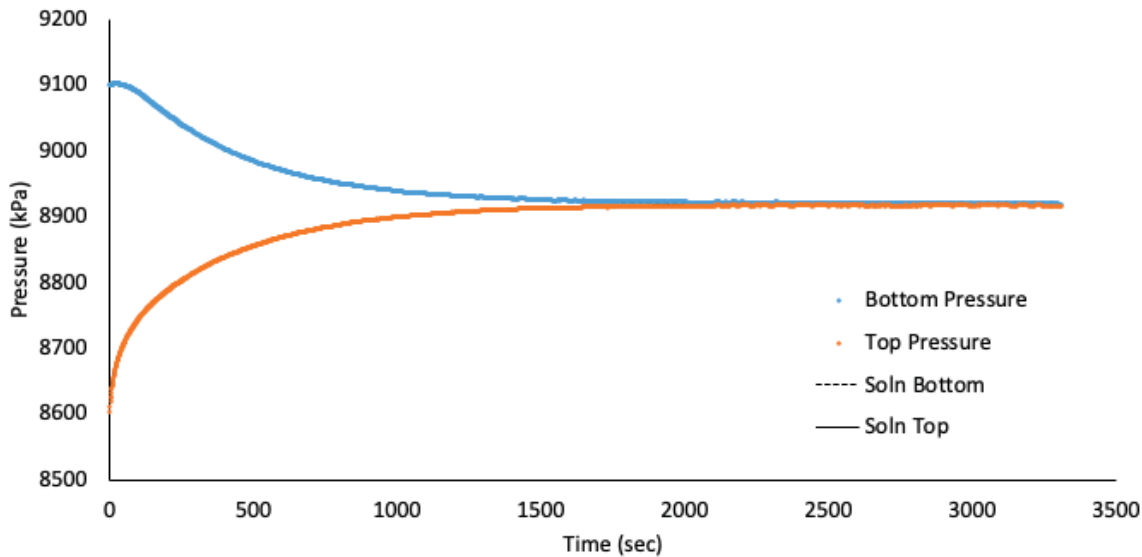


Figure 40 IG_BH04_PS003_HC61a: Effective Confining Stress = 17.51 MPa

	Sample Name		IG_BH04_PS005
	Specimen Name		IG_BH04_PS005_HC25a
	Specimen Top Depth		506.815
	Specimen Bottom Depth		506.850
	Test No		ES1
	Test Name		IG_BH04_PS005_HC25a_ES1
	Operator		StephenTalman/FrancyGuerrero
Dimensions	Length	mm	25.980
	Diameter	mm	25.350
	Length	m	0.02598
	Diameter	m	0.02535
Test Data Location	Raw Data File Name		IG-BH04-PS005-HC25a-001-C.dat
	Date & Time		2022-11-18 12:57:37
	Start Row		1374
	End Row		1472
Test Conditions	Avg Cell Temp	C	39.95
	Avg Confining Pressure	kPa	18568
	Pre Pulse Avg Pore Pressure	kPa	9148
	Pulse Pressure	kPa	-399
	Effective Stress	kPa	9420
	Post Pulse Avg Pore Pressure	kPa	8990
Pore Fluid & Conditions	Type		Water
	Salt	ppm	0
	Density	kg/m3	996.17
	Viscosity	kg.s/m	6.545E-04
	Compressibility	1/Pa	4.36E-10
Solution	Test System		System2-CELL1
Brace	Nominal Decay Time	s	490
	Brace Permeability	m2	5.21E-19
Hsieh	Permeability	m2	5.51E-19
	Specific Storage	1/m	5.76E-08
	Permeability	nD	558.0
	Hydraulic Conductivity	m/s	8.22E-12
	Pearson Coeff	()	0.9999335

IG_BH04_PS005_HC25a Eff Stress:9.42 MPa, HC=8.22e-12 m/s, SS=5.76e-8 1/m

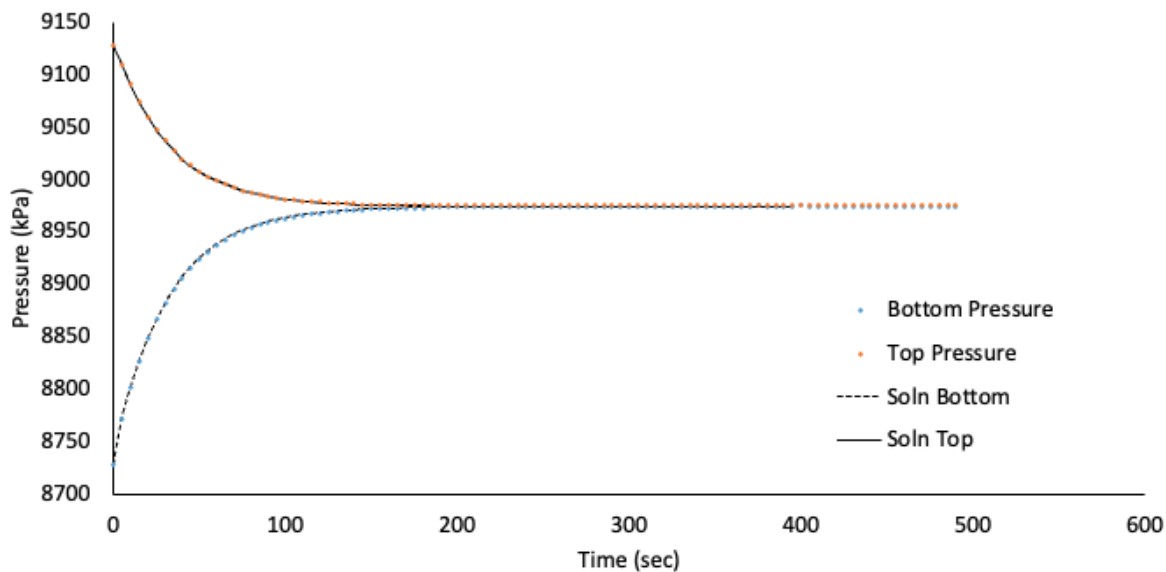


Figure 41 IG_BH04_PS005_HC25a: Effective Confining Stress = 9.42 MPa

	Sample Name		IG_BH04_PS005
	Specimen Name		IG_BH04_PS005_HC25a
	Specimen Top Depth		506.815
	Specimen Bottom Depth		506.850
	Test No		ES2
	Test Name		IG_BH04_PS005_HC25a_ES2
	Operator		StephenTalman/FrancyGuerrero
Dimensions	Length	mm	25.980
	Diameter	mm	25.350
	Length	m	0.02598
	Diameter	m	0.02535
Test Data Location	Raw Data File Name		IG-BH04-PS005-HC25a-002-B.dat
	Date & Time		2022-11-21 12:45:24
	Start Row		73
	End Row		600
Test Conditions	Avg Cell Temp	C	39.96
	Avg Confining Pressure	kPa	23541
	Pre Pulse Avg Pore Pressure	kPa	9427
	Pulse Pressure	kPa	516
	Effective Stress	kPa	14114
	Post Pulse Avg Pore Pressure	kPa	9165
Pore Fluid & Conditions	Type		Water
	Salt	ppm	0
	Density	kg/m3	996.29
	Viscosity	kg.s/m	6.544E-04
	Compressibility	1/Pa	4.36E-10
Solution	Test System		System2-CELL1
Brace	Nominal Decay Time	s	780
	Brace Permeability	m2	2.43E-19
Hsieh	Permeability	m2	2.55E-19
	Specific Storage	1/m	1.54E-07
	Permeability	nD	258.5
	Hydraulic Conductivity	m/s	3.81E-12
	Pearson Coeff	()	0.9998467

IG_BH04_PS005_HC25a Eff Stress:14.11 MPa, HC=3.81e-12 m/s, SS=1.54e-7 1/m

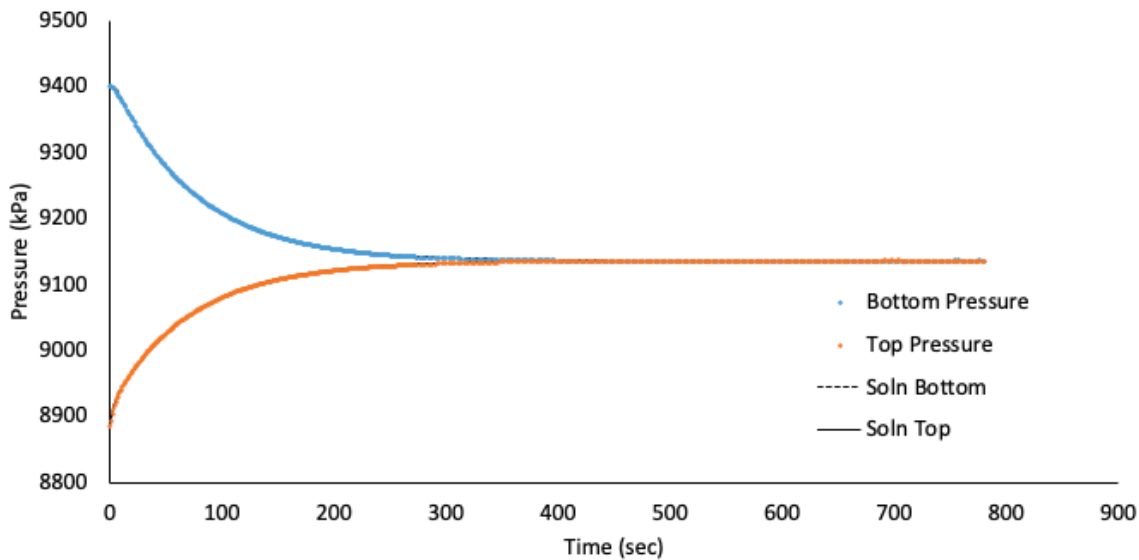


Figure 42 IG_BH04_PS005_HC25a: Effective Confining Stress = 14.11 MPa

	Sample Name		IG_BH04_PS005
	Specimen Name		IG_BH04_PS005_HC25a
	Specimen Top Depth		506.815
	Specimen Bottom Depth		506.850
	Test No		ES3
	Test Name		IG_BH04_PS005_HC25a_ES3
	Operator		StephenTalman/FrancyGuerrero
Dimensions	Length	mm	25.980
	Diameter	mm	25.350
	Length	m	0.02598
	Diameter	m	0.02535
Test Data Location	Raw Data File Name		IG-BH04-PS005-HC25a-003-A.dat
	Date & Time		2022-11-23 11:01:58
	Start Row		78
	End Row		800
Test Conditions	Avg Cell Temp	C	40.00
	Avg Confining Pressure	kPa	24943
	Pre Pulse Avg Pore Pressure	kPa	9120
	Pulse Pressure	kPa	-317
	Effective Stress	kPa	15823
	Post Pulse Avg Pore Pressure	kPa	9030
Pore Fluid & Conditions	Type		Water
	Salt	ppm	0
	Density	kg/m3	996.14
	Viscosity	kg.s/m	6.539E-04
	Compressibility	1/Pa	4.36E-10
Solution	Test System		System2-CELL1
Brace	Nominal Decay Time	s	1328
	Brace Permeability	m2	9.70E-20
Hsieh	Permeability	m2	9.18E-20
	Specific Storage	1/m	8.58E-08
	Permeability	nD	93.1
	Hydraulic Conductivity	m/s	1.37E-12
	Pearson Coeff	()	0.9997620

IG_BH04_PS005_HC25a Eff Stress:15.82 MPa, HC=1.37e-12 m/s, SS=8.58e-8 1/m

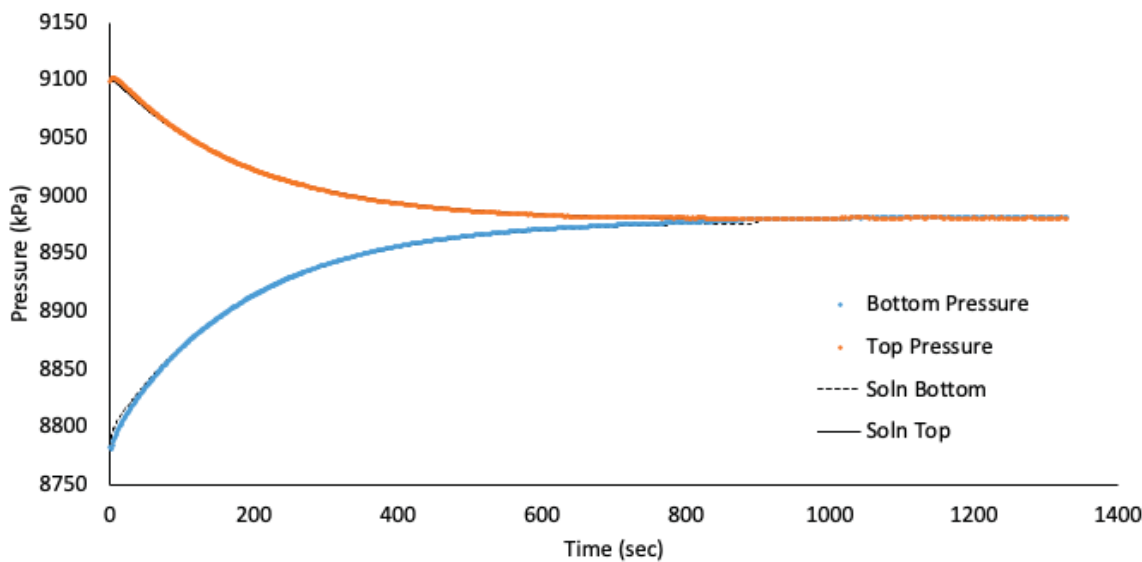


Figure 43 IG_BH04_PS005_HC25a: Effective Confining Stress = 15.82 MPa

	Sample Name		IG_BH04_PS005
	Specimen Name		IG_BH04_PS005_HC25r
	Specimen Top Depth		506.815
	Specimen Bottom Depth		506.850
	Test No		ES1
	Test Name		IG_BH04_PS005_HC25r_ES1
	Operator		Stephen Talman/ Francy Guerrero
Dimensions	Length	mm	24.830
	Diameter	mm	25.350
	Length	m	0.02483
	Diameter	m	0.02535
Test Data Location	Raw Data File Name		2022-11-18_13-03-14 System-2-CELL-3 IG-BH04-PS005-HC25r.csv
	Date & Time		2022-11-18 13:03:14
	Start Row		4288
	End Row		4700
Test Conditions	Avg Cell Temp	C	39.74
	Avg Confining Pressure	kPa	18402
	Pre Pulse Avg Pore Pressure	kPa	9157
	Pulse Pressure	kPa	-406
	Effective Stress	kPa	9245
	Post Pulse Avg Pore Pressure	kPa	8942
Pore Fluid & Conditions	Type		Water
	Salt	ppm	0
	Density	kg/m3	996.25
	Viscosity	kg.s/m	6.571E-04
	Compressibility	1/Pa	4.36E-10
Solution	Test System		System 2 - CELL 3
Brace	Nominal Decay Time	s	412
	Brace Permeability	m2	8.33E-19
Hsieh	Permeability	m2	8.33E-19
	Specific Storage	1/m	1.83E-08
	Permeability	nD	843.6
	Hydraulic Conductivity	m/s	1.24E-11
	Pearson Coeff	()	0.9998197

IG_BH04_PS005_HC25r Eff Stress:9.25 MPa, HC=1.24e-11 m/s, SS=1.83e-8 1/m

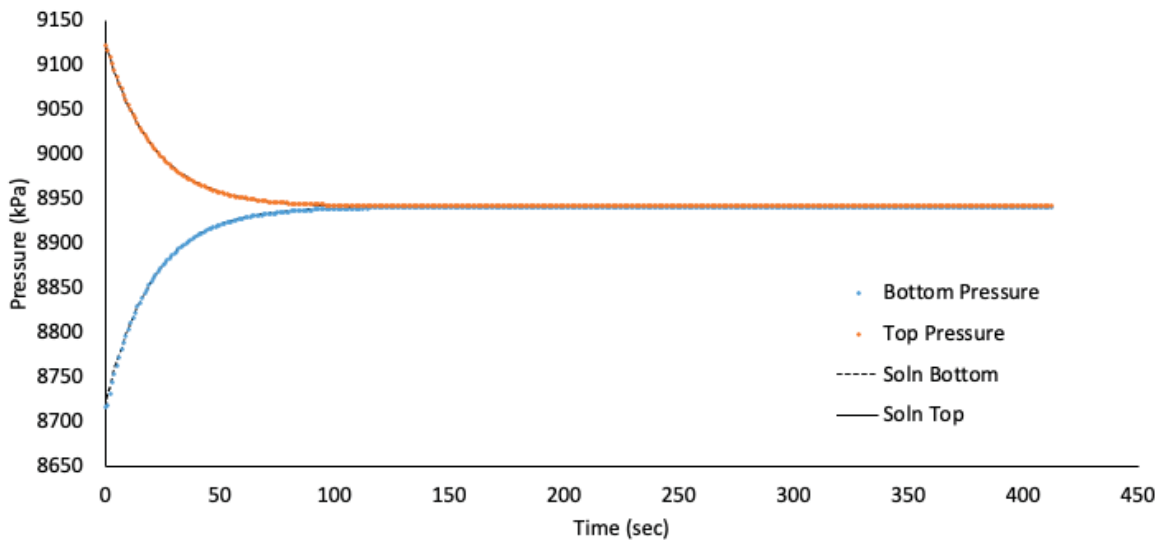


Figure 44 IG_BH04_PS005_HC25r: Effective Confining Stress = 9.25 MPa

	Sample Name		IG_BH04_PS005
	Specimen Name		IG_BH04_PS005_HC25r
	Specimen Top Depth		506.815
	Specimen Bottom Depth		506.850
	Test No		ES2
	Test Name		IG_BH04_PS005_HC25r_ES2
	Operator		Stephen Talman/ Francy Guerrero
Dimensions	Length	mm	24.830
	Diameter	mm	25.350
	Length	m	0.02483
	Diameter	m	0.02535
Test Data Location	Raw Data File Name		2022-11-18_13-03-14 System-2-CELL-3 IG-BH04-PS005-HC25r_P12.csv
	Date & Time		2022-11-18 13:03:14
	Start Row		8820
	End Row		9100
Test Conditions	Avg Cell Temp	C	39.69
	Avg Confining Pressure	kPa	18259
	Pre Pulse Avg Pore Pressure	kPa	10484
	Pulse Pressure	kPa	457
	Effective Stress	kPa	7775
	Post Pulse Avg Pore Pressure	kPa	10213
Pore Fluid & Conditions	Type		Water
	Salt	ppm	0
	Density	kg/m3	996.84
	Viscosity	kg.s/m	6.579E-04
	Compressibility	1/Pa	4.36E-10
Solution	Test System		System 2 - CELL 3
Brace	Nominal Decay Time	s	280
	Brace Permeability	m2	1.00E-18
Hsieh	Permeability	m2	1.00E-18
	Specific Storage	1/m	4.30E-08
	Permeability	nD	1013.6
	Hydraulic Conductivity	m/s	1.49E-11
	Pearson Coeff	()	0.9998883

IG_BH04_PS005_HC25r Eff Stress:7.77 MPa, HC=1.49e-11 m/s, SS=4.30e-8 1/m

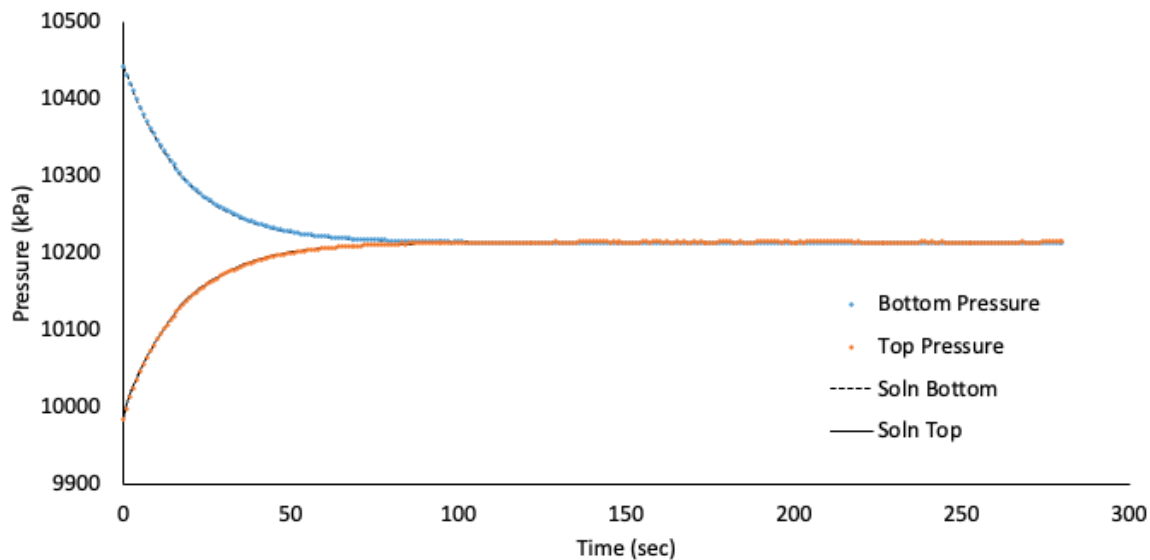


Figure 45 IG_BH04_PS005_HC25r: Effective Confining Stress = 7.77 MPa

	Sample Name		IG_BH04_PS005
	Specimen Name		IG_BH04_PS005_HC25r
	Specimen Top Depth		506.815
	Specimen Bottom Depth		506.850
	Test No		ES3
	Test Name		IG_BH04_PS005_HC25r_ES3
	Operator		Stephen Talman/ Francy Guerrero
Dimensions	Length	mm	24.830
	Diameter	mm	25.350
	Length	m	0.02483
	Diameter	m	0.02535
Test Data Location	Raw Data File Name		2022-11-18_13-03-14 System-2-CELL-3 IG-BH04-PS005-HC25r_Pt1.csv
	Date & Time		2022-11-23 11:04:50
	Start Row		1079
	End Row		2500
Test Conditions	Avg Cell Temp	C	39.75
	Avg Confining Pressure	kPa	25425
	Pre Pulse Avg Pore Pressure	kPa	9114
	Pulse Pressure	kPa	-320
	Effective Stress	kPa	16312
Pore Fluid & Conditions	Post Pulse Avg Pore Pressure	kPa	8978
	Type		Water
	Salt	ppm	0
	Density	kg/m3	996.23
	Viscosity	kg.s/m	6.570E-04
Solution	Compressibility	1/Pa	4.36E-10
	Test System		System 2 - CELL 3
Brace	Nominal Decay Time	s	1421
	Brace Permeability	m2	1.17E-19
Hsieh	Permeability	m2	1.18E-19
	Specific Storage	1/m	3.44E-08
	Permeability	nD	119.3
	Hydraulic Conductivity	m/s	1.75E-12
	Pearson Coeff	()	0.9975146

IG_BH04_PS005_HC25r Eff Stress:16.31 MPa, HC=1.75e-12 m/s, SS=3.44e-8 1/m

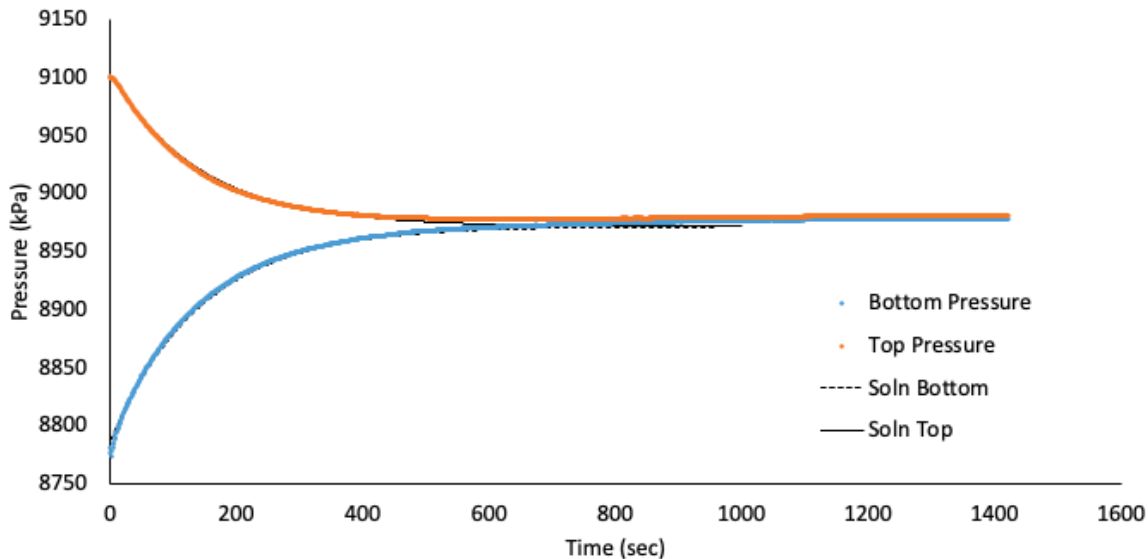


Figure 46 IG_BH04_PS005_HC25r: Effective Confining Stress = 16.31 MPa

	Sample Name		IG_BH04_PS005
	Specimen Name		IG_BH04_PS005_HC61a
	Specimen Top Depth		506.85
	Specimen Bottom Depth		506.912
	Test No		ES1
	Test Name		IG_BH04_PS005_HC61a_ES1
	Operator		StephenTalman/FrancyGuerrero
Dimensions	Length	mm	62.520
	Diameter	mm	61.140
	Length	m	0.06252
	Diameter	m	0.06114
Test Data Location	Raw Data File Name		IG-BH04-PS005-HC61a-001-C.dat
	Date & Time		2022-11-18 12:58:23
	Start Row		1373
	End Row		1450
Test Conditions	Avg Cell Temp	C	39.95
	Avg Confining Pressure	kPa	18513
	Pre Pulse Avg Pore Pressure	kPa	9135
	Pulse Pressure	kPa	-413
	Effective Stress	kPa	9378
	Post Pulse Avg Pore Pressure	kPa	9041
Pore Fluid & Conditions	Type		Water
	Salt	ppm	0
	Density	kg/m3	996.16
	Viscosity	kg.s/m	6.545E-04
	Compressibility	1/Pa	4.36E-10
Solution	Test System		System2-CELL2
Brace	Nominal Decay Time	s	385
	Brace Permeability	m2	5.23E-19
Hsieh	Permeability	m2	5.16E-19
	Specific Storage	1/m	9.66E-08
	Permeability	nD	522.5
	Hydraulic Conductivity	m/s	7.70E-12
	Pearson Coeff	()	0.9940769

IG_BH04_PS005_HC61a Eff Stress:9.38 MPa, HC=7.70e-12 m/s, SS=9.66e-8 1/m

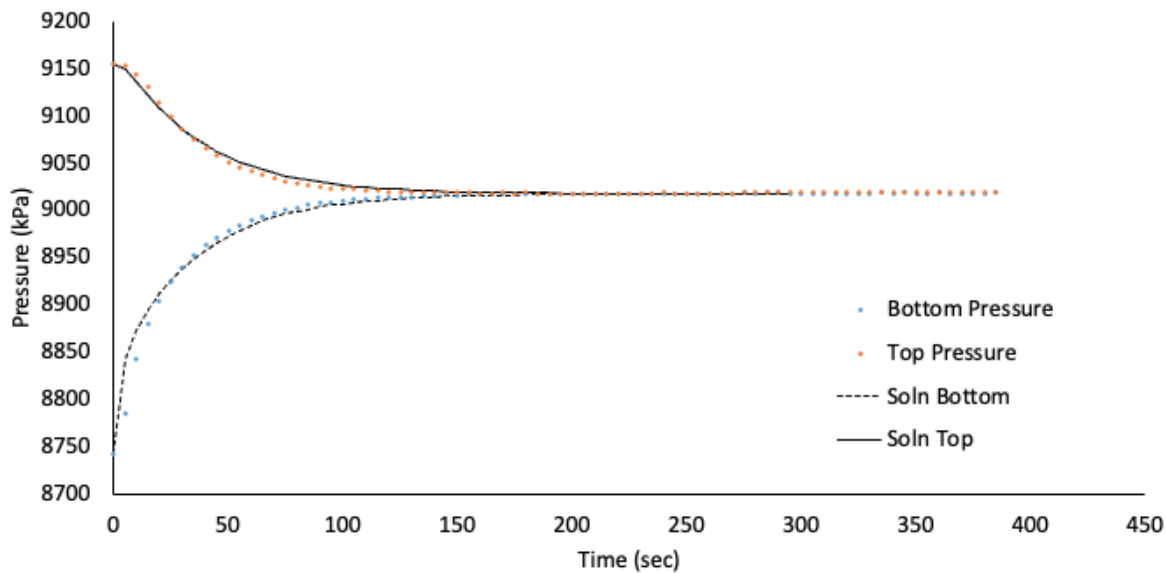


Figure 47 IG_BH04_PS005_HC61a: Effective Confining Stress = 9.38 MPa

	Sample Name		IG_BH04_PS005
	Specimen Name		IG_BH04_PS005_HC61a
	Specimen Top Depth		506.85
	Specimen Bottom Depth		506.912
	Test No		ES2
	Test Name		IG_BH04_PS005_HC61a_ES2
	Operator		StephenTalman/FrancyGuerrero
Dimensions	Length	mm	62.520
	Diameter	mm	61.140
	Length	m	0.06252
	Diameter	m	0.06114
Test Data Location	Raw Data File Name		IG-BH04-PS005-HC61a-002-B.dat
	Date & Time		2022-11-21 12:46:18
	Start Row		66
	End Row		600
Test Conditions	Avg Cell Temp	C	39.96
	Avg Confining Pressure	kPa	23472
	Pre Pulse Avg Pore Pressure	kPa	9398
	Pulse Pressure	kPa	499
	Effective Stress	kPa	14074
	Post Pulse Avg Pore Pressure	kPa	9278
Pore Fluid & Conditions	Type		Water
	Salt	ppm	0
	Density	kg/m3	996.27
	Viscosity	kg.s/m	6.544E-04
	Compressibility	1/Pa	4.36E-10
Solution	Test System		System2-CELL2
Brace	Nominal Decay Time	s	787
	Brace Permeability	m2	2.76E-19
Hsieh	Permeability	m2	3.45E-19
	Specific Storage	1/m	1.80E-07
	Permeability	nD	350.0
	Hydraulic Conductivity	m/s	5.16E-12
	Pearson Coeff	()	0.9995974

IG_BH04_PS005_HC61a Eff Stress:14.07 MPa, HC=5.16e-12 m/s, SS=1.80e-7 1/m

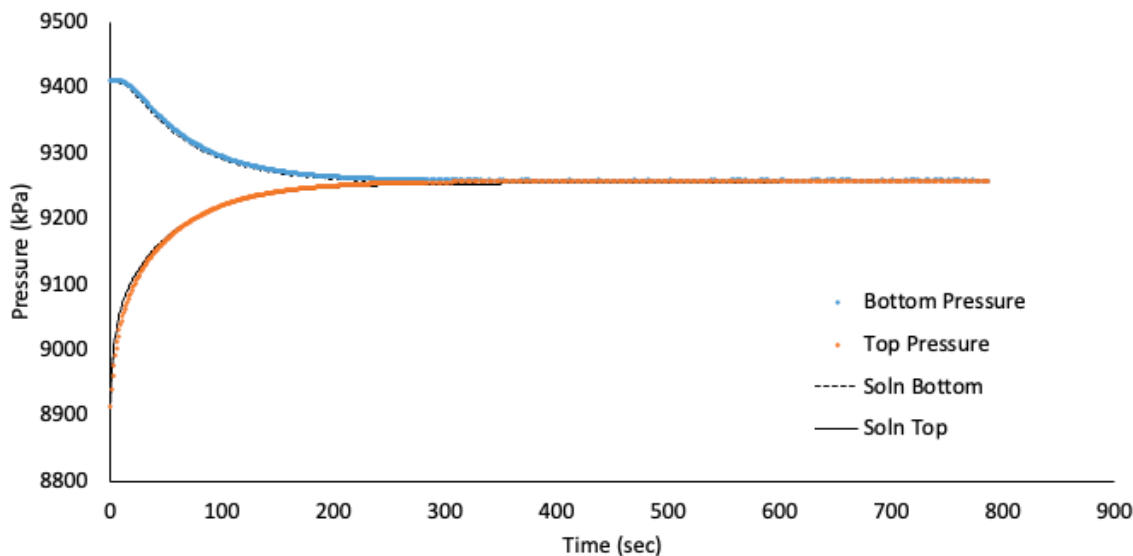


Figure 48 IG_BH04_PS005_HC61a: Effective Confining Stress = 14.07 MPa

	Sample Name		IG_BH04_PS005
	Specimen Name		IG_BH04_PS005_HC61a
	Specimen Top Depth		506.85
	Specimen Bottom Depth		506.912
	Test No		ES3
	Test Name		IG_BH04_PS005_HC61a_ES3
	Operator		StephenTalman/FrancyGuerrero
Dimensions	Length	mm	62.520
	Diameter	mm	61.140
	Length	m	0.06252
	Diameter	m	0.06114
Test Data Location	Raw Data File Name		IG-BH04-PS005-HC61a-003-A.dat
	Date & Time		2022-11-23 11:03:13
	Start Row		74
	End Row		700
Test Conditions	Avg Cell Temp	C	39.97
	Avg Confining Pressure	kPa	25072
	Pre Pulse Avg Pore Pressure	kPa	9103
	Pulse Pressure	kPa	-313
	Effective Stress	kPa	15969
Pore Fluid & Conditions	Post Pulse Avg Pore Pressure	kPa	9072
	Type		Water
	Salt	ppm	0
	Density	kg/m3	996.12
	Viscosity	kg.s/m	6.543E-04
Solution	Compressibility	1/Pa	4.36E-10
	Test System		System2-CELL2
Brace	Nominal Decay Time	s	1032
	Brace Permeability	m2	1.46E-19
Hsieh	Permeability	m2	1.36E-19
	Specific Storage	1/m	1.15E-07
	Permeability	nD	138.3
	Hydraulic Conductivity	m/s	2.04E-12
	Pearson Coeff	()	0.9991038

IG_BH04_PS005_HC61a Eff Stress:15.97 MPa, HC=2.04e-12 m/s, SS=1.15e-7 1/m

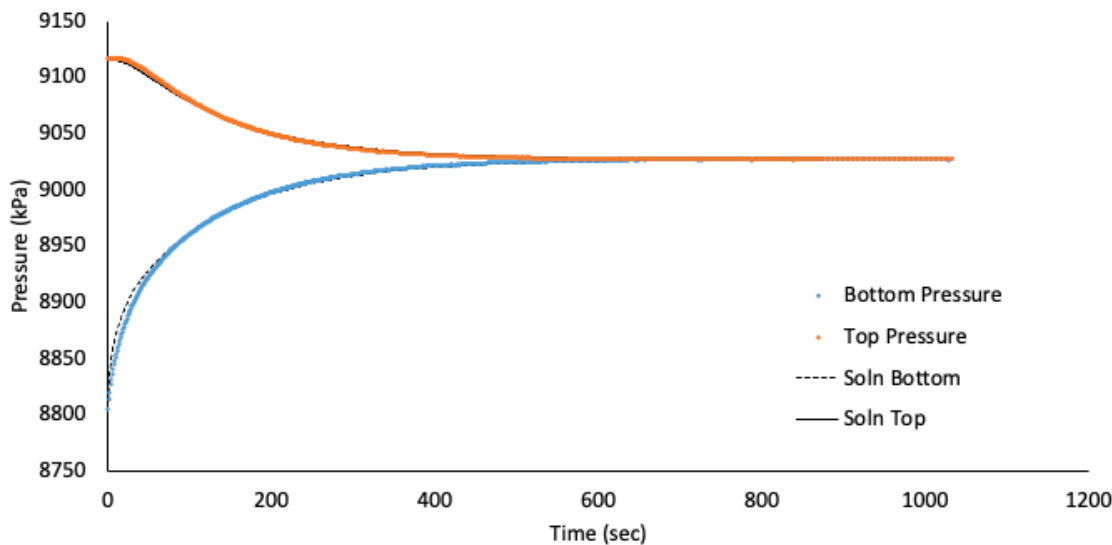


Figure 49 IG_BH04_PS005_HC61a: Effective Confining Stress = 15.97 MPa

	Sample Name		IG_BH04_PS006
	Specimen Name		IG_BH04_PS006_HC25a
	Specimen Top Depth		559.442
	Specimen Bottom Depth		559.477
	Test No		ES1
	Test Name		IG_BH04_PS006_HC25a_ES1
	Operator		StephenTalman/FrancyGuerrero
Dimensions	Length	mm	23.710
	Diameter	mm	25.340
	Length	m	0.02371
	Diameter	m	0.02534
Test Data Location	Raw Data File Name		IG-BH04-PS006-HC25a-004-B.dat
	Date & Time		2023-02-28 13:16:19
	Start Row		62
	End Row		700
Test Conditions	Avg Cell Temp	C	40.39
	Avg Confining Pressure	kPa	19675
	Pre Pulse Avg Pore Pressure	kPa	9219
	Pulse Pressure	kPa	-396
	Effective Stress	kPa	10456
Pore Fluid & Conditions	Post Pulse Avg Pore Pressure	kPa	9132
	Type		Water
	Salt	ppm	0
	Density	kg/m3	996.03
	Viscosity	kg.s/m	6.492E-04
Solution	Compressibility	1/Pa	4.36E-10
	Test System		System3-Cell1
Brace	Nominal Decay Time	s	1044
	Brace Permeability	m2	1.51E-19
Hsieh	Permeability	m2	1.59E-19
	Specific Storage	1/m	2.13E-07
	Permeability	nD	161.3
	Hydraulic Conductivity	m/s	2.40E-12
	Pearson Coeff	()	0.9998612

IG_BH04_PS006_HC25a Eff Stress:10.46 MPa, HC=2.40e-12 m/s, SS=2.13e-7 1/m

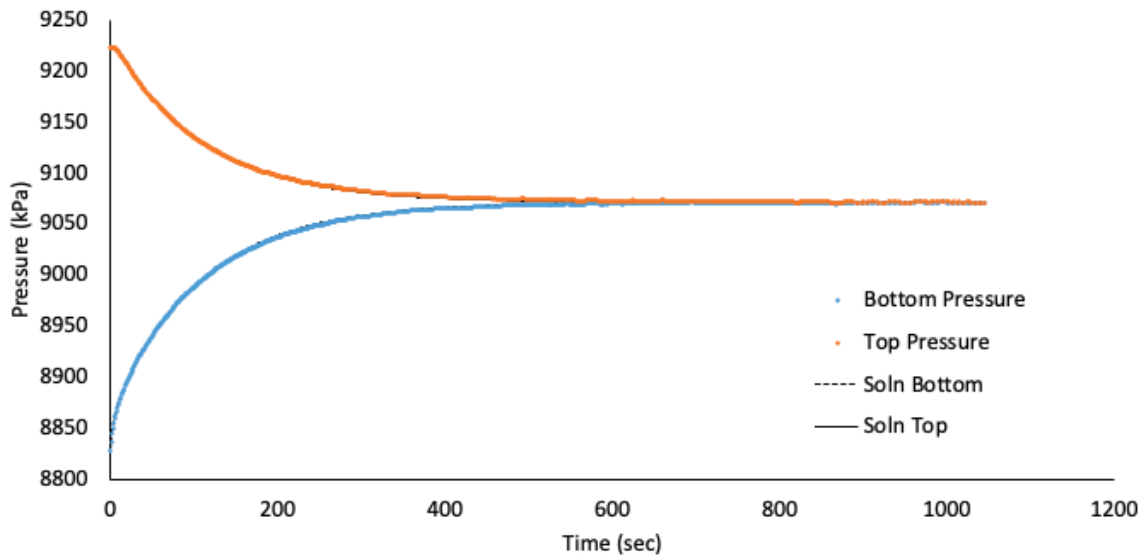


Figure 50 IG_BH04_PS006_HC25a: Effective Confining Stress = 10.46 MPa

	Sample Name		IG_BH04_PS006
	Specimen Name		IG_BH04_PS006_HC25a
	Specimen Top Depth		559.442
	Specimen Bottom Depth		559.477
	Test No		ES2
	Test Name		IG_BH04_PS006_HC25a_ES2
	Operator		StephenTalman/FrancyGuerrero
Dimensions	Length	mm	23.710
	Diameter	mm	25.340
	Length	m	0.02371
	Diameter	m	0.02534
Test Data Location	Raw Data File Name		IG-BH04-PS006-HC25a-005-D.dat
	Date & Time		2023-03-01 08:36:48
	Start Row		77
	End Row		966
Test Conditions	Avg Cell Temp	C	40.44
	Avg Confining Pressure	kPa	24673
	Pre Pulse Avg Pore Pressure	kPa	9197
	Pulse Pressure	kPa	-388
	Effective Stress	kPa	15476
	Post Pulse Avg Pore Pressure	kPa	9145
Pore Fluid & Conditions	Type		Water
	Salt	ppm	0
	Density	kg/m3	996
	Viscosity	kg.s/m	6.486E-04
	Compressibility	1/Pa	4.36E-10
Solution	Test System		System3-Cell1
Brace	Nominal Decay Time	s	1846
	Brace Permeability	m2	5.22E-20
Hsieh	Permeability	m2	4.71E-20
	Specific Storage	1/m	1.22E-07
	Permeability	nD	47.7
	Hydraulic Conductivity	m/s	7.10E-13
	Pearson Coeff	()	0.9996204

IG_BH04_PS006_HC25a Eff Stress:15.48 MPa, HC=7.10e-13 m/s, SS=1.22e-7 1/m

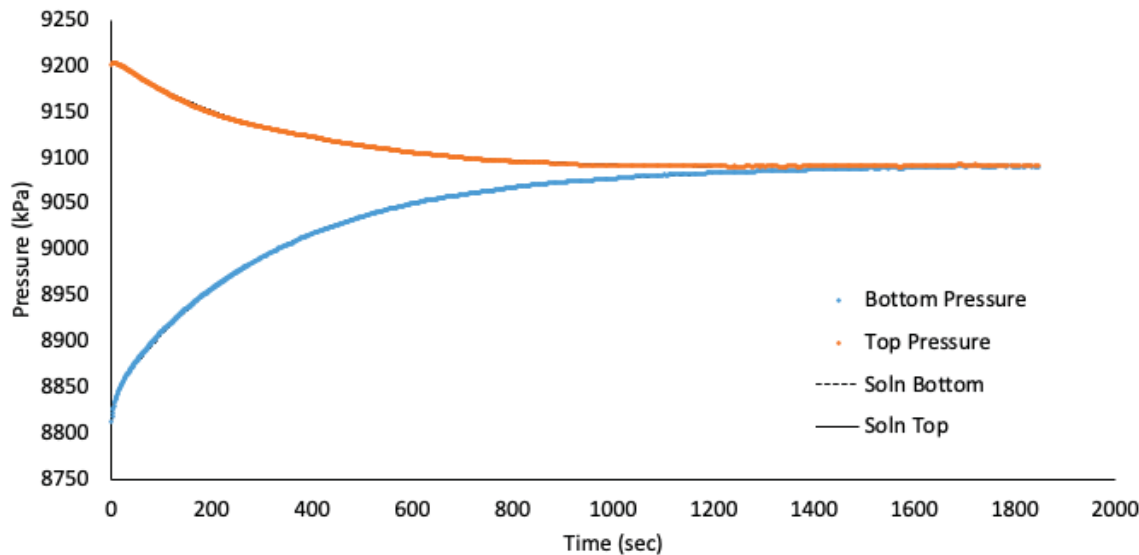


Figure 51 IG_BH04_PS006_HC25a: Effective Confining Stress = 15.48 MPa

	Sample Name		IG_BH04_PS006
	Specimen Name		IG_BH04_PS006_HC25a
	Specimen Top Depth		559.442
	Specimen Bottom Depth		559.477
	Test No		ES3
	Test Name		IG_BH04_PS006_HC25a_ES3
	Operator		StephenTalman/FrancyGuerrero
Dimensions	Length	mm	23.710
	Diameter	mm	25.340
	Length	m	0.02371
	Diameter	m	0.02534
Test Data Location	Raw Data File Name		IG-BH04-PS006-HC25a-005-H.dat
	Date & Time		2023-03-01 08:36:48
	Start Row		85
	End Row		1317
Test Conditions	Avg Cell Temp	C	40.39
	Avg Confining Pressure	kPa	26620
	Pre Pulse Avg Pore Pressure	kPa	9091
	Pulse Pressure	kPa	516
	Effective Stress	kPa	17529
Pore Fluid & Conditions	Post Pulse Avg Pore Pressure	kPa	8916
	Type		Water
	Salt	ppm	0
	Density	kg/m3	995.97
	Viscosity	kg.s/m	6.492E-04
Solution	Compressibility	1/Pa	4.36E-10
	Test System		System3-Cell1
Brace	Nominal Decay Time	s	3312
	Brace Permeability	m2	3.64E-20
Hsieh	Permeability	m2	3.85E-20
	Specific Storage	1/m	5.66E-08
	Permeability	nD	39.1
	Hydraulic Conductivity	m/s	5.80E-13
	Pearson Coeff	()	0.9998030

IG_BH04_PS006_HC25a Eff Stress:17.53 MPa, HC=5.80e-13 m/s, SS=5.66e-8 1/m

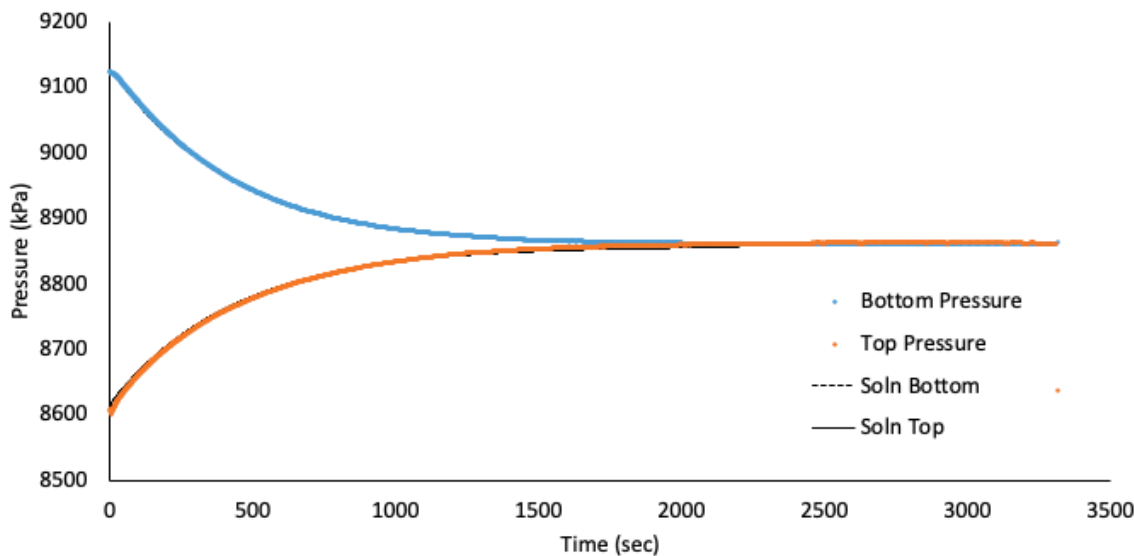


Figure 52 IG_BH04_PS006_HC25a: Effective Confining Stress = 17.53 MPa

	Sample Name		IG_BH04_PS006
	Specimen Name		IG_BH04_PS006_HC25r
	Specimen Top Depth		559.345
	Specimen Bottom Depth		559.380
	Test No		ES1
	Test Name		IG_BH04_PS006_HC25r_ES1
	Operator		Stephen Talman/ Francy Guerrero
Dimensions	Length	mm	23.940
	Diameter	mm	25.360
	Length	m	0.02394
	Diameter	m	0.02536
Test Data Location	Raw Data File Name		2022-11-09_15-01-42 System-3-Cell-3 IG-BH04-PS006-HC25r.csv
	Date & Time		2022-11-15 10:32:07
	Start Row		4966
	End Row		6500
Test Conditions	Avg Cell Temp	C	39.78
	Avg Confining Pressure	kPa	19532
	Pre Pulse Avg Pore Pressure	kPa	9312
	Pulse Pressure	kPa	132
	Effective Stress	kPa	10220
	Post Pulse Avg Pore Pressure	kPa	9351
Pore Fluid & Conditions	Type		Water
	Salt	ppm	0
	Density	kg/m3	996.3
	Viscosity	kg.s/m	6.566E-04
	Compressibility	1/Pa	4.36E-10
Solution	Test System		System 3 - Cell 3
Brace	Nominal Decay Time	s	1534
	Brace Permeability	m2	8.84E-20
Hsieh	Permeability	m2	9.73E-20
	Specific Storage	1/m	1.72E-07
	Permeability	nD	98.6
	Hydraulic Conductivity	m/s	1.45E-12
	Pearson Coeff	()	0.9990412

IG_BH04_PS006_HC25r Eff Stress:10.22 MPa, HC=1.45e-12 m/s, SS=1.72e-7 1/m

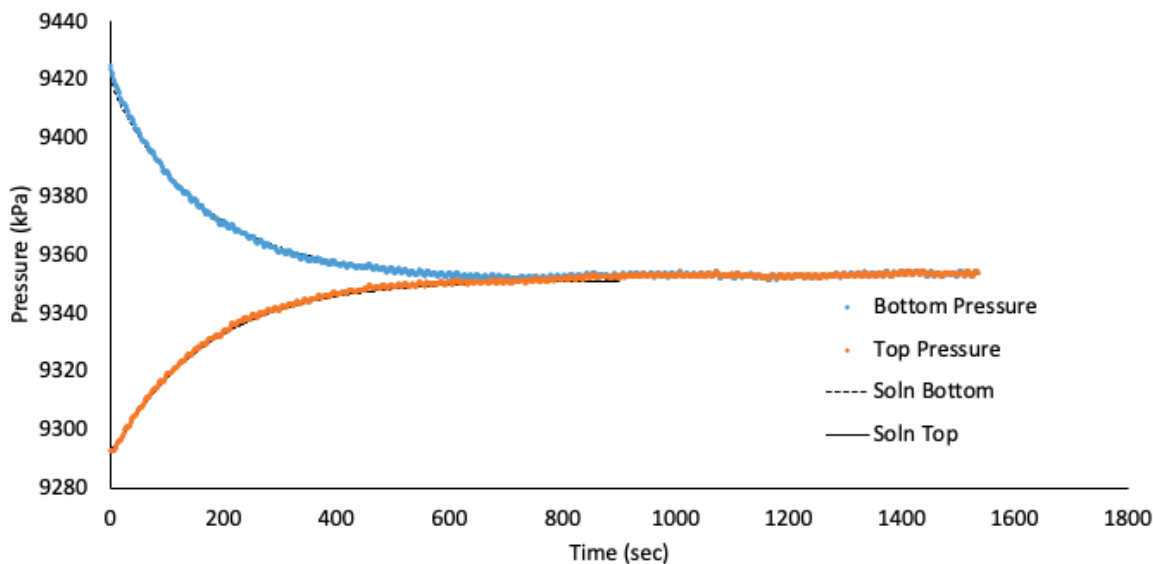


Figure 53 IG_BH04_PS006_HC25r: Effective Confining Stress = 10.22 MPa

	Sample Name		IG_BH04_PS006
	Specimen Name		IG_BH04_PS006_HC25r
	Specimen Top Depth		559.345
	Specimen Bottom Depth		559.380
	Test No		ES2
	Test Name		IG_BH04_PS006_HC25r_ES2
	Operator		Stephen Talman/ Francy Guerrero
Dimensions	Length	mm	23.940
	Diameter	mm	25.360
	Length	m	0.02394
	Diameter	m	0.02536
Test Data Location	Raw Data File Name		2022-11-09_15-01-42 System-3-Cell-3 IG-BH04-PS006-HC25r.csv
	Date & Time		2022-11-16 11:31:40
	Start Row		1345
	End Row		5530
Test Conditions	Avg Cell Temp	C	39.79
	Avg Confining Pressure	kPa	24508
	Pre Pulse Avg Pore Pressure	kPa	9173
	Pulse Pressure	kPa	-434
	Effective Stress	kPa	15335
	Post Pulse Avg Pore Pressure	kPa	8994
Pore Fluid & Conditions	Type		Water
	Salt	ppm	0
	Density	kg/m3	996.24
	Viscosity	kg.s/m	6.565E-04
	Compressibility	1/Pa	4.36E-10
Solution	Test System		System 3 - Cell 3
Brace	Nominal Decay Time	s	4185
	Brace Permeability	m2	3.24E-20
Hsieh	Permeability	m2	3.24E-20
	Specific Storage	1/m	7.82E-08
	Permeability	nD	32.8
	Hydraulic Conductivity	m/s	4.83E-13
	Pearson Coeff	()	0.9998239

IG_BH04_PS006_HC25r Eff Stress:15.33 MPa, HC=4.83e-13 m/s, SS=7.82e-8 1/m

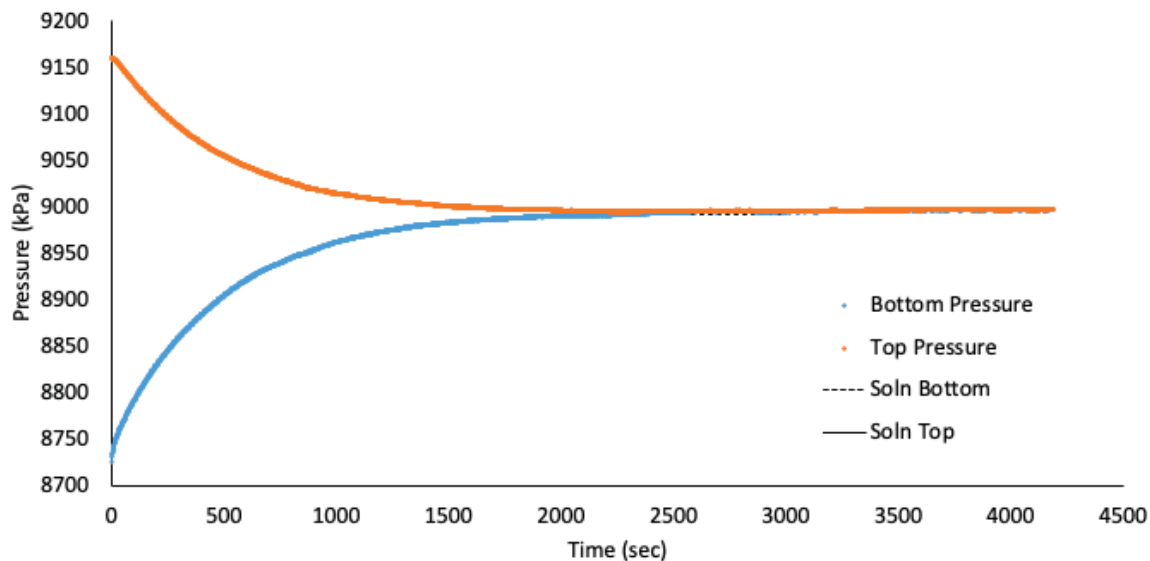


Figure 54 IG_BH04_PS006_HC25r: Effective Confining Stress = 15.33 MPa

	Sample Name		IG_BH04_PS006
	Specimen Name		IG_BH04_PS006_HC25r
	Specimen Top Depth		559.345
	Specimen Bottom Depth		559.380
	Test No		ES3
	Test Name		IG_BH04_PS006_HC25r_ES3
	Operator		Stephen Talman/ Francy Guerrero
Dimensions	Length	mm	23.940
	Diameter	mm	25.360
	Length	m	0.02394
	Diameter	m	0.02536
Test Data Location	Raw Data File Name		2022-11-09_15-01-42 System-3-Cell-3 IG-BH04-PS006-HC25r.csv
	Date & Time		2022-11-17 10:46:51
	Start Row		1898
	End Row		9000
Test Conditions	Avg Cell Temp	C	39.88
	Avg Confining Pressure	kPa	25094
	Pre Pulse Avg Pore Pressure	kPa	9840
	Pulse Pressure	kPa	611
	Effective Stress	kPa	15254
	Post Pulse Avg Pore Pressure	kPa	9607
Pore Fluid & Conditions	Type		Water
	Salt	ppm	0
	Density	kg/m3	996.49
	Viscosity	kg.s/m	6.555E-04
	Compressibility	1/Pa	4.36E-10
Solution	Test System		System 3 - Cell 3
Brace	Nominal Decay Time	s	7102
	Brace Permeability	m2	1.18E-20
Hsieh	Permeability	m2	1.29E-20
	Specific Storage	1/m	7.00E-08
	Permeability	nD	13.1
	Hydraulic Conductivity	m/s	1.93E-13
	Pearson Coeff	()	0.9999058

IG_BH04_PS006_HC25r Eff Stress:15.25 MPa, HC=1.93e-13 m/s, SS=7.00e-8 1/m

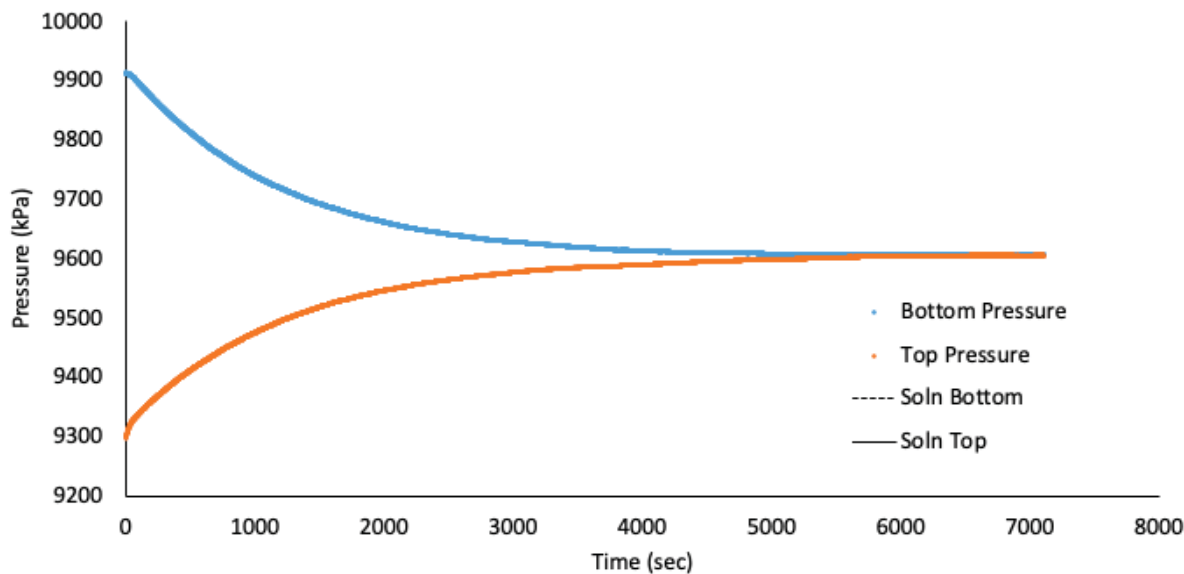


Figure 55 IG_BH04_PS006_HC25r: Effective Confining Stress = 15.25 MPa

	Sample Name		IG_BH04_PS006
	Specimen Name		IG_BH04_PS006_HC61a
	Specimen Top Depth		559.38
	Specimen Bottom Depth		559.442
	Test No		ES1
	Test Name		IG_BH04_PS006_HC61a_ES1
	Operator		Stephen Talman/ Francy Guerrero
Dimensions	Length	mm	63.030
	Diameter	mm	61.140
	Length	m	0.06303
	Diameter	m	0.06114
Test Data Location	Raw Data File Name		2022-11-15_10-32-01 System-3-Cell-2 IG-BH04-PS006-HC61a.csv
	Date & Time		2022-11-15 10:32:01
	Start Row		4174
	End Row		4960
Test Conditions	Avg Cell Temp	C	40.23
	Avg Confining Pressure	kPa	19571
	Pre Pulse Avg Pore Pressure	kPa	9283
	Pulse Pressure	kPa	-360
	Effective Stress	kPa	10288
	Post Pulse Avg Pore Pressure	kPa	9207
Pore Fluid & Conditions	Type		Water
	Salt	ppm	0
	Density	kg/m3	996.12
	Viscosity	kg.s/m	6.511E-04
	Compressibility	1/Pa	4.36E-10
Solution	Test System		System 3 - Cell 2
Brace	Nominal Decay Time	s	786
	Brace Permeability	m2	5.04E-20
Hsieh	Permeability	m2	4.70E-20
	Specific Storage	1/m	4.80E-08
	Permeability	nD	47.6
	Hydraulic Conductivity	m/s	7.06E-13
	Pearson Coeff	()	0.9993592

IG_BH04_PS006_HC61a Eff Stress:10.29 MPa, HC=7.06e-13 m/s, SS=4.80e-8 1/m

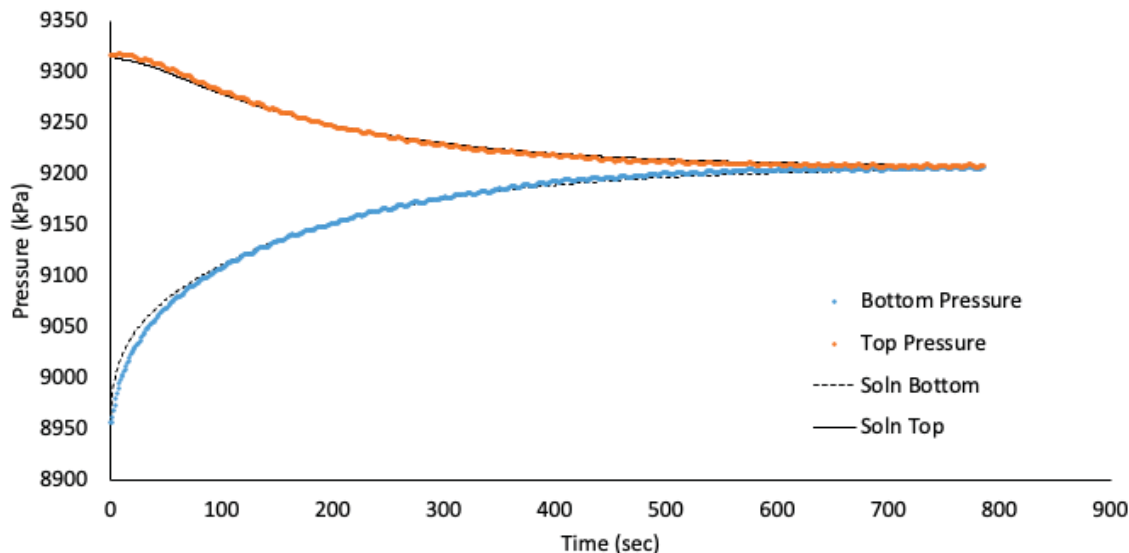


Figure 56 IG_BH04_PS006_HC61a: Effective Confining Stress = 10.29 MPa

	Sample Name		IG_BH04_PS006
	Specimen Name		IG_BH04_PS006_HC61a
	Specimen Top Depth		559.38
	Specimen Bottom Depth		559.442
	Test No		ES2
	Test Name		IG_BH04_PS006_HC61a_ES2
	Operator		Stephen Talman/ Francy Guerrero
Dimensions	Length	mm	63.030
	Diameter	mm	61.140
	Length	m	0.06303
	Diameter	m	0.06114
Test Data Location	Raw Data File Name		2022-11-15_10-32-01 System-3-Cell-2 IG-BH04-PS006-HC61a.csv
	Date & Time		2022-11-16 11:31:38
	Start Row		79573
	End Row		82000
Test Conditions	Avg Cell Temp	C	40.25
	Avg Confining Pressure	kPa	24558
	Pre Pulse Avg Pore Pressure	kPa	9127
	Pulse Pressure	kPa	-414
	Effective Stress	kPa	15431
	Post Pulse Avg Pore Pressure	kPa	9030
Pore Fluid & Conditions	Type		Water
	Salt	ppm	0
	Density	kg/m3	996.04
	Viscosity	kg.s/m	6.509E-04
	Compressibility	1/Pa	4.36E-10
Solution	Test System		System 3 - Cell 2
Brace	Nominal Decay Time	s	2427
	Brace Permeability	m2	2.16E-20
Hsieh	Permeability	m2	2.11E-20
	Specific Storage	1/m	6.27E-08
	Permeability	nD	21.4
	Hydraulic Conductivity	m/s	3.18E-13
	Pearson Coeff	()	0.9995493

IG_BH04_PS006_HC61a Eff Stress:15.43 MPa, HC=3.18e-13 m/s, SS=6.27e-8 1/m

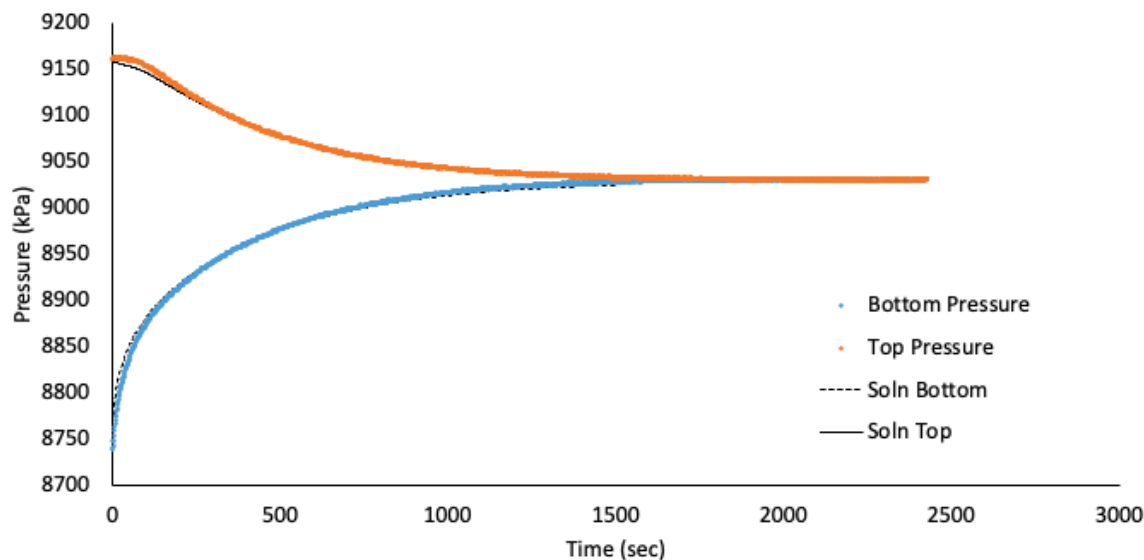


Figure 57 IG_BH04_PS006_HC61a: Effective Confining Stress = 15.43 MPa

	Sample Name		IG_BH04_PS006
	Specimen Name		IG_BH04_PS006_HC61a
	Specimen Top Depth		559.38
	Specimen Bottom Depth		559.442
	Test No		ES3
	Test Name		IG_BH04_PS006_HC61a_ES3
	Operator		Stephen Talman/ Francy Guerrero
Dimensions	Length	mm	63.030
	Diameter	mm	61.140
	Length	m	0.06303
	Diameter	m	0.06114
Test Data Location	Raw Data File Name		2022-11-17_10-46-49 System-3-Cell-2 IG-BH04-PS006-HC61a_filtered.csv
	Date & Time		2022-11-17 10:46:49
	Start Row		35739
	End Row		43000
Test Conditions	Avg Cell Temp	C	40.29
	Avg Confining Pressure	kPa	25193
	Pre Pulse Avg Pore Pressure	kPa	9428
	Pulse Pressure	kPa	-310
	Effective Stress	kPa	15766
	Post Pulse Avg Pore Pressure	kPa	9323
Pore Fluid & Conditions	Type		Water
	Salt	ppm	0
	Density	kg/m3	996.16
	Viscosity	kg.s/m	6.504E-04
	Compressibility	1/Pa	4.36E-10
Solution	Test System		System 3 - Cell 2
Brace	Nominal Decay Time	s	7261
	Brace Permeability	m2	8.63E-21
Hsieh	Permeability	m2	9.13E-21
	Specific Storage	1/m	3.23E-08
	Permeability	nD	9.2
	Hydraulic Conductivity	m/s	1.37E-13
	Pearson Coeff	()	0.9990771

IG_BH04_PS006_HC61a Eff Stress:15.77 MPa, HC=1.37e-13 m/s, SS=3.23e-8 1/m

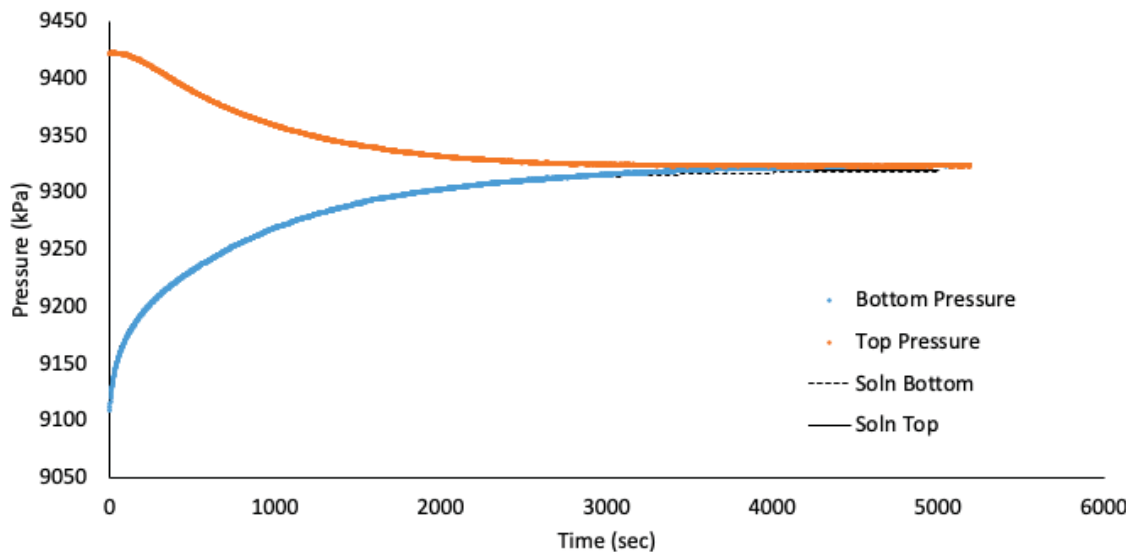


Figure 58 IG_BH04_PS006_HC61a: Effective Confining Stress = 15.77 MPa

	Sample Name		IG_BH04_PS008
	Specimen Name		IG_BH04_PS008_HC25a
	Specimen Top Depth		714.145
	Specimen Bottom Depth		714.180
	Test No		ES1
	Test Name		IG_BH04_PS008_HC25a_ES1
	Operator		StephenTalman/FrancyGuerrero
Dimensions	Length	mm	24.160
	Diameter	mm	25.390
	Length	m	0.02416
	Diameter	m	0.02539
Test Data Location	Raw Data File Name		IG-BH04-PS008-HC25a-001-A.dat
	Date & Time		2023-01-16 08:44:48
	Start Row		83
	End Row		1300
Test Conditions	Avg Cell Temp	C	40.33
	Avg Confining Pressure	kPa	22572
	Pre Pulse Avg Pore Pressure	kPa	9209
	Pulse Pressure	kPa	341
	Effective Stress	kPa	13363
	Post Pulse Avg Pore Pressure	kPa	9453
Pore Fluid & Conditions	Type		Water
	Salt	ppm	0
	Density	kg/m3	996.05
	Viscosity	kg.s/m	6.499E-04
	Compressibility	1/Pa	4.36E-10
Solution	Test System		System3-Cell1
Brace	Nominal Decay Time	s	3229
	Brace Permeability	m2	4.02E-20
Hsieh	Permeability	m2	4.35E-20
	Specific Storage	1/m	9.51E-08
	Permeability	nD	44.0
	Hydraulic Conductivity	m/s	6.54E-13
	Pearson Coeff	()	0.9997856

IG_BH04_PS008_HC25a Eff Stress:13.36 MPa, HC=6.54e-13 m/s, SS=9.51e-8 1/m

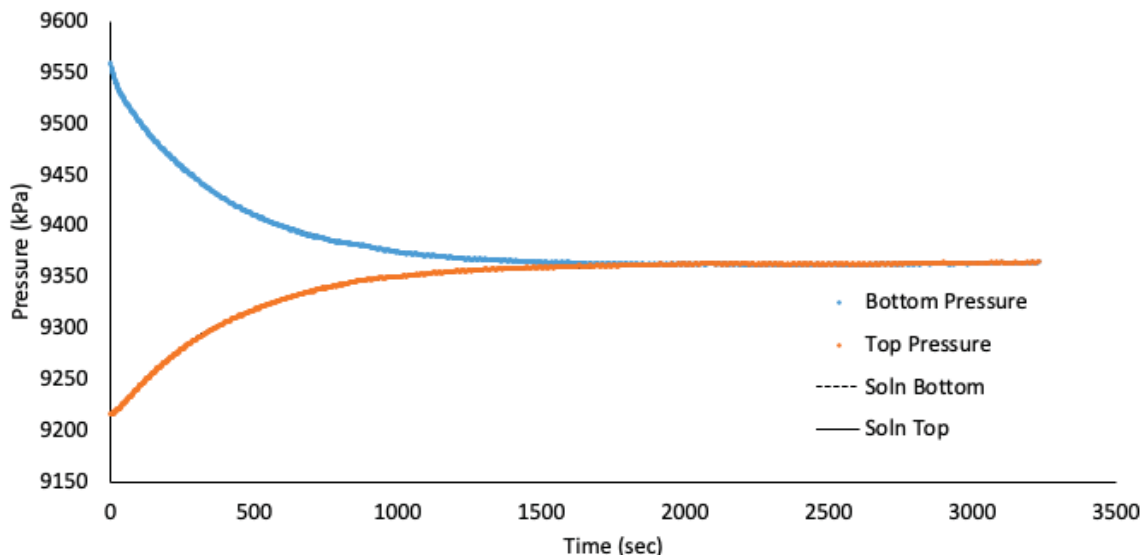


Figure 59 IG_BH04_PS008_HC25a: Effective Confining Stress = 13.36 MPa

	Sample Name		IG_BH04_PS008
	Specimen Name		IG_BH04_PS008_HC25a
	Specimen Top Depth		714.145
	Specimen Bottom Depth		714.180
	Test No		ES2
	Test Name		IG_BH04_PS008_HC25a_ES2
	Operator		StephenTalman/FrancyGuerrero
Dimensions	Length	mm	24.160
	Diameter	mm	25.390
	Length	m	0.02416
	Diameter	m	0.02539
Test Data Location	Raw Data File Name		IG-BH04-PS008-HC25a-002-C.dat
	Date & Time		2023-01-17 07:55:41
	Start Row		69
	End Row		2150
Test Conditions	Avg Cell Temp	C	40.37
	Avg Confining Pressure	kPa	27567
	Pre Pulse Avg Pore Pressure	kPa	9392
	Pulse Pressure	kPa	641
	Effective Stress	kPa	18175
	Post Pulse Avg Pore Pressure	kPa	9357
Pore Fluid & Conditions	Type		Water
	Salt	ppm	0
	Density	kg/m3	996.11
	Viscosity	kg.s/m	6.495E-04
	Compressibility	1/Pa	4.36E-10
Solution	Test System		System3-Cell1
Brace	Nominal Decay Time	s	8402
	Brace Permeability	m2	1.45E-20
Hsieh	Permeability	m2	1.53E-20
	Specific Storage	1/m	5.83E-08
	Permeability	nD	15.5
	Hydraulic Conductivity	m/s	2.30E-13
	Pearson Coeff	()	0.9996955

IG_BH04_PS008_HC25a Eff Stress:18.18 MPa, HC=2.30e-13 m/s, SS=5.83e-8 1/m

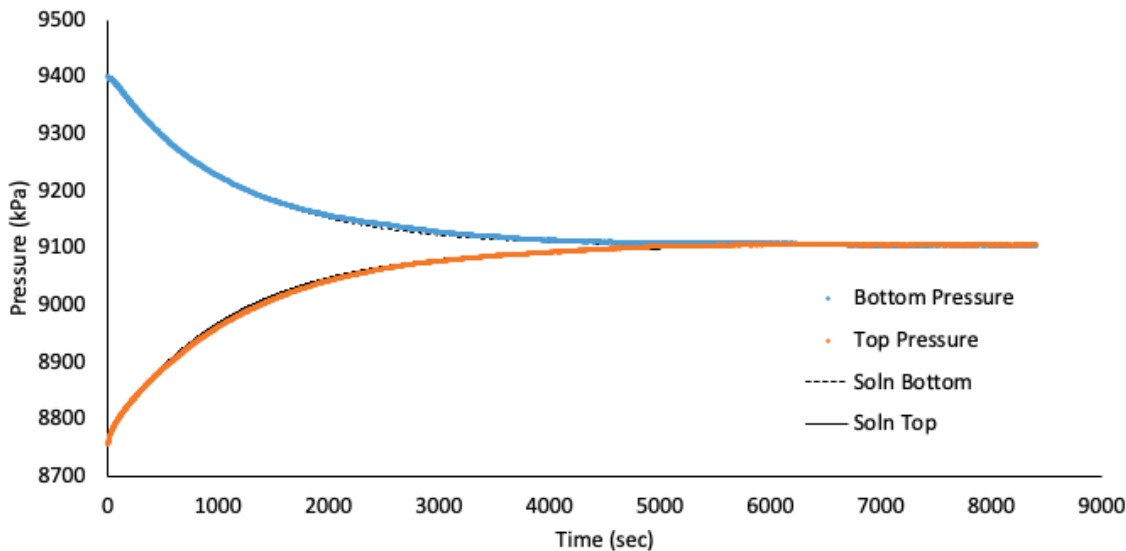


Figure 60 IG_BH04_PS008_HC25a: Effective Confining Stress = 18.18 MPa

	Sample Name		IG_BH04_PS008
	Specimen Name		IG_BH04_PS008_HC25a
	Specimen Top Depth		714.145
	Specimen Bottom Depth		714.180
	Test No		ES3
	Test Name		IG_BH04_PS008_HC25a_ES3
	Operator		StephenTalman/FrancyGuerrero
Dimensions	Length	mm	24.160
	Diameter	mm	25.390
	Length	m	0.02416
	Diameter	m	0.02539
Test Data Location	Raw Data File Name		IG-BH04-PS008-HC25a-003-C.dat
	Date & Time		2023-01-19 11:04:41
	Start Row		50
	End Row		3000
Test Conditions	Avg Cell Temp	C	40.38
	Avg Confining Pressure	kPa	32558
	Pre Pulse Avg Pore Pressure	kPa	9365
	Pulse Pressure	kPa	485
	Effective Stress	kPa	23193
	Post Pulse Avg Pore Pressure	kPa	9500
Pore Fluid & Conditions	Type		Water
	Salt	ppm	0
	Density	kg/m3	996.09
	Viscosity	kg.s/m	6.493E-04
	Compressibility	1/Pa	4.36E-10
Solution	Test System		System3-Cell1
Brace	Nominal Decay Time	s	16027
	Brace Permeability	m2	5.15E-21
Hsieh	Permeability	m2	5.20E-21
	Specific Storage	1/m	7.93E-09
	Permeability	nD	5.3
	Hydraulic Conductivity	m/s	7.83E-14
	Pearson Coeff	()	0.9986928

IG_BH04_PS008_HC25a Eff Stress:23.19 MPa, HC=7.83e-14 m/s, SS=7.93e-9 1/m

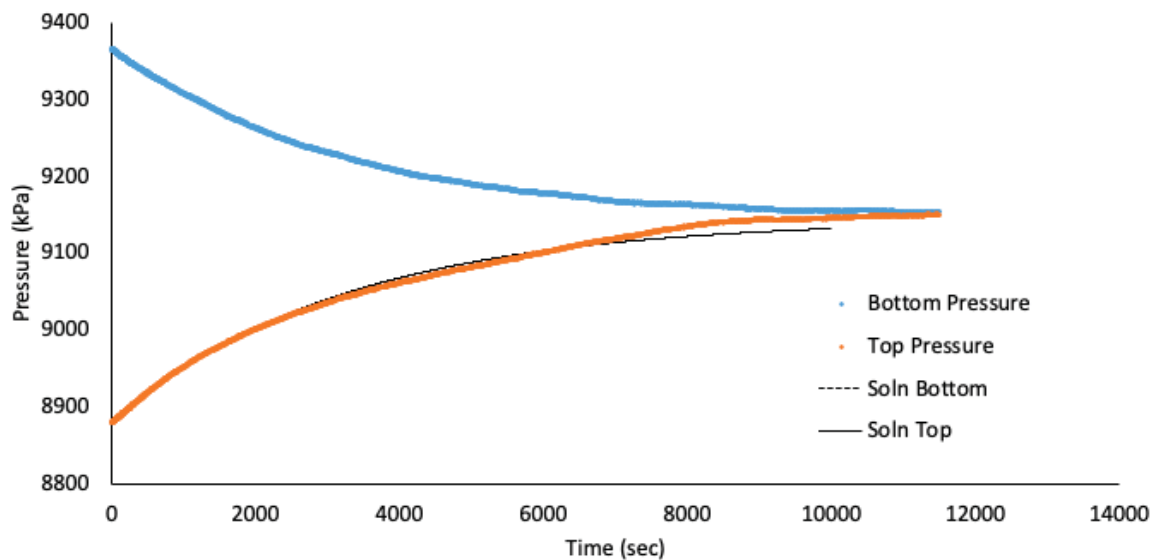


Figure 61 IG_BH04_PS008_HC25a: Effective Confining Stress = 23.19 MPa

	Sample Name		IG_BH04_PS008
	Specimen Name		IG_BH04_PS008_HC61a
	Specimen Top Depth		714.18
	Specimen Bottom Depth		714.242
	Test No		ES1
	Test Name		IG_BH04_PS008_HC61a_ES1
	Operator		StephenTalman/FrancyGuerrero
Dimensions	Length	mm	62.540
	Diameter	mm	61.590
	Length	m	0.06254
	Diameter	m	0.06159
Test Data Location	Raw Data File Name		IG-BH04-PS008-HC61a-001-B.dat
	Date & Time		2023-01-16 08:46:19
	Start Row		85
	End Row		1300
Test Conditions	Avg Cell Temp	C	40.18
	Avg Confining Pressure	kPa	22568
	Pre Pulse Avg Pore Pressure	kPa	9360
	Pulse Pressure	kPa	-413
	Effective Stress	kPa	13207
Pore Fluid & Conditions	Post Pulse Avg Pore Pressure	kPa	9243
	Type		Water
	Salt	ppm	0
	Density	kg/m3	996.17
	Viscosity	kg.s/m	6.519E-04
Solution	Compressibility	1/Pa	4.36E-10
	Test System		System3-Cell2
Brace	Nominal Decay Time	s	3227
	Brace Permeability	m2	5.23E-20
Hsieh	Permeability	m2	5.23E-20
	Specific Storage	1/m	8.64E-08
	Permeability	nD	53.0
	Hydraulic Conductivity	m/s	7.85E-13
	Pearson Coeff	()	0.9997292

IG_BH04_PS008_HC61a Eff Stress:13.21 MPa, HC=7.85e-13 m/s, SS=8.64e-8 1/m

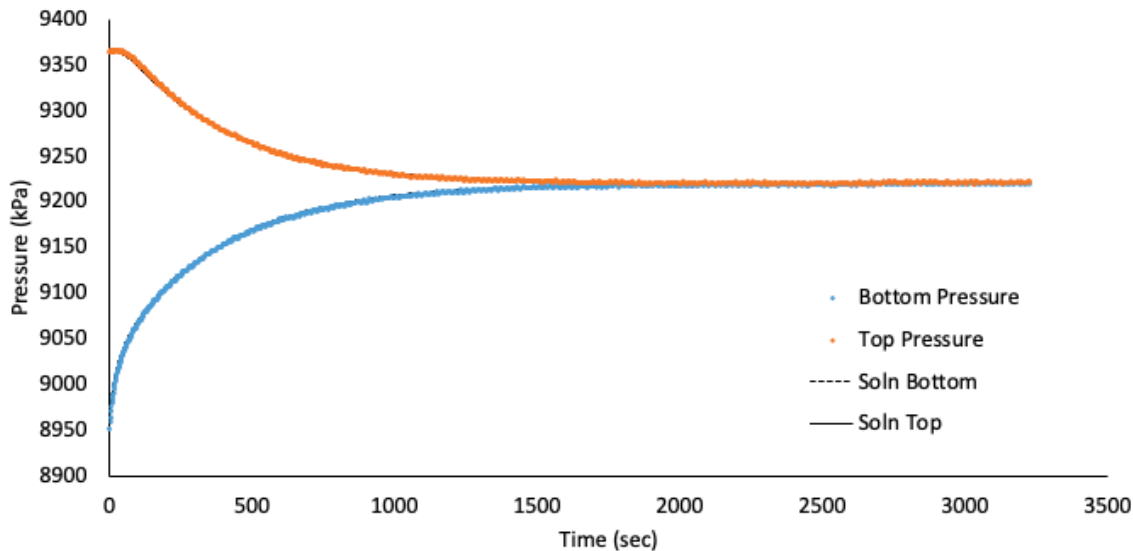


Figure 62 IG_BH04_PS008_HC61a: Effective Confining Stress = 13.21 MPa

	Sample Name		IG_BH04_PS008
	Specimen Name		IG_BH04_PS008_HC61a
	Specimen Top Depth		714.18
	Specimen Bottom Depth		714.242
	Test No		ES2
	Test Name		IG_BH04_PS008_HC61a_ES2
	Operator		StephenTalman/FrancyGuerrero
Dimensions	Length	mm	62.540
	Diameter	mm	61.590
	Length	m	0.06254
	Diameter	m	0.06159
Test Data Location	Raw Data File Name		IG-BH04-PS008-HC61a-002-C.dat
	Date & Time		2023-01-17 07:56:02
	Start Row		66
	End Row		2100
Test Conditions	Avg Cell Temp	C	40.17
	Avg Confining Pressure	kPa	27562
	Pre Pulse Avg Pore Pressure	kPa	9280
	Pulse Pressure	kPa	529
	Effective Stress	kPa	18282
	Post Pulse Avg Pore Pressure	kPa	9220
Pore Fluid & Conditions	Type		Water
	Salt	ppm	0
	Density	kg/m3	996.14
	Viscosity	kg.s/m	6.519E-04
	Compressibility	1/Pa	4.36E-10
Solution	Test System		System3-Cell2
Brace	Nominal Decay Time	s	8052
	Brace Permeability	m2	1.86E-20
Hsieh	Permeability	m2	2.14E-20
	Specific Storage	1/m	8.24E-08
	Permeability	nD	21.7
	Hydraulic Conductivity	m/s	3.21E-13
	Pearson Coeff	()	0.9994248

IG_BH04_PS008_HC61a Eff Stress:18.28 MPa, HC=3.21e-13 m/s, SS=8.24e-8 1/m

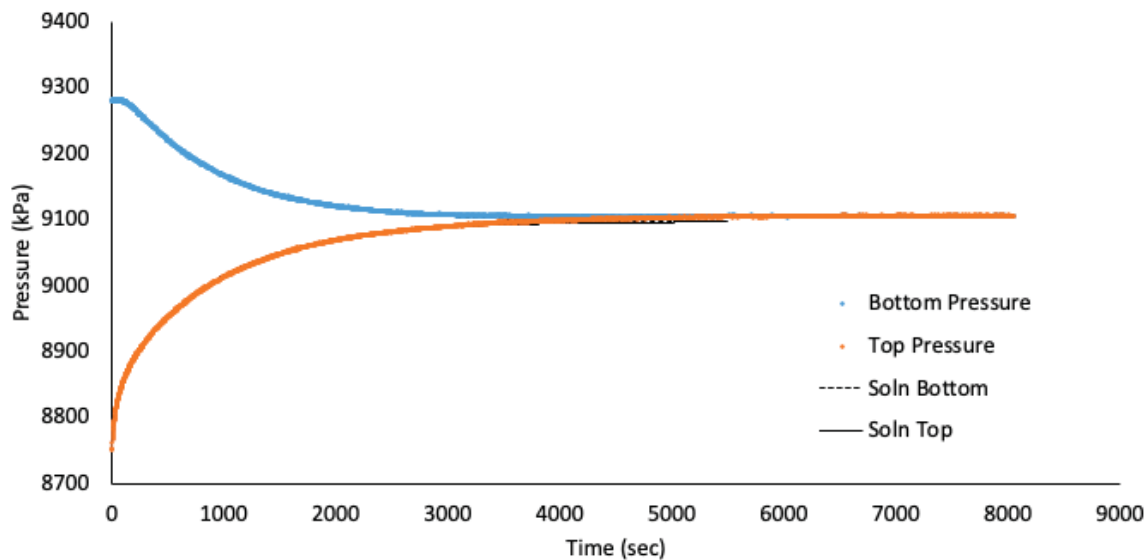


Figure 63 IG_BH04_PS008_HC61a: Effective Confining Stress = 18.28 MPa

	Sample Name		IG_BH04_PS008
	Specimen Name		IG_BH04_PS008_HC61a
	Specimen Top Depth		714.18
	Specimen Bottom Depth		714.242
	Test No		ES3
	Test Name		IG_BH04_PS008_HC61a_ES3
	Operator		StephenTalman/FrancyGuerrero
Dimensions	Length	mm	62.540
	Diameter	mm	61.590
	Length	m	0.06254
	Diameter	m	0.06159
Test Data Location	Raw Data File Name		IG-BH04-PS008-HC61a-003-B.dat
	Date & Time		2023-01-19 11:07:46
	Start Row		69
	End Row		3000
Test Conditions	Avg Cell Temp	C	40.17
	Avg Confining Pressure	kPa	32551
	Pre Pulse Avg Pore Pressure	kPa	9428
	Pulse Pressure	kPa	568
	Effective Stress	kPa	23123
	Post Pulse Avg Pore Pressure	kPa	9557
Pore Fluid & Conditions	Type		Water
	Salt	ppm	0
	Density	kg/m3	996.2
	Viscosity	kg.s/m	6.519E-04
	Compressibility	1/Pa	4.36E-10
Solution	Test System		System3-Cell2
Brace	Nominal Decay Time	s	16008
	Brace Permeability	m2	9.64E-21
Hsieh	Permeability	m2	8.99E-21
	Specific Storage	1/m	6.03E-08
	Permeability	nD	9.1
	Hydraulic Conductivity	m/s	1.35E-13
	Pearson Coeff	()	0.9970875

IG_BH04_PS008_HC61a Eff Stress:23.12 MPa, HC=1.35e-13 m/s, SS=6.03e-8 1/m

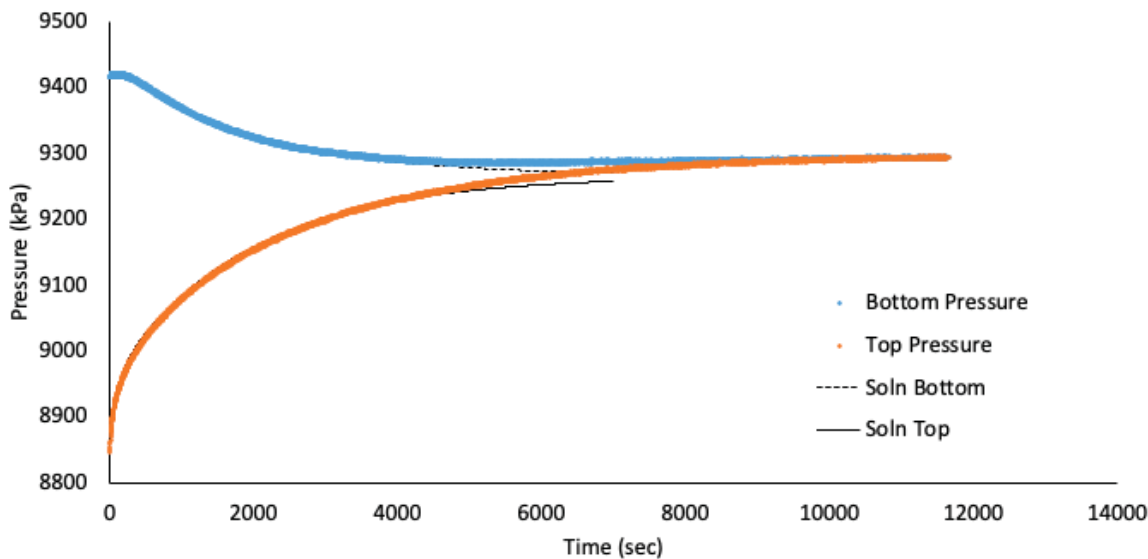


Figure 64 IG_BH04_PS008_HC61a: Effective Confining Stress = 23.12 MPa

Sample ID	IG_BH04_PS008			
Specimen Full Name	IG_BH04_PS008_SSG61a			
Top Depth (m)	714.242			
Bottom Depth (m)	714.304			
Test ID	SSG	ESL	ESM	ESH
Test Name	Steady State N2 Permeability			
Operator 1	A. Sanchez			
Operator 2				
Dimensions				
Length	mm	62.38		
Diameter	mm	61.59		
Length	m	0.06		
Diameter	m	0.06		
Test Data Location	Raw Data File Name	rawData_1	rawData_2	rawData_3
	Start Date & Time	2022-12-07		
	End Date & Time	2022-12-16		
Average Test Conditions and Pore Fluids Conditions	Cell Temp	C	33.2	33.2
	Fluid Type	Gas	Nitrogen	Nitrogen
	Density	kg/m3	81.2	86.5
	Viscosity	cP	0.0195	0.0196
	Effective Stress	MPa	13.6	18.6
Results	kapp	m2	2.03E-19	4.57E-20
NOTES:				
ESL	Effective stress - low test condition			
ESM	Effective stress - medium test condition			
ESH	Effective stress - high test condition			
kapp	Apparent gas permeability			

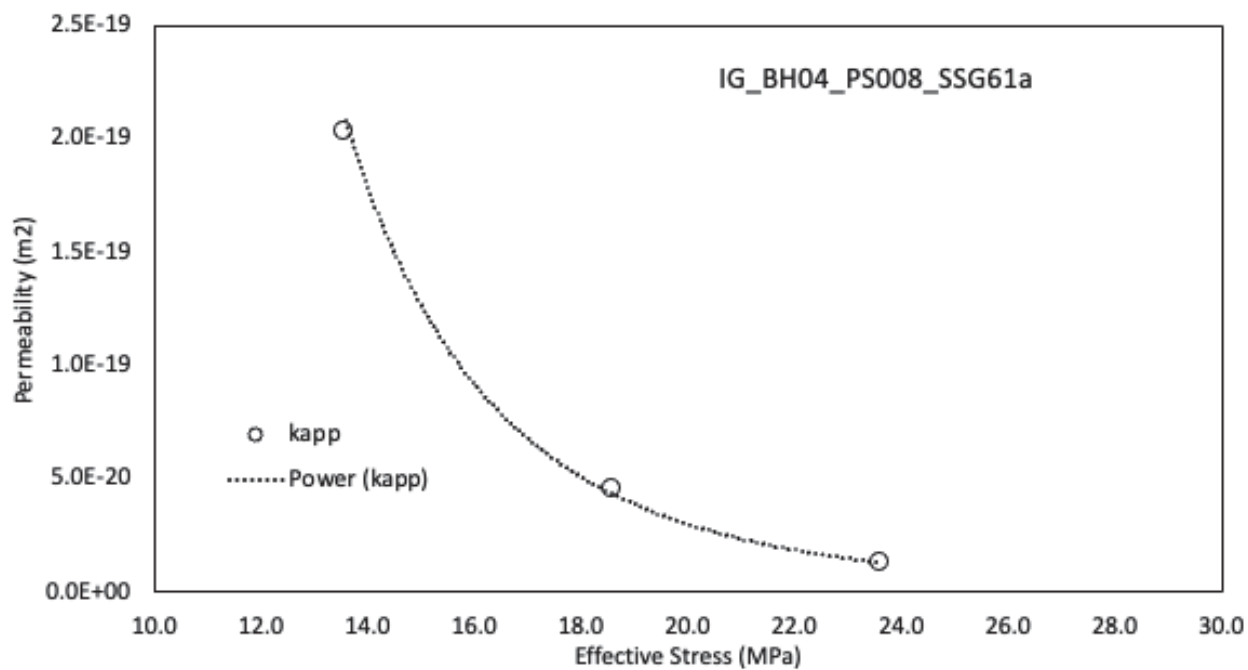


Figure 65 IG_BH04_PS008_SSG61a: Effective Confining Stresses of 13.6 MPa, 18.6 MPa and 23.6 MPa

	Sample Name		IG_BH04_PS009
	Specimen Name		IG_BH04_PS009_HC25a
	Specimen Top Depth		828.145
	Specimen Bottom Depth		828.180
	Test No		ES1
	Test Name		IG_BH04_PS009_HC25a_ES1
	Operator		Stephen Talman/ Francy Guerrero
Dimensions	Length	mm	25.330
	Diameter	mm	24.760
	Length	m	0.02533
	Diameter	m	0.02476
Test Data Location	Raw Data File Name		2023-03-28_12-22-32 System-1-Cell-1 IG-BH04-PS009-HC25a.csv
	Date & Time		2023-08-31 13:23:48
	Start Row		73984
	End Row		74700
Test Conditions	Avg Cell Temp	C	40.37
	Avg Confining Pressure	kPa	24744
	Pre Pulse Avg Pore Pressure	kPa	8861
	Pulse Pressure	kPa	504
	Effective Stress	kPa	15883
Pore Fluid & Conditions	Post Pulse Avg Pore Pressure	kPa	9036
	Type		Water
	Salt	ppm	0
	Density	kg/m3	995.88
	Viscosity	kg.s/m	6.494E-04
Solution	Compressibility	1/Pa	4.36E-10
	Test System		System 3 - Cell 1
Brace	Nominal Decay Time	s	716
	Brace Permeability	m2	1.86E-19
Hsieh	Permeability	m2	1.96E-19
	Specific Storage	1/m	7.79E-08
	Permeability	nD	198.1
	Hydraulic Conductivity	m/s	2.94E-12
	Pearson Coeff	()	0.9998180

IG_BH04_PS009_HC25a Eff Stress:15.88 MPa, HC=2.94e-12 m/s, SS=7.79e-8 1/m

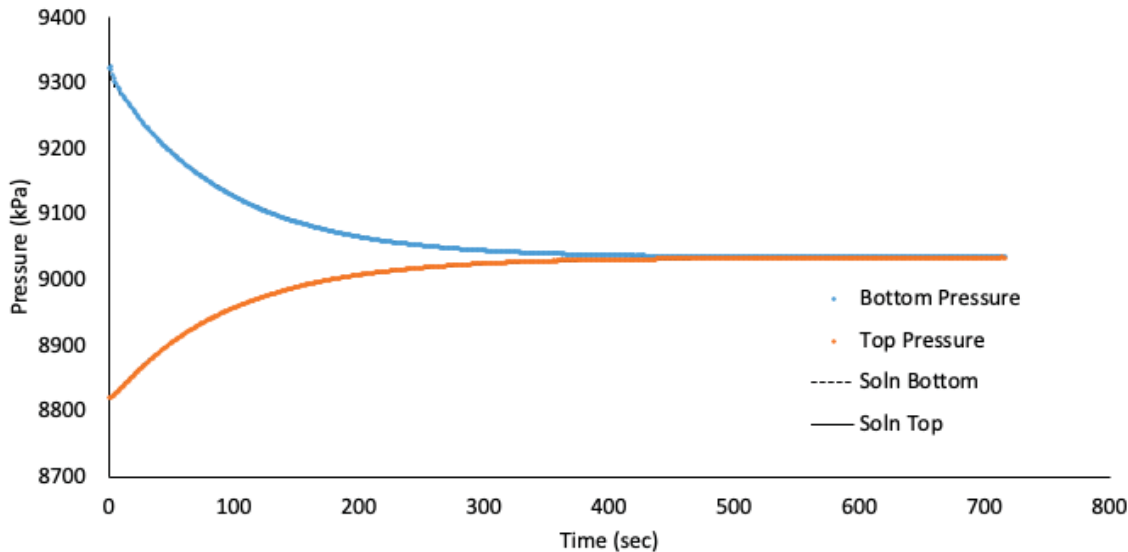


Figure 66 IG_BH04_PS009_HC25a: Effective Confining Stress = 15.88 MPa

	Sample Name		IG_BH04_PS009
	Specimen Name		IG_BH04_PS009_HC25a
	Specimen Top Depth		828.145
	Specimen Bottom Depth		828.180
	Test No		ES2
	Test Name		IG_BH04_PS009_HC25a_ES2
	Operator		Stephen Talman/ Francy Guerrero
Dimensions	Length	mm	25.330
	Diameter	mm	24.760
	Length	m	0.02533
	Diameter	m	0.02476
Test Data Location	Raw Data File Name		2023-03-28_12-22-32 System-1-Cell-1 IG-BH04-PS009-HC25a.csv
	Date & Time		2023-09-01 12:15:17
	Start Row		164
	End Row		2300
Test Conditions	Avg Cell Temp	C	40.36
	Avg Confining Pressure	kPa	29753
	Pre Pulse Avg Pore Pressure	kPa	8557
	Pulse Pressure	kPa	498
	Effective Stress	kPa	21196
	Post Pulse Avg Pore Pressure	kPa	8731
Pore Fluid & Conditions	Type		Water
	Salt	ppm	0
	Density	kg/m3	995.76
	Viscosity	kg.s/m	6.495E-04
	Compressibility	1/Pa	4.36E-10
Solution			System 3 - Cell 1
Brace	Nominal Decay Time	s	2136
	Brace Permeability	m2	7.98E-20
Hsieh	Permeability	m2	8.38E-20
	Specific Storage	1/m	4.87E-08
	Permeability	nD	84.9
	Hydraulic Conductivity	m/s	1.26E-12
	Pearson Coeff	()	0.9998327

IG_BH04_PS009_HC25a Eff Stress:21.2 MPa, HC=1.26e-12 m/s, SS=4.87e-8 1/m

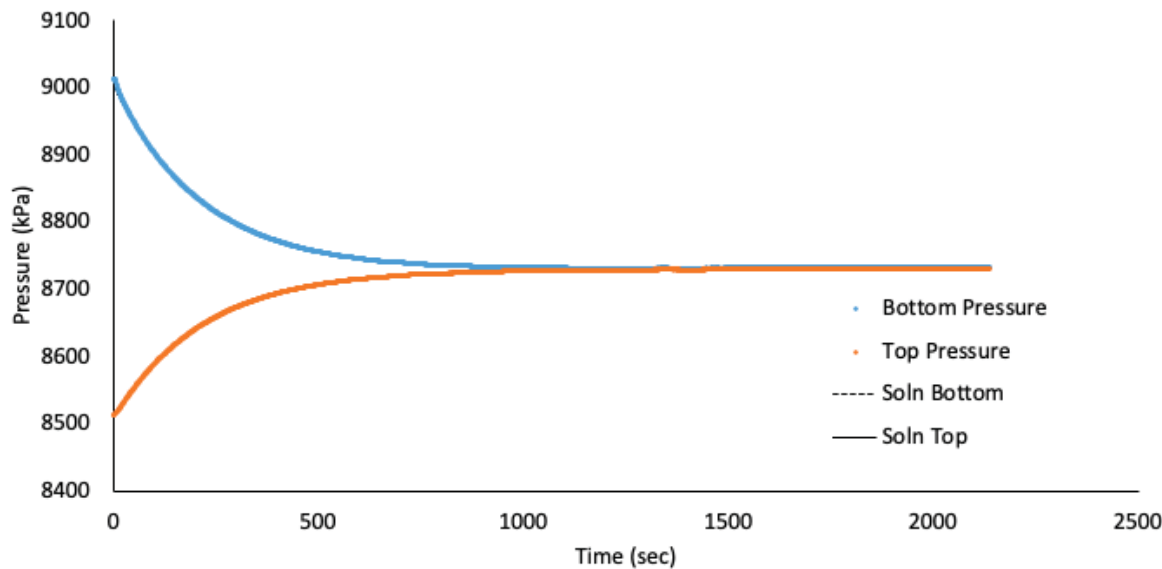


Figure 67 IG_BH04_PS009_HC25a: Effective Confining Stress = 21.20 MPa

	Sample Name		IG_BH04_PS009
	Specimen Name		IG_BH04_PS009_HC25a
	Specimen Top Depth		828.145
	Specimen Bottom Depth		828.180
	Test No		ES3
	Test Name		IG_BH04_PS009_HC25a_ES3
	Operator		Stephen Talman/ Francy Guerrero
Dimensions	Length	mm	25.330
	Diameter	mm	24.760
	Length	m	0.02533
	Diameter	m	0.02476
Test Data Location	Raw Data File Name		2023-08-28_14-13-09 System-3-Cell-1 IG-BH04-PS009-HC25a.csv
	Date & Time		2023-09-03 00:48:02
	Start Row		722
	End Row		3110
Test Conditions	Avg Cell Temp	C	40.40
	Avg Confining Pressure	kPa	34761
	Pre Pulse Avg Pore Pressure	kPa	8860
	Pulse Pressure	kPa	482
	Effective Stress	kPa	25900
	Post Pulse Avg Pore Pressure	kPa	8999
Pore Fluid & Conditions	Type		Water
	Salt	ppm	0
	Density	kg/m3	995.87
	Viscosity	kg.s/m	6.490E-04
	Compressibility	1/Pa	4.36E-10
Solution	Test System		System 3 - Cell 1
Brace	Nominal Decay Time	s	2388
	Brace Permeability	m2	4.43E-20
Hsieh	Permeability	m2	4.43E-20
	Specific Storage	1/m	7.95E-08
	Permeability	nD	44.9
	Hydraulic Conductivity	m/s	6.67E-13
	Pearson Coeff	()	0.9995736

IG_BH04_PS009_HC25a Eff Stress:25.9 MPa, HC=6.67e-13 m/s, SS=7.95e-8 1/m

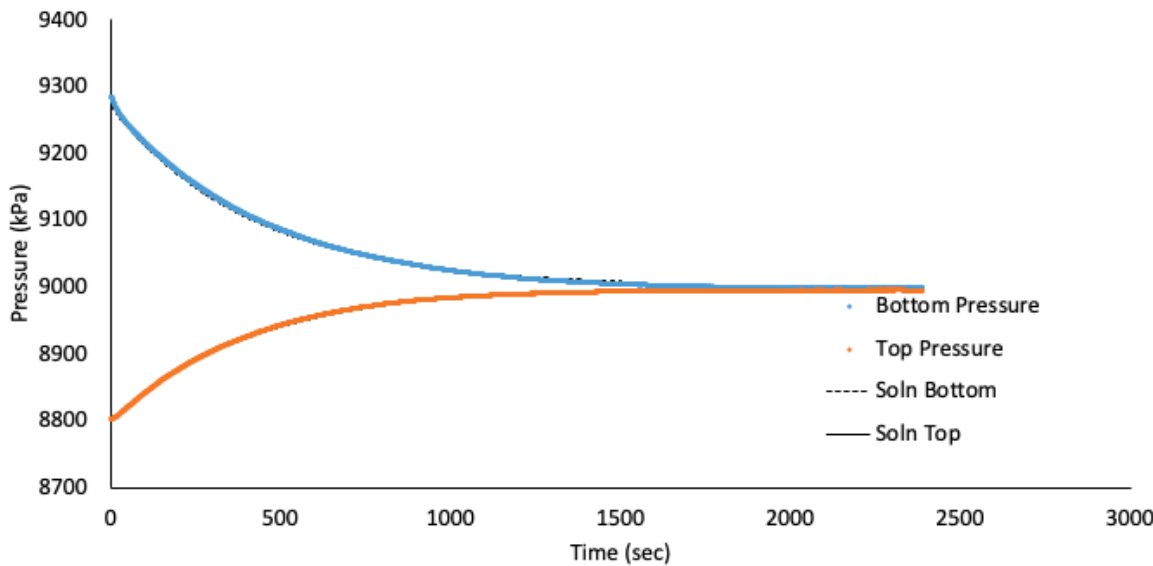


Figure 68 IG_BH04_PS009_HC25a: Effective Confining Stress = 25.9 MPa

Sample ID	IG_BH04_PS009			
Specimen Name	IG_BH04_PS009_SSG61a			
Top Depth (m)	828.242			
Bottom Depth (m)	828.304			
Test ID	SSG	ESL	ESM	ESH
Test Name	Steady State N2 Permeability			
Operator 1	A. Sanchez			
Operator 2				
Dimensions	Length	mm	62.27	
	Diameter	mm	61.31	
	Length	m	0.06	
	Diameter	m	0.06	
Test Data Location	Raw Data File Name		rawData_1	rawData_2
	Start Date & Time	2022-10-27		
	End Date & Time	2022-11-15		
Average Test Conditions and Pore Fluids Conditions	Cell Temp	C	33.5	33.5
	Fluid Type	Gas	Nitrogen	Nitrogen
	Density	kg/m3	100.3	98.2
	Viscosity	Pa.s or kg.s/m	0.0200	0.0199
	Effective Stress	MPa	15.5	20.8
Results	kapp	m ²	1.74E-19	5.69E-20
				2.74E-20

NOTES:

ESL Effective stress - low test condition
 ESM Effective stress - medium test condition
 ESH Effective stress - high test condition
 kapp Apparent gas permeability

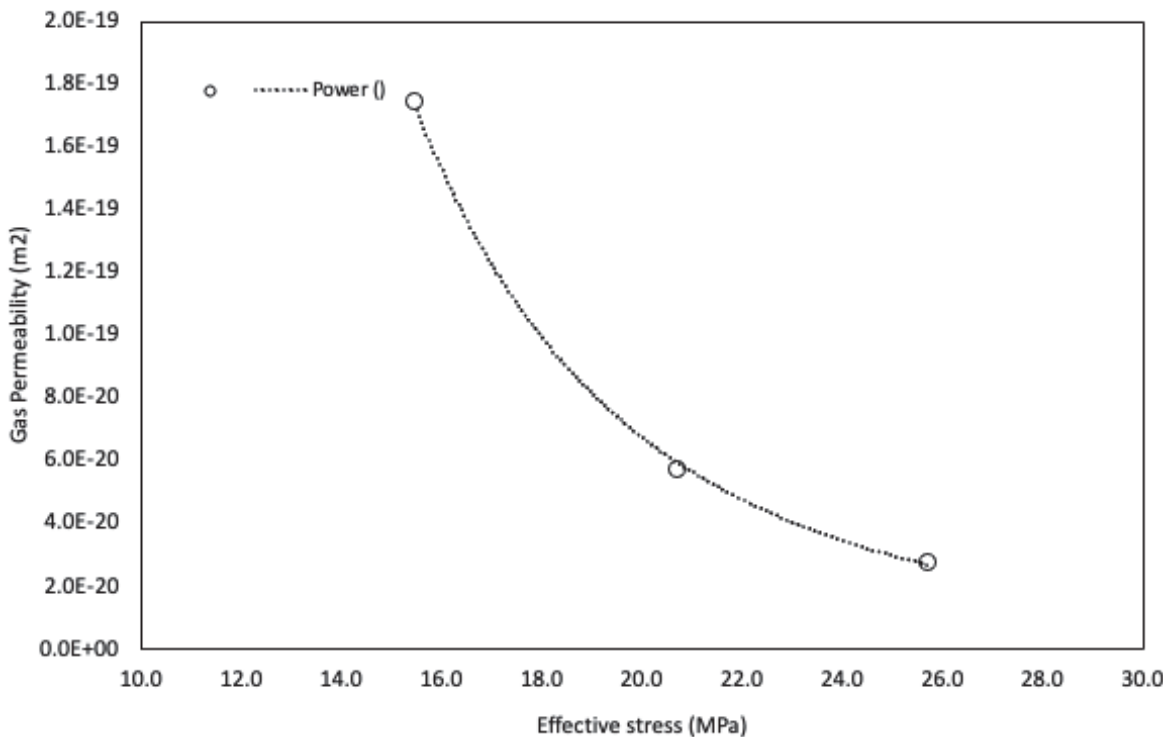


Figure 69 IG_BH04_PS009_SSG61a: Effective Confining Stresses of 15.5 MPa, 20.8 MPa and 25.7 MPa

	Sample Name		IG_BH04_PS010
	Specimen Name		IG_BH04_PS010_HC25r
	Specimen Top Depth		888.67
	Specimen Bottom Depth		888.705
	Test No		ES1
	Test Name		IG_BH04_PS010_HC25r_ES1
	Operator		Stephen Talman/ Francy Guerrero
Dimensions	Length	mm	23.350
	Diameter	mm	24.810
	Length	m	0.02335
	Diameter	m	0.02481
Test Data Location	Raw Data File Name		2023-04-03_08-58-45 System-2-CELL-3 IG-BH04-PS0010-HC25r.csv
	Date & Time		2023-04-03 08:58:45
	Start Row		14922
	End Row		38000
Test Conditions	Avg Cell Temp	C	39.73
	Avg Confining Pressure	kPa	25566
	Pre Pulse Avg Pore Pressure	kPa	9324
	Pulse Pressure	kPa	526
	Effective Stress	kPa	16242
	Post Pulse Avg Pore Pressure	kPa	9188
Pore Fluid & Conditions	Type		Water
	Salt	ppm	0
	Density	kg/m3	996.33
	Viscosity	kg.s/m	6.572E-04
	Compressibility	1/Pa	4.36E-10
Solution	Test System		System 2 - CELL 3
Brace	Nominal Decay Time	s	23078
	Brace Permeability	m2	4.09E-21
Hsieh	Permeability	m2	4.91E-21
	Specific Storage	1/m	1.87E-07
	Permeability	nD	5.0
	Hydraulic Conductivity	m/s	7.30E-14
	Pearson Coeff	()	0.9977326

IG_BH04_PS010_HC25r Eff Stress:16.24 MPa, HC=7.30e-14 m/s, SS=1.87e-7 1/m

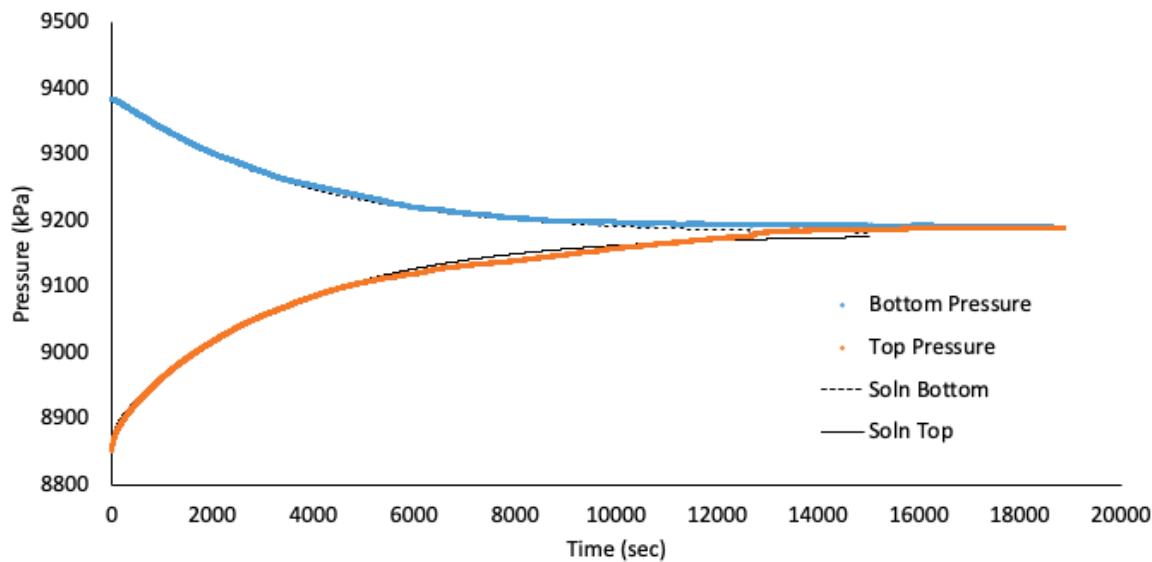


Figure 70 IG_BH04_PS010_HC25r: Effective Confining Stress = 16.24 MPa

Sample ID	IG_BH04_PS010			
Specimen Full Name	IG_BH04_PS010_SSG61a			
Top Depth (m)	888.705			
Bottom Depth (m)	888.767			
Test ID	SSG	ESL	ESM	ESH
Test Name	Steady State N2 Permeability			
Operator 1	A. Sanchez			
Operator 2				
Dimensions				
Length	mm	62.63		
Diameter	mm	61.37		
Length	m	0.06		
Diameter	m	0.06		
Test Data Location	Raw Data File Name	rawData_1	rawData_2	rawData_3
	Start Date & Time	2022-11-24		
	End Date & Time	2022-12-06		
Average Test Conditions and Pore Fluids Conditions	Cell Temp	C	33.3	33.1
	Fluid Type	Gas	Nitrogen	Nitrogen
	Density	kg/m3	103.6	103.7
	Viscosity	cP	0.0201	0.0200
	Effective Stress	MPa	16.9	21.9
Results	kapp	m2	1.53E-19	2.95E-20
				6.90E-21

NOTES:

ESL Effective stress - low test condition
 ESM Effective stress - medium test condition
 ESH Effective stress - high test condition
 kapp Apparent gas permeability

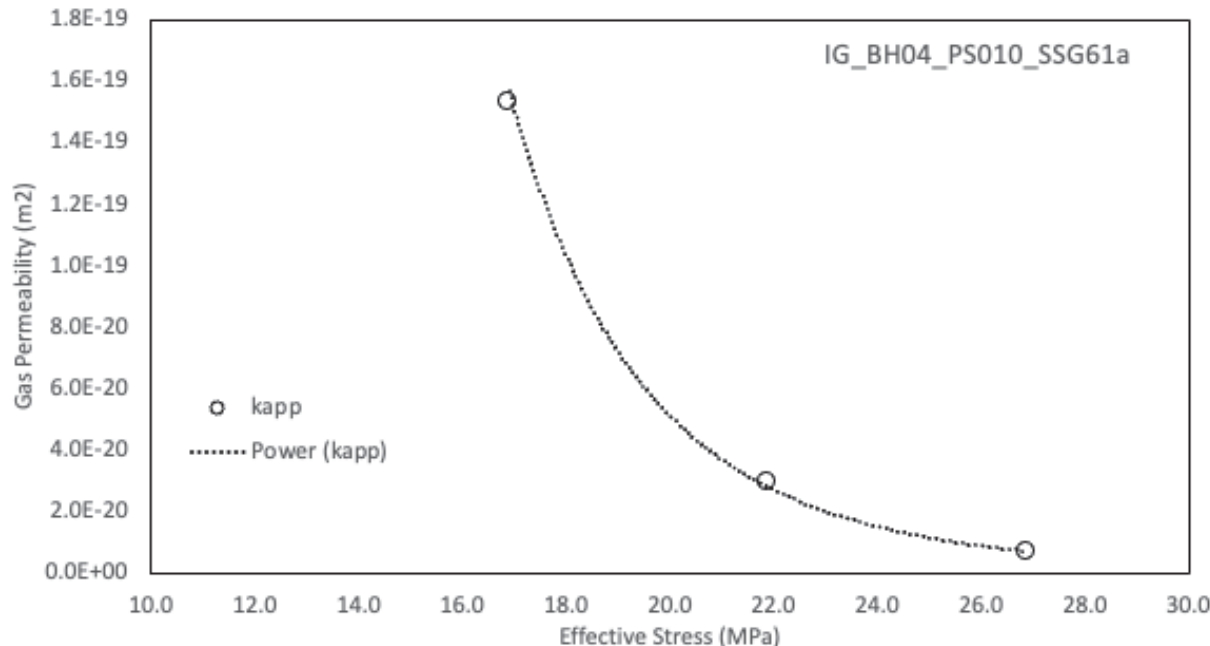


Figure 71 IG_BH04_PS010_SSG61a: Effective Confining Stresses of 16.9 MPa, 21.9 MPa and 26.9 MPa

	Sample Name		IG_BH04_PS011
	Specimen Name		IG_BH04_PS011_HC25a
	Specimen Top Depth		934.39
	Specimen Bottom Depth		934.430
	Test No		ES2
	Test Name		IG_BH04_PS011_HC25a_ES2
	Operator		Stephen Talman/ Francy Guerrero
Dimensions	Length	mm	25.390
	Diameter	mm	25.350
	Length	m	0.02539
	Diameter	m	0.02535
Test Data Location	Raw Data File Name		2023-02-03_11-24-08 System-3-Cell-1 IG-BH04-PS011-HC25a.csv
	Date & Time		2023-02-06 12:33:43
	Start Row		80359
	End Row		84550
Test Conditions	Avg Cell Temp	C	40.39
	Avg Confining Pressure	kPa	31757
	Pre Pulse Avg Pore Pressure	kPa	9134
	Pulse Pressure	kPa	298
	Effective Stress	kPa	22623
	Post Pulse Avg Pore Pressure	kPa	9251
Pore Fluid & Conditions	Type		Water
	Salt	ppm	0
	Density	kg/m3	995.99
	Viscosity	kg.s/m	6.492E-04
	Compressibility	1/Pa	4.36E-10
Solution	Test System		System 3 - Cell 1
Brace	Nominal Decay Time	s	4191
	Brace Permeability	m2	2.39E-20
Hsieh	Permeability	m2	2.39E-20
	Specific Storage	1/m	2.52E-07
	Permeability	nD	24.2
	Hydraulic Conductivity	m/s	3.59E-13
	Pearson Coeff	()	0.9987952

IG_BH04_PS011_HC25a Eff Stress:22.62 MPa, HC=3.59e-13 m/s, SS=2.52e-7 1/m

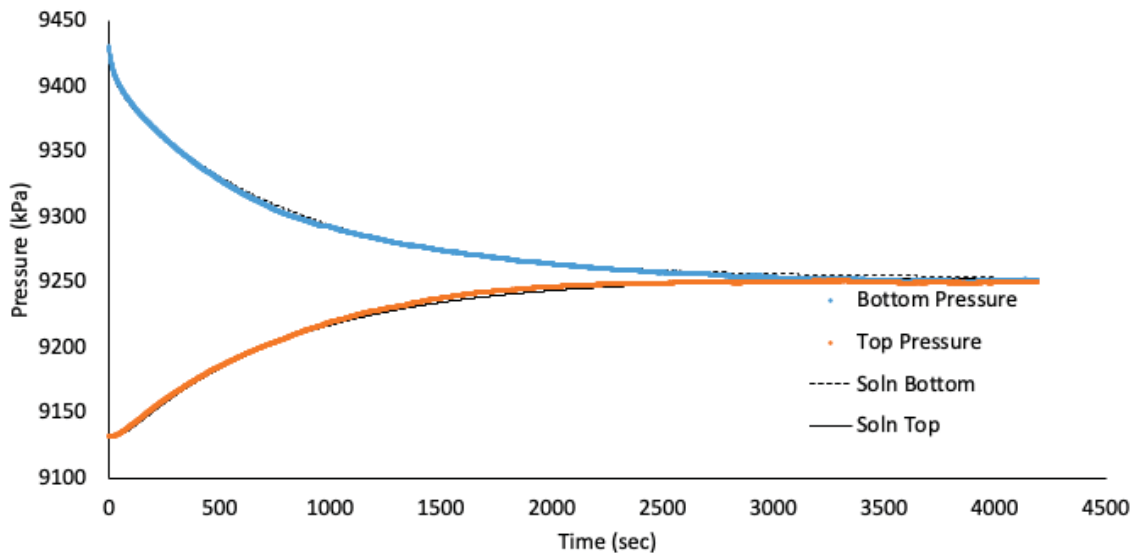


Figure 72 IG_BH04_PS011_HC25a: Effective Confining Stress = 22.62 MPa

	Sample Name		IG_BH04_PS011
	Specimen Name		IG_BH04_PS011_HC25a
	Specimen Top Depth		934.39
	Specimen Bottom Depth		934.430
	Test No		ES3
	Test Name		IG_BH04_PS011_HC25a_ES3
	Operator		Stephen Talman/ Francy Guerrero
Dimensions	Length	mm	25.390
	Diameter	mm	25.350
	Length	m	0.02539
	Diameter	m	0.02535
Test Data Location	Raw Data File Name		2023-02-03_11-24-08 System-3-Cell-1 IG-BH04-PS0011+HC25a.csv
	Date & Time		2023-02-07 12:12:38
	Start Row		173
	End Row		9500
Test Conditions	Avg Cell Temp	C	40.38
	Avg Confining Pressure	kPa	36746
	Pre Pulse Avg Pore Pressure	kPa	9135
	Pulse Pressure	kPa	272
	Effective Stress	kPa	27611
	Post Pulse Avg Pore Pressure	kPa	9266
Pore Fluid & Conditions	Type		Water
	Salt	ppm	0
	Density	kg/m3	996
	Viscosity	kg.s/m	6.493E-04
	Compressibility	1/Pa	4.36E-10
Solution	Test System		System 3 - Cell 1
Brace	Nominal Decay Time	s	9327
	Brace Permeability	m2	1.32E-20
Hsieh	Permeability	m2	1.32E-20
	Specific Storage	1/m	1.06E-07
	Permeability	nD	13.4
	Hydraulic Conductivity	m/s	1.99E-13
	Pearson Coeff	()	0.9985787

IG_BH04_PS011_HC25a Eff Stress:27.61 MPa, HC=1.99e-13 m/s, SS=1.06e-7 1/m

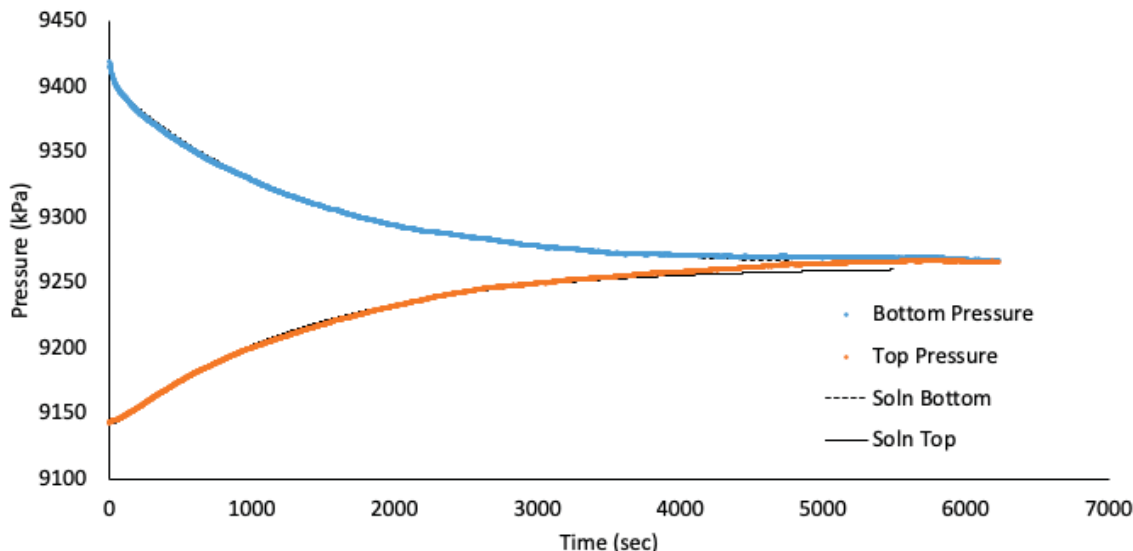


Figure 73 IG_BH04_PS011_HC25a: Effective Confining Stress = 27.61 MPa

	Sample Name		IG_BH04_PS011
	Specimen Name		IG_BH04_PS011_HC25r
	Specimen Top Depth		934.395
	Specimen Bottom Depth		934.430
	Test No		ES2
	Test Name		IG_BH04_PS011_HC25r_ES2
	Operator		Stephen Talman/ Francy Guerrero
Dimensions	Length	mm	25.550
	Diameter	mm	25.240
	Length	m	0.02555
	Diameter	m	0.02524
Test Data Location	Raw Data File Name		2023-02-06_12-35-13_System-3-Cell-3_IG-BH04-PS0011-HC25r_filtered.csv
	Date & Time		2023-02-06 12:35:13
	Start Row		2746
	End Row		7120
Test Conditions	Avg Cell Temp	C	39.80
	Avg Confining Pressure	kPa	31677
	Pre Pulse Avg Pore Pressure	kPa	9154
	Pulse Pressure	kPa	308
	Effective Stress	kPa	22524
	Post Pulse Avg Pore Pressure	kPa	9154
Pore Fluid & Conditions	Type		Water
	Salt	ppm	0
	Density	kg/m3	996.23
	Viscosity	kg.s/m	6.564E-04
	Compressibility	1/Pa	4.36E-10
Solution	Test System		System 3 - Cell 3
Brace	Nominal Decay Time	s	4374
	Brace Permeability	m2	2.38E-20
Hsieh	Permeability	m2	2.33E-20
	Specific Storage	1/m	1.76E-07
	Permeability	nD	23.6
	Hydraulic Conductivity	m/s	3.48E-13
	Pearson Coeff	()	0.9970743

IG_BH04_PS011_HC25r Eff Stress:22.52 MPa, HC=3.48e-13 m/s, SS=1.76e-7 1/m

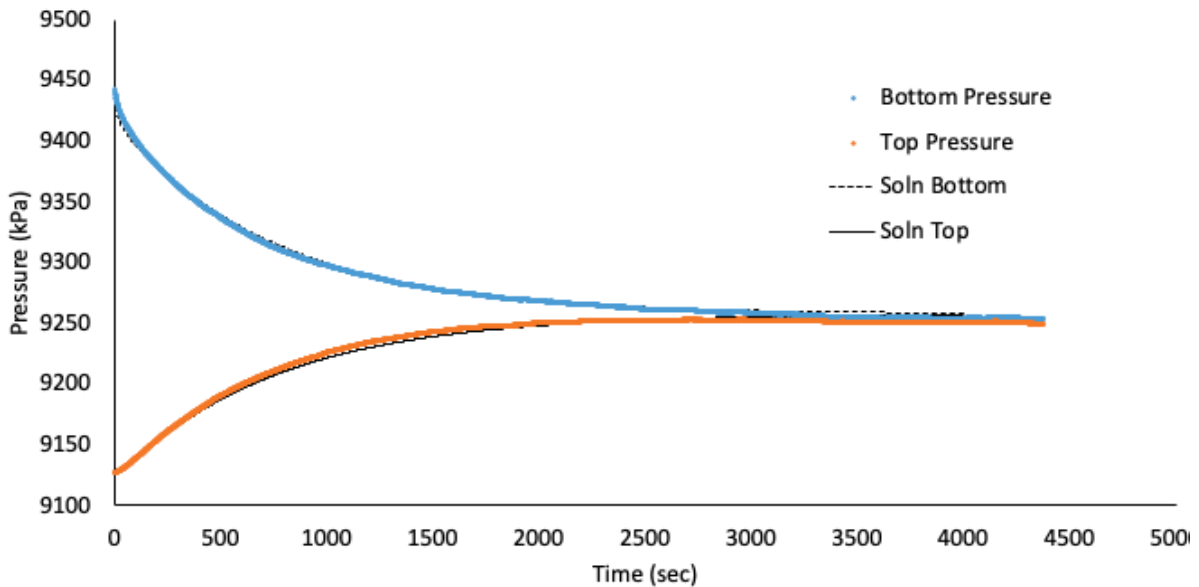


Figure 74 IG_BH04_PS011_HC25r: Effective Confining Stress = 22.52 MPa

	Sample Name		IG_BH04_PS011
	Specimen Name		IG_BH04_PS011_HC25r
	Specimen Top Depth		934.395
	Specimen Bottom Depth		934.430
	Test No		ES3
	Test Name		IG_BH04_PS011_HC25r_ES3
	Operator		Stephen Talman/ Francy Guerrero
Dimensions	Length	mm	25.550
	Diameter	mm	25.240
	Length	m	0.02555
	Diameter	m	0.02524
Test Data Location	Raw Data File Name		2023-02-01_12-38-53 System-3-Cell-3 IG-BH04-PS0011-HC25r.csv
	Date & Time		2023-02-07 12:16:34
	Start Row		438
	End Row		6400
Test Conditions	Avg Cell Temp	C	39.78
	Avg Confining Pressure	kPa	36653
	Pre Pulse Avg Pore Pressure	kPa	9191
	Pulse Pressure	kPa	240
	Effective Stress	kPa	27463
	Post Pulse Avg Pore Pressure	kPa	9191
Pore Fluid & Conditions	Type		Water
	Salt	ppm	0
	Density	kg/m3	996.25
	Viscosity	kg.s/m	6.566E-04
	Compressibility	1/Pa	4.36E-10
Solution	Test System		System 3 - Cell 3
Brace	Nominal Decay Time	s	5962
	Brace Permeability	m2	1.24E-20
Hsieh	Permeability	m2	1.26E-20
	Specific Storage	1/m	2.10E-07
	Permeability	nD	12.8
	Hydraulic Conductivity	m/s	1.88E-13
	Pearson Coeff	()	0.9988224

IG_BH04_PS011_HC25r Eff Stress:27.46 MPa, HC=1.88e-13 m/s, SS=2.10e-7 1/m

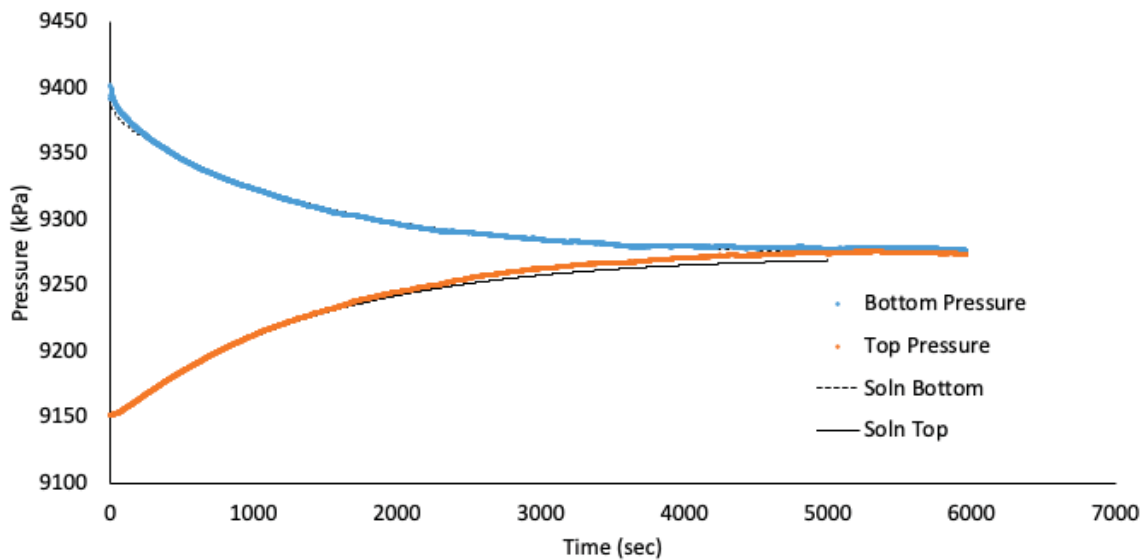


Figure 75 IG_BH04_PS011_HC25r: Effective Confining Stress = 27.46 MPa

	Sample Name		IG_BH04_PS011
	Specimen Name		IG_BH04_PS011_HC61a
	Specimen Top Depth		934.43
	Specimen Bottom Depth		934.492
	Test No		ES2
	Test Name		IG_BH04_PS011_HC61a_ES2
	Operator		Stephen Talman/ Francy Guerrero
Dimensions	Length	mm	62.010
	Diameter	mm	61.270
	Length	m	0.06201
	Diameter	m	0.06127
Test Data Location	Raw Data File Name		2023-02-06_12-34-21 System-3-Cell-2 IG-BH04-PS0011-HC61a.csv
	Date & Time		2023-02-06 12:34:21
	Start Row		839
	End Row		1400
Test Conditions	Avg Cell Temp	C	40.21
	Avg Confining Pressure	kPa	31753
	Pre Pulse Avg Pore Pressure	kPa	9124
	Pulse Pressure	kPa	306
	Effective Stress	kPa	22629
	Post Pulse Avg Pore Pressure	kPa	9124
Pore Fluid & Conditions	Type		Water
	Salt	ppm	0
	Density	kg/m3	996.06
	Viscosity	kg.s/m	6.514E-04
	Compressibility	1/Pa	4.36E-10
Solution	Test System		System 3 - Cell 2
Brace	Nominal Decay Time	s	561
	Brace Permeability	m2	3.05E-19
Hsieh	Permeability	m2	3.05E-19
	Specific Storage	1/m	1.07E-07
	Permeability	nD	308.9
	Hydraulic Conductivity	m/s	4.57E-12
	Pearson Coeff	()	0.9987689

IG_BH04_PS011_HC61a Eff Stress:22.63 MPa, HC=4.57e-12 m/s, SS=1.07e-7 1/m

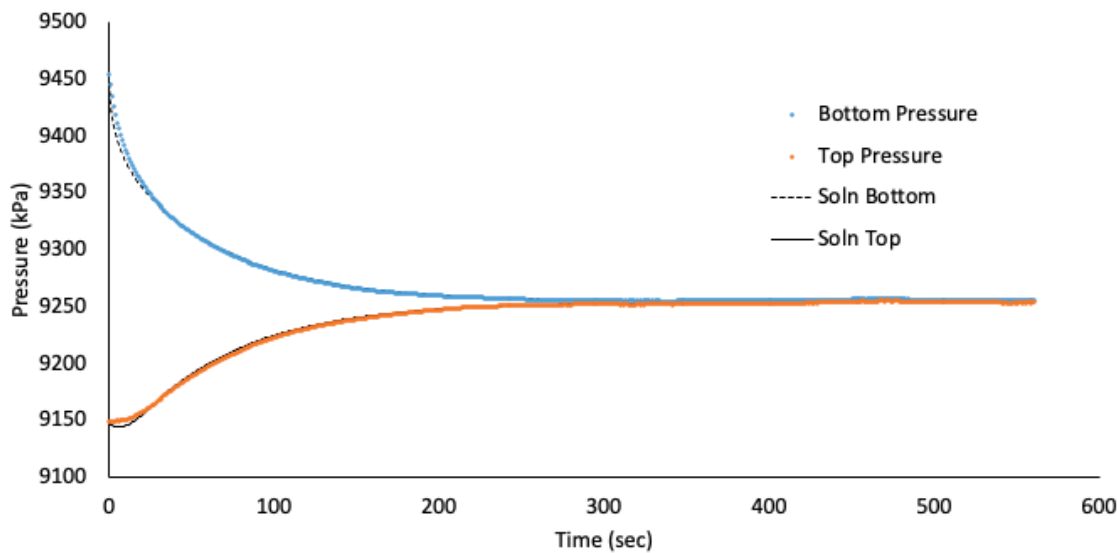


Figure 76 IG_BH04_PS011_HC61a: Effective Confining Stress = 22.63 MPa

	Sample Name		IG_BH04_PS011
	Specimen Name		IG_BH04_PS011_HC61a
	Specimen Top Depth		934.43
	Specimen Bottom Depth		934.492
	Test No		ES3
	Test Name		9349.82150542561_ES3
	Operator		Stephen Taiman/ Francy Guerrero
Dimensions	Length	mm	62.010
	Diameter	mm	61.270
	Length	m	0.06201
	Diameter	m	0.06127
Test Data Location	Raw Data File Name		2023-02-07_12-11-46 System-3-Cell-2 IG-BH04-PS0011-HC61a_filtered.csv
	Date & Time		2023-02-07 12:11:46
	Start Row		2686
	End Row		4000
Test Conditions	Avg Cell Temp	C	40.19
	Avg Confining Pressure	kPa	36740
	Pre Pulse Avg Pore Pressure	kPa	9409
	Pulse Pressure	kPa	339
	Effective Stress	kPa	27331
	Post Pulse Avg Pore Pressure	kPa	9409
Pore Fluid & Conditions	Type		Water
	Salt	ppm	0
	Density	kg/m3	996.19
	Viscosity	kg.s/m	6.516E-04
Solution	Compressibility	1/Pa	4.36E-10
	Test System		System 3 - Cell 2
Brace	Nominal Decay Time	s	1314
	Brace Permeability	m2	1.69E-19
Hsieh	Permeability	m2	1.69E-19
	Specific Storage	1/m	9.13E-08
	Permeability	nD	171.7
	Hydraulic Conductivity	m/s	2.54E-12
	Pearson Coeff	()	0.9966958

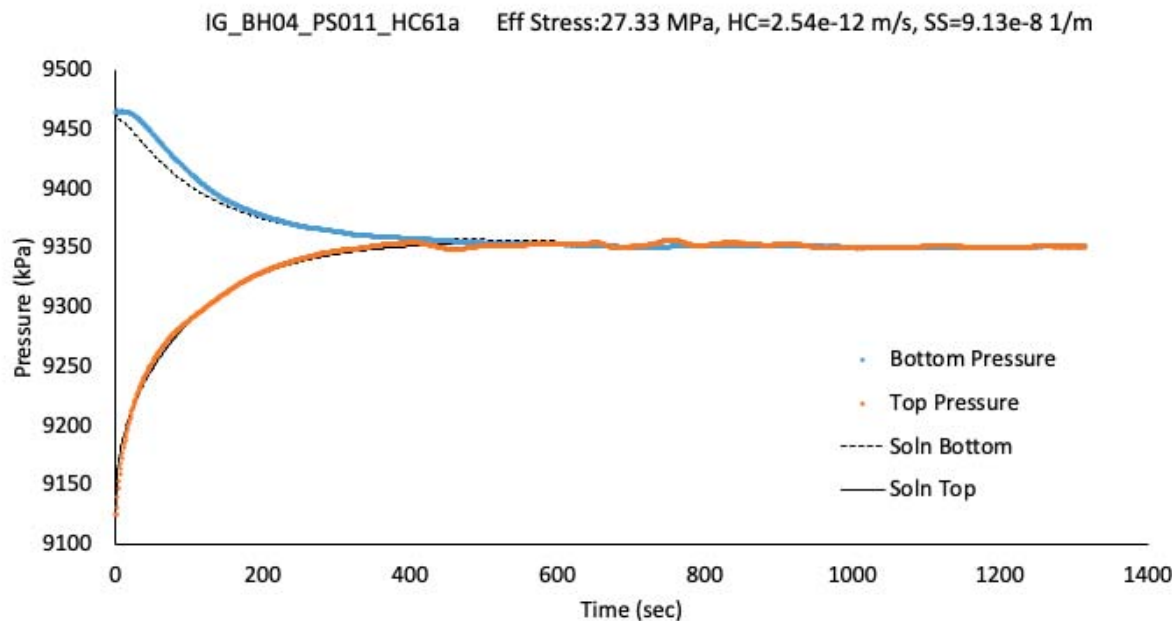


Figure 77 IG_BH04_PS011_HC61a: Effective Confining Stress = 27.33 MPa

**Appendix C: Hydraulic Conductivity and Steady State Gas Permeability Test Summaries
– IG_BH05**

CONTENTS

	Page
Figure 78 IG_BH05_AR044_SSG61a: Effective Confining Stresses of 15.0MPa, 20.0MPa and 25.0MPa.....	122
Figure 79 IG_BH05_PS002_HC25a: Effective Confining Stress = 8.02 MPa	123
Figure 80 IG_BH05_PS002_HC25a: Effective Confining Stress = 13.55 MPa	124
Figure 81 IG_BH05_PS002_HC25a: Effective Confining Stress = 18.24 MPa	125
Figure 82 IG_BH05_PS002_HC25r: Effective Confining Stress = 8.02 MPa	126
Figure 83 IG_BH05_PS002_HC25r: Effective Confining Stress = 13.52 MPa	127
Figure 84 IG_BH05_PS002_HC61a: Effective Confining Stress = 8.01 MPa	128
Figure 85 IG_BH05_PS002_HC61a: Effective Confining Stress = 13.56 MPa	129
Figure 86 IG_BH05_PS003_HC25a: Effective Confining Stress = 10.09 MPa	130
Figure 87 IG_BH05_PS003_HC25a: Effective Confining Stress = 14.82 MPa	131
Figure 88 IG_BH05_PS003_HC25a: Effective Confining Stress = 19.75 MPa	132
Figure 89 IG_BH05_PS003_HC25r: Effective Confining Stress = 9.99 MPa	133
Figure 90 IG_BH05_PS003_HC25r: Effective Confining Stress = 14.56 MPa	134
Figure 91 IG_BH05_PS003_HC25r: Effective Confining Stress = 19.59 MPa	135
Figure 92 IG_BH05_PS003_HC61a: Effective Confining Stress = 9.78 MPa	136
Figure 93 IG_BH05_PS004_HC25a: Effective Confining Stress = 11.65 MPa	137
Figure 94 IG_BH05_PS004_HC25a: Effective Confining Stress = 16.79 MPa	138
Figure 95 IG_BH05_PS004_HC25a: Effective Confining Stress = 21.83 MPa	139
Figure 96 IG_BH05_PS004_HC25r: Effective Confining Stress = 11.62 MPa	140
Figure 97 IG_BH05_PS004_HC25r: Effective Confining Stress = 16.61 MPa	141
Figure 98 IG_BH05_PS004_HC25r: Effective Confining Stress = 22.30 MPa	142
Figure 99 IG_BH05_PS004_HC61a: Effective Confining Stress = 11.64 MPa	143
Figure 100 IG_BH05_PS004_HC61a: Effective Confining Stress = 16.77 MPa	144
Figure 101 IG_BH05_PS005_HC25a: Effective Confining Stress = 14.48 MPa	145
Figure 102 IG_BH05_PS005_HC25a: Effective Confining Stress = 18.77 MPa	146
Figure 103 IG_BH05_PS005_HC25a: Effective Confining Stress = 23.66 MPa	147
Figure 104 IG_BH05_PS005_HC25r: Effective Confining Stress = 14.35 MPa	148
Figure 105 IG_BH05_PS005_HC25r: Effective Confining Stress = 18.59 MPa	149
Figure 106 IG_BH05_PS005_HC25r: Effective Confining Stress = 23.46 MPa	150

Figure 107	IG_BH05_PS005_HC61a: Effective Confining Stress = 14.58 MPa	151
Figure 108	IG_BH05_PS005_HC61a: Effective Confining Stress = 18.89 MPa	152
Figure 109	IG_BH05_PS005_HC61a: Effective Confining Stress = 23.79 MPa	153
Figure 110	IG_BH05_PS005_SSG61a: Effective Confining Stresses of 14.3MPa, 19.4MPa and 24.3MPa.....	154
Figure 111	IG_BH05_PS006_HC25a: Effective Confining Stress = 15.5 MPa	155
Figure 112	IG_BH05_PS006_HC25a: Effective Confining Stress = 20.69 MPa	156
Figure 113	IG_BH05_PS006_HC25r: Effective Confining Stress = 15.10 MPa	157
Figure 114	IG_BH05_PS006_HC25r: Effective Confining Stress = 20.46 MPa	158
Figure 115	IG_BH05_PS006_HC25r: Effective Confining Stress = 24.36 MPa	159
Figure 116	IG_BH05_PS006_HC61a: Effective Confining Stress = 15.37 MPa	160
Figure 117	IG_BH05_PS006_HC61a: Effective Confining Stress = 20.78 MPa	161
Figure 118	IG_BH05_PS006_HC61a: Effective Confining Stress = 24.71 MPa	162

Sample ID	IG_BH05_AR044			
Specimen Full Name	IG_BH05_AR044_SSG61a			
Top Depth (m)	788.412			
Bottom Depth (m)	788.474			
Test ID	SSG	ESL	ESM	ESH
Test Name	Steady State N2 Permeability			
Operator 1	A. Sanchez			
Operator 2				
Dimensions	Length	mm	61.47	
	Diameter	mm	61.07	
	Length	m	0.06	
	Diameter	m	0.06	
Test Data Location	Raw Data File Name		rawData_ESL	rawData_ESM
	Start Date & Time	2023-02-13	rawData_ESL	rawData_ESM
	End Date & Time	2023-02-25	rawData_ESL	rawData_ESM
Average Test Conditions and Pore Fluids Conditions	Cell Temp	C	33.1	33.1
	Fluid Type	Gas	Nitrogen	Nitrogen
	Density	kg/m3	104.8	94.1
	Viscosity	cP	0.0201	0.0198
	Effective Stress	MPa	15.0	20.0
Results	kapp	m2	5.60E-21	7.34E-22
Results	kapp	m2	5.60E-21	7.34E-22

NOTES:

- ESL Effective stress - low test condition
 ESM Effective stress - medium test condition
 ESH Effective stress - high test condition
 kapp Apparent gas permeability

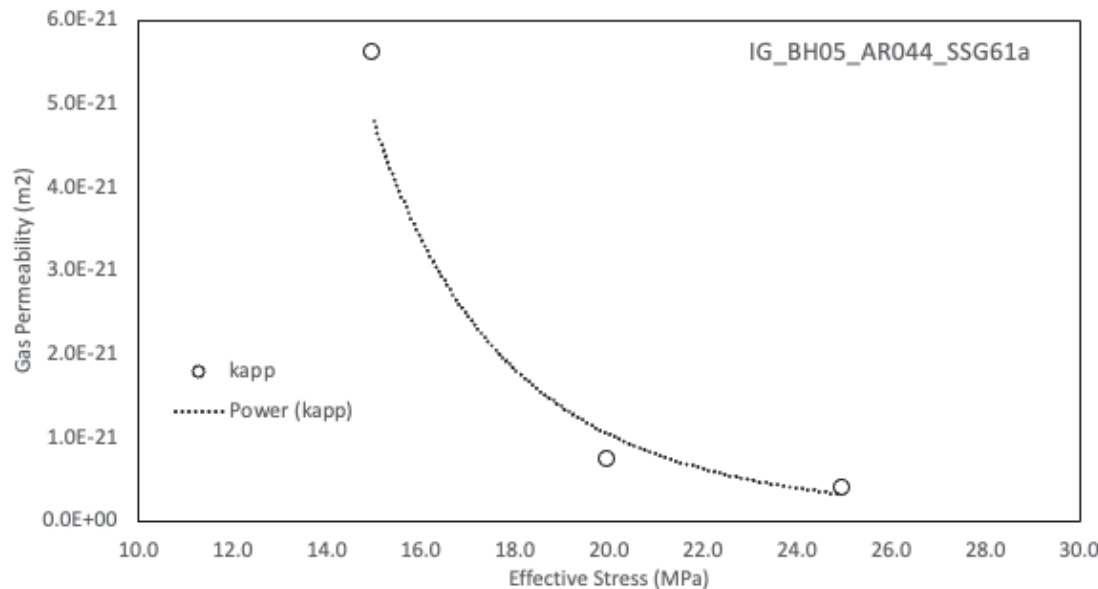


Figure 78 IG_BH05_AR044_SSG61a: Effective Confining Stresses of 15.0 MPa, 20.0 MPa and 25.0 MPa

	Sample Name		IG_BH05_PS002
	Specimen Name		IG_BH05_PS002_HC25a
	Specimen Top Depth		434.045
	Specimen Bottom Depth		434.080
	Test No		ES1
	Test Name		8980.32283845163_ES1
	Operator		Stephen Talman/ Francy Guerrero
Dimensions	Length	mm	25.900
	Diameter	mm	25.430
	Length	m	0.0259
	Diameter	m	0.02543
Test Data Location	Raw Data File Name		2023-05-03_14-33-29 System-3-Cell-1 IG-BH05-PS002-HC25a.csv
	Date & Time		2023-05-03 14:33:29
	Start Row		23451
	End Row		24500
Test Conditions	Avg Cell Temp	C	40.15
	Avg Confining Pressure	kPa	17275
	Pre Pulse Avg Pore Pressure	kPa	9252
	Pulse Pressure	kPa	515
	Effective Stress	kPa	8023
Pore Fluid & Conditions	Post Pulse Avg Pore Pressure	kPa	9252
	Type		Water
	Salt	ppm	0
	Density	kg/m3	996.13
	Viscosity	kg.s/m	6.521E-04
Solution	Compressibility	1/Pa	4.36E-10
	Test System		System 3 - Cell 1
Brace	Nominal Decay Time	s	1049
	Brace Permeability	m2	1.73E-19
Hsieh	Permeability	m2	1.90E-19
	Specific Storage	1/m	1.31E-07
	Permeability	nD	192.4
	Hydraulic Conductivity	m/s	2.85E-12
	Pearson Coeff	()	0.9995009

IG_BH05_PS002_HC25a Eff Stress:8.02 MPa, HC=2.85e-12 m/s, SS=1.31e-7 1/m

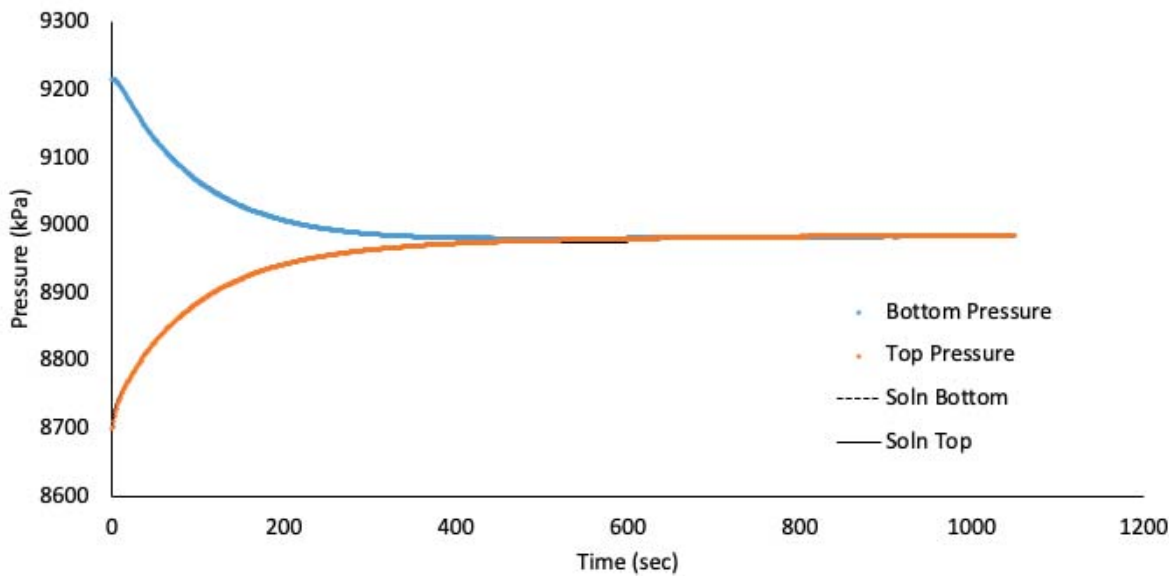


Figure 79 IG_BH05_PS002_HC25a: Effective Confining Stress = 8.02 MPa

	Sample Name		IG_BH05_PS002
	Specimen Name		IG_BH05_PS002_HC25a
	Specimen Top Depth		434.045
	Specimen Bottom Depth		434.080
	Test No		ES2
	Test Name		8904.66796430941_ES2
	Operator		Stephen Talman/ Francy Guerrero
Dimensions	Length	mm	25.900
	Diameter	mm	25.430
	Length	m	0.0259
	Diameter	m	0.02543
Test Data Location	Raw Data File Name		2023-05-04_07-00-08 System-3-Cell-1 IG-BH05-PS002-HC25a.csv
	Date & Time		2023-05-04 07:00:08
	Start Row		9601
	End Row		12000
Test Conditions	Avg Cell Temp	C	39.40
	Avg Confining Pressure	kPa	22276
	Pre Pulse Avg Pore Pressure	kPa	8731
	Pulse Pressure	kPa	500
	Effective Stress	kPa	13545
	Post Pulse Avg Pore Pressure	kPa	8731
Pore Fluid & Conditions	Type		Water
	Salt	ppm	0
	Density	kg/m3	996.2
	Viscosity	kg.s/m	6.612E-04
	Compressibility	1/Pa	4.36E-10
Solution	Test System		System 3 - Cell 1
Brace	Nominal Decay Time	s	2399
	Brace Permeability	m2	5.60E-20
Hsieh	Permeability	m2	5.60E-20
	Specific Storage	1/m	1.23E-07
	Permeability	nD	56.8
	Hydraulic Conductivity	m/s	8.28E-13
	Pearson Coeff	()	0.9996754

IG_BH05_PS002_HC25a Eff Stress:13.55 MPa, HC=8.28e-13 m/s, SS=1.23e-7 1/m

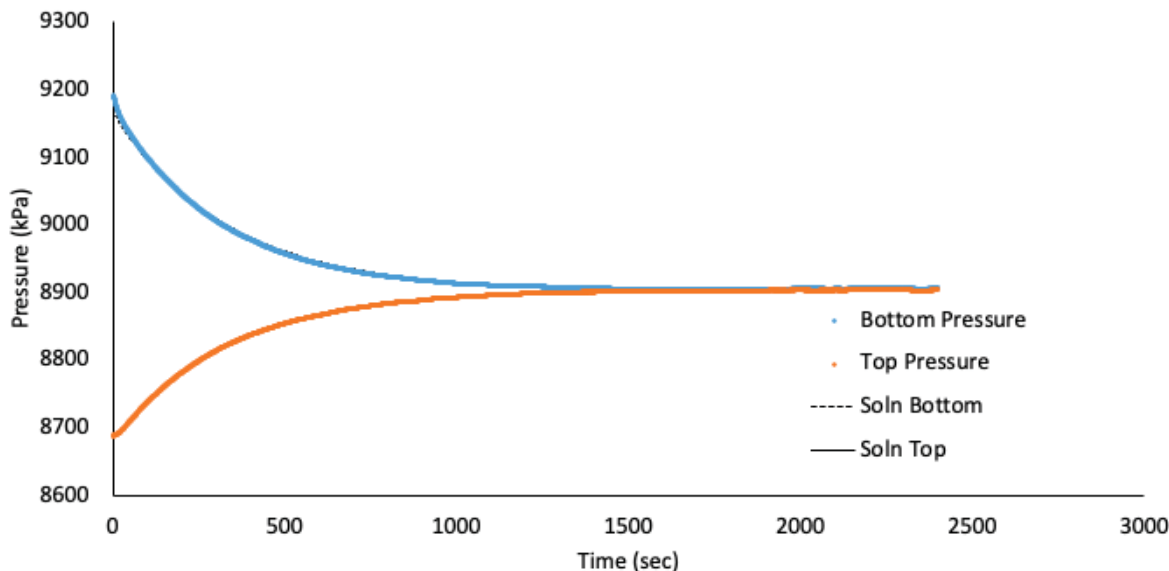


Figure 80 IG_BH05_PS002_HC25a: Effective Confining Stress = 13.55 MPa

	Sample Name		IG_BH05_PS002
	Specimen Name		IG_BH05_PS002_HC25a
	Specimen Top Depth		434.045
	Specimen Bottom Depth		434.080
	Test No		ES3
	Test Name		IG_BH05_PS002_HC25a_ES3
	Operator		Stephen Talman/ Francy Guerrero
Dimensions	Length	mm	25.900
	Diameter	mm	25.430
	Length	m	0.0259
	Diameter	m	0.02543
Test Data Location	Raw Data File Name		2023-05-05_10-13-23 System-3-Cell-1 IG-BH05-PS002-HC25a_filtered.csv
	Date & Time		2023-05-05 10:13:23
	Start Row		1190
	End Row		8000
Test Conditions	Avg Cell Temp	C	40.41
	Avg Confining Pressure	kPa	27234
	Pre Pulse Avg Pore Pressure	kPa	8990
	Pulse Pressure	kPa	491
	Effective Stress	kPa	18244
	Post Pulse Avg Pore Pressure	kPa	8990
Pore Fluid & Conditions	Type		Water
	Salt	ppm	0
	Density	kg/m3	995.92
	Viscosity	kg.s/m	6.489E-04
	Compressibility	1/Pa	4.36E-10
Solution			System 3 - Cell 1
Brace	Nominal Decay Time	s	6810
	Brace Permeability	m2	1.89E-20
Hsieh	Permeability	m2	1.95E-20
	Specific Storage	1/m	5.03E-08
	Permeability	nD	19.7
	Hydraulic Conductivity	m/s	2.93E-13
	Pearson Coeff	()	0.9999741

IG_BH05_PS002_HC25a Eff Stress:18.24 MPa, HC=2.93e-13 m/s, SS=5.03e-8 1/m

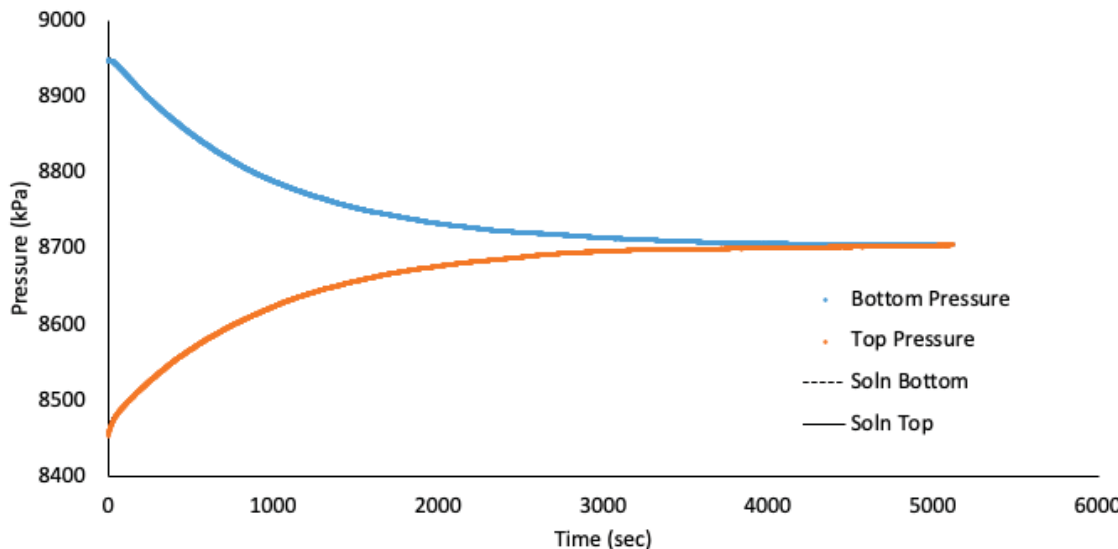


Figure 81 IG_BH05_PS002_HC25a: Effective Confining Stress = 18.24 MPa

	Sample Name		IG_BH05_PS002
	Specimen Name		IG_BH05_PS002_HC25r
	Specimen Top Depth		434.045
	Specimen Bottom Depth		434.080
	Test No		ES1
	Test Name		9004.66039633333_ES1
	Operator		StephenTalman/FrancyGuerrero
Dimensions	Length	mm	26.630
	Diameter	mm	25.340
	Length	m	0.02663
	Diameter	m	0.02534
Test Data Location	Raw Data File Name		IG-BH05-PS002-HC25r-001-B.dat
	Date & Time		2023-05-03 14:35:04
	Start Row		69
	End Row		764
Test Conditions	Avg Cell Temp	C	39.77
	Avg Confining Pressure	kPa	17244
	Pre Pulse Avg Pore Pressure	kPa	9225
	Pulse Pressure	kPa	504
	Effective Stress	kPa	8019
	Post Pulse Avg Pore Pressure	kPa	9225
Pore Fluid & Conditions	Type		Water
	Salt	ppm	0
	Density	kg/m3	996.27
	Viscosity	kg.s/m	6.567E-04
	Compressibility	1/Pa	4.36E-10
Solution	Test System		System3-Cell3
Brace	Nominal Decay Time	s	1229
	Brace Permeability	m2	1.07E-19
Hsieh	Permeability	m2	1.13E-19
	Specific Storage	1/m	1.39E-07
	Permeability	nD	114.4
	Hydraulic Conductivity	m/s	1.68E-12
	Pearson Coeff	()	0.9998999

IG_BH05_PS002_HC25r Eff Stress:8.02 MPa, HC=1.68e-12 m/s, SS=1.39e-7 1/m

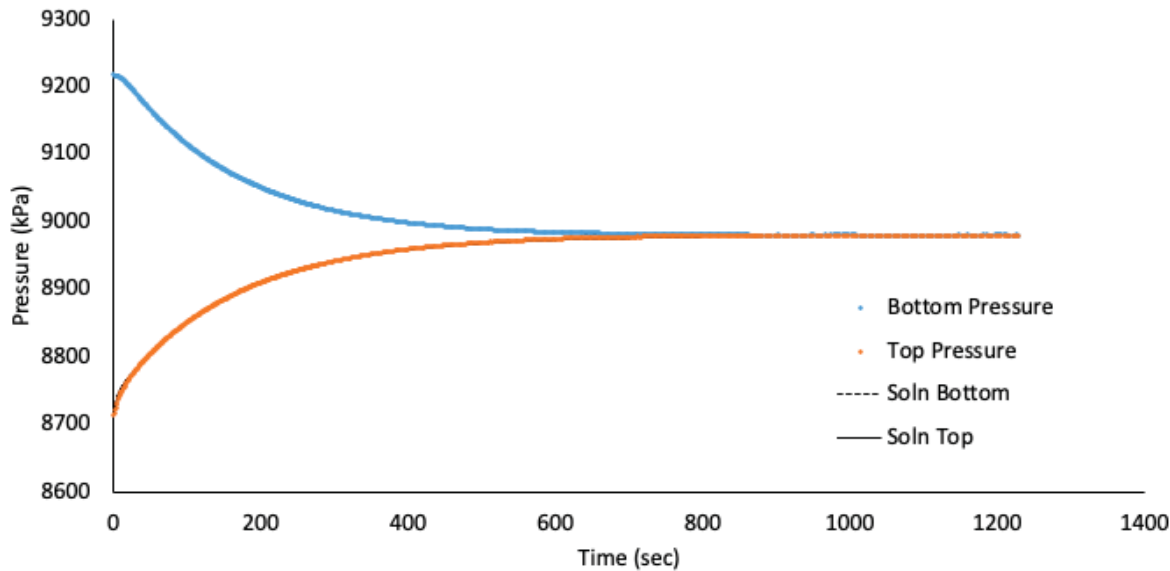


Figure 82 IG_BH05_PS002_HC25r: Effective Confining Stress = 8.02 MPa

	Sample Name		IG_BH05_PS002
	Specimen Name		IG_BH05_PS002_HC25r
	Specimen Top Depth		434.045
	Specimen Bottom Depth		434.080
	Test No		ES2
	Test Name		9005.5132605_ES2
	Operator		StephenTalman/FrancyGuerrero
Dimensions	Length	mm	26.630
	Diameter	mm	25.340
	Length	m	0.02663
	Diameter	m	0.02534
Test Data Location	Raw Data File Name		IG-BH05-PS002-HC25r-002-A.dat
	Date & Time		2023-05-04 07:01:13
	Start Row		86
	End Row		1350
Test Conditions	Avg Cell Temp	C	39.72
	Avg Confining Pressure	kPa	22233
	Pre Pulse Avg Pore Pressure	kPa	8714
	Pulse Pressure	kPa	484
	Effective Stress	kPa	13519
	Post Pulse Avg Pore Pressure	kPa	8714
Pore Fluid & Conditions	Type		Water
	Salt	ppm	0
	Density	kg/m3	996.07
	Viscosity	kg.s/m	6.573E-04
	Compressibility	1/Pa	4.36E-10
Solution	Test System		System3-Cell3
Brace	Nominal Decay Time	s	3476
	Brace Permeability	m2	3.29E-20
Hsieh	Permeability	m2	3.15E-20
	Specific Storage	1/m	1.07E-07
	Permeability	nD	31.9
	Hydraulic Conductivity	m/s	4.69E-13
	Pearson Coeff	()	0.9993282

IG_BH05_PS002_HC25r Eff Stress:13.52 MPa, HC=4.69e-13 m/s, SS=1.07e-7 1/m

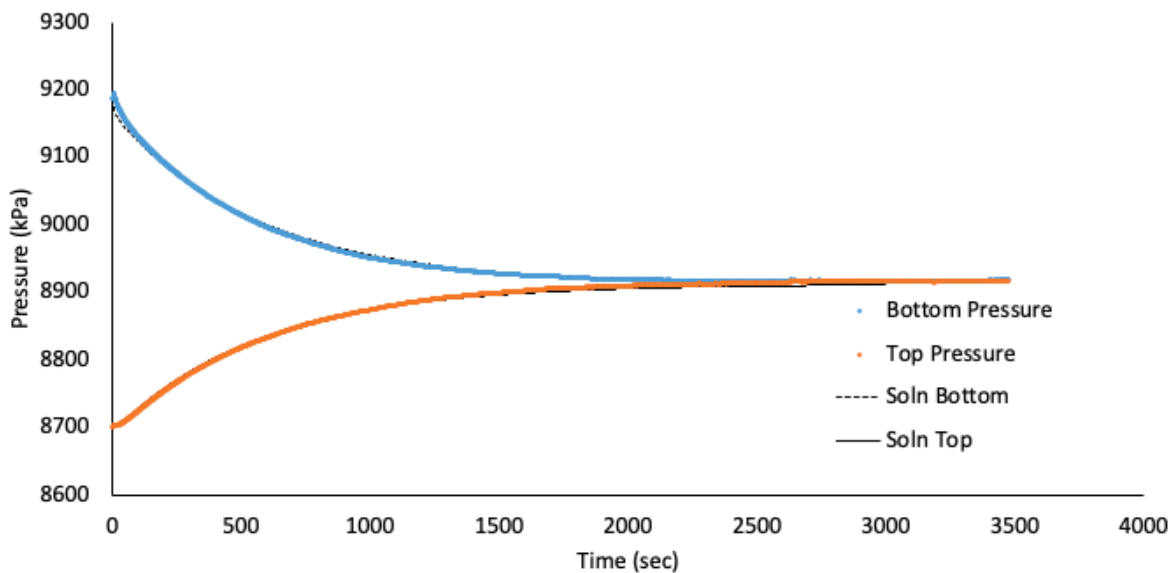


Figure 83 IG_BH05_PS002_HC25r: Effective Confining Stress = 13.52 MPa

	Sample Name		IG_BH05_PS002
	Specimen Name		IG_BH05_PS002_HC61a
	Specimen Top Depth		933.405
	Specimen Bottom Depth		933.44
	Test No		ES1
	Test Name		IG_BH05_PS002_HC61a_ES1
	Operator		Stephen Talman/ Francy Guerrero
Dimensions	Length	mm	61.820
	Diameter	mm	61.670
	Length	m	0.06182
	Diameter	m	0.06167
Test Data Location	Raw Data File Name		2023-05-03_14-34-38 System-3-Cell-2 IG-BH05-PS002-HC61a.csv
	Date & Time		2023-05-03 14:34:38
	Start Row		939
	End Row		2160
Test Conditions	Avg Cell Temp	°C	40.10
	Avg Confining Pressure	kPa	17273
	Pre Pulse Avg Pore Pressure	kPa	9262
	Pulse Pressure	kPa	521
	Effective Stress	kPa	8011
	Post Pulse Avg Pore Pressure	kPa	9262
Pore Fluid & Conditions	Type		Water
	Salt	ppm	0
	Density	kg/m³	996.16
	Viscosity	kg.s/m	6.527E-04
	Compressibility	1/Pa	4.36E-10
Solution	System and Cell		System 3 - Cell 2
Brace	Nominal Decay Time	s	1221
	Brace Permeability	m²	9.14E-20
Hsieh	Permeability	m²	8.81E-20
	Specific Storage	1/m	1.06E-07
	Permeability	nD	89.3
	Hydraulic Conductivity	m/s	1.32E-12
	Pearson Coeff	()	0.9973792

IG_BH05_PS002_HC61a Eff Stress:8.01 MPa, HC=1.32e-12 m/s, SS=1.06e-7 1/m

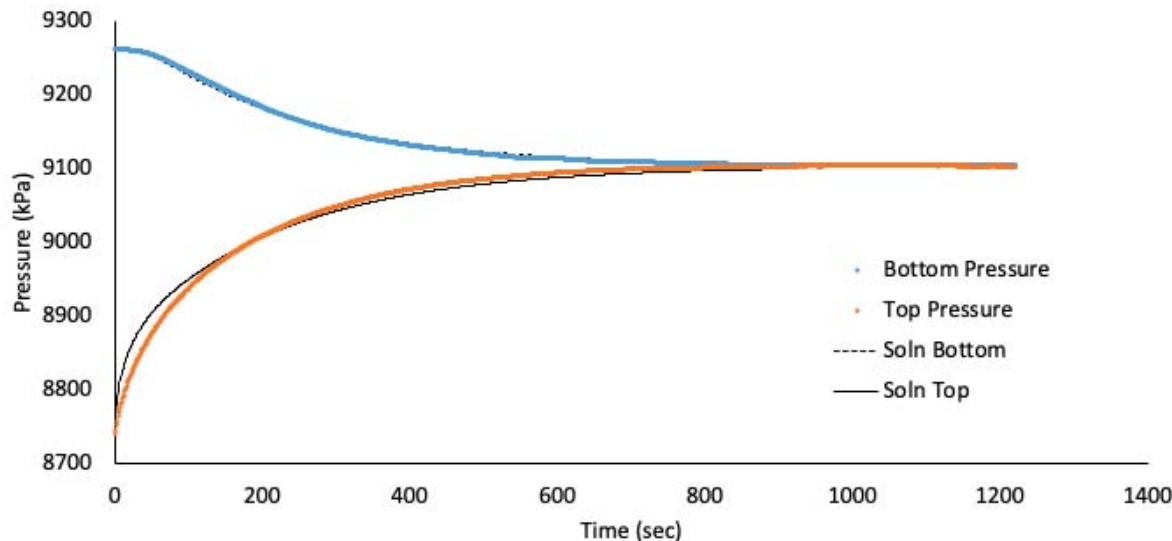


Figure 84 IG_BH05_PS002_HC61a: Effective Confining Stress = 8.01 MPa

	Sample Name		IG_BH05_PS002
	Specimen Name		IG_BH05_PS002_HC61a
	Specimen Top Depth		933.405
	Specimen Bottom Depth		933.44
	Test No		ES2
	Test Name		IG_BH05_PS002_HC61a_ES2
	Operator		Stephen Talman/ Francy Guerrero
Dimensions	Length	mm	61.820
	Diameter	mm	61.670
	Length	m	0.06182
	Diameter	m	0.06167
Test Data Location	Raw Data File Name		2023-05-03_14-34-38 System-3-Cell-2 IG-BH05-PS002-HC61a.csv
	Date & Time		2023-05-04 07:00:49
	Start Row		265
	End Row		3600
Test Conditions	Avg Cell Temp	C	40.06
	Avg Confining Pressure	kPa	22271
	Pre Pulse Avg Pore Pressure	kPa	8716
	Pulse Pressure	kPa	475
	Effective Stress	kPa	13556
	Post Pulse Avg Pore Pressure	kPa	8716
Pore Fluid & Conditions	Type		Water
	Salt	ppm	0
	Density	kg/m3	995.94
	Viscosity	kg.s/m	6.531E-04
	Compressibility	1/Pa	4.36E-10
Solution	System and Cell		System 3 - Cell 2
Brace	Nominal Decay Time	s	3335
	Brace Permeability	m2	3.34E-20
Hsieh	Permeability	m2	4.01E-20
	Specific Storage	1/m	1.79E-07
	Permeability	nD	40.6
	Hydraulic Conductivity	m/s	6.00E-13
	Pearson Coeff	()	0.9968619

IG_BH05_PS002_HC61a Eff Stress:13.56 MPa, HC=6.00e-13 m/s, SS=1.79e-7 1/m

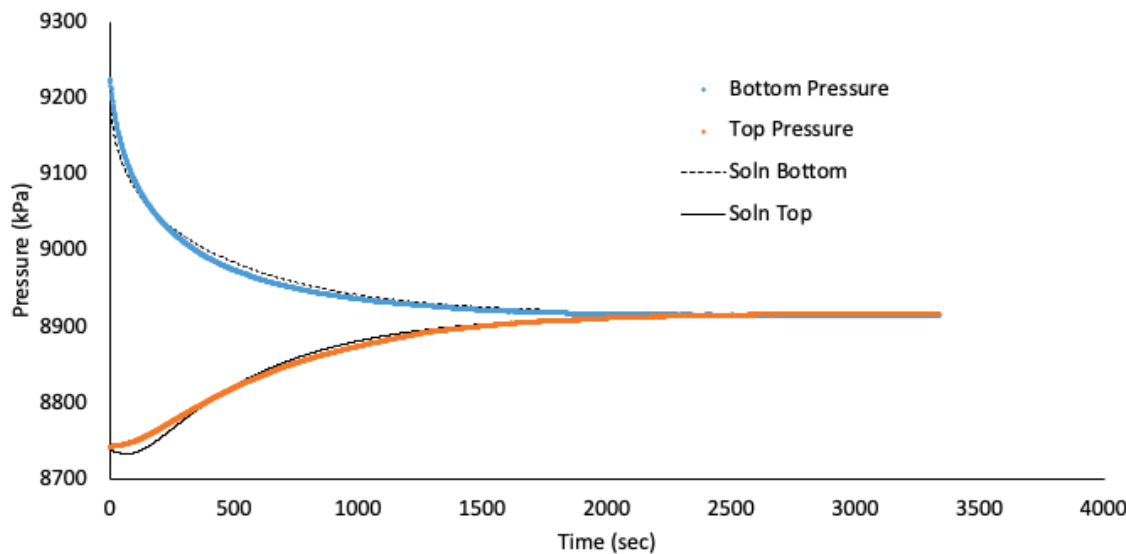


Figure 85 IG_BH05_PS002_HC61a: Effective Confining Stress = 13.56 MPa

	Sample Name		IG_BH05_PS003
	Specimen Name		IG_BH05_PS003_HC25a
	Specimen Top Depth		527.64
	Specimen Bottom Depth		527.674
	Test No		ES1
	Test Name		9075.086156_ES1
	Operator		Stephen Talman/ Francy Guerrero
Dimensions	Length	mm	24.950
	Diameter	mm	25.180
	Length	m	0.02495
	Diameter	m	0.02518
Test Data Location	Raw Data File Name		2023-05-10_11-24-34 System-2-CELL-1 IG-BH05-PS003-HC25a.csv
	Date & Time		2023-05-10 11:24:34
	Start Row		1045
	End Row		3500
Test Conditions	Avg Cell Temp	C	39.86
	Avg Confining Pressure	kPa	18945
	Pre Pulse Avg Pore Pressure	kPa	8855
	Pulse Pressure	kPa	-501
	Effective Stress	kPa	10090
	Post Pulse Avg Pore Pressure	kPa	8855
Pore Fluid & Conditions	Type		Water
	Salt	ppm	0
	Density	kg/m3	996.07
	Viscosity	kg.s/m	6.556E-04
	Compressibility	1/Pa	4.36E-10
Solution	Test System		System 2 - CELL 1
Brace	Nominal Decay Time	s	2455
	Brace Permeability	m2	3.55E-20
Hsieh	Permeability	m2	4.26E-20
	Specific Storage	1/m	1.37E-07
	Permeability	nD	43.2
	Hydraulic Conductivity	m/s	6.36E-13
	Pearson Coeff	()	0.9957702

IG_BH05_PS003_HC25a Eff Stress:10.09 MPa, HC=6.36e-13 m/s, SS=1.37e-7 1/m

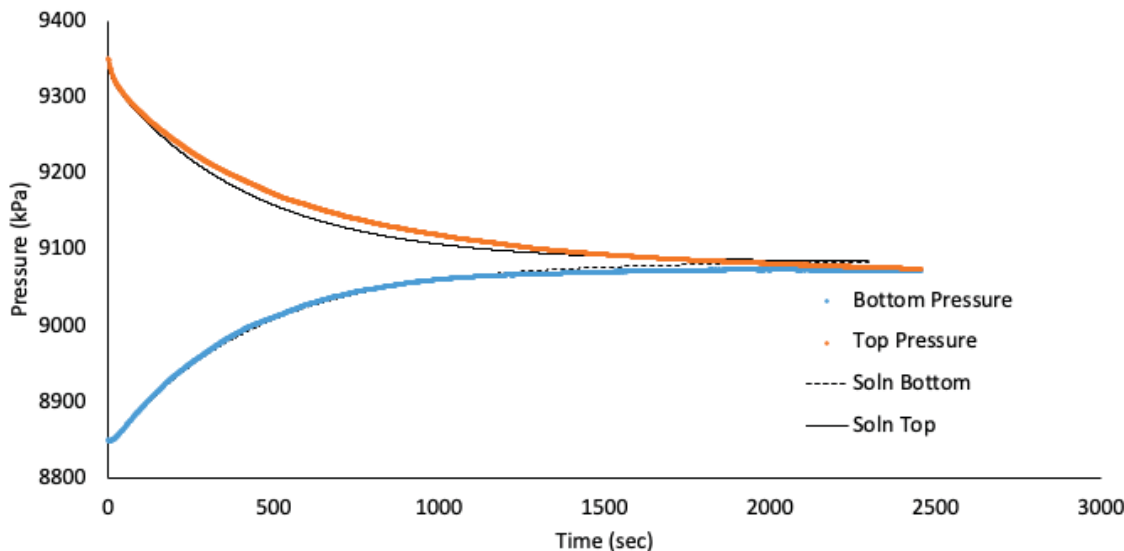


Figure 86 IG_BH05_PS003_HC25a: Effective Confining Stress = 10.09 MPa

	Sample Name		IG_BH05_PS003
	Specimen Name		IG_BH05_PS003_HC25a
	Specimen Top Depth		527.64
	Specimen Bottom Depth		527.674
	Test No		ES2
	Test Name		8964.35895374332_ES2
	Operator		Stephen Talman/ Francy Guerrero
Dimensions	Length	mm	24.950
	Diameter	mm	25.180
	Length	m	0.02495
	Diameter	m	0.02518
Test Data Location	Raw Data File Name		2023-05-11_07-55-01 System-2-CELL-1 IG-BH05-PS003-HC25a.csv
	Date & Time		2023-05-11 07:55:01
	Start Row		8299
	End Row		15000
Test Conditions	Avg Cell Temp	C	39.87
	Avg Confining Pressure	kPa	23922
	Pre Pulse Avg Pore Pressure	kPa	9101
	Pulse Pressure	kPa	241
	Effective Stress	kPa	14821
Pore Fluid & Conditions	Post Pulse Avg Pore Pressure	kPa	9101
	Type		Water
	Salt	ppm	0
	Density	kg/m3	996.18
	Viscosity	kg.s/m	6.555E-04
Solution	Compressibility	1/Pa	4.36E-10
	Test System		System 2 - CELL 1
Brace	Nominal Decay Time	s	6701
	Brace Permeability	m2	1.69E-20
Hsieh	Permeability	m2	1.95E-20
	Specific Storage	1/m	9.06E-08
	Permeability	nD	19.7
	Hydraulic Conductivity	m/s	2.90E-13
	Pearson Coeff	()	0.9970758

IG_BH05_PS003_HC25a Eff Stress:14.82 MPa, HC=2.90e-13 m/s, SS=9.06e-8 1/m

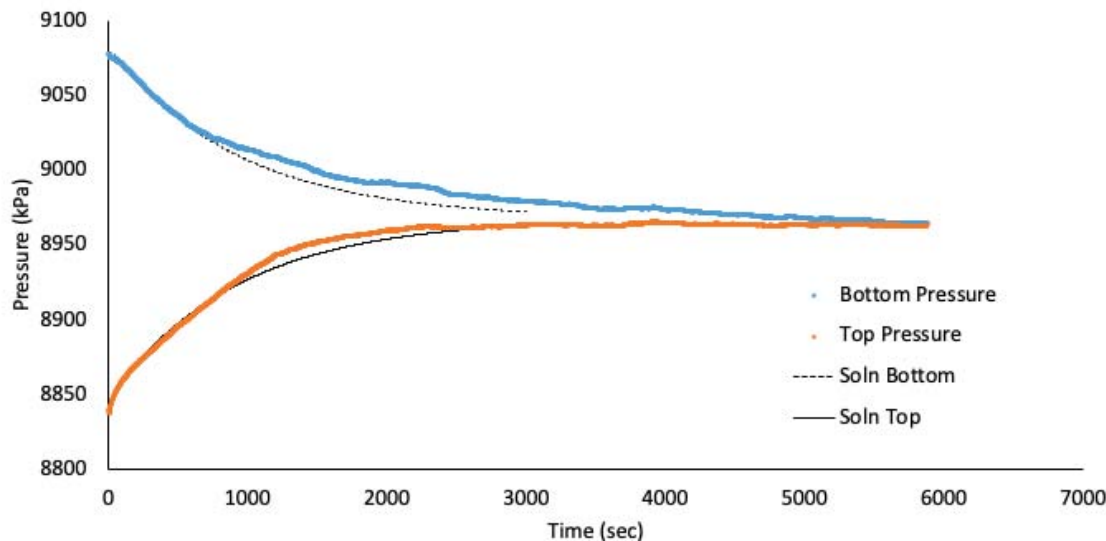


Figure 87 IG_BH05_PS003_HC25a: Effective Confining Stress = 14.82 MPa

	Sample Name		IG_BH05_PS003
	Specimen Name		IG_BH05_PS003_HC25a
	Specimen Top Depth		527.64
	Specimen Bottom Depth		527.674
	Test No		ES3
	Test Name		8804.04122008607_ES3
	Operator		Stephen Talman/ Francy Guerrero
Dimensions	Length	mm	24.950
	Diameter	mm	25.180
	Length	m	0.02495
	Diameter	m	0.02518
Test Data Location	Raw Data File Name		2023-05-10_11-24-34 System-2-CELL-1 IG-BH05-PS003-HC25a.csv
	Date & Time		2023-05-12 09:34:44
	Start Row		16235
	End Row		40000
Test Conditions	Avg Cell Temp	C	39.89
	Avg Confining Pressure	kPa	28898
	Pre Pulse Avg Pore Pressure	kPa	9147
	Pulse Pressure	kPa	488
	Effective Stress	kPa	19751
	Post Pulse Avg Pore Pressure	kPa	9147
Pore Fluid & Conditions	Type		Water
	Salt	ppm	0
	Density	kg/m3	996.19
	Viscosity	kg.s/m	6.553E-04
	Compressibility	1/Pa	4.36E-10
Solution	Test System		System 2 - CELL 1
Brace	Nominal Decay Time	s	23765
	Brace Permeability	m2	6.09E-21
Hsieh	Permeability	m2	6.39E-21
	Specific Storage	1/m	1.15E-07
	Permeability	nD	6.5
	Hydraulic Conductivity	m/s	9.53E-14
	Pearson Coeff	()	0.9952240

IG_BH05_PS003_HC25a Eff Stress:19.75 MPa, HC=9.53e-14 m/s, SS=1.15e-7 1/m

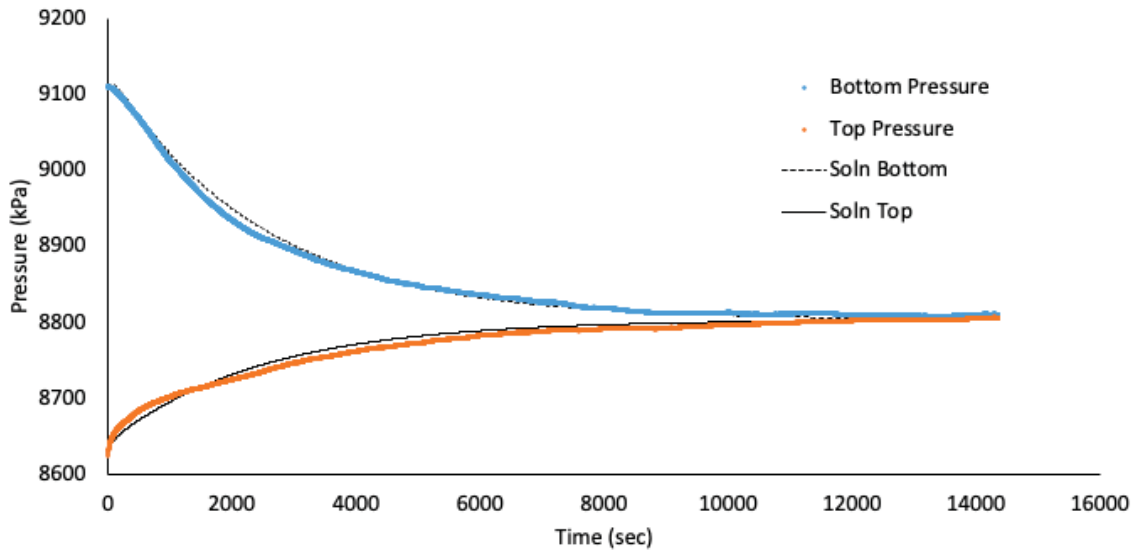


Figure 88 IG_BH05_PS003_HC25a: Effective Confining Stress = 19.75 MPa

	Sample Name		IG_BH05_PS003
	Specimen Name		IG_BH05_PS003_HC25r
	Specimen Top Depth		527.736
	Specimen Bottom Depth		527.771
	Test No		ES1
	Test Name		9111.96181266667_ES1
	Operator		StephenTalman/FrancyGuerrero
Dimensions	Length	mm	25.300
	Diameter	mm	25.150
	Length	m	0.0253
	Diameter	m	0.02515
Test Data Location	Raw Data File Name		IG-BH05-PS003-HC25r-001-A.dat
	Date & Time		2023-05-10 11:25:35
	Start Row		69
	End Row		1000
Test Conditions	Avg Cell Temp	C	39.62
	Avg Confining Pressure	kPa	18800
	Pre Pulse Avg Pore Pressure	kPa	8810
	Pulse Pressure	kPa	-506
	Effective Stress	kPa	9990
	Post Pulse Avg Pore Pressure	kPa	8810
Pore Fluid & Conditions	Type		Water
	Salt	ppm	0
	Density	kg/m3	996.15
	Viscosity	kg.s/m	6.585E-04
	Compressibility	1/Pa	4.36E-10
Solution	Test System		System2-CELL3
Brace	Nominal Decay Time	s	1990
	Brace Permeability	m2	5.89E-20
Hsieh	Permeability	m2	6.23E-20
	Specific Storage	1/m	1.43E-07
	Permeability	nD	63.1
	Hydraulic Conductivity	m/s	9.25E-13
	Pearson Coeff	()	0.9996942

IG_BH05_PS003_HC25r Eff Stress:9.99 MPa, HC=9.25e-13 m/s, SS=1.43e-7 1/m

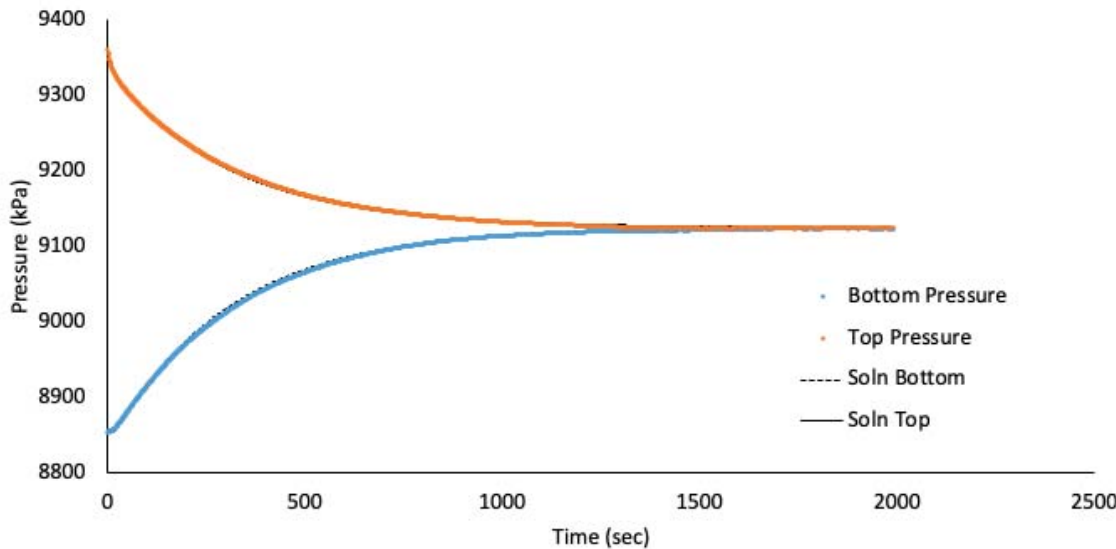


Figure 89 IG_BH05_PS003_HC25r: Effective Confining Stress = 9.99 MPa

	Sample Name		IG_BH05_PS003
	Specimen Name		IG_BH05_PS003_HC25r
	Specimen Top Depth		527.736
	Specimen Bottom Depth		527.771
	Test No		ES2
	Test Name		9104.41544616667_ES2
	Operator		StephenTalman/FrancyGuerrero
Dimensions	Length	mm	25.300
	Diameter	mm	25.150
	Length	m	0.0253
	Diameter	m	0.02515
Test Data Location	Raw Data File Name		IG-BH05-PS003-HC25r-002-A.dat
	Date & Time		2023-05-11 07:55:41
	Start Row		73
	End Row		1296
Test Conditions	Avg Cell Temp	C	39.63
	Avg Confining Pressure	kPa	23743
	Pre Pulse Avg Pore Pressure	kPa	9180
	Pulse Pressure	kPa	-450
	Effective Stress	kPa	14563
	Post Pulse Avg Pore Pressure	kPa	9180
Pore Fluid & Conditions	Type		Water
	Salt	ppm	0
	Density	kg/m3	996.31
	Viscosity	kg.s/m	6.585E-04
	Compressibility	1/Pa	4.36E-10
Solution	Test System		System2-CELL3
Brace	Nominal Decay Time	s	3219
	Brace Permeability	m2	2.68E-20
Hsieh	Permeability	m2	2.65E-20
	Specific Storage	1/m	1.43E-07
	Permeability	nD	26.9
	Hydraulic Conductivity	m/s	3.93E-13
	Pearson Coeff	()	0.9997476

IG_BH05_PS003_HC25r Eff Stress:14.56 MPa, HC=3.93e-13 m/s, SS=1.43e-7 1/m

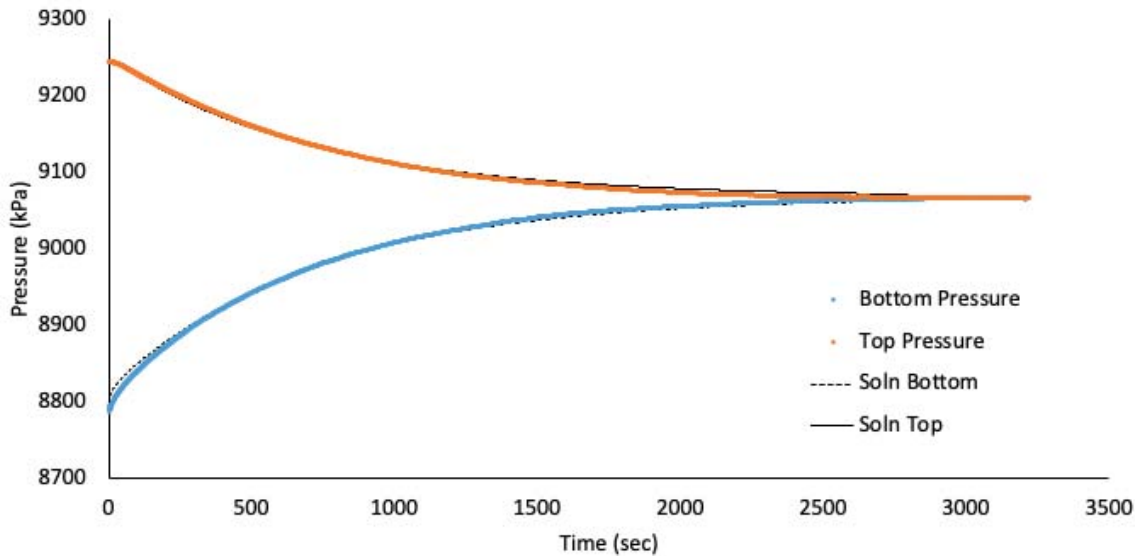


Figure 90 IG_BH05_PS003_HC25r: Effective Confining Stress = 14.56 MPa

	Sample Name		IG_BH05_PS003
	Specimen Name		IG_BH05_PS003_HC25r
	Specimen Top Depth		527.736
	Specimen Bottom Depth		527.771
	Test No		ES3
	Test Name		8960.23087283333_ES3
	Operator		StephenTalman/FrancyGuerrero
Dimensions	Length	mm	25.300
	Diameter	mm	25.150
	Length	m	0.0253
	Diameter	m	0.02515
Test Data Location	Raw Data File Name		IG-BH05-PS003-HC25r-003-B.dat
	Date & Time		2023-05-12 09:35:28
	Start Row		67
	End Row		2700
Test Conditions	Avg Cell Temp	C	39.67
	Avg Confining Pressure	kPa	28686
	Pre Pulse Avg Pore Pressure	kPa	9096
	Pulse Pressure	kPa	483
	Effective Stress	kPa	19590
	Post Pulse Avg Pore Pressure	kPa	9096
Pore Fluid & Conditions	Type		Water
	Salt	ppm	0
	Density	kg/m3	996.25
	Viscosity	kg.s/m	6.580E-04
	Compressibility	1/Pa	4.36E-10
Solution	Test System		System2-CELL3
Brace	Nominal Decay Time	s	13057
	Brace Permeability	m2	9.81E-21
Hsieh	Permeability	m2	1.01E-20
	Specific Storage	1/m	1.32E-07
	Permeability	nD	10.2
	Hydraulic Conductivity	m/s	1.50E-13
	Pearson Coeff	()	0.9997877

IG_BH05_PS003_HC25r Eff Stress:19.59 MPa, HC=1.50e-13 m/s, SS=1.32e-7 1/m

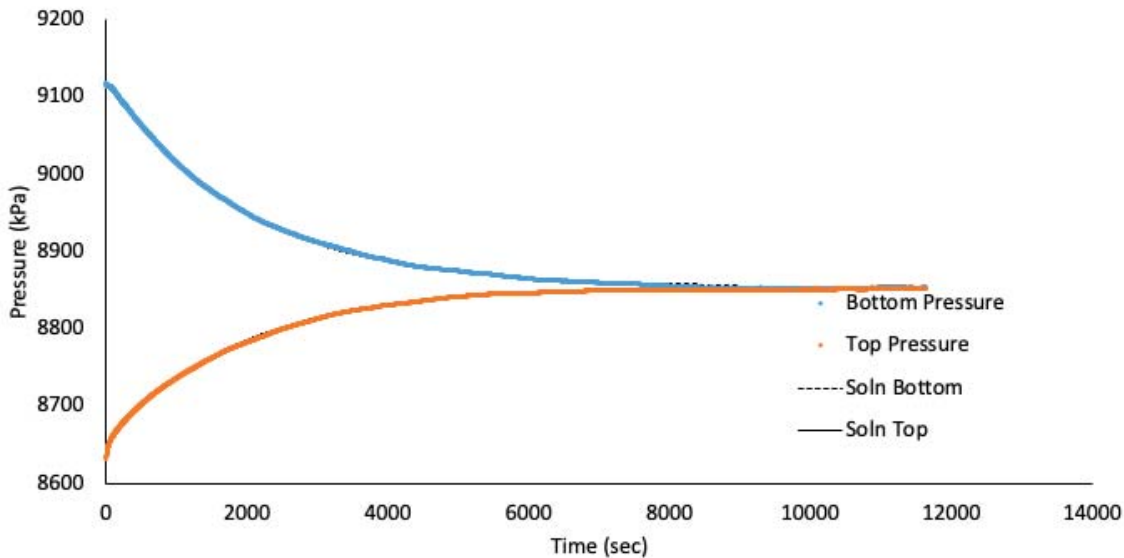


Figure 91 IG_BH05_PS003_HC25r: Effective Confining Stress = 19.59 MPa

	Sample Name		IG_BH05_PS003
	Specimen Name		IG_BH05_PS003_HC61a
	Specimen Top Depth		527.674
	Specimen Bottom Depth		527.736
	Test No		ES1
	Test Name		9116.4371874407_ES1
	Operator		Stephen Talman/ Francy Guerrero
Dimensions	Length	mm	61.370
	Diameter	mm	61.120
	Length	m	0.06137
	Diameter	m	0.06112
Test Data Location	Raw Data File Name		2023-05-10_11-24-56 System-2-CELL-2 IG-BH05-PS003-HC61a.csv
	Date & Time		2023-05-10 11:24:56
	Start Row		7467
	End Row		9800
Test Conditions	Avg Cell Temp	C	39.84
	Avg Confining Pressure	kPa	19036
	Pre Pulse Avg Pore Pressure	kPa	9252
	Pulse Pressure	kPa	-480
	Effective Stress	kPa	9784
	Post Pulse Avg Pore Pressure	kPa	9252
Pore Fluid & Conditions	Type		Water
	Salt	ppm	0
	Density	kg/m3	996.25
	Viscosity	kg.s/m	6.559E-04
	Compressibility	1/Pa	4.36E-10
Solution	Test System		System 2 - CELL 2
Brace	Nominal Decay Time	s	2333
	Brace Permeability	m2	4.84E-20
Hsieh	Permeability	m2	5.13E-20
	Specific Storage	1/m	1.19E-07
	Permeability	nD	52.0
	Hydraulic Conductivity	m/s	7.64E-13
	Pearson Coeff	()	0.9987422

IG_BH05_PS003_HC61a Eff Stress:9.78 MPa, HC=7.64e-13 m/s, SS=1.19e-7 1/m

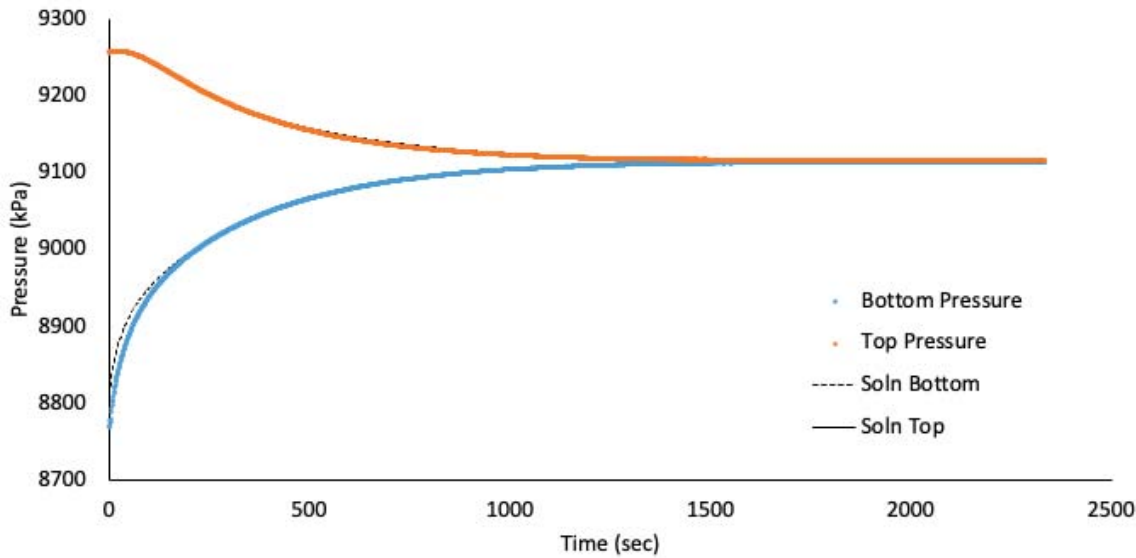


Figure 92 IG_BH05_PS003_HC61a: Effective Confining Stress = 9.78 MPa

	Sample Name		IG_BH05_PS004
	Specimen Name		IG_BH05_PS004_HC25a
	Specimen Top Depth		641.495
	Specimen Bottom Depth		641.530
	Test No		ES1
	Test Name		9320.14770556694_ES1
	Operator		Stephen Talman/ Francy Guerrero
Dimensions	Length	mm	25.210
	Diameter	mm	24.470
	Length	m	0.02521
	Diameter	m	0.02447
Test Data Location	Raw Data File Name		2023-05-19_08-42-40 System-3-Cell-1 IG-BH05-PS004-HC25a.csv
	Date & Time		2023-05-19 08:42:40
	Start Row		968
	End Row		2000
Test Conditions	Avg Cell Temp	C	40.32
	Avg Confining Pressure	kPa	21201
	Pre Pulse Avg Pore Pressure	kPa	9552
	Pulse Pressure	kPa	-475
	Effective Stress	kPa	11648
Pore Fluid & Conditions	Post Pulse Avg Pore Pressure	kPa	9552
	Type		Water
	Salt	ppm	0
	Density	kg/m3	996.2
	Viscosity	kg.s/m	6.501E-04
Solution	Compressibility	1/Pa	4.36E-10
	Test System		System 3 - Cell 1
Brace	Nominal Decay Time	s	1032
	Brace Permeability	m2	1.45E-19
Hsieh	Permeability	m2	1.45E-19
	Specific Storage	1/m	8.18E-08
	Permeability	nD	146.6
	Hydraulic Conductivity	m/s	2.18E-12
	Pearson Coeff	()	0.9994433

IG_BH05_PS004_HC25a Eff Stress:11.65 MPa, HC=2.18e-12 m/s, SS=8.18e-8 1/m

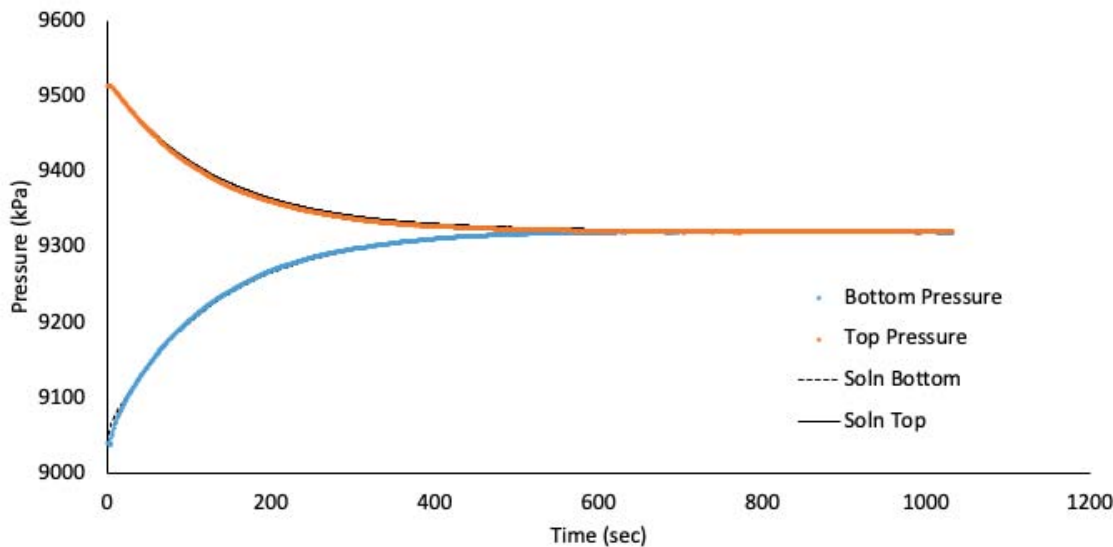


Figure 93 IG_BH05_PS004_HC25a: Effective Confining Stress = 11.65 MPa

	Sample Name		IG_BH05_PS004
	Specimen Name		IG_BH05_PS004_HC25a
	Specimen Top Depth		641.495
	Specimen Bottom Depth		641.530
	Test No		ES2
	Test Name		IG_BH05_PS004_HC25a_ES2
	Operator		Stephen Talman/ Francy Guerrero
Dimensions	Length	mm	25.210
	Diameter	mm	24.470
	Length	m	0.02521
	Diameter	m	0.02447
Test Data Location	Raw Data File Name		2023-05-19_08-42-40 System-3-Cell-1 IG-BH05-PS004-HC25a.csv
	Date & Time		2023-05-21 19:19:51
	Start Row		12249
	End Row		14300
Test Conditions	Avg Cell Temp	C	40.36
	Avg Confining Pressure	kPa	26191
	Pre Pulse Avg Pore Pressure	kPa	9404
	Pulse Pressure	kPa	538
	Effective Stress	kPa	16787
	Post Pulse Avg Pore Pressure	kPa	9404
Pore Fluid & Conditions	Type		Water
	Salt	ppm	0
	Density	kg/m3	996.12
	Viscosity	kg.s/m	6.496E-04
	Compressibility	1/Pa	4.36E-10
Solution	Test System		System 3 - Cell 1
Brace	Nominal Decay Time	s	2051
	Brace Permeability	m2	5.42E-20
Hsieh	Permeability	m2	5.42E-20
	Specific Storage	1/m	9.10E-08
	Permeability	nD	54.9
	Hydraulic Conductivity	m/s	8.16E-13
	Pearson Coeff	()	0.9998048

IG_BH05_PS004_HC25a Eff Stress:16.79 MPa, HC=8.16e-13 m/s, SS=9.10e-8 1/m

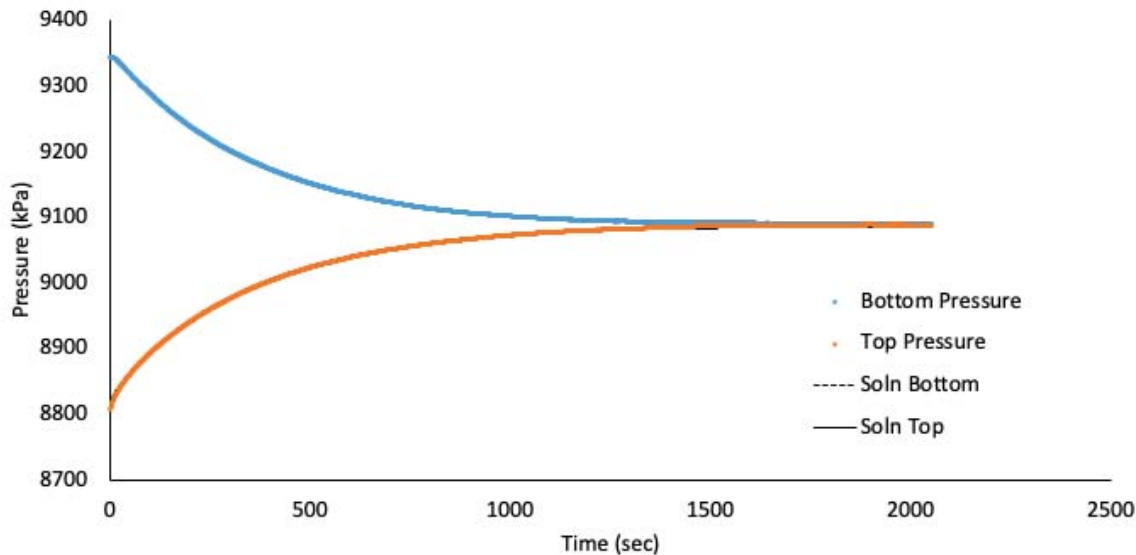


Figure 94 IG_BH05_PS004_HC25a: Effective Confining Stress = 16.79 MPa

	Sample Name		IG_BH05_PS004
	Specimen Name		IG_BH05_PS004_HC25a
	Specimen Top Depth		641.495
	Specimen Bottom Depth		641.530
	Test No		ES3
	Test Name		IG_BH05_PS004_HC25a_ES3
	Operator		Stephen Talman/ Francy Guerrero
Dimensions	Length	mm	25.210
	Diameter	mm	24.470
	Length	m	0.02521
	Diameter	m	0.02447
Test Data Location	Raw Data File Name		2023-05-19_08-42-40 System-3-Cell-1 IG-BH05-PS004-HC25a.csv
	Date & Time		2023-05-23 08:12:44
	Start Row		1170
	End Row		5699
Test Conditions	Avg Cell Temp	C	40.40
	Avg Confining Pressure	kPa	31187
	Pre Pulse Avg Pore Pressure	kPa	9356
	Pulse Pressure	kPa	462
	Effective Stress	kPa	21831
	Post Pulse Avg Pore Pressure	kPa	9356
Pore Fluid & Conditions	Type		Water
	Salt	ppm	0
	Density	kg/m3	996.08
	Viscosity	kg.s/m	6.491E-04
	Compressibility	1/Pa	4.36E-10
Solution	Test System		System 3 - Cell 1
Brace	Nominal Decay Time	s	4529
	Brace Permeability	m2	4.30E-20
Hsieh	Permeability	m2	4.30E-20
	Specific Storage	1/m	6.57E-08
	Permeability	nD	43.6
	Hydraulic Conductivity	m/s	6.48E-13
	Pearson Coeff	()	0.9996490

IG_BH05_PS004_HC25a Eff Stress:21.83 MPa, HC=6.48e-13 m/s, SS=6.57e-8 1/m

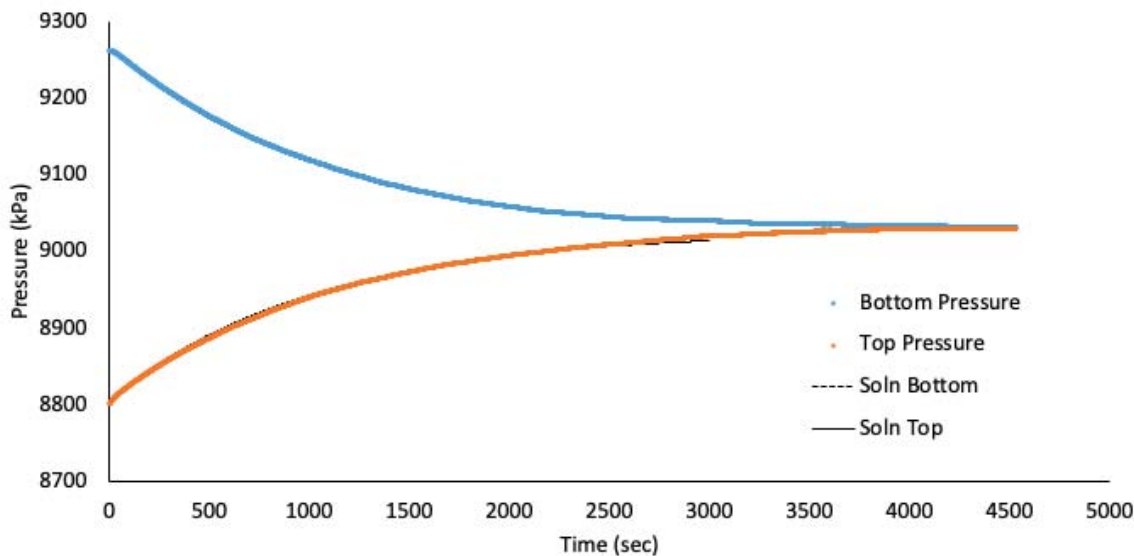


Figure 95 IG_BH05_PS004_HC25a: Effective Confining Stress = 21.83 MPa

	Sample Name		IG_BH05_PS004
	Specimen Name		IG_BH05_PS004_HC25r
	Specimen Top Depth		641.495
	Specimen Bottom Depth		641.530
	Test No		ES1
	Test Name		IG_BH05_PS004_HC25r_ES1
	Operator		Stephen Talman/ Francy Guerrero
Dimensions	Length	mm	24.920
	Diameter	mm	25.040
	Length	m	0.02492
	Diameter	m	0.02504
Test Data Location	Raw Data File Name		2023-05-19_08-43-40 System-3-Cell-3 IG-BH05-PS004-HC25r.csv
	Date & Time		2023-05-19 08:43:40
	Start Row		891
	End Row		2000
Test Conditions	Avg Cell Temp	C	39.54
	Avg Confining Pressure	kPa	21154
	Pre Pulse Avg Pore Pressure	kPa	9536
	Pulse Pressure	kPa	-491
	Effective Stress	kPa	11617
Pore Fluid & Conditions	Post Pulse Avg Pore Pressure	kPa	9536
	Type		Water
	Salt	ppm	0
	Density	kg/m3	996.49
	Viscosity	kg.s/m	6.596E-04
Solution	Compressibility	1/Pa	4.36E-10
	Test System		System 3 - Cell 3
Brace	Nominal Decay Time	s	1109
	Brace Permeability	m2	1.44E-19
Hsieh	Permeability	m2	1.53E-19
	Specific Storage	1/m	5.56E-08
	Permeability	nD	154.5
	Hydraulic Conductivity	m/s	2.26E-12
	Pearson Coeff	()	0.9995266

IG_BH05_PS004_HC25r Eff Stress:11.62 MPa, HC=2.26e-12 m/s, SS=5.56e-8 1/m

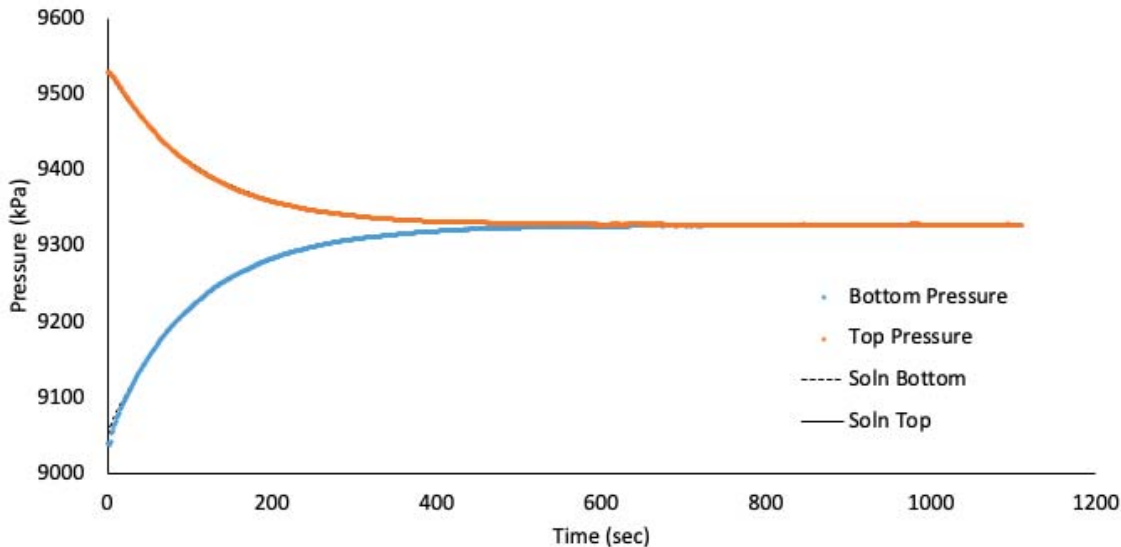


Figure 96 IG_BH05_PS004_HC25r: Effective Confining Stress = 11.62 MPa

	Sample Name		IG_BH05_PS004
	Specimen Name		IG_BH05_PS004_HC25r
	Specimen Top Depth		641.495
	Specimen Bottom Depth		641.530
	Test No		ES2
	Test Name		IG_BH05_PS004_HC25r_ES2
	Operator		Stephen Talman/ Francy Guerrero
Dimensions	Length	mm	24.920
	Diameter	mm	25.040
	Length	m	0.02492
	Diameter	m	0.02504
Test Data Location	Raw Data File Name		2023-05-21_19-19-55 System-3-Cell-3 IG-BH05-PS004-HC25r.csv
	Date & Time		2023-05-21 19:19:55
	Start Row		9417
	End Row		11200
Test Conditions	Avg Cell Temp	C	39.72
	Avg Confining Pressure	kPa	26131
	Pre Pulse Avg Pore Pressure	kPa	9517
	Pulse Pressure	kPa	-485
	Effective Stress	kPa	16614
	Post Pulse Avg Pore Pressure	kPa	9517
Pore Fluid & Conditions	Type		Water
	Salt	ppm	0
	Density	kg/m3	996.42
	Viscosity	kg.s/m	6.574E-04
	Compressibility	1/Pa	4.36E-10
Solution	Test System		System 3 - Cell 3
Brace	Nominal Decay Time	s	1783
	Brace Permeability	m2	4.41E-20
Hsieh	Permeability	m2	4.58E-20
	Specific Storage	1/m	1.00E-07
	Permeability	nD	46.4
	Hydraulic Conductivity	m/s	6.82E-13
	Pearson Coeff	()	0.9985371

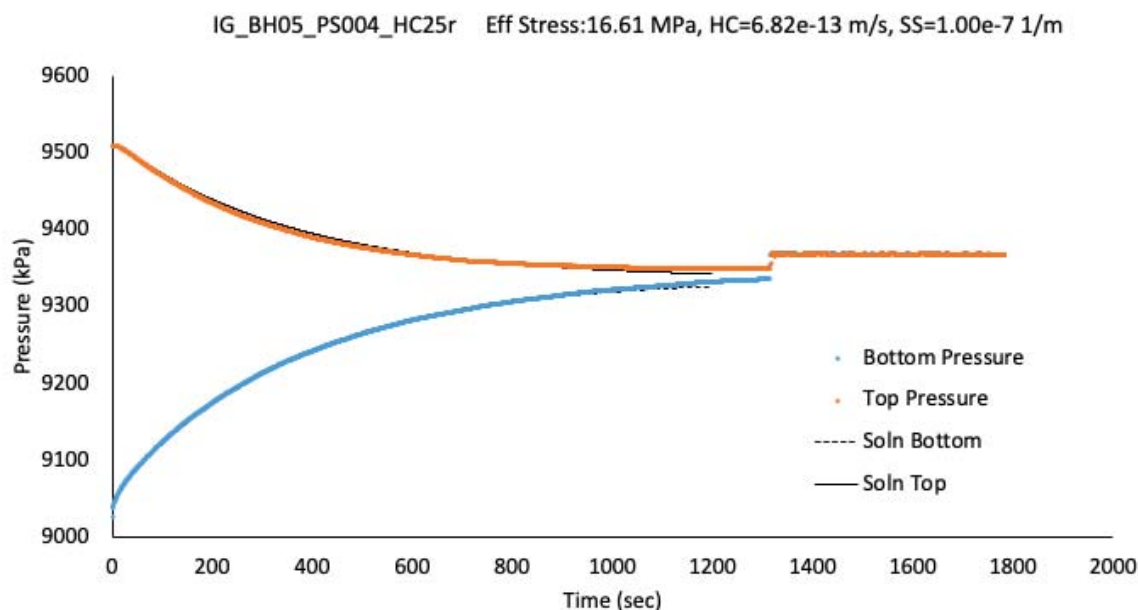


Figure 97 IG_BH05_PS004_HC25r: Effective Confining Stress = 16.61 MPa

	Sample Name		IG_BH05_PS004
	Specimen Name		IG_BH05_PS004_HC25r
	Specimen Top Depth		641.495
	Specimen Bottom Depth		641.530
	Test No		ES3
	Test Name		IG_BH05_PS004_HC25r_ES3
	Operator		Stephen Talman/ Francy Guerrero
Dimensions	Length	mm	24.920
	Diameter	mm	25.040
	Length	m	0.02492
	Diameter	m	0.02504
Test Data Location	Raw Data File Name		2023-05-19_08-43-40 System-3-Cell-3 IG-BH05-PS004-HC25r.csv
	Date & Time		2023-05-23 08:13:46
	Start Row		2843
	End Row		7600
Test Conditions	Avg Cell Temp	C	39.64
	Avg Confining Pressure	kPa	31116
	Pre Pulse Avg Pore Pressure	kPa	8813
	Pulse Pressure	kPa	519
	Effective Stress	kPa	22303
	Post Pulse Avg Pore Pressure	kPa	8813
Pore Fluid & Conditions	Type		Water
	Salt	ppm	0
	Density	kg/m3	996.14
	Viscosity	kg.s/m	6.583E-04
	Compressibility	1/Pa	4.36E-10
Solution	Test System		System 3 - Cell 3
Brace	Nominal Decay Time	s	4757
	Brace Permeability	m2	1.36E-20
Hsieh	Permeability	m2	1.38E-20
	Specific Storage	1/m	8.72E-08
	Permeability	nD	14.0
	Hydraulic Conductivity	m/s	2.06E-13
	Pearson Coeff	()	0.9976477

IG_BH05_PS004_HC25r Eff Stress:22.3 MPa, HC=2.06e-13 m/s, SS=8.72e-8 1/m

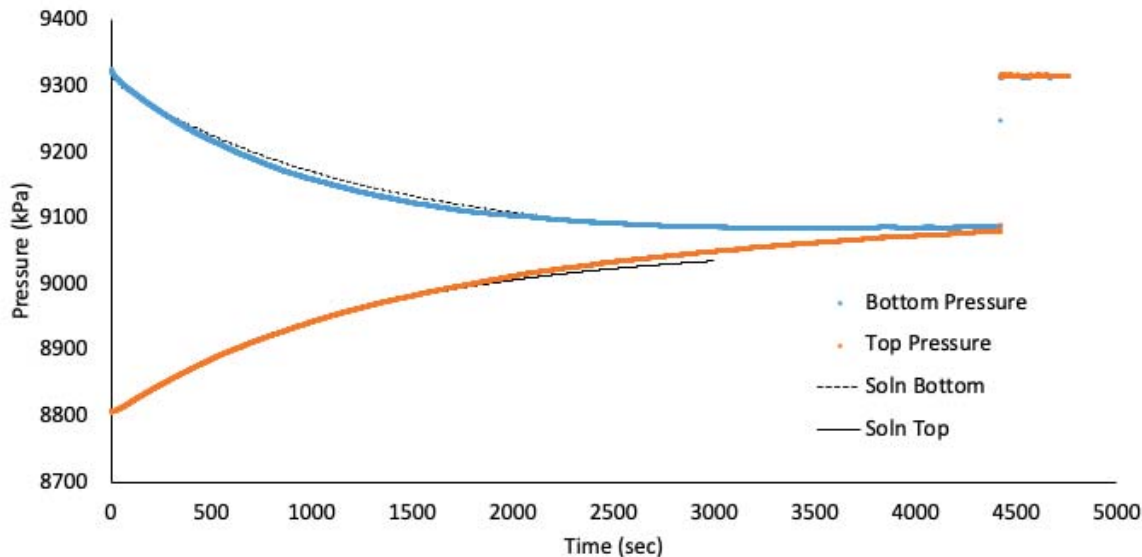


Figure 98 IG_BH05_PS004_HC25r: Effective Confining Stress = 22.30 MPa

	Sample Name		IG_BH05_PS004
	Specimen Name		IG_BH05_PS004_HC61a
	Specimen Top Depth		641.53
	Specimen Bottom Depth		641.592
	Test No		ES1
	Test Name		IG_BH05_PS004_HC61a_ES1
	Operator		Stephen Talman/ Francy Guerrero
Dimensions	Length	mm	61.680
	Diameter	mm	61.420
	Length	m	0.06168
	Diameter	m	0.06142
Test Data Location	Raw Data File Name		2023-05-19_08-43-06 System-3-Cell-2 IG-BH05-PS004-HC61a.csv
	Date & Time		2023-05-19 08:43:06
	Start Row		936
	End Row		2500
Test Conditions	Avg Cell Temp	C	40.10
	Avg Confining Pressure	kPa	21189
	Pre Pulse Avg Pore Pressure	kPa	9546
	Pulse Pressure	kPa	-514
	Effective Stress	kPa	11642
	Post Pulse Avg Pore Pressure	kPa	9546
Pore Fluid & Conditions	Type		Water
	Salt	ppm	0
	Density	kg/m3	996.28
	Viscosity	kg.s/m	6.528E-04
	Compressibility	1/Pa	4.36E-10
Solution	Test System		System 3 - Cell 2
Brace	Nominal Decay Time	s	1564
	Brace Permeability	m2	1.01E-19
Hsieh	Permeability	m2	1.07E-19
	Specific Storage	1/m	8.53E-08
	Permeability	nD	108.0
	Hydraulic Conductivity	m/s	1.60E-12
	Pearson Coeff	()	0.9988340

IG_BH05_PS004_HC61a Eff Stress:11.64 MPa, HC=1.60e-12 m/s, SS=8.53e-8 1/m

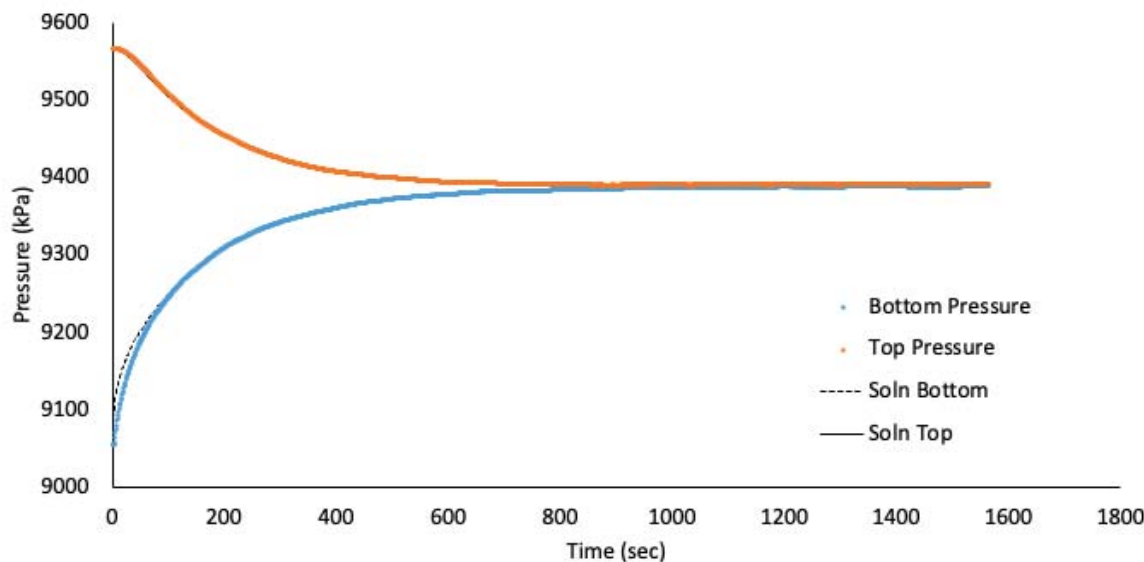


Figure 99 IG_BH05_PS004_HC61a: Effective Confining Stress = 11.64 MPa

	Sample Name		IG_BH05_PS004
	Specimen Name		IG_BH05_PS004_HC61a
	Specimen Top Depth		641.53
	Specimen Bottom Depth		641.592
	Test No		ES2
	Test Name		IG_BH05_PS004_HC61a_ES2
	Operator		Stephen Talman/ Francy Guerrero
Dimensions	Length	mm	61.680
	Diameter	mm	61.420
	Length	m	0.06168
	Diameter	m	0.06142
Test Data Location	Raw Data File Name		2023-05-19_08-43-06 System-3-Cell-2 IG-BH05-PS004-HC61a.csv
	Date & Time		2023-05-21 19:19:53
	Start Row		12244
	End Row		14320
Test Conditions	Avg Cell Temp	C	40.14
	Avg Confining Pressure	kPa	26176
	Pre Pulse Avg Pore Pressure	kPa	9401
	Pulse Pressure	kPa	502
	Effective Stress	kPa	16775
Pore Fluid & Conditions	Post Pulse Avg Pore Pressure	kPa	9401
	Type		Water
	Salt	ppm	0
	Density	kg/m3	996.2
	Viscosity	kg.s/m	6.523E-04
Solution	Compressibility	1/Pa	4.36E-10
			System 3 - Cell 2
Brace	Nominal Decay Time	s	2076
	Brace Permeability	m2	4.53E-20
Hsieh	Permeability	m2	4.67E-20
	Specific Storage	1/m	7.40E-08
	Permeability	nD	47.3
	Hydraulic Conductivity	m/s	7.00E-13
	Pearson Coeff	()	0.9989549

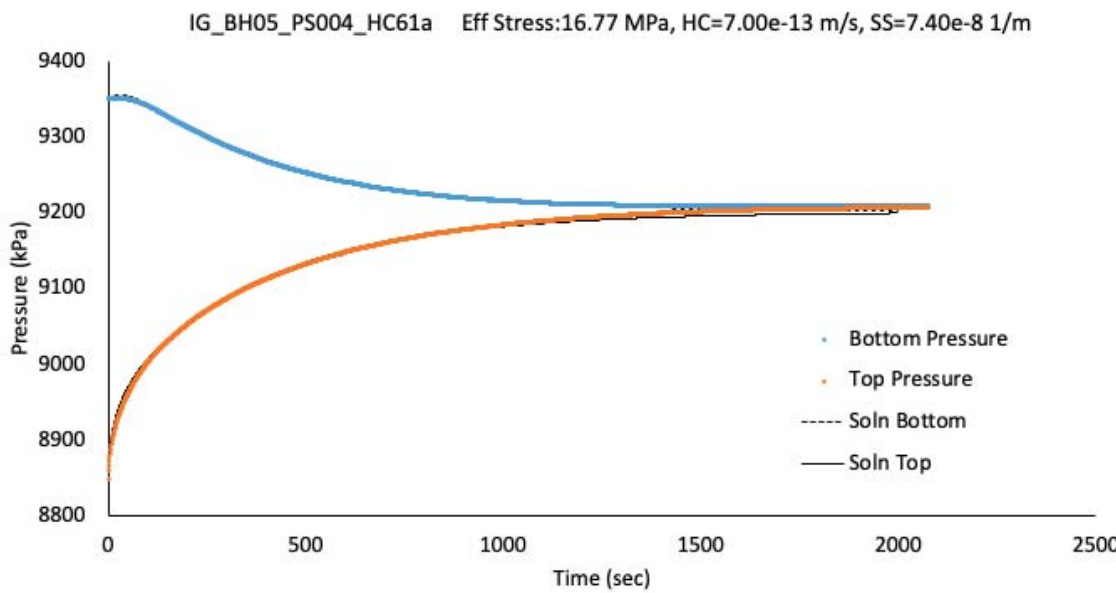


Figure 100 IG_BH05_PS004_HC61a: Effective Confining Stress = 16.77 MPa

	Sample Name		IG_BH05_PS005
	Specimen Name		IG_BH05_PS005_HC25a
	Specimen Top Depth		752.555
	Specimen Bottom Depth		752.590
	Test No		ES1
	Test Name		8922.01399713673_ES1
	Operator		Stephen Talman/ Francy Guerrero
Dimensions	Length	mm	25.800
	Diameter	mm	25.140
	Length	m	0.0258
	Diameter	m	0.02514
Test Data Location	Raw Data File Name		2023-06-01_06-35-24 System-2-CELL-1 IG-BH05-PS005-HC25a.csv
	Date & Time		2023-06-01 06:35:24
	Start Row		14852
	End Row		20000
Test Conditions	Avg Cell Temp	C	39.74
	Avg Confining Pressure	kPa	23166
	Pre Pulse Avg Pore Pressure	kPa	8683
	Pulse Pressure	kPa	504
	Effective Stress	kPa	14483
	Post Pulse Avg Pore Pressure	kPa	8683
Pore Fluid & Conditions	Type		Water
	Salt	ppm	0
	Density	kg/m3	996.05
	Viscosity	kg.s/m	6.570E-04
	Compressibility	1/Pa	4.36E-10
Solution	Test System		System 2 - CELL 1
Brace	Nominal Decay Time	s	5348
	Brace Permeability	m2	3.17E-20
Hsieh	Permeability	m2	3.32E-20
	Specific Storage	1/m	1.23E-07
	Permeability	nD	33.7
	Hydraulic Conductivity	m/s	4.94E-13
	Pearson Coeff	()	0.9918044

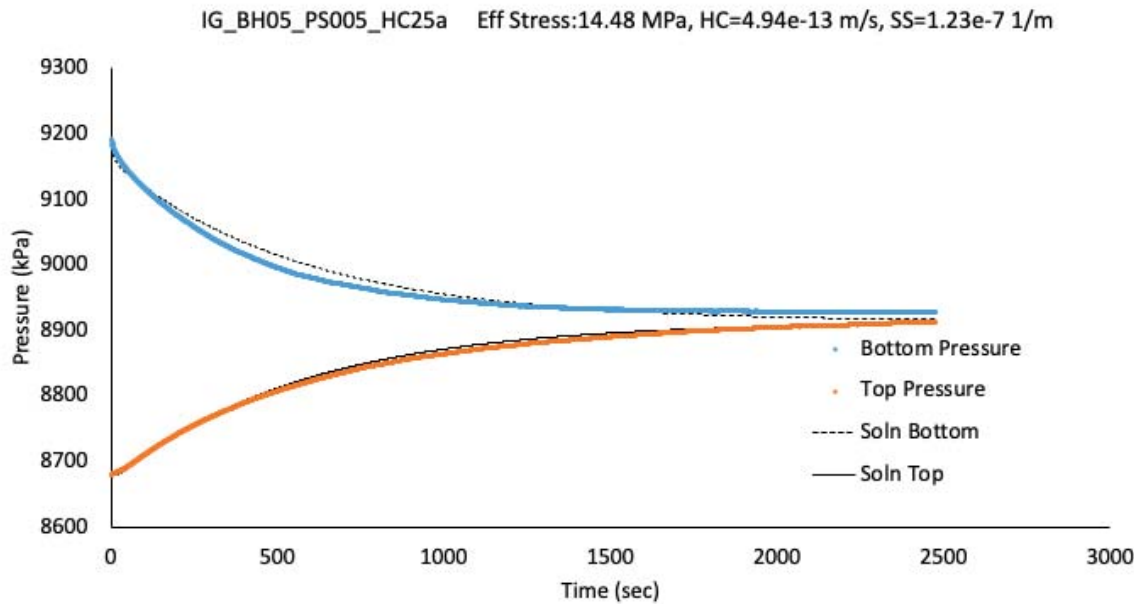


Figure 101 IG_BH05_PS005_HC25a: Effective Confining Stress = 14.48 MPa

	Sample Name		IG_BH05_PS005
	Specimen Name		IG_BH05_PS005_HC25a
	Specimen Top Depth		752.555
	Specimen Bottom Depth		752.590
	Test No		ES2
	Test Name		9155.34327034012_ES2
	Operator		Stephen Talman/ Francy Guerrero
Dimensions	Length	mm	25.800
	Diameter	mm	25.140
	Length	m	0.0258
	Diameter	m	0.02514
Test Data Location	Raw Data File Name		2023-06-01_06-35-24 System-2-CELL-1 IG-BH05-PS005-HC25a.csv
	Date & Time		2023-06-02 07:44:49
	Start Row		949
	End Row		5750
Test Conditions	Avg Cell Temp	C	39.74
	Avg Confining Pressure	kPa	28144
	Pre Pulse Avg Pore Pressure	kPa	9374
	Pulse Pressure	kPa	-496
	Effective Stress	kPa	18770
	Post Pulse Avg Pore Pressure	kPa	9374
Pore Fluid & Conditions	Type		Water
	Salt	ppm	0
	Density	kg/m3	996.34
	Viscosity	kg.s/m	6.571E-04
	Compressibility	1/Pa	4.36E-10
Solution	Test System		System 2 - CELL 1
Brace	Nominal Decay Time	s	4801
	Brace Permeability	m2	1.76E-20
Hsieh	Permeability	m2	1.62E-20
	Specific Storage	1/m	9.69E-08
	Permeability	nD	16.4
	Hydraulic Conductivity	m/s	2.41E-13
	Pearson Coeff	()	0.9993668

IG_BH05_PS005_HC25a Eff Stress:18.77 MPa, HC=2.41e-13 m/s, SS=9.69e-8 1/m

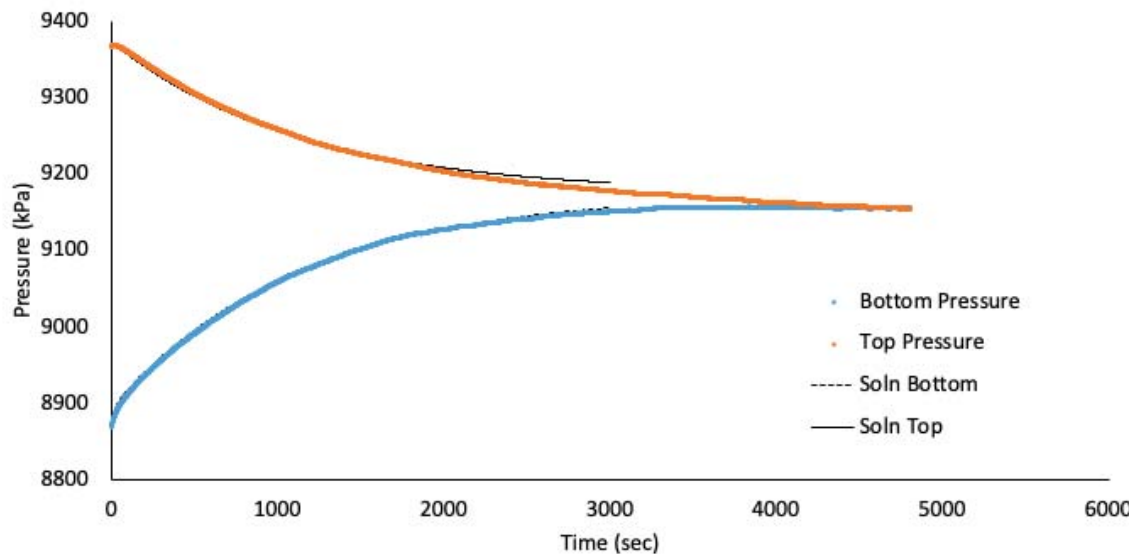


Figure 102 IG_BH05_PS005_HC25a: Effective Confining Stress = 18.77 MPa

	Sample Name		IG_BH05_PS005
	Specimen Name		IG_BH05_PS005_HC25a
	Specimen Top Depth		752.555
	Specimen Bottom Depth		752.590
	Test No		ES3
	Test Name		9168.344226_ES3
	Operator		Stephen Talman/ Francy Guerrero
Dimensions	Length	mm	25.800
	Diameter	mm	25.140
	Length	m	0.0258
	Diameter	m	0.02514
Test Data Location	Raw Data File Name		2023-06-01_06-35-24 System-2-CELL-1 IG-BH05-PS005-HC25a.csv
	Date & Time		2023-06-03 12:39:09
	Start Row		1310
	End Row		11570
Test Conditions	Avg Cell Temp	C	39.79
	Avg Confining Pressure	kPa	33110
	Pre Pulse Avg Pore Pressure	kPa	9448
	Pulse Pressure	kPa	507
	Effective Stress	kPa	23662
	Post Pulse Avg Pore Pressure	kPa	9448
Pore Fluid & Conditions	Type		Water
	Salt	ppm	0
	Density	kg/m3	996.36
	Viscosity	kg.s/m	6.565E-04
	Compressibility	1/Pa	4.36E-10
Solution	Test System		System 2 - CELL 1
Brace	Nominal Decay Time	s	10260
	Brace Permeability	m2	5.27E-21
Hsieh	Permeability	m2	5.17E-21
	Specific Storage	1/m	1.70E-07
	Permeability	nD	5.2
	Hydraulic Conductivity	m/s	7.69E-14
	Pearson Coeff	()	0.9988787

IG_BH05_PS005_HC25a Eff Stress:23.66 MPa, HC=7.69e-14 m/s, SS=1.70e-7 1/m

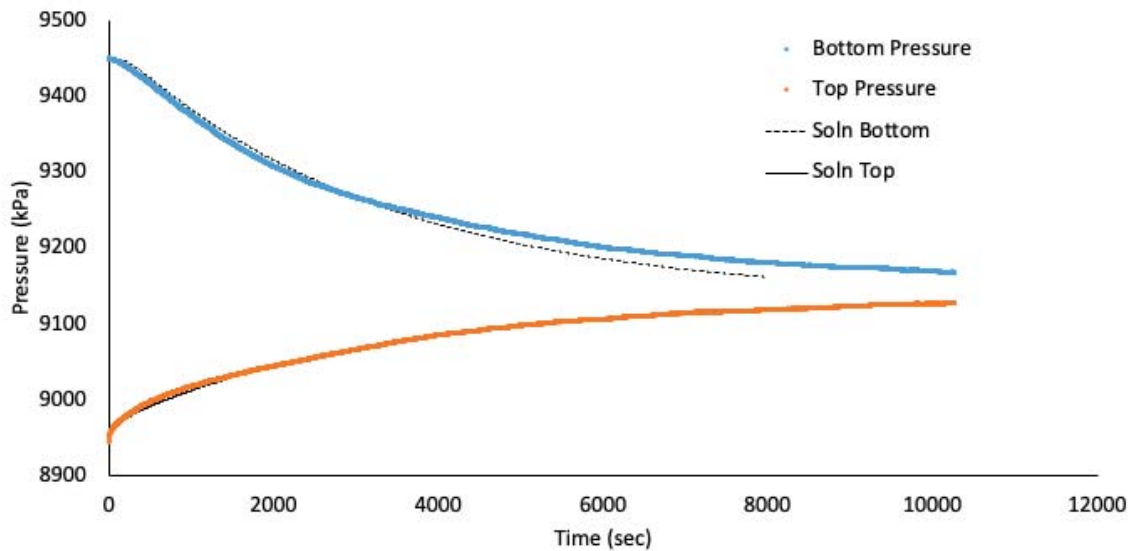


Figure 103 IG_BH05_PS005_HC25a: Effective Confining Stress = 23.66 MPa

	Sample Name		IG_BH05_PS005
	Specimen Name		IG_BH05_PS005_HC25r
	Specimen Top Depth		752.555
	Specimen Bottom Depth		752.590
	Test No		ES1
	Test Name		8889.40794399093_ES1
	Operator		Stephen Talman/ Francy Guerrero
Dimensions	Length	mm	20.650
	Diameter	mm	24.490
	Length	m	0.02065
	Diameter	m	0.02449
Test Data Location	Raw Data File Name		2023-06-01_06-36-37 System-2-CELL-3 IG-BH05-PS005-HC25r.csv
	Date & Time		2023-06-01 06:36:37
	Start Row		14561
	End Row		18000
Test Conditions	Avg Cell Temp	C	39.52
	Avg Confining Pressure	kPa	22989
	Pre Pulse Avg Pore Pressure	kPa	8644
	Pulse Pressure	kPa	516
	Effective Stress	kPa	14345
	Post Pulse Avg Pore Pressure	kPa	8644
Pore Fluid & Conditions	Type		Water
	Salt	ppm	0
	Density	kg/m3	996.11
	Viscosity	kg.s/m	6.597E-04
	Compressibility	1/Pa	4.36E-10
Solution	Test System		System 2 - CELL 3
Brace	Nominal Decay Time	s	3439
	Brace Permeability	m2	3.54E-20
Hsieh	Permeability	m2	3.61E-20
	Specific Storage	1/m	1.29E-07
	Permeability	nD	36.6
	Hydraulic Conductivity	m/s	5.35E-13
	Pearson Coeff	()	0.9998489

IG_BH05_PS005_HC25r Eff Stress:14.35 MPa, HC=5.35e-13 m/s, SS=1.29e-7 1/m

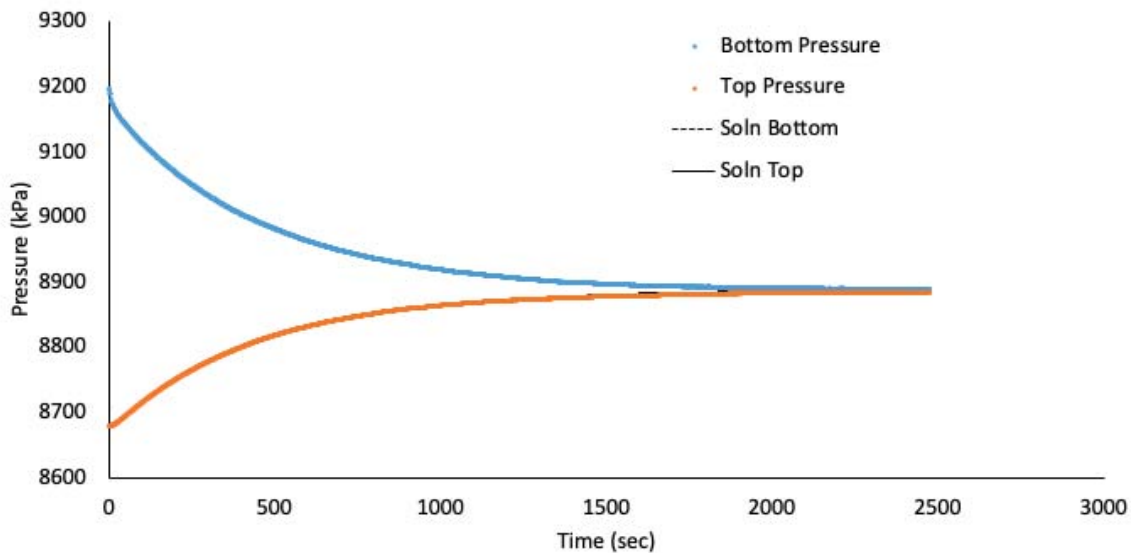


Figure 104 IG_BH05_PS005_HC25r: Effective Confining Stress = 14.35 MPa

	Sample Name		IG_BH05_PS005
	Specimen Name		IG_BH05_PS005_HC25r
	Specimen Top Depth		752.555
	Specimen Bottom Depth		752.590
	Test No		ES2
	Test Name		9183.732712_ES2
	Operator		Stephen Talman/ Francy Guerrero
Dimensions	Length	mm	20.650
	Diameter	mm	24.490
	Length	m	0.02065
	Diameter	m	0.02449
Test Data Location	Raw Data File Name		2023-06-01_06-36-37 System-2-CELL-3 IG-BH05-PS005-HC25r.csv
	Date & Time		2023-06-02 07:45:47
	Start Row		873
	End Row		5650
Test Conditions	Avg Cell Temp	C	39.50
	Avg Confining Pressure	kPa	27935
	Pre Pulse Avg Pore Pressure	kPa	9342
	Pulse Pressure	kPa	-495
	Effective Stress	kPa	18593
	Post Pulse Avg Pore Pressure	kPa	9342
Pore Fluid & Conditions	Type		Water
	Salt	ppm	0
	Density	kg/m3	996.42
	Viscosity	kg.s/m	6.601E-04
	Compressibility	1/Pa	4.36E-10
Solution	Test System		System 2 - CELL 3
Brace	Nominal Decay Time	s	4777
	Brace Permeability	m2	1.37E-20
Hsieh	Permeability	m2	1.37E-20
	Specific Storage	1/m	1.08E-07
	Permeability	nD	13.9
	Hydraulic Conductivity	m/s	2.03E-13
	Pearson Coeff	()	0.9995758

IG_BH05_PS005_HC25r Eff Stress:18.59 MPa, HC=2.03e-13 m/s, SS=1.08e-7 1/m

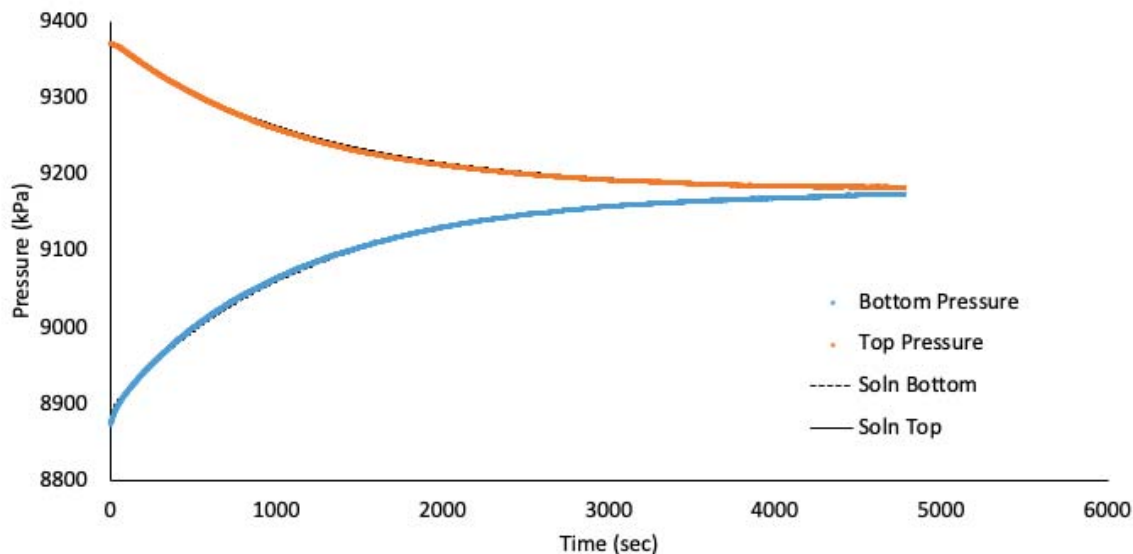


Figure 105 IG_BH05_PS005_HC25r: Effective Confining Stress = 18.59 MPa

	Sample Name		IG_BH05_PS005
	Specimen Name		IG_BH05_PS005_HC25r
	Specimen Top Depth		752.555
	Specimen Bottom Depth		752.590
	Test No		ES3
	Test Name		9268.420566_ES3
	Operator		Stephen Talman/ Francy Guerrero
Dimensions	Length	mm	20.650
	Diameter	mm	24.490
	Length	m	0.02065
	Diameter	m	0.02449
Test Data Location	Raw Data File Name		2023-06-01_06-36-37 System-2-CELL-3 IG-BH05-PS005-HC25r.csv
	Date & Time		2023-06-03 12:39:49
	Start Row		141
	End Row		8500
Test Conditions	Avg Cell Temp	C	39.57
	Avg Confining Pressure	kPa	32876
	Pre Pulse Avg Pore Pressure	kPa	9419
	Pulse Pressure	kPa	-481
	Effective Stress	kPa	23457
	Post Pulse Avg Pore Pressure	kPa	9419
Pore Fluid & Conditions	Type		Water
	Salt	ppm	0
	Density	kg/m3	996.43
	Viscosity	kg.s/m	6.592E-04
	Compressibility	1/Pa	4.36E-10
Solution			System 2 - CELL 3
Brace	Nominal Decay Time	s	8359
	Brace Permeability	m2	5.38E-21
Hsieh	Permeability	m2	5.38E-21
	Specific Storage	1/m	7.82E-08
	Permeability	nD	5.5
	Hydraulic Conductivity	m/s	7.98E-14
	Pearson Coeff	()	0.9998935

IG_BH05_PS005_HC25r Eff Stress:23.46 MPa, HC=7.98e-14 m/s, SS=7.82e-8 1/m

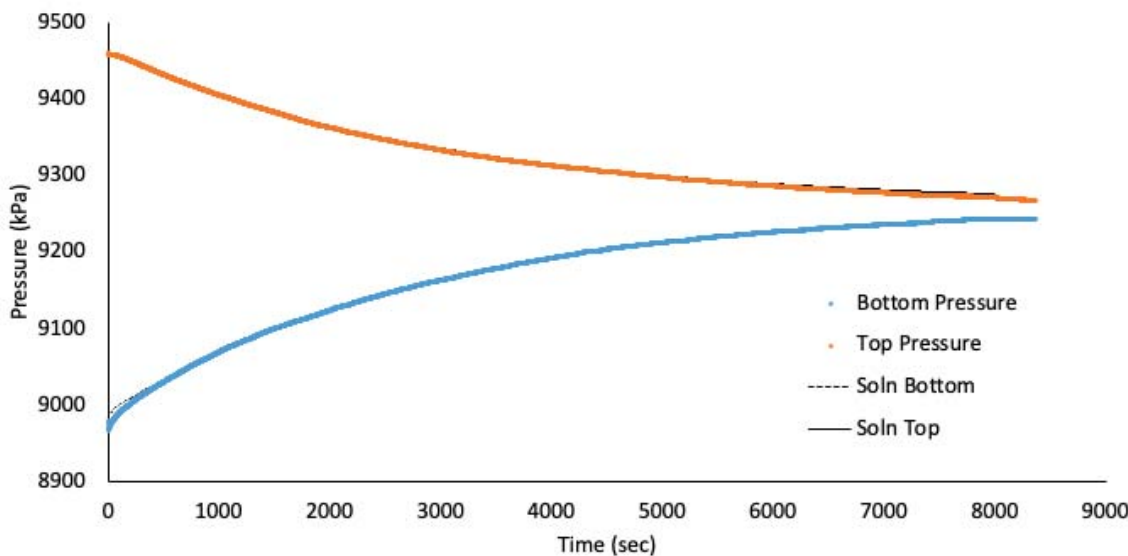


Figure 106 IG_BH05_PS005_HC25r: Effective Confining Stress = 23.46 MPa

	Sample Name		IG_BH05_PS005
	Specimen Name		IG_BH05_PS005_HC61a
	Specimen Top Depth		752.652
	Specimen Bottom Depth		752.714
	Test No		ES1
	Test Name		IG_BH05_PS005_HC61a_ES1
	Operator		Stephen Talman/ Francy Guerrero
Dimensions	Length	mm	62.320
	Diameter	mm	61.090
	Length	m	0.06232
	Diameter	m	0.06109
Test Data Location	Raw Data File Name		2023-06-01_06-35-53 System-2-CELL-2 IG-BH05-PS005-HC61a.csv
	Date & Time		2023-06-01 06:35:53
	Start Row		14613
	End Row		18000
Test Conditions	Avg Cell Temp	C	39.69
	Avg Confining Pressure	kPa	23277
	Pre Pulse Avg Pore Pressure	kPa	8701
	Pulse Pressure	kPa	496
	Effective Stress	kPa	14576
	Post Pulse Avg Pore Pressure	kPa	8701
Pore Fluid & Conditions	Type		Water
	Salt	ppm	0
	Density	kg/m3	996.08
	Viscosity	kg.s/m	6.577E-04
	Compressibility	1/Pa	4.36E-10
Solution	Test System		System 2 - CELL 2
Brace	Nominal Decay Time	s	3387
	Brace Permeability	m2	2.62E-20
Hsieh	Permeability	m2	2.75E-20
	Specific Storage	1/m	8.43E-08
	Permeability	nD	27.9
	Hydraulic Conductivity	m/s	4.09E-13
	Pearson Coeff	()	0.9991463

IG_BH05_PS005_HC61a Eff Stress:14.58 MPa, HC=4.09e-13 m/s, SS=8.43e-8 1/m

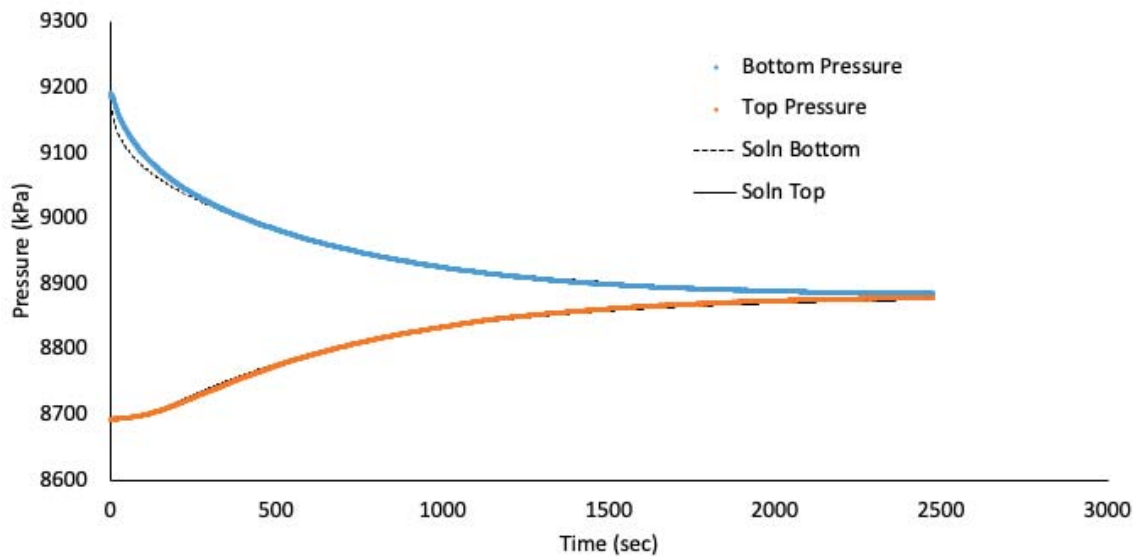


Figure 107 IG_BH05_PS005_HC61a: Effective Confining Stress = 14.58 MPa

	Sample Name		IG_BH05_PS005
	Specimen Name		IG_BH05_PS005_HC61a
	Specimen Top Depth		752.652
	Specimen Bottom Depth		752.714
	Test No		ES2
	Test Name		9228.04384981537_ES2
	Operator		Stephen Talman/ Francy Guerrero
Dimensions	Length	mm	62.320
	Diameter	mm	61.090
	Length	m	0.06232
	Diameter	m	0.06109
Test Data Location	Raw Data File Name		2023-06-01_06-35-53 System-2-CELL-2 IG-BH05-PS005-HC61a.csv
	Date & Time		2023-06-02 07:45:15
	Start Row		21148
	End Row		30000
Test Conditions	Avg Cell Temp	C	39.68
	Avg Confining Pressure	kPa	28279
	Pre Pulse Avg Pore Pressure	kPa	9389
	Pulse Pressure	kPa	508
	Effective Stress	kPa	18890
	Post Pulse Avg Pore Pressure	kPa	9389
Pore Fluid & Conditions	Type		Water
	Salt	ppm	0
	Density	kg/m3	996.38
	Viscosity	kg.s/m	6.579E-04
	Compressibility	1/Pa	4.36E-10
Solution	Test System		System 2 - CELL 2
Brace	Nominal Decay Time	s	8852
	Brace Permeability	m2	1.23E-20
Hsieh	Permeability	m2	1.23E-20
	Specific Storage	1/m	6.96E-08
	Permeability	nD	12.5
	Hydraulic Conductivity	m/s	1.83E-13
	Pearson Coeff	()	0.9992181

IG_BH05_PS005_HC61a Eff Stress:18.89 MPa, HC=1.83e-13 m/s, SS=6.96e-8 1/m

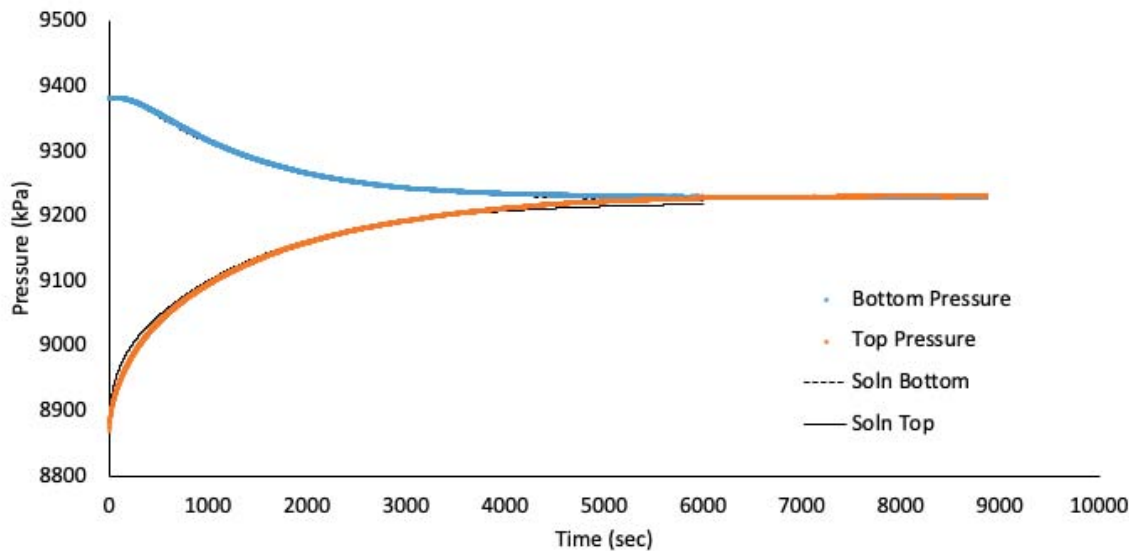


Figure 108 IG_BH05_PS005_HC61a: Effective Confining Stress = 18.89 MPa

	Sample Name		IG_BH05_PS005
	Specimen Name		IG_BH05_PS005_HC61a
	Specimen Top Depth		752.652
	Specimen Bottom Depth		752.714
	Test No		ES3
	Test Name		9347.702306_ES3
	Operator		Stephen Talman/ Francy Guerrero
Dimensions	Length	mm	62.320
	Diameter	mm	61.090
	Length	m	0.06232
	Diameter	m	0.06109
Test Data Location	Raw Data File Name		2023-06-01_06-35-53 System-2-CELL-2 IG-BH05-PS005-HC61a.csv
	Date & Time		2023-06-03 12:39:33
	Start Row		165
	End Row		8520
Test Conditions	Avg Cell Temp	C	39.66
	Avg Confining Pressure	kPa	33275
	Pre Pulse Avg Pore Pressure	kPa	9481
	Pulse Pressure	kPa	-506
	Effective Stress	kPa	23794
Pore Fluid & Conditions	Post Pulse Avg Pore Pressure	kPa	9481
	Type		Water
	Salt	ppm	0
	Density	kg/m3	996.42
	Viscosity	kg.s/m	6.581E-04
Solution	Compressibility	1/Pa	4.36E-10
	Test System		System 2 - CELL 2
Brace	Nominal Decay Time	s	8355
	Brace Permeability	m2	6.17E-21
Hsieh	Permeability	m2	6.17E-21
	Specific Storage	1/m	8.69E-08
	Permeability	nD	6.2
	Hydraulic Conductivity	m/s	9.16E-14
	Pearson Coeff	()	0.9996496

IG_BH05_PS005_HC61a Eff Stress:23.79 MPa, HC=9.16e-14 m/s, SS=8.69e-8 1/m

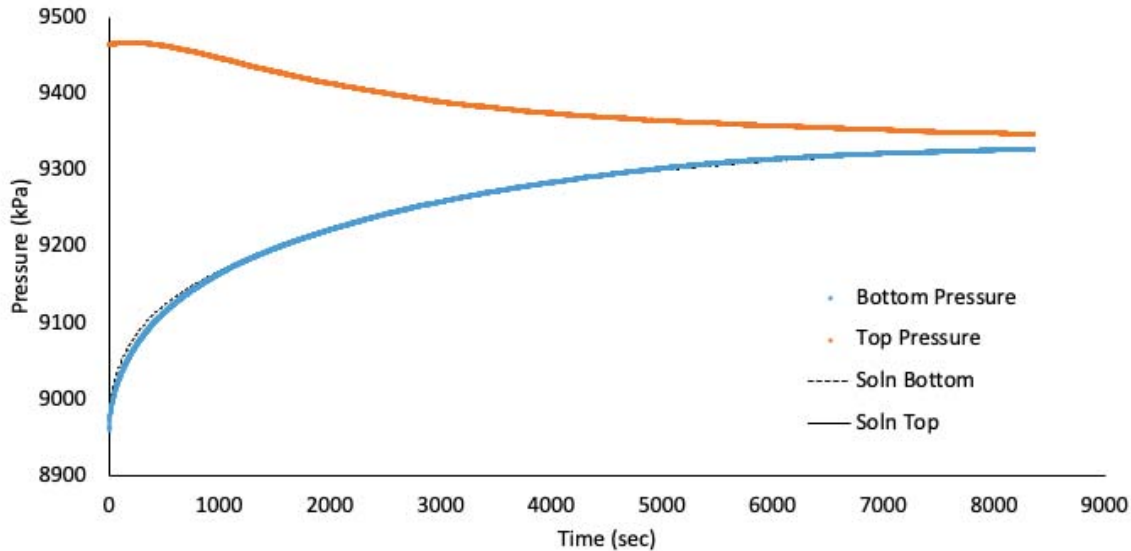


Figure 109 IG_BH05_PS005_HC61a: Effective Confining Stress = 23.79 MPa

Sample ID	IG_BH05_PS005			
Specimen Full Name	IG_BH05_PS005_SSG61a			
Top Depth (m)	752.714			
Bottom Depth (m)	752.775			
Test ID	SSG	ESL	ESM	ESH
Test Name	Steady State N2 Permeability			
Operator 1	A. Sanchez			
Operator 2				
Dimensions	Length mm	61.70		
	Diameter mm	61.11		
	Length m	0.06		
	Diameter m	0.06		
Test Data Location	Raw Data File Name	rawData_ESL	rawData_ESM	rawData_ESH
	Start Date & Time	2023-01-22		
	End Date & Time	2023-02-02		
Average Test Conditions and Pore Fluids Conditions	Cell Temp C	32.8	32.8	32.9
	Fluid Type Gas	Nitrogen	Nitrogen	Nitrogen
	Density kg/m3	96.4	91.0	91.0
	Viscosity cP	0.0199	0.0197	0.0197
	Effective Stress MPa	14.3	19.4	24.3
Results	kapp m2	4.27E-19	5.27E-20	4.05E-21

NOTES:

ESL Effective stress - low test condition
 ESM Effective stress - medium test condition
 ESH Effective stress - high test condition
 kapp Apparent gas permeability

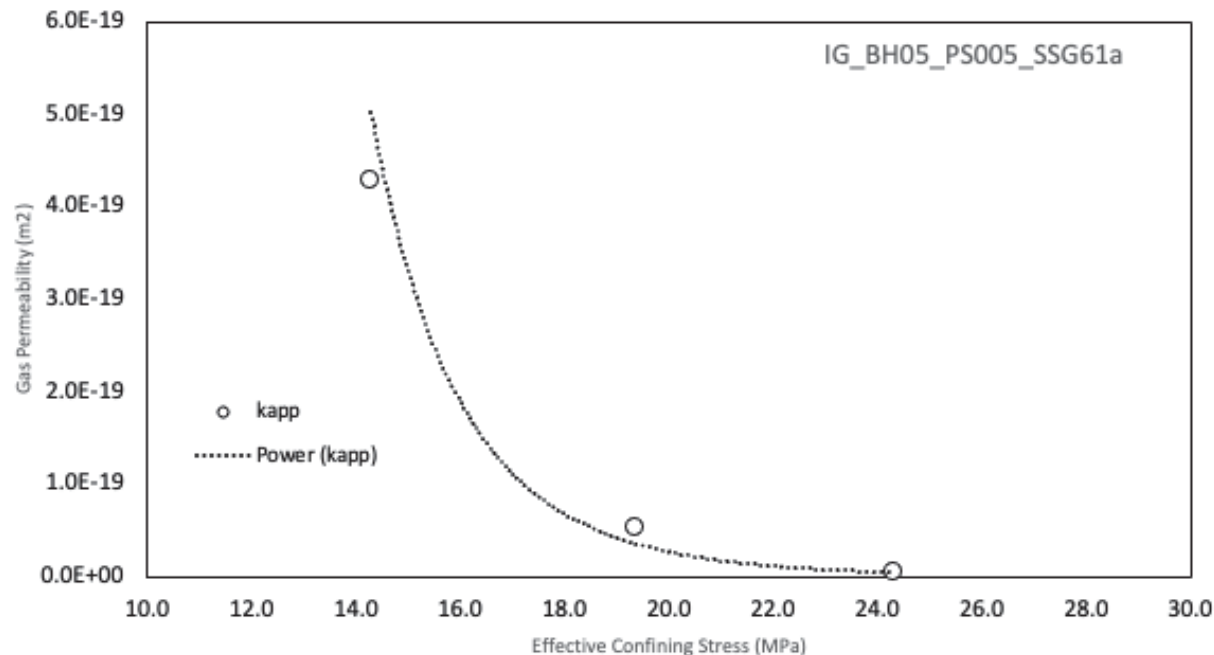


Figure 110 IG_BH05_PS005_SSG61a: Effective Confining Stresses of 14.3 MPa, 19.4 MPa and 24.3 MPa

	Sample Name		IG_BH05_PS006
	Specimen Name		IG_BH05_PS006_HC25a
	Specimen Top Depth		852.57
	Specimen Bottom Depth		852.605
	Test No		ES1
	Test Name		9172.40065840611_ES1
	Operator		Stephen Talman/ Francy Guerrero
Dimensions	Length	mm	25.350
	Diameter	mm	25.160
	Length	m	0.02535
	Diameter	m	0.02516
Test Data Location	Raw Data File Name		2023-06-16_11-00-35 System-2-CELL-1 IG-BH05-PS006-HC25a.csv
	Date & Time		2023-06-16 11:00:35
	Start Row		7827
	End Row		14500
Test Conditions	Avg Cell Temp	C	39.85
	Avg Confining Pressure	kPa	25051
	Pre Pulse Avg Pore Pressure	kPa	9552
	Pulse Pressure	kPa	719
	Effective Stress	kPa	15499
	Post Pulse Avg Pore Pressure	kPa	9552
Pore Fluid & Conditions	Type		Water
	Salt	ppm	0
	Density	kg/m3	996.38
	Viscosity	kg.s/m	6.558E-04
	Compressibility	1/Pa	4.36E-10
Solution	Test System		System 2 - CELL 1
Brace	Nominal Decay Time	s	6673
	Brace Permeability	m2	1.89E-20
Hsieh	Permeability	m2	2.27E-20
	Specific Storage	1/m	2.10E-07
	Permeability	nD	23.0
	Hydraulic Conductivity	m/s	3.39E-13
	Pearson Coeff	()	0.9992952

IG_BH05_PS006_HC25a Eff Stress:15.5 MPa, HC=3.39e-13 m/s, SS=2.10e-7 1/m

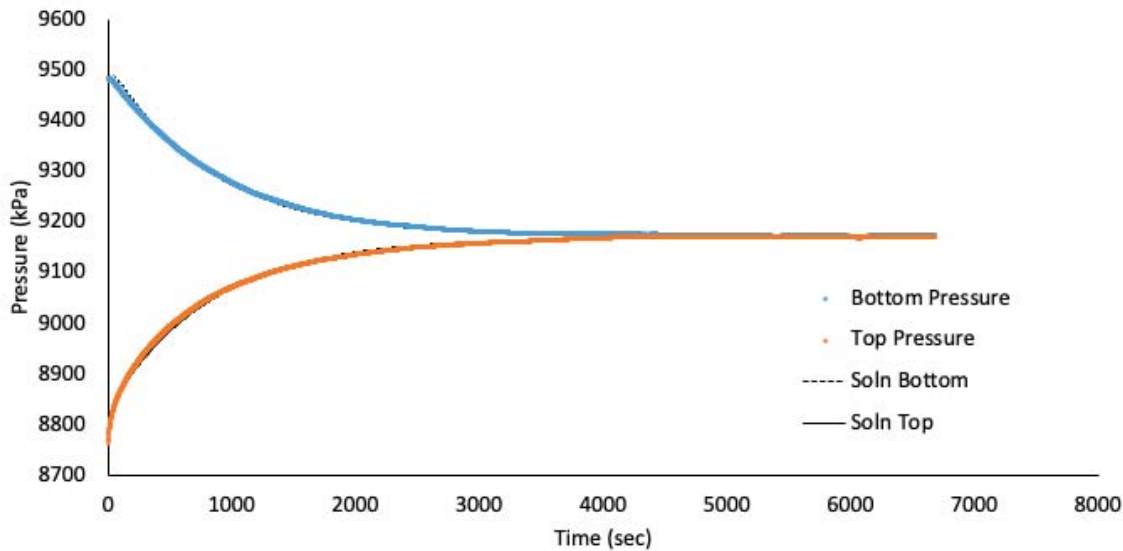


Figure 111 IG_BH05_PS006_HC25a: Effective Confining Stress = 15.5 MPa

	Sample Name		IG_BH05_PS006
	Specimen Name		IG_BH05_PS006_HC25a
	Specimen Top Depth		852.57
	Specimen Bottom Depth		852.605
	Test No		ES2
	Test Name		9001.521803_ES2
	Operator		Stephen Talman/ Francy Guerrero
Dimensions	Length	mm	25.350
	Diameter	mm	25.160
	Length	m	0.02535
	Diameter	m	0.02516
Test Data Location	Raw Data File Name		2023-06-16_11-00-35 System-2-CELL-1 IG-BH05-PS006-HC25a.csv
	Date & Time		2023-06-17 13:13:15
	Start Row		13320
	End Row		21400
Test Conditions	Avg Cell Temp	C	39.85
	Avg Confining Pressure	kPa	30027
	Pre Pulse Avg Pore Pressure	kPa	9342
	Pulse Pressure	kPa	563
	Effective Stress	kPa	20685
	Post Pulse Avg Pore Pressure	kPa	9342
Pore Fluid & Conditions	Type		Water
	Salt	ppm	0
	Density	kg/m3	996.29
	Viscosity	kg.s/m	6.558E-04
	Compressibility	1/Pa	4.36E-10
Solution			System 2 - CELL 1
Brace	Nominal Decay Time	s	8080
	Brace Permeability	m2	7.58E-21
Hsieh	Permeability	m2	9.09E-21
	Specific Storage	1/m	1.38E-07
	Permeability	nD	9.2
	Hydraulic Conductivity	m/s	1.36E-13
	Pearson Coeff	()	0.9998466

IG_BH05_PS006_HC25a Eff Stress:20.69 MPa, HC=1.36e-13 m/s, SS=1.38e-7 1/m

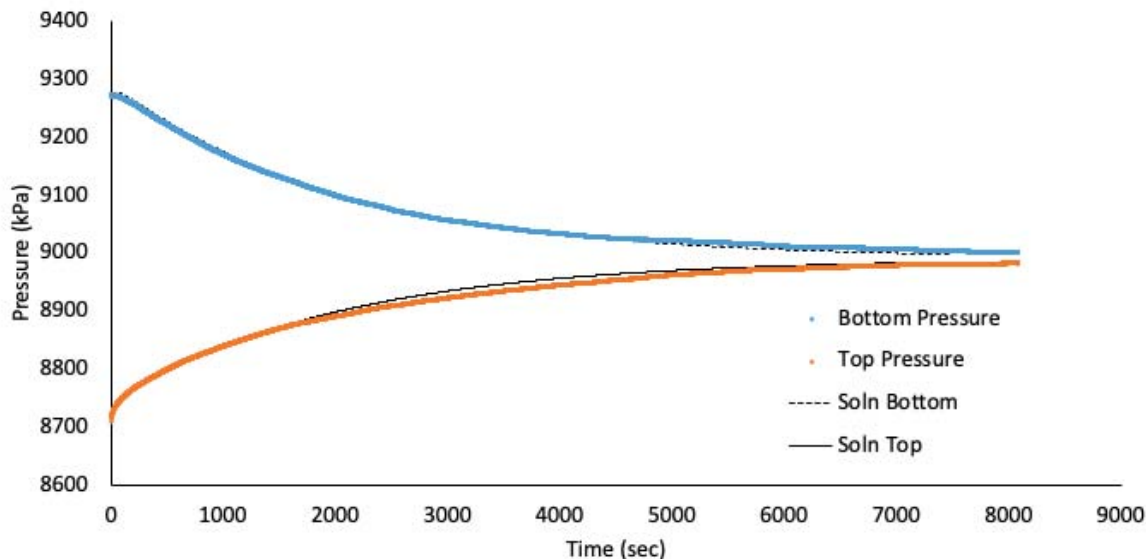


Figure 112 IG_BH05_PS006_HC25a: Effective Confining Stress = 20.69 MPa

	Sample Name		IG_BH05_PS006
	Specimen Name		IG_BH05_PS006_HC25r
	Specimen Top Depth		852.57
	Specimen Bottom Depth		852.605
	Test No		ES1
	Test Name		9499.803497_ES1
	Operator		Stephen Talman/ Francy Guerrero
Dimensions	Length	mm	25.050
	Diameter	mm	24.530
	Length	m	0.02505
	Diameter	m	0.02453
Test Data Location	Raw Data File Name		2023-06-16_11-00-31 System-2-CELL-3 IG-BH05-PS006-HC25r.csv
	Date & Time		2023-06-16 11:00:31
	Start Row		1223
	End Row		4650
Test Conditions	Avg Cell Temp	C	39.61
	Avg Confining Pressure	kPa	24861
	Pre Pulse Avg Pore Pressure	kPa	9766
	Pulse Pressure	kPa	-825
	Effective Stress	kPa	15096
	Post Pulse Avg Pore Pressure	kPa	9766
Pore Fluid & Conditions	Type		Water
	Salt	ppm	0
	Density	kg/m3	996.57
	Viscosity	kg.s/m	6.588E-04
	Compressibility	1/Pa	4.36E-10
Solution	Test System		System 2 - CELL 3
Brace	Nominal Decay Time	s	3427
	Brace Permeability	m2	1.67E-20
Hsieh	Permeability	m2	1.84E-20
	Specific Storage	1/m	2.25E-07
	Permeability	nD	18.6
	Hydraulic Conductivity	m/s	2.73E-13
	Pearson Coeff	()	0.9997362

IG_BH05_PS006_HC25r Eff Stress:15.1 MPa, HC=2.73e-13 m/s, SS=2.25e-7 1/m

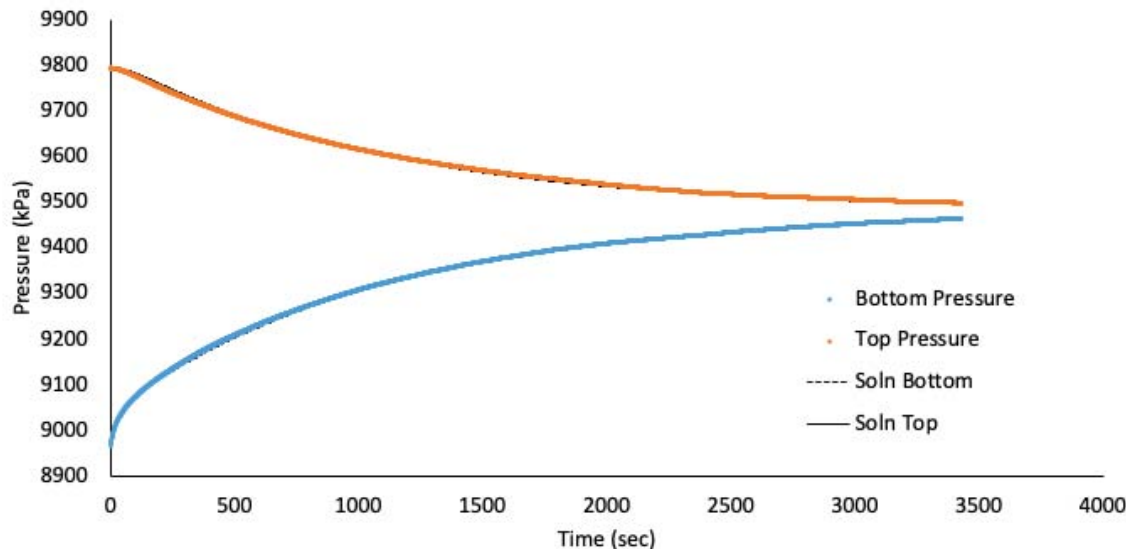


Figure 113 IG_BH05_PS006_HC25r: Effective Confining Stress = 15.10 MPa

	Sample Name		IG_BH05_PS006
	Specimen Name		IG_BH05_PS006_HC25r
	Specimen Top Depth		852.57
	Specimen Bottom Depth		852.605
	Test No		ES2
	Test Name		9194.33595_ES2
	Operator		Stephen Talman/ Francy Guerrero
Dimensions	Length	mm	25.050
	Diameter	mm	24.530
	Length	m	0.02505
	Diameter	m	0.02453
Test Data Location	Raw Data File Name		2023-06-16_11-00-31 System-2-CELL-3 IG-BH05-PS006-HC25r.csv
	Date & Time		2023-06-17 13:13:19
	Start Row		613
	End Row		7050
Test Conditions	Avg Cell Temp	C	39.63
	Avg Confining Pressure	kPa	29806
	Pre Pulse Avg Pore Pressure	kPa	9342
	Pulse Pressure	kPa	-611
	Effective Stress	kPa	20464
	Post Pulse Avg Pore Pressure	kPa	9342
Pore Fluid & Conditions	Type		Water
	Salt	ppm	0
	Density	kg/m3	996.37
	Viscosity	kg.s/m	6.585E-04
	Compressibility	1/Pa	4.36E-10
Solution	Test System		System 2 - CELL 3
Brace	Nominal Decay Time	s	6437
	Brace Permeability	m2	7.43E-21
Hsieh	Permeability	m2	7.43E-21
	Specific Storage	1/m	1.22E-07
	Permeability	nD	7.5
	Hydraulic Conductivity	m/s	1.10E-13
	Pearson Coeff	()	0.9996801

IG_BH05_PS006_HC25r Eff Stress:20.46 MPa, HC=1.10e-13 m/s, SS=1.22e-7 1/m

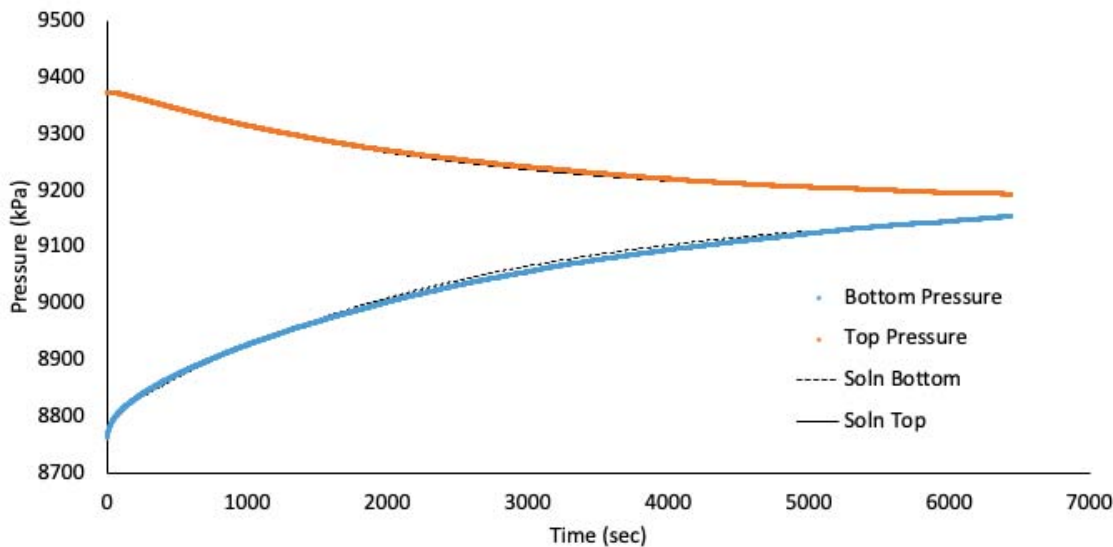


Figure 114 IG_BH05_PS006_HC25r: Effective Confining Stress = 20.46 MPa

	Sample Name		IG_BH05_PS006
	Specimen Name		IG_BH05_PS006_HC25r
	Specimen Top Depth		852.57
	Specimen Bottom Depth		852.605
	Test No		ES3
	Test Name		10086.0623907222_ES3
	Operator		Stephen Talman/ Francy Guerrero
Dimensions	Length	mm	25.050
	Diameter	mm	24.530
	Length	m	0.02505
	Diameter	m	0.02453
Test Data Location	Raw Data File Name		2023-06-16_11-00-31 System-2-CELL-3 IG-BH05-PS006-HC25r.csv
	Date & Time		2023-06-17 13:13:19
	Start Row		3466
	End Row		55000
Test Conditions	Avg Cell Temp	C	39.58
	Avg Confining Pressure	kPa	34747
	Pre Pulse Avg Pore Pressure	kPa	10389
	Pulse Pressure	kPa	797
	Effective Stress	kPa	24358
Pore Fluid & Conditions	Post Pulse Avg Pore Pressure	kPa	10389
	Type		Water
	Salt	ppm	0
	Density	kg/m3	996.84
	Viscosity	kg.s/m	6.592E-04
Solution	Compressibility	1/Pa	4.36E-10
	Test System		System 2 - CELL 3
Brace	Nominal Decay Time	s	51534
	Brace Permeability	m2	1.95E-21
Hsieh	Permeability	m2	2.01E-21
	Specific Storage	1/m	4.06E-08
	Permeability	nD	2.0
	Hydraulic Conductivity	m/s	2.98E-14
	Pearson Coeff	()	0.9979019

IG_BH05_PS006_HC25r Eff Stress:24.36 MPa, HC=2.98e-14 m/s, SS=4.06e-8 1/m

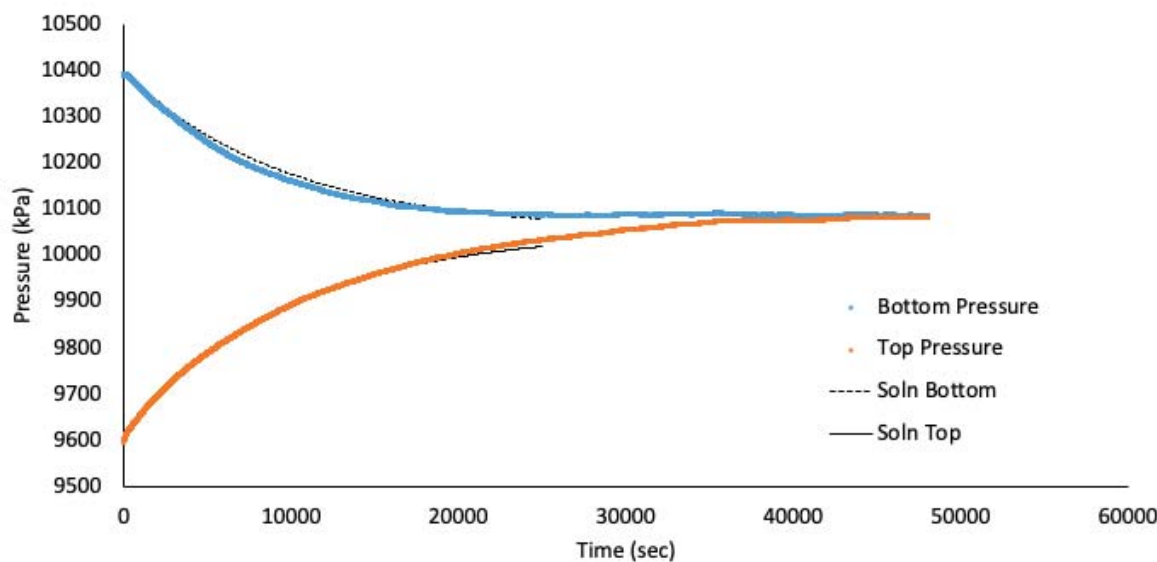


Figure 115 IG_BH05_PS006_HC25r: Effective Confining Stress = 24.36 MPa

	Sample Name		IG_BH05_PS006
	Specimen Name		IG_BH05_PS006_HC61a
	Specimen Top Depth		852.605
	Specimen Bottom Depth		852.667
	Test No		ES1
	Test Name		9557.65129_ES1
	Operator		Stephen Talman/ Francy Guerrero
Dimensions	Length	mm	61.450
	Diameter	mm	61.090
	Length	m	0.06145
	Diameter	m	0.06109
Test Data Location	Raw Data File Name		2023-06-16_11-00-33 System-2-CELL-2 IG-BH05-PS006-HC61a.csv
	Date & Time		2023-06-16 11:00:33
	Start Row		1210
	End Row		4650
Test Conditions	Avg Cell Temp	C	39.83
	Avg Confining Pressure	kPa	25173
	Pre Pulse Avg Pore Pressure	kPa	9806
	Pulse Pressure	kPa	-821
	Effective Stress	kPa	15367
Pore Fluid & Conditions	Post Pulse Avg Pore Pressure	kPa	9806
	Type		Water
	Salt	ppm	0
	Density	kg/m3	996.5
	Viscosity	kg.s/m	6.561E-04
Solution	Compressibility	1/Pa	4.36E-10
	Test System		System 2 - CELL 2
Brace	Nominal Decay Time	s	3440
	Brace Permeability	m2	1.82E-20
Hsieh	Permeability	m2	2.13E-20
	Specific Storage	1/m	8.14E-08
	Permeability	nD	21.6
	Hydraulic Conductivity	m/s	3.17E-13
	Pearson Coeff	()	0.9995894

IG_BH05_PS006_HC61a Eff Stress:15.37 MPa, HC=3.17e-13 m/s, SS=8.14e-8 1/m

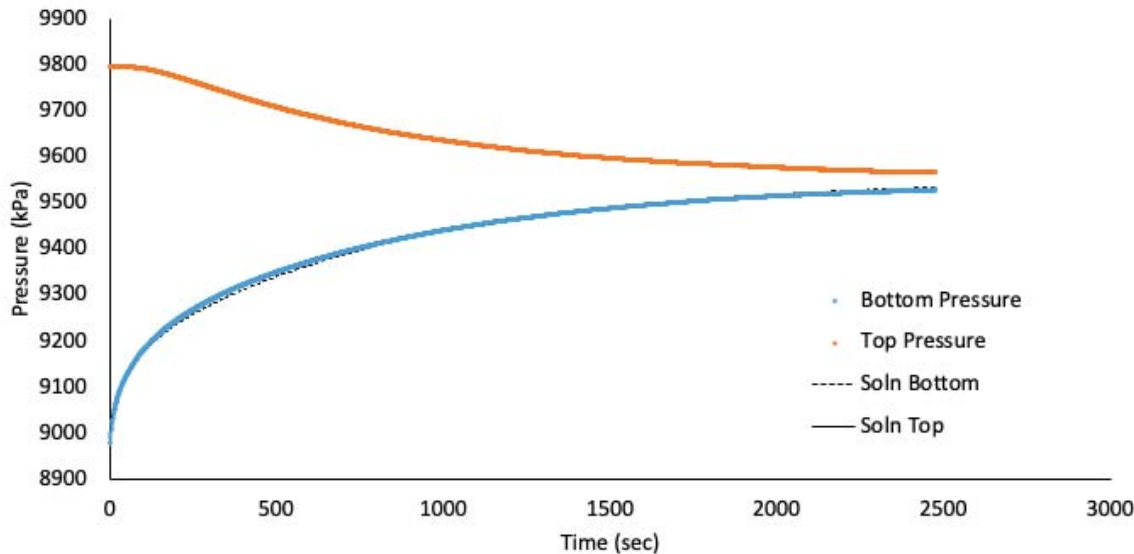


Figure 116 IG_BH05_PS006_HC61a: Effective Confining Stress = 15.37 MPa

	Sample Name		IG_BH05_PS006
	Specimen Name		IG_BH05_PS006_HC61a
	Specimen Top Depth		852.605
	Specimen Bottom Depth		852.667
	Test No		ES2
	Test Name		9213.191654_ES2
	Operator		Stephen Talman/ Francy Guerrero
Dimensions	Length	mm	61.450
	Diameter	mm	61.090
	Length	m	0.06145
	Diameter	m	0.06109
Test Data Location	Raw Data File Name		2023-06-16_11-00-33 System-2-CELL-2 IG-BH05-PS006-HC61a.csv
	Date & Time		2023-06-17 13:13:17
	Start Row		620
	End Row		7140
Test Conditions	Avg Cell Temp	C	39.85
	Avg Confining Pressure	kPa	30173
	Pre Pulse Avg Pore Pressure	kPa	9396
	Pulse Pressure	kPa	-620
	Effective Stress	kPa	20776
	Post Pulse Avg Pore Pressure	kPa	9396
Pore Fluid & Conditions	Type		Water
	Salt	ppm	0
	Density	kg/m3	996.32
	Viscosity	kg.s/m	6.558E-04
	Compressibility	1/Pa	4.36E-10
Solution	Test System		System 2 - CELL 2
Brace	Nominal Decay Time	s	6520
	Brace Permeability	m2	9.09E-21
Hsieh	Permeability	m2	9.63E-21
	Specific Storage	1/m	8.14E-08
	Permeability	nD	9.8
	Hydraulic Conductivity	m/s	1.44E-13
	Pearson Coeff	()	0.9996192

IG_BH05_PS006_HC61a Eff Stress:20.78 MPa, HC=1.44e-13 m/s, SS=8.14e-8 1/m

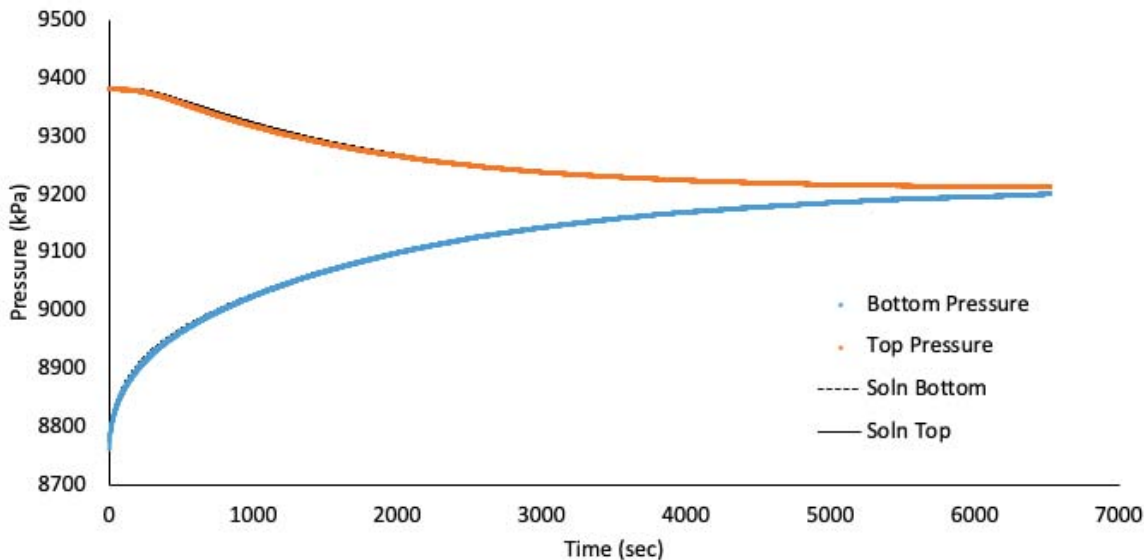


Figure 117 IG_BH05_PS006_HC61a: Effective Confining Stress = 20.78 MPa

	Sample Name		IG_BH05_PS006
	Specimen Name		IG_BH05_PS006_HC61a
	Specimen Top Depth		852.605
	Specimen Bottom Depth		852.667
	Test No		ES3
	Test Name		IG_BH05_PS006_HC61a_ES3
	Operator		Stephen Talman/ Francy Guerrero
Dimensions	Length	mm	61.450
	Diameter	mm	61.090
	Length	m	0.06145
	Diameter	m	0.06109
Test Data Location	Raw Data File Name		2023-06-16_11-00-33 System-2-CELL-2 IG-BH05-PS006-HC61a.csv
	Date & Time		2023-06-19 10:35:59
	Start Row		5175
	End Row		35000
Test Conditions	Avg Cell Temp	C	39.80
	Avg Confining Pressure	kPa	35167
	Pre Pulse Avg Pore Pressure	kPa	10457
	Pulse Pressure	kPa	809
	Effective Stress	kPa	24710
	Post Pulse Avg Pore Pressure	kPa	10457
Pore Fluid & Conditions	Type		Water
	Salt	ppm	0
	Density	kg/m3	996.79
	Viscosity	kg.s/m	6.565E-04
	Compressibility	1/Pa	
Solution			
Brace	Nominal Decay Time	s	1789500
	Brace Permeability	m2	3.94E-21
Hsieh	Permeability	m2	4.18E-21
	Specific Storage	1/m	3.92E-08
	Permeability	nD	4.2
	Hydraulic Conductivity	m/s	6.23E-14
	Pearson Coeff	()	0.9998526

IG_BH05_PS006_HC61a Eff Stress:24.71 MPa, HC=6.23e-14 m/s, SS=3.92e-8 1/m

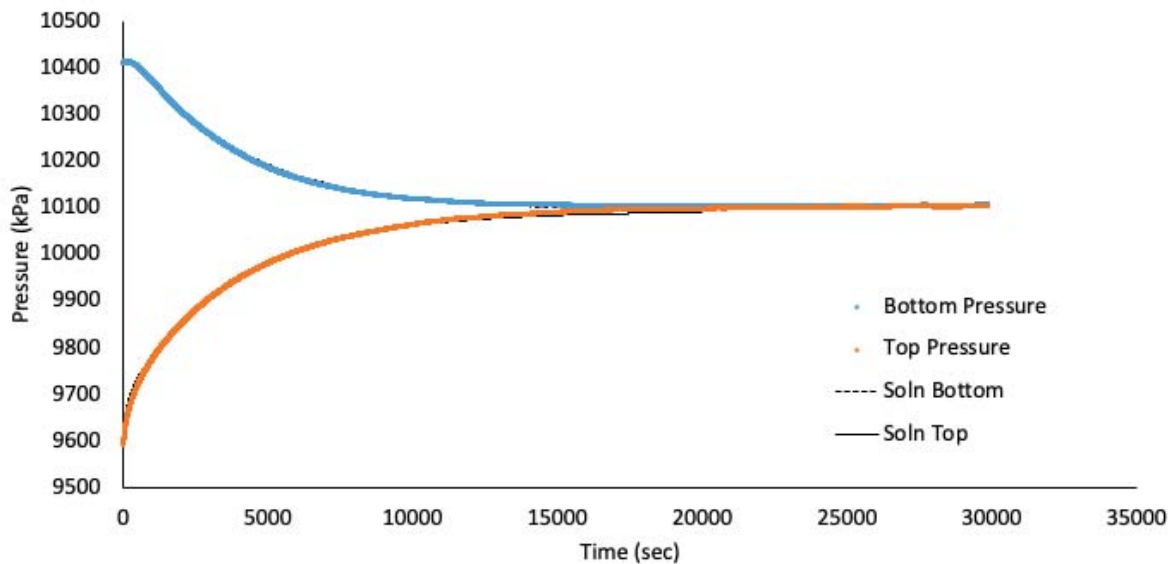


Figure 118 IG_BH05_PS006_HC61a: Effective Confining Stress = 24.71 MPa

**Appendix D: Hydraulic Conductivity and Steady State Gas Permeability Test Summaries
– IG_BH06**

CONTENTS

	Page
Figure 119 IG_BH06_AR011_HC25a: Effective Confining Stress = 7.82 MPa	165
Figure 120 IG_BH06_AR011_HC25a: Effective Confining Stress = 12.75 MPa	166
Figure 121 IG_BH06_AR011_HC25r: Effective Confining Stress = 8.22 MPa	167
Figure 122 IG_BH06_AR011_HC25r: Effective Confining Stress = 12.77 MPa	168
Figure 123 IG_BH06_AR011_HC61a: Effective Confining Stress = 8.25 MPa	169
Figure 124 IG_BH06_AR011_HC61a: Effective Confining Stress = 12.79 MPa	170
Figure 125 IG_BH06_AR011_HC61a: Effective Confining Stress = 16.91 MPa	171
Figure 126 IG_BH06_AR056_HC25a: Effective Confining Stress = 16.74 MPa	172
Figure 127 IG_BH06_AR056_HC61a: Effective Confining Stress = 17.46 MPa	173
Figure 128 IG_BH06_AR056_SSG61a: Effective Confining Stresses of 17.3MPa and 22.3MPa.....	174
Figure 129 IG_BH06_PS001_HC25a: Effective Confining Stress = 6.86 MPa	175
Figure 130 IG_BH06_PS001_HC25a: Effective Confining Stress = 11.91 MPa	176
Figure 131 IG_BH06_PS001_HC25a: Effective Confining Stress = 15.52 MPa	177
Figure 132 IG_BH06_PS001_HC25r: Effective Confining Stress = 7.09 MPa	178
Figure 133 IG_BH06_PS001_HC25r: Effective Confining Stress = 11.82 MPa	179
Figure 134 IG_BH06_PS001_HC25r: Effective Confining Stress = 15.39 MPa	180
Figure 135 IG_BH06_PS001_HC61a: Effective Confining Stress = 7.23 MPa	181
Figure 136 IG_BH06_PS001_HC61a: Effective Confining Stress = 12.02 MPa	182
Figure 137 IG_BH06_PS001_HC61a: Effective Confining Stress = 15.6 MPa	183
Figure 138 IG_BH06_PS002_HC25a: Effective Confining Stress = 10.43 MPa	184
Figure 139 IG_BH06_PS002_HC25a: Effective Confining Stress = 15.51 MPa	185
Figure 140 IG_BH06_PS002_HC25a: Effective Confining Stress = 20.9 MPa	186
Figure 141 IG_BH06_PS002_HC25r: Effective Confining Stress = 10.67 MPa	187
Figure 142 IG_BH06_PS002_HC25r: Effective Confining Stress = 15.76 MPa	188
Figure 143 IG_BH06_PS002_HC25r: Effective Confining Stress = 20.71 MPa	189
Figure 144 IG_BH06_PS002_HC61a: Effective Confining Stress = 10.88 MPa	190
Figure 145 IG_BH06_PS002_HC61a: Effective Confining Stress = 16.03 MPa	191
Figure 146 IG_BH06_PS002_HC61a: Effective Confining Stress = 21.05 MPa	192
Figure 147 IG_BH06_PS003_HC25a: Effective Confining Stress = 12.46 MPa	193

Figure 148	IG_BH06_PS003_HC25a: Effective Confining Stress = 17.64 MPa	194
Figure 149	IG_BH06_PS003_HC25a: Effective Confining Stress = 22.23 MPa	195
Figure 150	IG_BH06_PS003_HC25r: Effective Confining Stress = 12.35 MPa	196
Figure 151	IG_BH06_PS003_HC25r: Effective Confining Stress = 17.5 MPa	197
Figure 152	IG_BH06_PS003_HC25r: Effective Confining Stress = 22.0 MPa	198
Figure 153	IG_BH06_PS003_HC61a: Effective Confining Stress = 12.58 MPa	199
Figure 154	IG_BH06_PS003_HC61a: Effective Confining Stress = 17.79 MPa	200
Figure 155	IG_BH06_PS003_HC61a: Effective Confining Stress = 22.40 MPa	201
Figure 156	IG_BH06_PS004_HC25a: Effective Confining Stress = 13.33 MPa	202
Figure 157	IG_BH06_PS004_HC25a: Effective Confining Stress = 18.43 MPa	203
Figure 158	IG_BH06_PS004_HC25a: Effective Confining Stress = 23.51 MPa	204
Figure 159	IG_BH06_PS004_HC25r: Effective Confining Stress = 13.35 MPa	205
Figure 160	IG_BH06_PS004_HC25r: Effective Confining Stress = 18.37 MPa	206
Figure 161	IG_BH06_PS004_HC25r: Effective Confining Stress = 23.71 MPa	207
Figure 162	IG_BH06_PS004_HC61a: Effective Confining Stress = 13.36 MPa	208
Figure 163	IG_BH06_PS004_HC61a: Effective Confining Stress = 18.36 MPa	209
Figure 164	IG_BH06_PS004_HC61a: Effective Confining Stress = 23.71 MPa	210
Figure 165	IG_BH06_PS004_SSG61a: Effective Confining Stresses of 13.0MPa, 18.9MPa and 23.9MPa.....	211
Figure 166	IG_BH06_PS006_HC25a: Effective Confining Stress = 16.08 MPa	212
Figure 167	IG_BH06_PS006_HC25a: Effective Confining Stress = 21.07 MPa	213
Figure 168	IG_BH06_PS006_HC25a: Effective Confining Stress = 26.12 MPa	214
Figure 169	IG_BH06_PS006_HC25r: Effective Confining Stress = 16.18 MPa	215
Figure 170	IG_BH06_PS006_HC25r: Effective Confining Stress = 20.98 MPa	216
Figure 171	IG_BH06_PS006_HC25r: Effective Confining Stress = 25.97 MPa	217
Figure 172	IG_BH06_PS006_SSG61a: Effective Confining Stresses of 16.8MPa, 21.8MPa and 26.8MPa.....	218
Figure 173	IG_BH06_PS007_HC25a: Effective Confining Stress = 17.70 MPa	219
Figure 174	IG_BH06_PS007_HC25a: Effective Confining Stress = 22.26 MPa	220
Figure 175	IG_BH06_PS007_HC25a: Effective Confining Stress = 27.26 MPa	221
Figure 176	IG_BH06_PS007_HC25r: Effective Confining Stress = 17.53 MPa	222
Figure 177	IG_BH06_PS007_HC25r: Effective Confining Stress = 22.04 MPa	223
Figure 178	IG_BH06_PS007_HC25r: Effective Confining Stress = 27.05 MPa	224
Figure 179	IG_BH06_PS007_HC61a: Effective Confining Stress = 17.82 MPa	225

	Sample Name		IG_BH06_AR011
	Specimen Name		IG_BH06_AR011_HC25a
	Specimen Top Depth		398.93
	Specimen Bottom Depth		398.965
	Test No		ES1
	Test Name		8912.08492584372_ES1
	Operator		0
Dimensions	Length	mm	25.480
	Diameter	mm	25.160
	Length	m	0.02548
	Diameter	m	0.02516
Test Data Location	Raw Data File Name		2023-07-19_08-17-08 System-3-Cell-1 IG-BH06-AR011-HC25a.csv
	Date & Time		2023-07-24 11:49:29
	Start Row		26665
	End Row		42625
Test Conditions	Avg Cell Temp	C	40.56
	Avg Confining Pressure	kPa	17066
	Pre Pulse Avg Pore Pressure	kPa	9248
	Pulse Pressure	kPa	588
	Effective Stress	kPa	7818
Pore Fluid & Conditions	Post Pulse Avg Pore Pressure	kPa	9248
	Type		Water
	Salt	ppm	0
	Density	kg/m3	995.97
	Viscosity	kg.s/m	6.472E-04
Solution	Compressibility	1/Pa	4.36E-10
	Test System		System 3 - Cell 1
Brace	Nominal Decay Time	s	15960
	Brace Permeability	m2	5.81E-21
Hsieh	Permeability	m2	6.39E-21
	Specific Storage	1/m	2.36E-07
	Permeability	nD	6.5
	Hydraulic Conductivity	m/s	9.64E-14
	Pearson Coeff	()	0.9997058

IG_BH06_AR011_HC25a Eff Stress:7.82 MPa, HC=9.64e-14 m/s, SS=2.36e-7 1/m

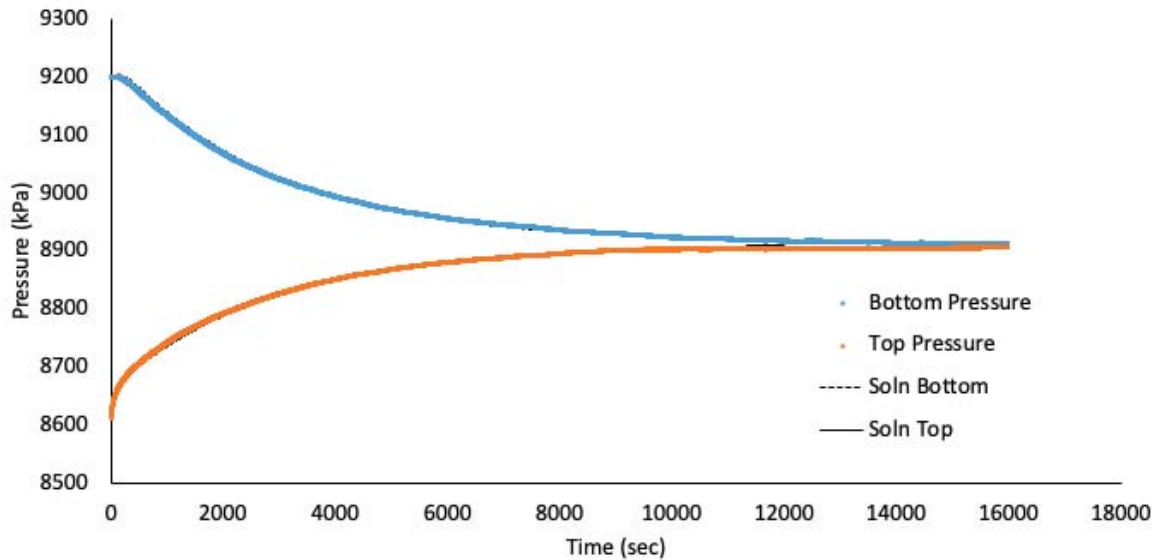


Figure 119 IG_BH06_AR011_HC25a: Effective Confining Stress = 7.82 MPa

	Sample Name		IG_BH06_AR011
	Specimen Name		IG_BH06_AR011_HC25a
	Specimen Top Depth		398.93
	Specimen Bottom Depth		398.965
	Test No		ES2
	Test Name		8997.51859601816_ES2
	Operator		0
Dimensions	Length	mm	25.480
	Diameter	mm	25.160
	Length	m	0.02548
	Diameter	m	0.02516
Test Data Location	Raw Data File Name		2023-07-19_08-17-08 System-3-Cell-1 IG-BH06-AR011-HC25a.csv
	Date & Time		2023-07-19 08:17:08
	Start Row		20330
	End Row		40000
Test Conditions	Avg Cell Temp	C	40.59
	Avg Confining Pressure	kPa	22104
	Pre Pulse Avg Pore Pressure	kPa	9356
	Pulse Pressure	kPa	463
	Effective Stress	kPa	12748
	Post Pulse Avg Pore Pressure	kPa	9356
Pore Fluid & Conditions	Type		Water
	Salt	ppm	0
	Density	kg/m3	996.01
	Viscosity	kg.s/m	6.468E-04
	Compressibility	1/Pa	4.36E-10
Solution	Test System		System 3 - Cell 1
Brace	Nominal Decay Time	s	19670
	Brace Permeability	m2	4.65E-21
Hsieh	Permeability	m2	4.88E-21
	Specific Storage	1/m	1.45E-07
	Permeability	nD	4.9
	Hydraulic Conductivity	m/s	7.37E-14
	Pearson Coeff	()	0.9994302

IG_BH06_AR011_HC25a Eff Stress:12.75 MPa, HC=7.37e-14 m/s, SS=1.45e-7 1/m

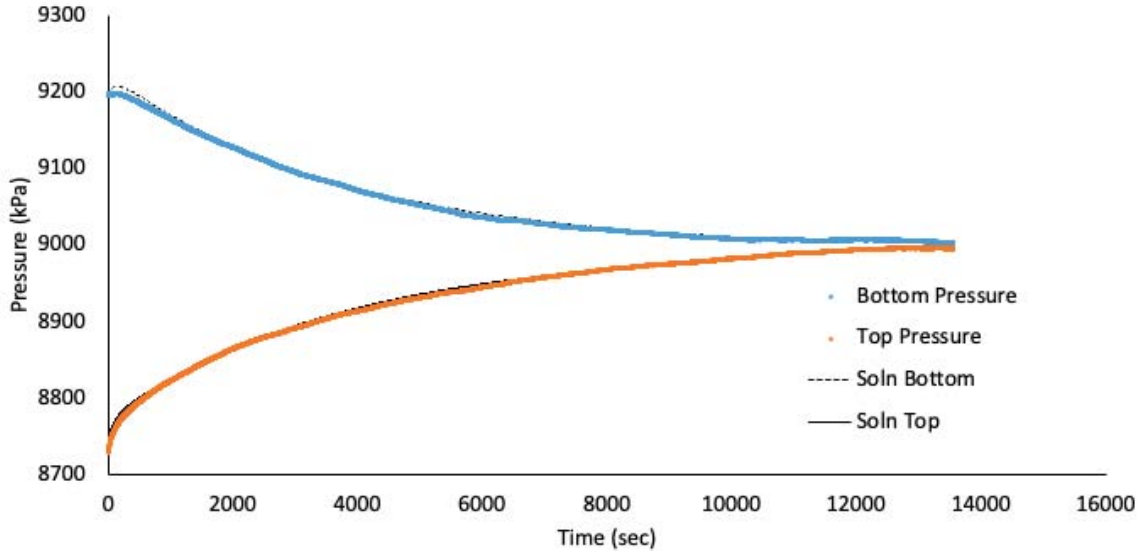


Figure 120 IG_BH06_AR011_HC25a: Effective Confining Stress = 12.75 MPa

	Sample Name		IG_BH06_AR011
	Specimen Name		IG_BH06_AR011_HC25r
	Specimen Top Depth		398.93
	Specimen Bottom Depth		398.965
	Test No		ES1
	Test Name		9082.373951_ES1
	Operator		0
Dimensions	Length	mm	25.980
	Diameter	mm	24.570
	Length	m	0.02598
	Diameter	m	0.02457
Test Data Location	Raw Data File Name		2023-07-18_09-17-48 System-3-Cell-3 IG-BH06-AR011-HC25r.csv
	Date & Time		2023-07-18 09:17:48
	Start Row		658
	End Row		9050
Test Conditions	Avg Cell Temp	C	39.84
	Avg Confining Pressure	kPa	17082
	Pre Pulse Avg Pore Pressure	kPa	8864
	Pulse Pressure	kPa	496
	Effective Stress	kPa	8218
	Post Pulse Avg Pore Pressure	kPa	8864
Pore Fluid & Conditions	Type		Water
	Salt	ppm	0
	Density	kg/m3	996.09
	Viscosity	kg.s/m	6.558E-04
	Compressibility	1/Pa	4.36E-10
Solution	Test System		System 3 - Cell 3
Brace	Nominal Decay Time	s	8392
	Brace Permeability	m2	6.64E-21
Hsieh	Permeability	m2	7.30E-21
	Specific Storage	1/m	2.02E-07
	Permeability	nD	7.4
	Hydraulic Conductivity	m/s	1.09E-13
	Pearson Coeff	()	0.9998243

IG_BH06_AR011_HC25r Eff Stress:8.22 MPa, HC=1.09e-13 m/s, SS=2.02e-7 1/m

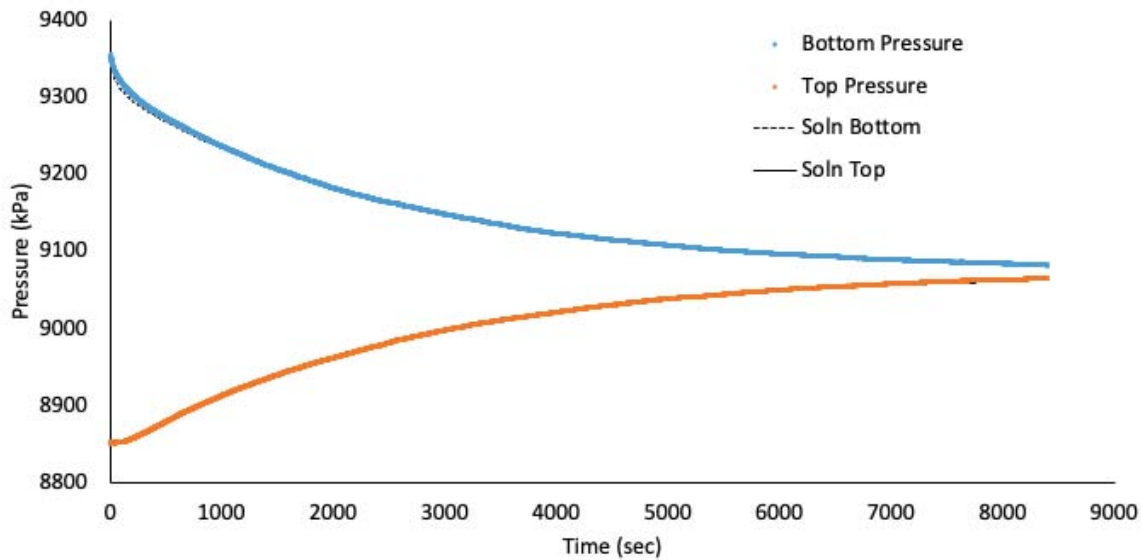


Figure 121 IG_BH06_AR011_HC25r: Effective Confining Stress = 8.22 MPa

	Sample Name		IG_BH06_AR011
	Specimen Name		IG_BH06_AR011_HC25r
	Specimen Top Depth		398.93
	Specimen Bottom Depth		398.965
	Test No		ES2
	Test Name		9079.07772386199_ES2
	Operator		0
Dimensions	Length	mm	25.980
	Diameter	mm	24.570
	Length	m	0.02598
	Diameter	m	0.02457
Test Data Location	Raw Data File Name		2023-07-19_08-16-16 System-3-Cell-3 IG-BH06-AR011-HC25r.csv
	Date & Time		2023-07-19 08:16:16
	Start Row		20368
	End Row		45900
Test Conditions	Avg Cell Temp	C	39.92
	Avg Confining Pressure	kPa	22066
	Pre Pulse Avg Pore Pressure	kPa	9298
	Pulse Pressure	kPa	538
	Effective Stress	kPa	12767
	Post Pulse Avg Pore Pressure	kPa	9298
Pore Fluid & Conditions	Type		Water
	Salt	ppm	0
	Density	kg/m3	996.25
	Viscosity	kg.s/m	6.549E-04
	Compressibility	1/Pa	4.36E-10
Solution	Test System		System 3 - Cell 3
Brace	Nominal Decay Time	s	25532
	Brace Permeability	m2	3.91E-21
Hsieh	Permeability	m2	4.10E-21
	Specific Storage	1/m	1.50E-07
	Permeability	nD	4.2
	Hydraulic Conductivity	m/s	6.13E-14
	Pearson Coeff	()	0.9960689

IG_BH06_AR011_HC25r Eff Stress:12.77 MPa, HC=6.13e-14 m/s, SS=1.50e-7 1/m

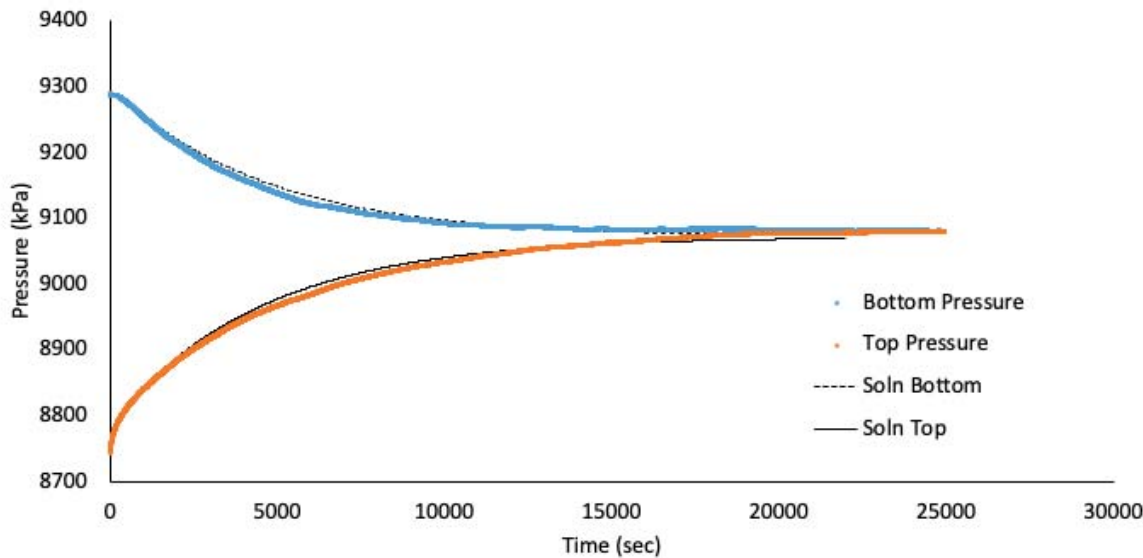


Figure 122 IG_BH06_AR011_HC25r: Effective Confining Stress = 12.77 MPa

	Sample Name		IG_BH06_AR011
	Specimen Name		IG_BH06_AR011_HC61a
	Specimen Top Depth		398.965
	Specimen Bottom Depth		399.027
	Test No		ES1
	Test Name		9116.97939033333_ES1
	Operator		0
Dimensions	Length	mm	62.160
	Diameter	mm	61.110
	Length	m	0.06216
	Diameter	m	0.06111
Test Data Location	Raw Data File Name		2023-07-18_09-16-58 System-3-Cell-2 IG-BH06-AR011-HC61a.csv
	Date & Time		2023-07-18 09:16:58
	Start Row		716
	End Row		9110
Test Conditions	Avg Cell Temp	C	40.28
	Avg Confining Pressure	kPa	17110
	Pre Pulse Avg Pore Pressure	kPa	8856
	Pulse Pressure	kPa	503
	Effective Stress	kPa	8254
	Post Pulse Avg Pore Pressure	kPa	8856
Pore Fluid & Conditions	Type		Water
	Salt	ppm	0
	Density	kg/m3	995.92
	Viscosity	kg.s/m	6.505E-04
	Compressibility	1/Pa	4.36E-10
Solution	Test System		System 3 - Cell 2
Brace	Nominal Decay Time	s	8394
	Brace Permeability	m2	4.26E-21
Hsieh	Permeability	m2	5.20E-21
	Specific Storage	1/m	9.42E-08
	Permeability	nD	5.3
	Hydraulic Conductivity	m/s	7.81E-14
	Pearson Coeff	()	0.9988604

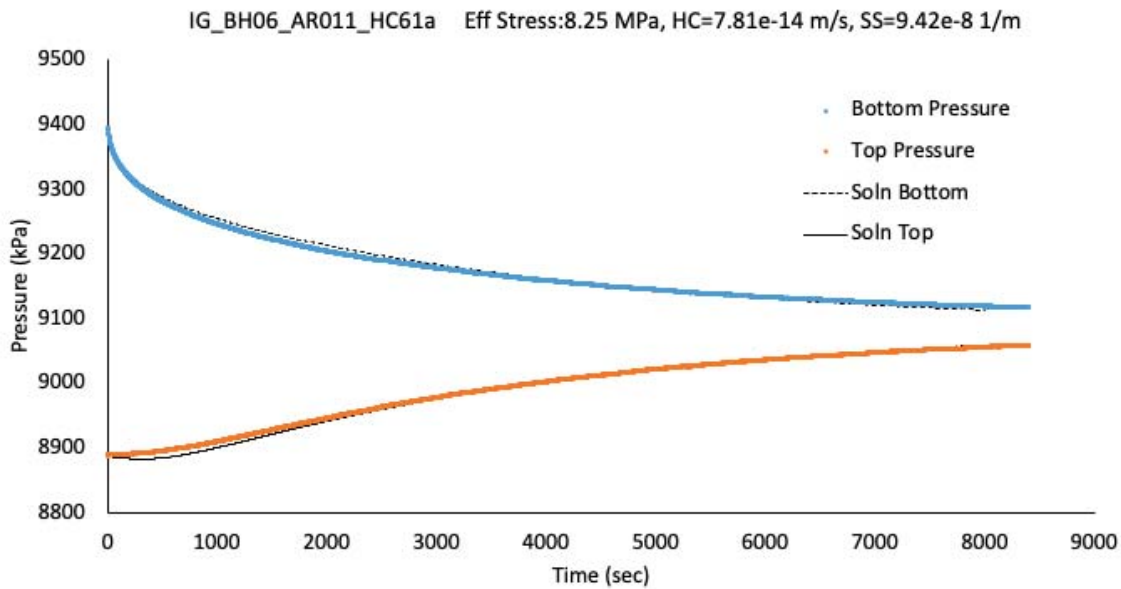


Figure 123 IG_BH06_AR011_HC61a: Effective Confining Stress = 8.25 MPa

	Sample Name		IG_BH06_AR011
	Specimen Name		IG_BH06_AR011_HC61a
	Specimen Top Depth		398.965
	Specimen Bottom Depth		399.027
	Test No		ES2
	Test Name		9197.68646333333_ES2
	Operator		0
Dimensions	Length	mm	62.160
	Diameter	mm	61.110
	Length	m	0.06216
	Diameter	m	0.06111
Test Data Location	Raw Data File Name		2023-07-18_09-16-58 System-3-Cell-2 IG-BH06-AR011-HC61a.csv
	Date & Time		2023-07-19 08:15:52
	Start Row		20399
	End Row		45990
Test Conditions	Avg Cell Temp	C	40.31
	Avg Confining Pressure	kPa	22104
	Pre Pulse Avg Pore Pressure	kPa	9314
	Pulse Pressure	kPa	542
	Effective Stress	kPa	12790
	Post Pulse Avg Pore Pressure	kPa	9314
Pore Fluid & Conditions	Type		Water
	Salt	ppm	0
	Density	kg/m3	996.1
	Viscosity	kg.s/m	6.502E-04
	Compressibility	1/Pa	4.36E-10
Solution	Test System		System 3 - Cell 2
Brace	Nominal Decay Time	s	25591
	Brace Permeability	m2	3.41E-21
Hsieh	Permeability	m2	3.41E-21
	Specific Storage	1/m	1.12E-07
	Permeability	nD	3.5
	Hydraulic Conductivity	m/s	5.12E-14
	Pearson Coeff	()	0.9970516

IG_BH06_AR011_HC61a Eff Stress:12.79 MPa, HC=5.12e-14 m/s, SS=1.12e-7 1/m

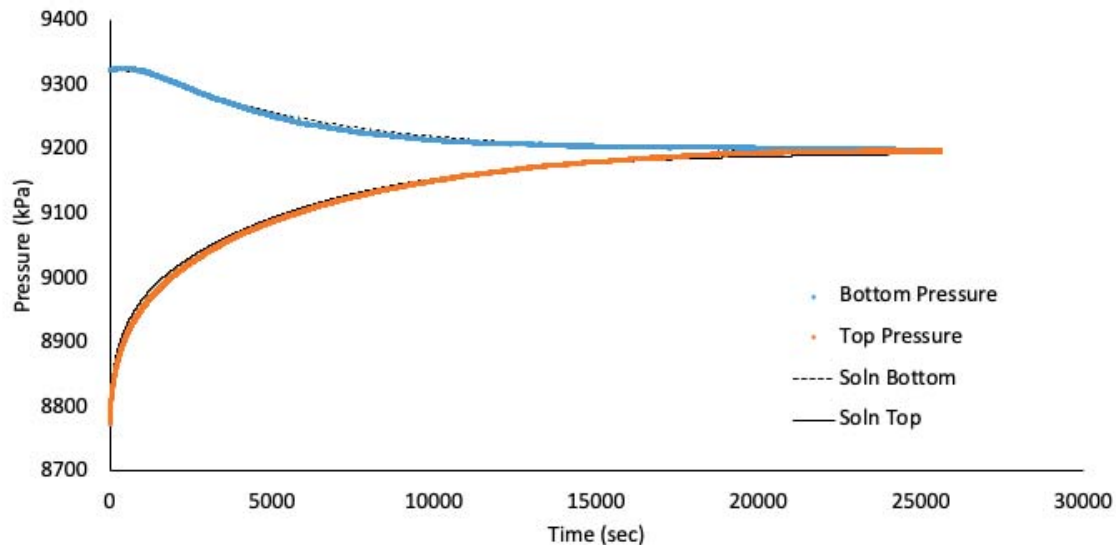


Figure 124 IG_BH06_AR011_HC61a: Effective Confining Stress = 12.79 MPa

	Sample Name		IG_BH06_AR011
	Specimen Name		IG_BH06_AR011_HC61a
	Specimen Top Depth		398.965
	Specimen Bottom Depth		399.027
	Test No		ES3
	Test Name		9888.13991266385_ES3
	Operator		0
Dimensions	Length	mm	62.160
	Diameter	mm	61.110
	Length	m	0.06216
	Diameter	m	0.06111
Test Data Location	Raw Data File Name		2023-07-18_09-16-58 System-3-Cell-2 IG-BH06-AR011-HC61a.csv
	Date & Time		2023-07-20 08:51:32
	Start Row		776
	End Row		50000
Test Conditions	Avg Cell Temp	C	40.30
	Avg Confining Pressure	kPa	27074
	Pre Pulse Avg Pore Pressure	kPa	10164
	Pulse Pressure	kPa	972
	Effective Stress	kPa	16910
	Post Pulse Avg Pore Pressure	kPa	10164
Pore Fluid & Conditions	Type		Water
	Salt	ppm	0
	Density	kg/m3	996.47
	Viscosity	kg.s/m	6.504E-04
	Compressibility	1/Pa	4.36E-10
Solution			System 3 - Cell 2
Brace	Nominal Decay Time	s	49301
	Brace Permeability	m2	2.30E-21
Hsieh	Permeability	m2	2.30E-21
	Specific Storage	1/m	1.26E-07
	Permeability	nD	2.3
	Hydraulic Conductivity	m/s	3.46E-14
	Pearson Coeff	()	0.9999330

IG_BH06_AR011_HC61a Eff Stress:16.91 MPa, HC=3.46e-14 m/s, SS=1.26e-7 1/m

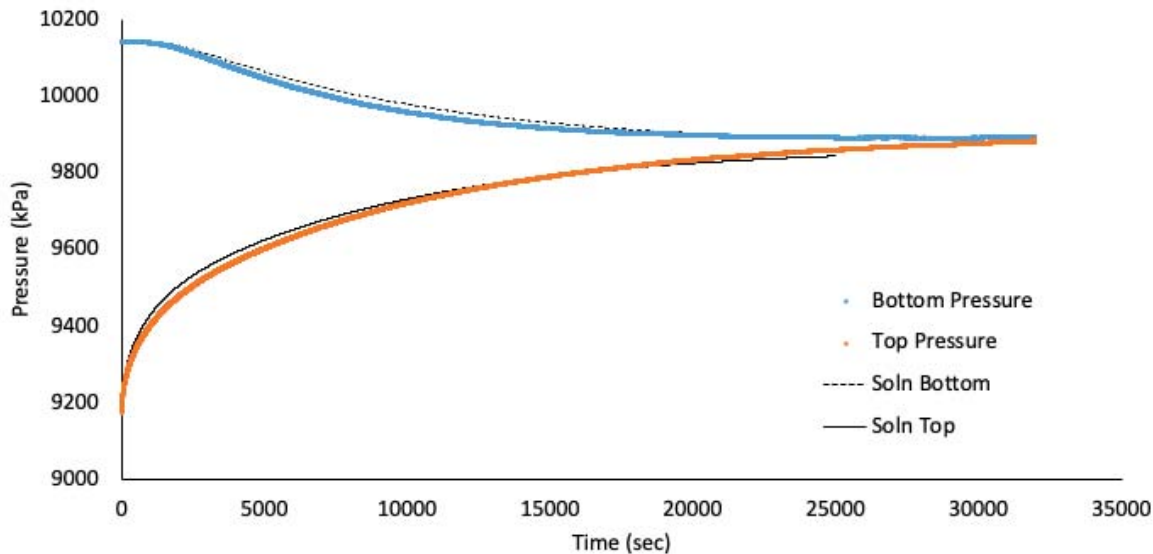


Figure 125 IG_BH06_AR011_HC61a: Effective Confining Stress = 16.91 MPa

	Sample Name		IG_BH06_AR056
	Specimen Name		IG_BH06_AR056_HC25a
	Specimen Top Depth		909.325
	Specimen Bottom Depth		909.360
	Test No		ES1
	Test Name		9251.73147366667_ES1
	Operator		Stephen Talman/ Francy Guerrero
Dimensions	Length	mm	25.520
	Diameter	mm	25.330
	Length	m	0.025552
	Diameter	m	0.02533
Test Data Location	Raw Data File Name		2023-08-09_09-30-19 System-2-CELL-1 IG-BH06-AR056-HC25a.csv
	Date & Time		2023-08-16 08:57:12
	Start Row		17950
	End Row		29600
Test Conditions	Avg Cell Temp	C	39.87
	Avg Confining Pressure	kPa	26152
	Pre Pulse Avg Pore Pressure	kPa	9414
	Pulse Pressure	kPa	603
	Effective Stress	kPa	16738
	Post Pulse Avg Pore Pressure	kPa	9414
Pore Fluid & Conditions	Type		Water
	Salt	ppm	0
	Density	kg/m3	996.31
	Viscosity	kg.s/m	6.555E-04
	Compressibility	1/Pa	4.36E-10
Solution	Test System		System 2 - CELL 1
Brace	Nominal Decay Time	s	11650
	Brace Permeability	m2	1.20E-21
Hsieh	Permeability	m2	1.44E-21
	Specific Storage	1/m	8.96E-08
	Permeability	nD	1.5
	Hydraulic Conductivity	m/s	2.14E-14
	Pearson Coeff	()	0.9906883

IG_BH06_AR056_HC25a Eff Stress:16.74 MPa, HC=2.14e-14 m/s, SS=8.96e-8 1/m

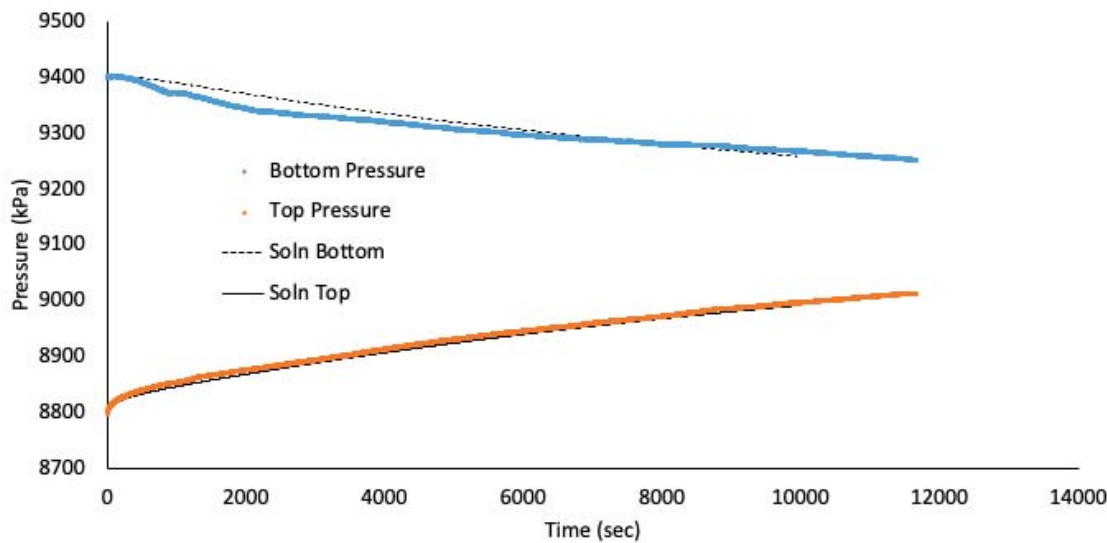


Figure 126 IG_BH06_AR056_HC25a: Effective Confining Stress = 16.74 MPa

	Sample Name		IG_BH06_AR056
	Specimen Name		IG_BH06_AR056_HC61a
	Specimen Top Depth		909.36
	Specimen Bottom Depth		909.422
	Test No		ES1
	Test Name		9210.72341166666_ES1
	Operator		Stephen Talman/ Francy Guerrero
Dimensions	Length	mm	62.140
	Diameter	mm	61.120
	Length	m	0.06214
	Diameter	m	0.06112
Test Data Location	Raw Data File Name		2023-08-09_09-30-44 System-2-CELL-2 IG-BH06-AR056-HC61a.csv
	Date & Time		2023-08-16 08:57:33
	Start Row		718
	End Row		9800
Test Conditions	Avg Cell Temp	C	39.83
	Avg Confining Pressure	kPa	26277
	Pre Pulse Avg Pore Pressure	kPa	8814
	Pulse Pressure	kPa	587
	Effective Stress	kPa	17463
	Post Pulse Avg Pore Pressure	kPa	8814
Pore Fluid & Conditions	Type		Water
	Salt	ppm	0
	Density	kg/m3	996.07
	Viscosity	kg.s/m	6.560E-04
	Compressibility	1/Pa	4.36E-10
Solution	System and Cell		System 2 - CELL 2
Brace	Nominal Decay Time	s	9082
	Brace Permeability	m2	9.18E-22
Hsieh	Permeability	m2	1.29E-21
	Specific Storage	1/m	8.30E-08
	Permeability	nD	1.3
	Hydraulic Conductivity	m/s	1.92E-14
	Pearson Coeff	()	0.9957065

IG_BH06_AR056_HC61a Eff Stress:17.46 MPa, HC=1.92e-14 m/s, SS=8.30e-8 1/m

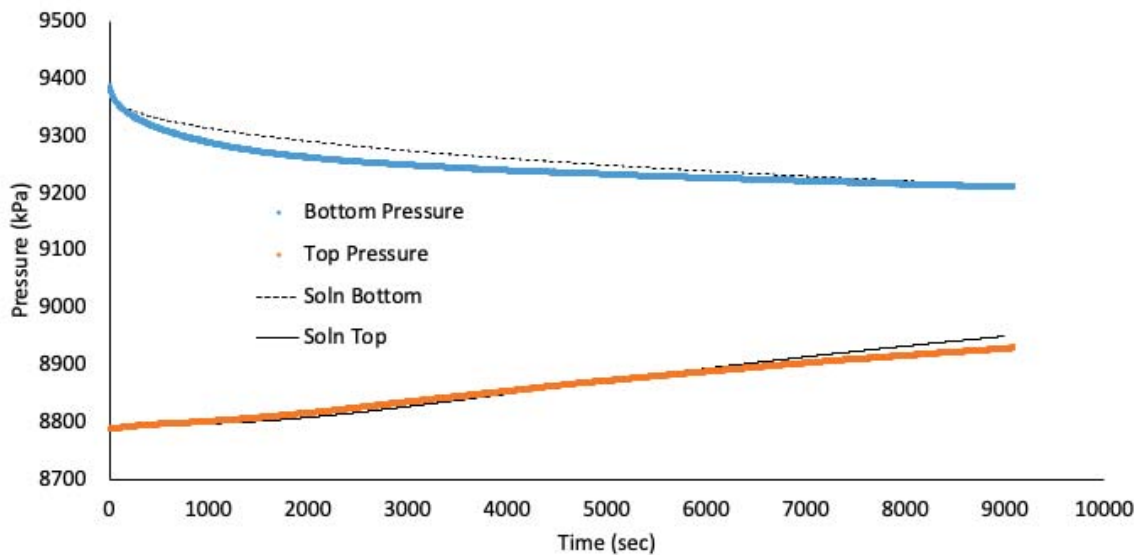


Figure 127 IG_BH06_AR056_HC61a: Effective Confining Stress = 17.46 MPa

Sample ID	IG_BH06_AR056			
Specimen Full Name	IG_BH06_AR056_SSG61a			
Top Depth (m)	909.422			
Bottom Depth (m)	909.484			
Test ID	SSG	ESL	ESM	ESH
Test Name	Steady State N2 Permeability			
Operator 1	A. Sanchez			
Operator 2				
Dimensions	Length	mm	62.11	
	Diameter	mm	61.12	
	Length	m	0.06	
	Diameter	m	0.06	
Test Data Location	Raw Data File Name		rawData_ESL	rawData_ESM
	Start Date & Time	2023-04-12	rawData_ESL	rawData_ESM
	End Date & Time	2023-04-19	rawData_ESL	rawData_ESM
Average Test Conditions and Pore Fluids Conditions	Cell Temp	C	33.0	33.1
	Fluid Type	Gas	Nitrogen	Nitrogen
	Density	kg/m3	105.8	105.8
	Viscosity	cP	0.0201	0.0201
Results	Effective Stress	MPa	17.3	22.3
	kapp	m2	1.96E-19	7.47E-20

NOTES:

- ESL Effective stress - low test condition
 ESM Effective stress - medium test condition
 ESH Effective stress - high test condition
 kapp Apparent gas permeability

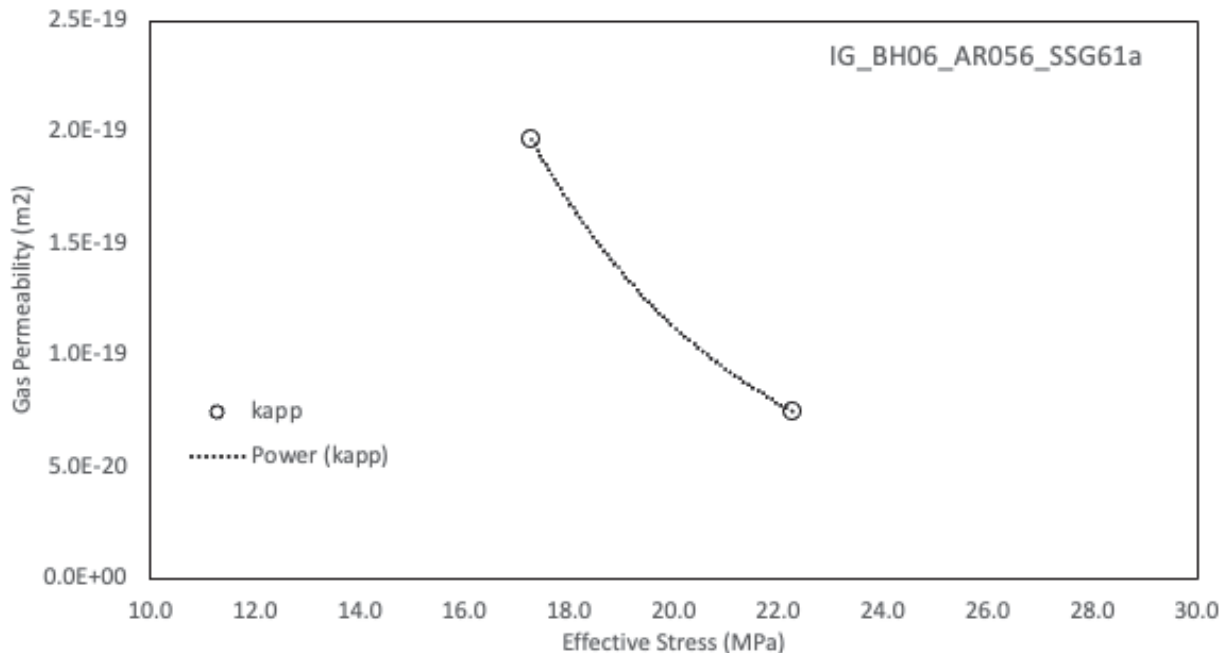


Figure 128 IG_BH06_AR056_SSG61a: Effective Confining Stresses of 17.3 MPa and 22.3 MPa

	Sample Name		IG_BH06_PS001
	Specimen Name		IG_BH06_PS001_HC25a
	Specimen Top Depth		371.705
	Specimen Bottom Depth		371.740
	Test No		ES1
	Test Name		8812.83721204438_ES1
	Operator		Stephen Talman/ Francy Guerrero
Dimensions	Length	mm	25.010
	Diameter	mm	25.260
	Length	m	0.02501
	Diameter	m	0.02526
Test Data Location	Raw Data File Name		2023-07-07_21-51-52 System-2-CELL-1 IG-BH06-PS001-HC25a.csv
	Date & Time		2023-07-11 11:26:23
	Start Row		41616
	End Row		43700
Test Conditions	Avg Cell Temp	C	39.81
	Avg Confining Pressure	kPa	16030
	Pre Pulse Avg Pore Pressure	kPa	9170
	Pulse Pressure	kPa	649
	Effective Stress	kPa	6860
	Post Pulse Avg Pore Pressure	kPa	9170
Pore Fluid & Conditions	Type		Water
	Salt	ppm	0
	Density	kg/m3	996.23
	Viscosity	kg.s/m	6.562E-04
	Compressibility	1/Pa	4.36E-10
Solution	Test System		System 2 - CELL 1
Brace	Nominal Decay Time	s	2084
	Brace Permeability	m2	5.23E-20
Hsieh	Permeability	m2	5.39E-20
	Specific Storage	1/m	1.39E-07
	Permeability	nD	54.6
	Hydraulic Conductivity	m/s	8.02E-13
	Pearson Coeff	()	0.9998342

IG_BH06_PS001_HC25a Eff Stress:6.86 MPa, HC=8.02e-13 m/s, SS=1.39e-7 1/m

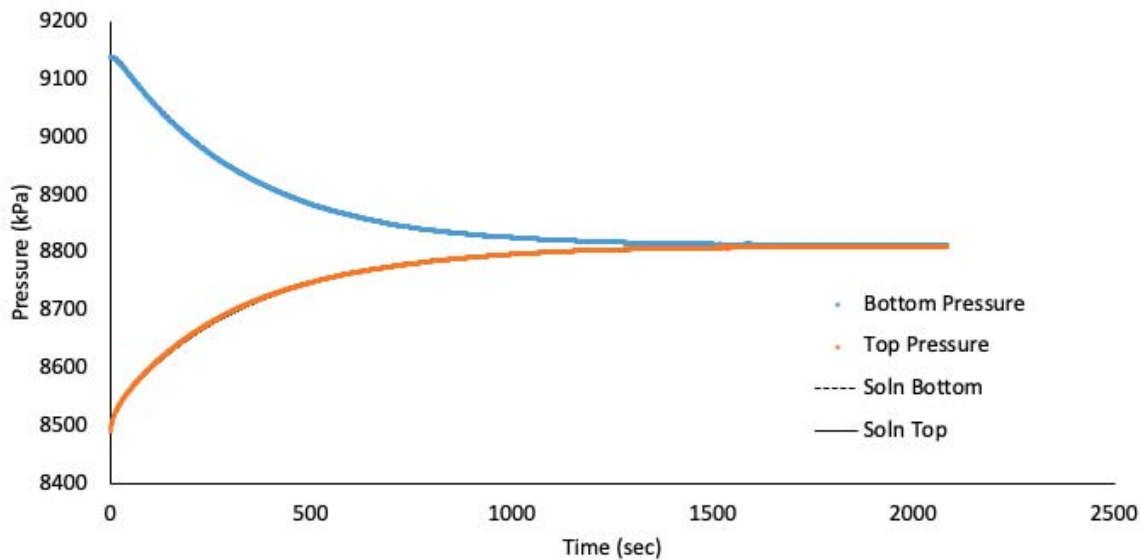


Figure 129 IG_BH06_PS001_HC25a: Effective Confining Stress = 6.86 MPa

	Sample Name		IG_BH06_PS001
	Specimen Name		IG_BH06_PS001_HC25a
	Specimen Top Depth		371.705
	Specimen Bottom Depth		371.740
	Test No		ES2
	Test Name		8826.84416545198_ES2
	Operator		Stephen Talman/ Francy Guerrero
Dimensions	Length	mm	25.010
	Diameter	mm	25.260
	Length	m	0.02501
	Diameter	m	0.02526
Test Data Location	Raw Data File Name		2023-07-07_21-51-52 System-2-CELL-1 IG-BH06-PS001-HC25a.csv
	Date & Time		2023-07-10 12:55:28
	Start Row		66569
	End Row		71200
Test Conditions	Avg Cell Temp	C	39.75
	Avg Confining Pressure	kPa	20994
	Pre Pulse Avg Pore Pressure	kPa	9082
	Pulse Pressure	kPa	-508
	Effective Stress	kPa	11913
	Post Pulse Avg Pore Pressure	kPa	9082
Pore Fluid & Conditions	Type		Water
	Salt	ppm	0
	Density	kg/m3	996.22
	Viscosity	kg.s/m	6.570E-04
	Compressibility	1/Pa	4.36E-10
Solution	Test System		System 2 - CELL 1
Brace	Nominal Decay Time	s	4631
	Brace Permeability	m2	2.53E-20
Hsieh	Permeability	m2	2.63E-20
	Specific Storage	1/m	1.30E-07
	Permeability	nD	26.7
	Hydraulic Conductivity	m/s	3.92E-13
	Pearson Coeff	()	0.9995020

IG_BH06_PS001_HC25a Eff Stress:11.91 MPa, HC=3.92e-13 m/s, SS=1.30e-7 1/m

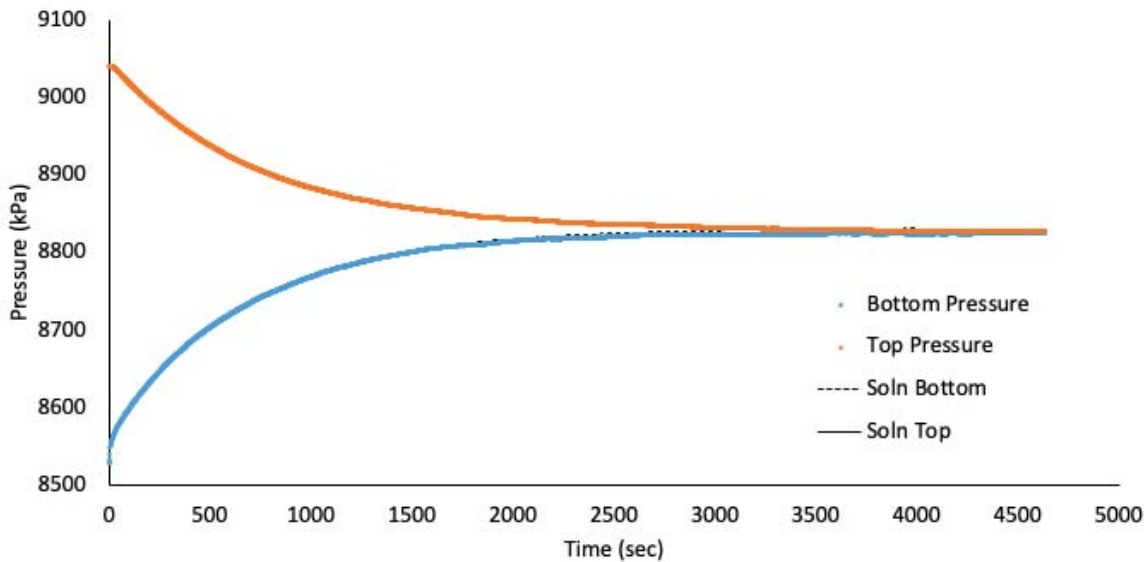


Figure 130 IG_BH06_PS001_HC25a: Effective Confining Stress = 11.91 MPa

	Sample Name		IG_BH06_PS001
	Specimen Name		IG_BH06_PS001_HC25a
	Specimen Top Depth		371.705
	Specimen Bottom Depth		371.740
	Test No		ES3
	Test Name		9339.52385034798_ES3
	Operator		Stephen Talman/ Francy Guerrero
Dimensions	Length	mm	25.010
	Diameter	mm	25.260
	Length	m	0.02501
	Diameter	m	0.02526
Test Data Location	Raw Data File Name		2023-07-07_21-51-52 System-2-CELL-1 IG-BH06-PS001-HC25a.csv
	Date & Time		2023-07-07 21:51:52
	Start Row		10198
	End Row		16000
Test Conditions	Avg Cell Temp	C	39.83
	Avg Confining Pressure	kPa	25089
	Pre Pulse Avg Pore Pressure	kPa	9573
	Pulse Pressure	kPa	-487
	Effective Stress	kPa	15516
	Post Pulse Avg Pore Pressure	kPa	9573
Pore Fluid & Conditions	Type		Water
	Salt	ppm	0
	Density	kg/m3	996.4
	Viscosity	kg.s/m	6.561E-04
	Compressibility	1/Pa	4.36E-10
Solution	Test System		System 2 - CELL 1
Brace	Nominal Decay Time	s	5802
	Brace Permeability	m2	2.02E-20
Hsieh	Permeability	m2	2.02E-20
	Specific Storage	1/m	1.29E-07
	Permeability	nD	20.5
	Hydraulic Conductivity	m/s	3.02E-13
	Pearson Coeff	()	0.9996649

IG_BH06_PS001_HC25a Eff Stress:15.52 MPa, HC=3.02e-13 m/s, SS=1.29e-7 1/m

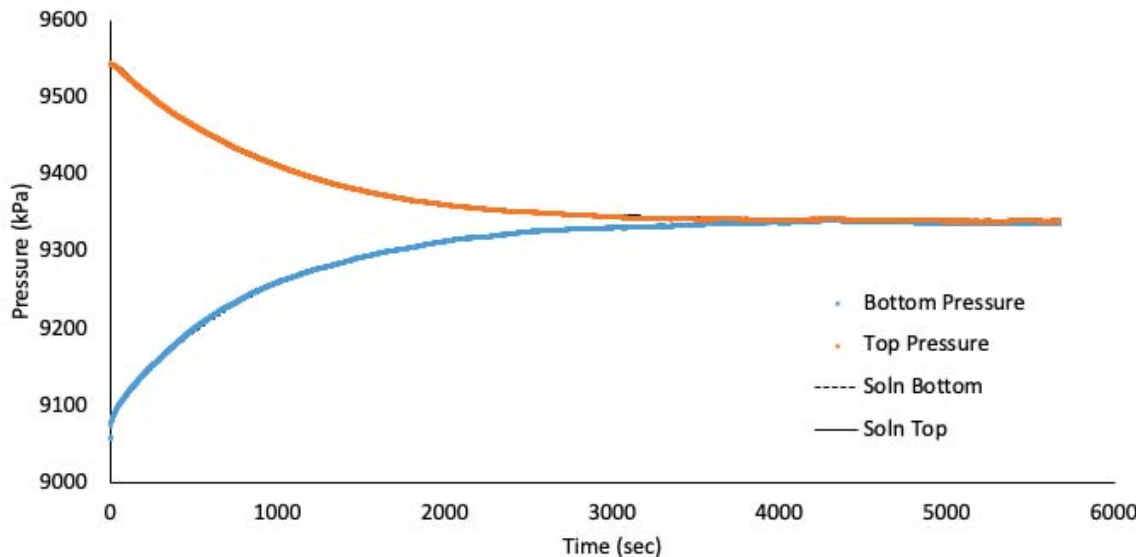


Figure 131 IG_BH06_PS001_HC25a: Effective Confining Stress = 15.52 MPa

	Sample Name		IG_BH06_PS001
	Specimen Name		IG_BH06_PS001_HC25r
	Specimen Top Depth		371.705
	Specimen Bottom Depth		371.740
	Test No		ES1
	Test Name		9059.26724782291_ES1
	Operator		Stephen Talman/ Francy Guerrero
Dimensions	Length	mm	25.180
	Diameter	mm	24.490
	Length	m	0.02518
	Diameter	m	0.02449
Test Data Location	Raw Data File Name		2023-07-07_21-51-55 System-2-CELL-3 IG-BH06-PS001-HC25r.csv
	Date & Time		2023-07-11 11:27:24
	Start Row		510
	End Row		3000
Test Conditions	Avg Cell Temp	C	39.59
	Avg Confining Pressure	kPa	15907
	Pre Pulse Avg Pore Pressure	kPa	8821
	Pulse Pressure	kPa	584
	Effective Stress	kPa	7086
	Post Pulse Avg Pore Pressure	kPa	8821
Pore Fluid & Conditions	Type		Water
	Salt	ppm	0
	Density	kg/m3	996.17
	Viscosity	kg.s/m	6.589E-04
	Compressibility	1/Pa	4.36E-10
Solution	Test System		System 2 - CELL 3
Brace	Nominal Decay Time	s	2490
	Brace Permeability	m2	5.06E-20
Hsieh	Permeability	m2	5.06E-20
	Specific Storage	1/m	2.28E-07
	Permeability	nD	51.3
	Hydraulic Conductivity	m/s	7.51E-13
	Pearson Coeff	()	0.9997395

IG_BH06_PS001_HC25r Eff Stress:7.09 MPa, HC=7.51e-13 m/s, SS=2.28e-7 1/m

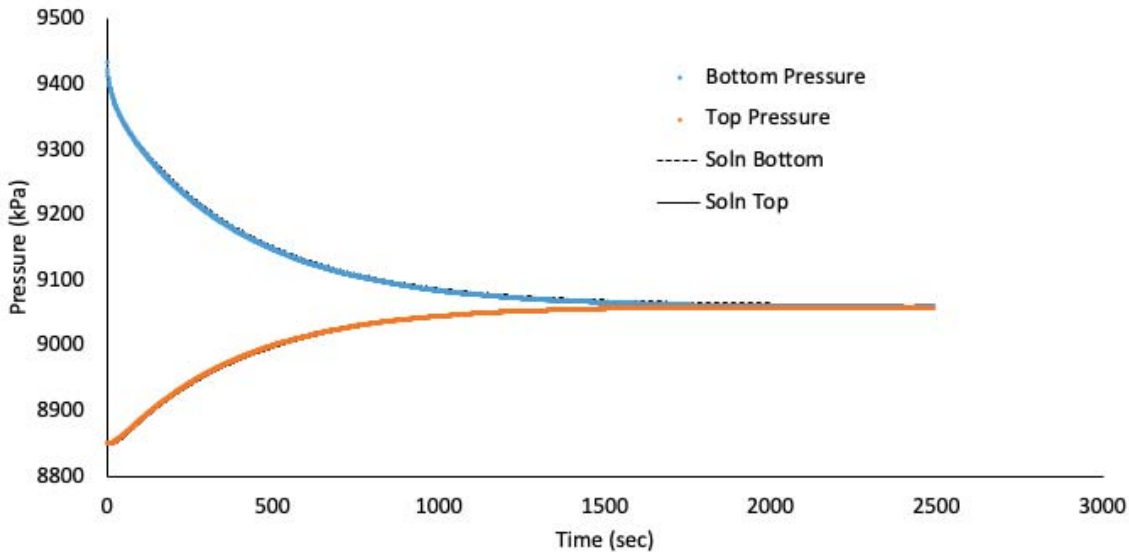


Figure 132 IG_BH06_PS001_HC25r: Effective Confining Stress = 7.09 MPa

	Sample Name		IG_BH06_PS001
	Specimen Name		IG_BH06_PS001_HC25r
	Specimen Top Depth		371.705
	Specimen Bottom Depth		371.740
	Test No		ES2
	Test Name		8833.46345999999_ES2
	Operator		Stephen Talman/ Francy Guerrero
Dimensions	Length	mm	25.180
	Diameter	mm	24.490
	Length	m	0.02518
	Diameter	m	0.02449
Test Data Location	Raw Data File Name		2023-07-07_21-51-55 System-2-CELL-3 IG-BH06-PS001-HC25r.csv
	Date & Time		2023-07-10 12:56:36
	Start Row		133
	End Row		4950
Test Conditions	Avg Cell Temp	C	39.50
	Avg Confining Pressure	kPa	20837
	Pre Pulse Avg Pore Pressure	kPa	9013
	Pulse Pressure	kPa	-502
	Effective Stress	kPa	11824
Pore Fluid & Conditions	Post Pulse Avg Pore Pressure	kPa	9013
	Type		Water
	Salt	ppm	0
	Density	kg/m3	996.28
	Viscosity	kg.s/m	6.600E-04
Solution	Compressibility	1/Pa	4.36E-10
	Test System		System 2 - CELL 3
Brace	Nominal Decay Time	s	4817
	Brace Permeability	m2	2.25E-20
Hsieh	Permeability	m2	2.39E-20
	Specific Storage	1/m	9.35E-08
	Permeability	nD	24.2
	Hydraulic Conductivity	m/s	3.54E-13
	Pearson Coeff	()	0.9998480

IG_BH06_PS001_HC25r Eff Stress:11.82 MPa, HC=3.54e-13 m/s, SS=9.35e-8 1/m

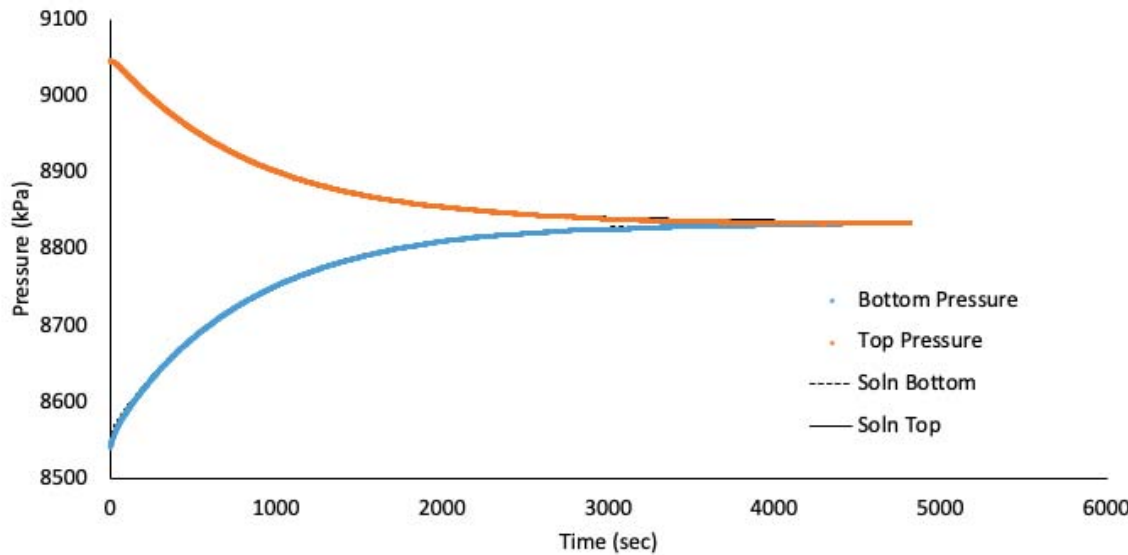


Figure 133 IG_BH06_PS001_HC25r: Effective Confining Stress = 11.82 MPa

	Sample Name		IG_BH06_PS001
	Specimen Name		IG_BH06_PS001_HC25r
	Specimen Top Depth		371.705
	Specimen Bottom Depth		371.740
	Test No		ES3
	Test Name		9334.02882725728_ES3
	Operator		Stephen Talman/ Francy Guerrero
Dimensions	Length	mm	25.180
	Diameter	mm	24.490
	Length	m	0.02518
	Diameter	m	0.02449
Test Data Location	Raw Data File Name		2023-07-07_21-51-55 System-2-CELL-3 IG-BH06-PS001-HC25r.csv
	Date & Time		2023-07-07 21:51:55
	Start Row		11622
	End Row		20050
Test Conditions	Avg Cell Temp	C	39.58
	Avg Confining Pressure	kPa	24902
	Pre Pulse Avg Pore Pressure	kPa	9510
	Pulse Pressure	kPa	-504
	Effective Stress	kPa	15392
	Post Pulse Avg Pore Pressure	kPa	9510
Pore Fluid & Conditions	Type		Water
	Salt	ppm	0
	Density	kg/m3	996.47
	Viscosity	kg.s/m	6.591E-04
	Compressibility	1/Pa	4.36E-10
Solution	Test System		System 2 - CELL 3
Brace	Nominal Decay Time	s	8428
	Brace Permeability	m2	1.69E-20
Hsieh	Permeability	m2	1.69E-20
	Specific Storage	1/m	1.11E-07
	Permeability	nD	17.1
	Hydraulic Conductivity	m/s	2.50E-13
	Pearson Coeff	()	0.9995424

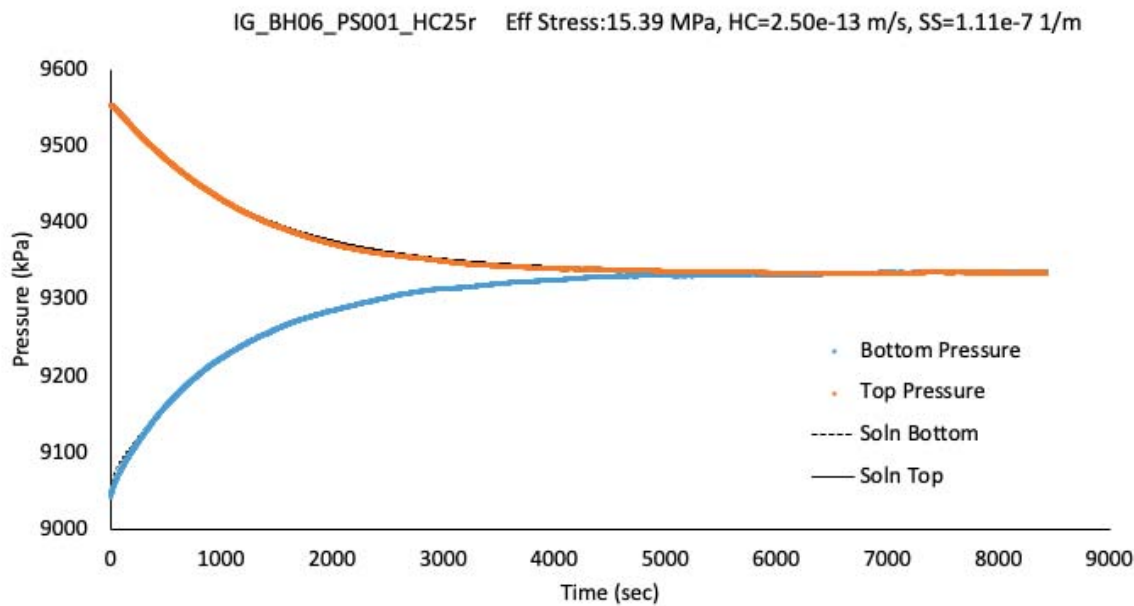


Figure 134 IG_BH06_PS001_HC25r: Effective Confining Stress = 15.39 MPa

	Sample Name		IG_BH06_PS001
	Specimen Name		IG_BH06_PS001_HC61a
	Specimen Top Depth		371.74
	Specimen Bottom Depth		371.802
	Test No		ES1
	Test Name		9006.83614354417_ES1
	Operator		Stephen Talman/ Francy Guerrero
Dimensions	Length	mm	61.860
	Diameter	mm	61.050
	Length	m	0.06186
	Diameter	m	0.06105
Test Data Location	Raw Data File Name		2023-07-07_21-51-54 System-2-CELL-2 IG-BH06-PS001-HC61a.csv
	Date & Time		2023-07-11 11:26:52
	Start Row		2569
	End Row		5320
Test Conditions	Avg Cell Temp	C	39.82
	Avg Confining Pressure	kPa	16108
	Pre Pulse Avg Pore Pressure	kPa	8876
	Pulse Pressure	kPa	571
	Effective Stress	kPa	7232
	Post Pulse Avg Pore Pressure	kPa	8876
Pore Fluid & Conditions	Type		Water
	Salt	ppm	0
	Density	kg/m3	996.1
	Viscosity	kg.s/m	6.561E-04
	Compressibility	1/Pa	4.36E-10
Solution	Test System		System 2 - CELL 2
Brace	Nominal Decay Time	s	2751
	Brace Permeability	m2	3.82E-20
Hsieh	Permeability	m2	3.82E-20
	Specific Storage	1/m	1.22E-07
	Permeability	nD	38.7
	Hydraulic Conductivity	m/s	5.69E-13
	Pearson Coeff	()	0.9990781

IG_BH06_PS001_HC61a Eff Stress:7.23 MPa, HC=5.69e-13 m/s, SS=1.22e-7 1/m

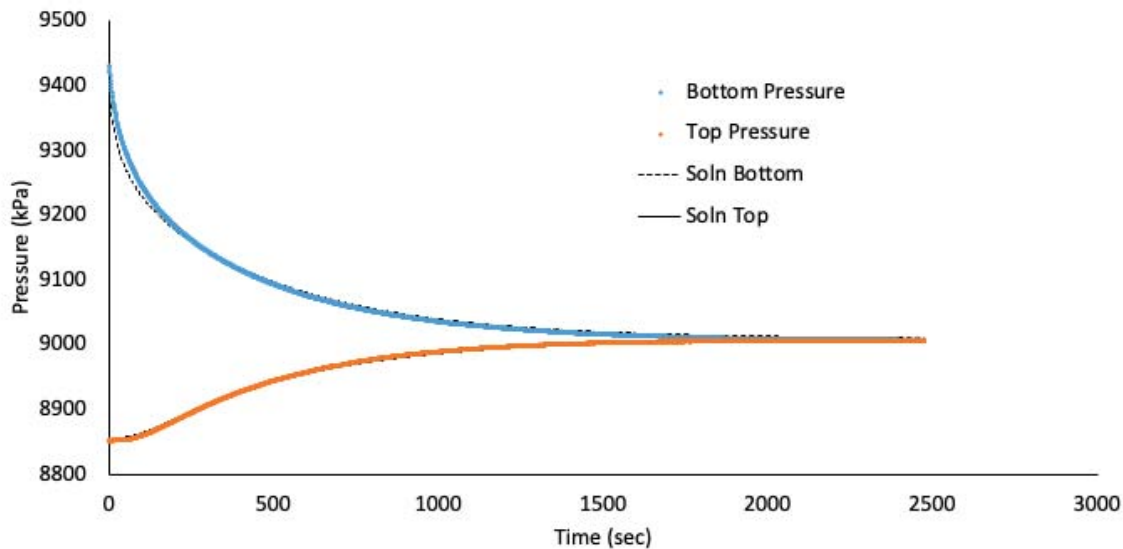


Figure 135 IG_BH06_PS001_HC61a: Effective Confining Stress = 7.23 MPa

	Sample Name		IG_BH06_PS001
	Specimen Name		IG_BH06_PS001_HC61a
	Specimen Top Depth		371.74
	Specimen Bottom Depth		371.802
	Test No		ES2
	Test Name		8857.40689326788_ES2
	Operator		Stephen Talman/ Francy Guerrero
Dimensions	Length	mm	61.860
	Diameter	mm	61.050
	Length	m	0.06186
	Diameter	m	0.06105
Test Data Location	Raw Data File Name		2023-07-07_21-51-54 System-2-CELL-2 IG-BH06-PS001-HC61a.csv
	Date & Time		2023-07-10 12:56:16
	Start Row		3169
	End Row		8000
Test Conditions	Avg Cell Temp	C	39.75
	Avg Confining Pressure	kPa	21097
	Pre Pulse Avg Pore Pressure	kPa	9079
	Pulse Pressure	kPa	-531
	Effective Stress	kPa	12018
	Post Pulse Avg Pore Pressure	kPa	9079
Pore Fluid & Conditions	Type		Water
	Salt	ppm	0
	Density	kg/m3	996.22
	Viscosity	kg.s/m	6.570E-04
	Compressibility	1/Pa	4.36E-10
Solution	Test System		System 2 - CELL 2
Brace	Nominal Decay Time	s	4831
	Brace Permeability	m2	1.99E-20
Hsieh	Permeability	m2	2.09E-20
	Specific Storage	1/m	6.45E-08
	Permeability	nD	21.2
	Hydraulic Conductivity	m/s	3.11E-13
	Pearson Coeff	()	0.9995953

IG_BH06_PS001_HC61a Eff Stress:12.02 MPa, HC=3.11e-13 m/s, SS=6.45e-8 1/m

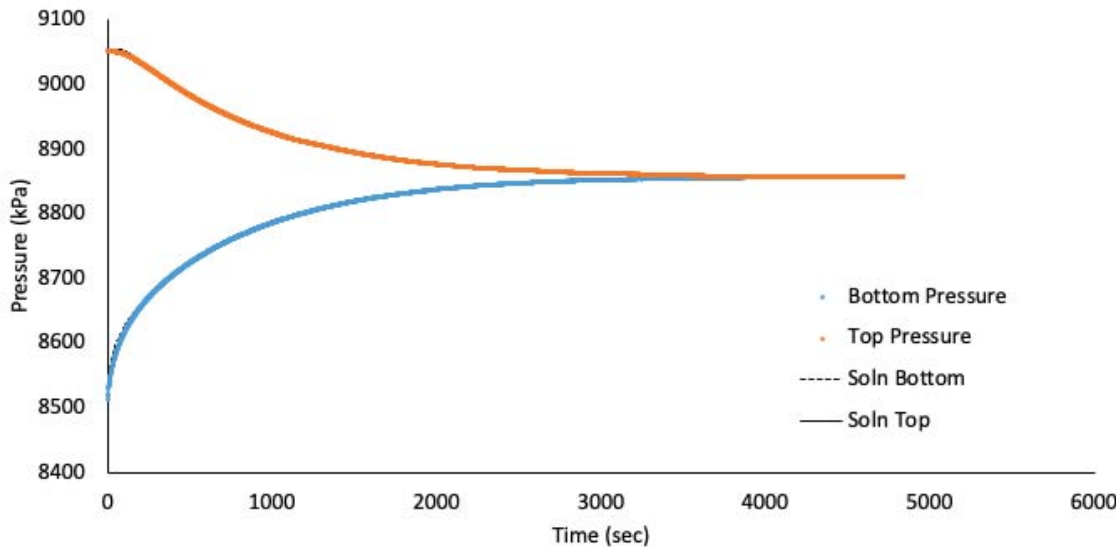


Figure 136 IG_BH06_PS001_HC61a: Effective Confining Stress = 12.02 MPa

	Sample Name		IG_BH06_PS001
	Specimen Name		IG_BH06_PS001_HC61a
	Specimen Top Depth		371.74
	Specimen Bottom Depth		371.802
	Test No		ES3
	Test Name		9359.26466973315_ES3
	Operator		Stephen Talman/ Francy Guerrero
Dimensions	Length	mm	61.860
	Diameter	mm	61.050
	Length	m	0.06186
	Diameter	m	0.06105
Test Data Location	Raw Data File Name		2023-07-07_21-51-54 System-2-CELL-2 IG-BH06-PS001-HC61a.csv
	Date & Time		2023-07-07 21:51:54
	Start Row		1148
	End Row		10200
Test Conditions	Avg Cell Temp	C	39.82
	Avg Confining Pressure	kPa	25211
	Pre Pulse Avg Pore Pressure	kPa	9610
	Pulse Pressure	kPa	-573
	Effective Stress	kPa	15601
	Post Pulse Avg Pore Pressure	kPa	9610
Pore Fluid & Conditions	Type		Water
	Salt	ppm	0
	Density	kg/m3	996.42
	Viscosity	kg.s/m	6.562E-04
	Compressibility	1/Pa	4.36E-10
Solution	Test System		System 2 - CELL 2
Brace	Nominal Decay Time	s	9052
	Brace Permeability	m2	1.22E-20
Hsieh	Permeability	m2	1.41E-20
	Specific Storage	1/m	4.18E-08
	Permeability	nD	14.2
	Hydraulic Conductivity	m/s	2.09E-13
	Pearson Coeff	()	0.9973269

IG_BH06_PS001_HC61a Eff Stress:15.6 MPa, HC=2.09e-13 m/s, SS=4.18e-8 1/m

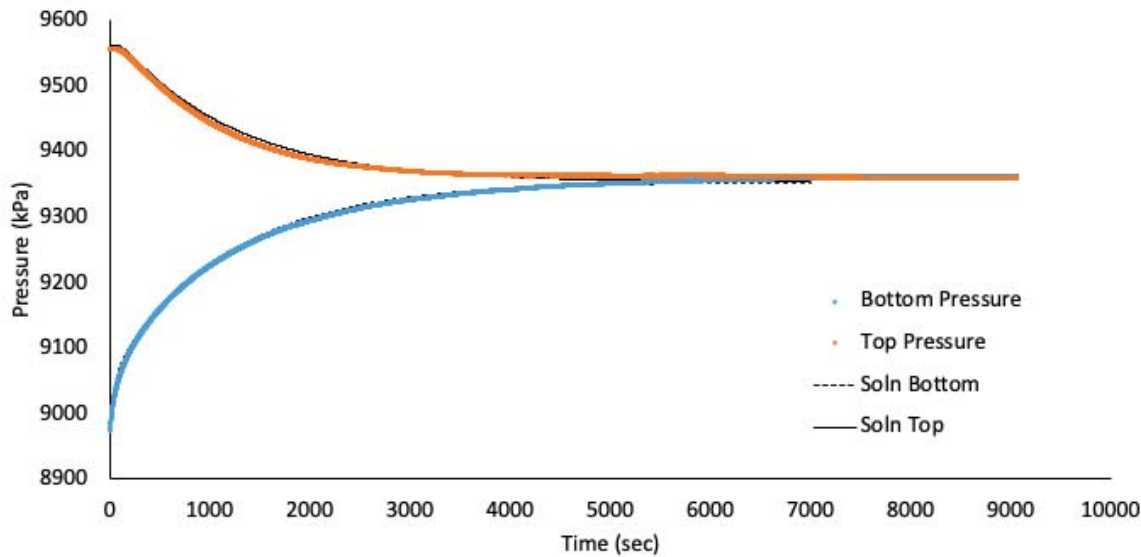


Figure 137 IG_BH06_PS001_HC61a: Effective Confining Stress = 15.6 MPa

	Sample Name		IG_BH06_PS002
	Specimen Name		IG_BH06_PS002_HC25a
	Specimen Top Depth		565.445
	Specimen Bottom Depth		565.480
	Test No		ES1
	Test Name		IG_BH06_PS002_HC25a_ES1
	Operator		Stephen Talman/ Francy Guerrero
Dimensions	Length	mm	25.690
	Diameter	mm	25.210
	Length	m	0.02569
	Diameter	m	0.02521
Test Data Location	Raw Data File Name		2023-07-19_08-47-41 System-2-CELL-1 IG-BH06-PS002-HC25a.csv
	Date & Time		2023-07-19 08:47:41
	Start Row		21521
	End Row		25700
Test Conditions	Avg Cell Temp	C	39.85
	Avg Confining Pressure	kPa	19613
	Pre Pulse Avg Pore Pressure	kPa	9181
	Pulse Pressure	kPa	498
	Effective Stress	kPa	10432
	Post Pulse Avg Pore Pressure	kPa	9181
Pore Fluid & Conditions	Type		Water
	Salt	ppm	0
	Density	kg/m3	996.22
	Viscosity	kg.s/m	6.558E-04
	Compressibility	1/Pa	4.36E-10
Solution	Test System		System 2 - CELL 1
Brace	Nominal Decay Time	s	4179
	Brace Permeability	m2	3.82E-20
Hsieh	Permeability	m2	4.02E-20
	Specific Storage	1/m	6.73E-08
	Permeability	nD	40.7
	Hydraulic Conductivity	m/s	5.99E-13
	Pearson Coeff	()	0.9990681

IG_BH06_PS002_HC25a Eff Stress:10.43 MPa, HC=5.99e-13 m/s, SS=6.73e-8 1/m

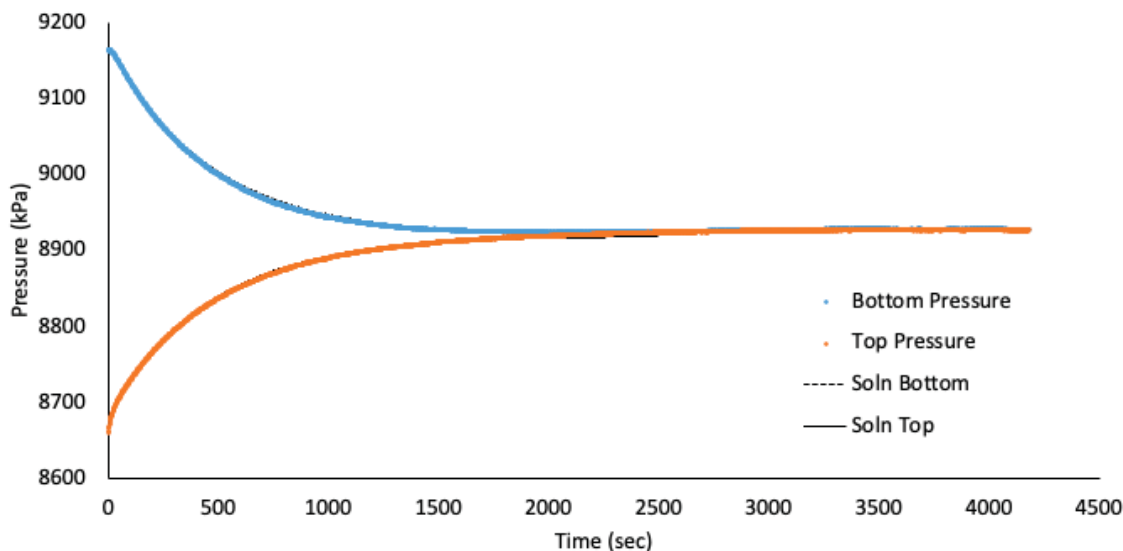


Figure 138 IG_BH06_PS002_HC25a: Effective Confining Stress = 10.43 MPa

	Sample Name		IG_BH06_PS002
	Specimen Name		IG_BH06_PS002_HC25a
	Specimen Top Depth		565.445
	Specimen Bottom Depth		565.480
	Test No		ES2
	Test Name		IG_BH06_PS002_HC25a_ES2
	Operator		Stephen Talman/ Francy Guerrero
Dimensions	Length	mm	25.690
	Diameter	mm	25.210
	Length	m	0.02569
	Diameter	m	0.02521
Test Data Location	Raw Data File Name		2023-07-19_08-47-41 System-2-CELL-1 IG-BH06-PS002-HC25a.csv
	Date & Time		2023-07-20 08:33:26
	Start Row		14129
	End Row		19000
Test Conditions	Avg Cell Temp	C	39.88
	Avg Confining Pressure	kPa	24591
	Pre Pulse Avg Pore Pressure	kPa	9081
	Pulse Pressure	kPa	497
	Effective Stress	kPa	15511
	Post Pulse Avg Pore Pressure	kPa	9081
Pore Fluid & Conditions	Type		Water
	Salt	ppm	0
	Density	kg/m3	996.17
	Viscosity	kg.s/m	6.554E-04
	Compressibility	1/Pa	4.36E-10
Solution			System 2 - CELL 1
Brace	Nominal Decay Time	s	4871
	Brace Permeability	m2	2.08E-20
Hsieh	Permeability	m2	2.08E-20
	Specific Storage	1/m	9.54E-08
	Permeability	nD	21.1
	Hydraulic Conductivity	m/s	3.11E-13
	Pearson Coeff	()	0.9984572

IG_BH06_PS002_HC25a Eff Stress:15.51 MPa, HC=3.11e-13 m/s, SS=9.54e-8 1/m

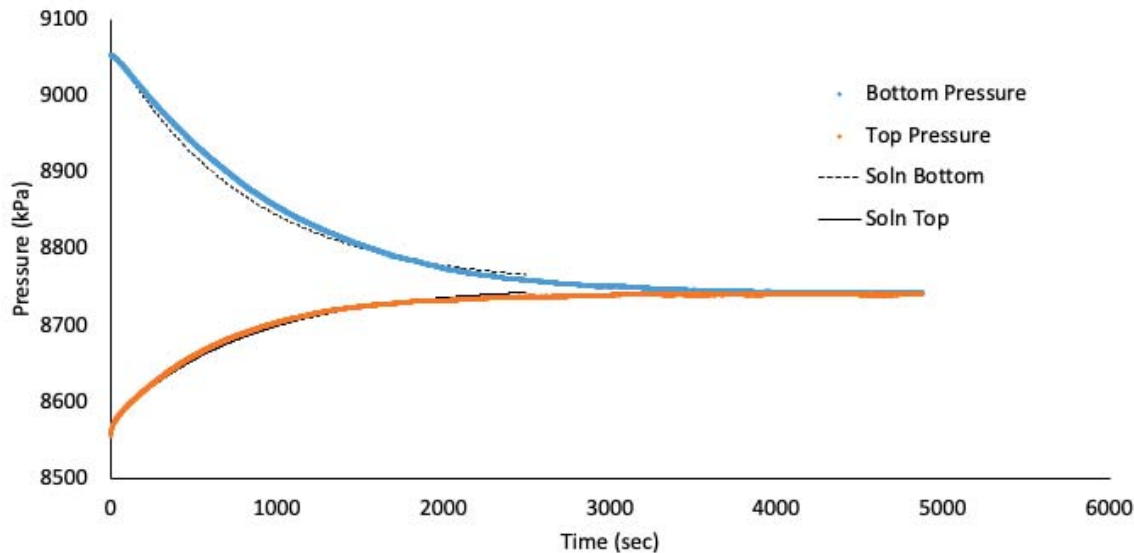


Figure 139 IG_BH06_PS002_HC25a: Effective Confining Stress = 15.51 MPa

	Sample Name		IG_BH06_PS002
	Specimen Name		IG_BH06_PS002_HC25a
	Specimen Top Depth		565.445
	Specimen Bottom Depth		565.480
	Test No		ES3
	Test Name		IG_BH06_PS002_HC25a_ES3
	Operator		Stephen Talman/ Francy Guerrero
Dimensions	Length	mm	25.690
	Diameter	mm	25.210
	Length	m	0.02569
	Diameter	m	0.02521
Test Data Location	Raw Data File Name		2023-07-19_08-47-41 System-2-CELL-1 IG-BH06-PS002-HC25a.csv
	Date & Time		2023-07-21 08:00:13
	Start Row		601
	End Row		7000
Test Conditions	Avg Cell Temp	C	39.88
	Avg Confining Pressure	kPa	29570
	Pre Pulse Avg Pore Pressure	kPa	8670
	Pulse Pressure	kPa	488
	Effective Stress	kPa	20900
	Post Pulse Avg Pore Pressure	kPa	8670
Pore Fluid & Conditions	Type		Water
	Salt	ppm	0
	Density	kg/m3	995.99
	Viscosity	kg.s/m	6.553E-04
	Compressibility	1/Pa	4.36E-10
Solution	Test System		System 2 - CELL 1
Brace	Nominal Decay Time	s	6399
	Brace Permeability	m2	1.04E-20
Hsieh	Permeability	m2	1.04E-20
	Specific Storage	1/m	7.97E-08
	Permeability	nD	10.6
	Hydraulic Conductivity	m/s	1.55E-13
	Pearson Coeff	()	0.9988007

IG_BH06_PS002_HC25a Eff Stress:20.9 MPa, HC=1.55e-13 m/s, SS=7.97e-8 1/m

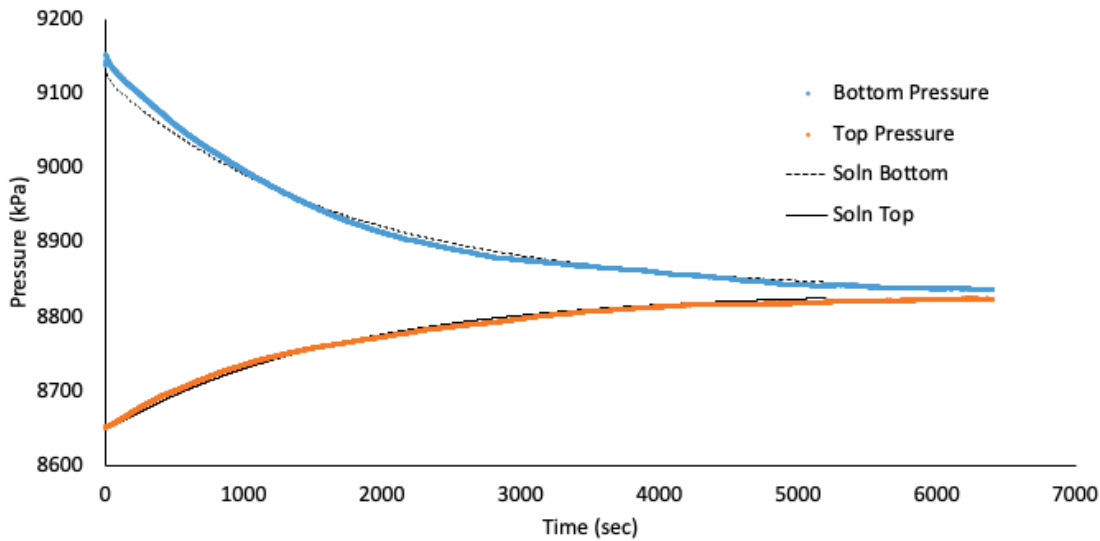


Figure 140 IG_BH06_PS002_HC25a: Effective Confining Stress = 20.9 MPa

	Sample Name		IG_BH06_PS002
	Specimen Name		IG_BH06_PS002_HC25r
	Specimen Top Depth		565.445
	Specimen Bottom Depth		565.480
	Test No		ES1
	Test Name		IG_BH06_PS002_HC25r_ES1
	Operator		Stephen Talman/ Francy Guerrero
Dimensions	Length	mm	26.410
	Diameter	mm	24.560
	Length	m	0.02641
	Diameter	m	0.02456
Test Data Location	Raw Data File Name		2023-07-19_08-48-22 System-2-CELL-3 IG-BH06-PS002-HC25r.csv
	Date & Time		2023-07-19 08:48:22
	Start Row		15981
	End Row		18800
Test Conditions	Avg Cell Temp	C	39.66
	Avg Confining Pressure	kPa	19462
	Pre Pulse Avg Pore Pressure	kPa	8793
	Pulse Pressure	kPa	499
	Effective Stress	kPa	10669
	Post Pulse Avg Pore Pressure	kPa	8793
Pore Fluid & Conditions	Type		Water
	Salt	ppm	0
	Density	kg/m3	996.13
	Viscosity	kg.s/m	6.580E-04
	Compressibility	1/Pa	4.36E-10
Solution	Test System		System 2 - CELL 3
Brace	Nominal Decay Time	s	2819
	Brace Permeability	m2	5.86E-20
Hsieh	Permeability	m2	6.03E-20
	Specific Storage	1/m	1.16E-07
	Permeability	nD	61.1
	Hydraulic Conductivity	m/s	8.96E-13
	Pearson Coeff	()	0.9998479

IG_BH06_PS002_HC25r Eff Stress:10.67 MPa, HC=8.96e-13 m/s, SS=1.16e-7 1/m

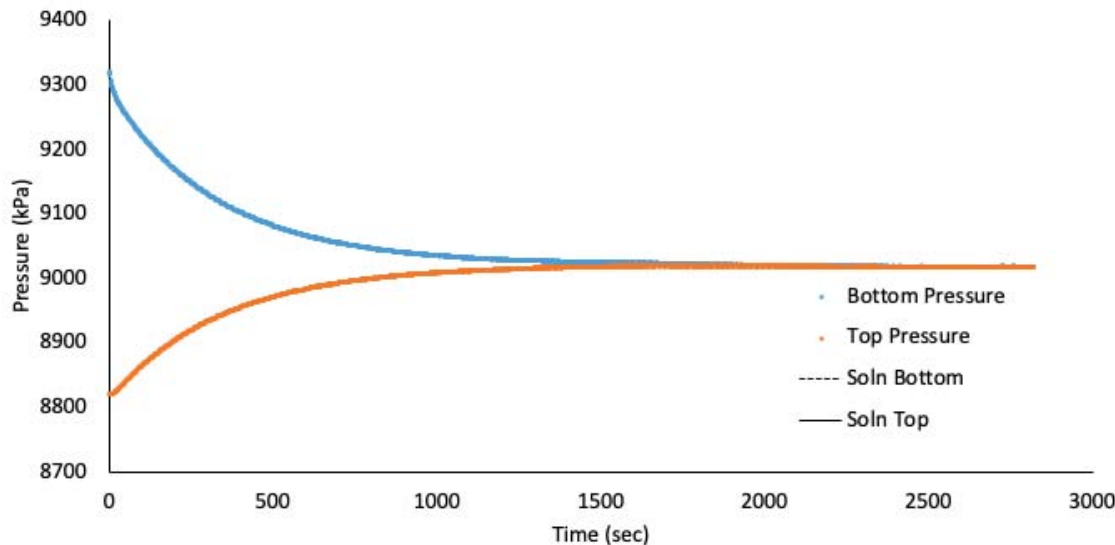


Figure 141 IG_BH06_PS002_HC25r: Effective Confining Stress = 10.67 MPa

	Sample Name		IG_BH06_PS002
	Specimen Name		IG_BH06_PS002_HC25r
	Specimen Top Depth		565.48
	Specimen Bottom Depth		565.505
	Test No		ES2
	Test Name		8865.19833458317_ES2
	Operator		Stephen Talman/ Francy Guerrero
Dimensions	Length	mm	26.410
	Diameter	mm	24.560
	Length	m	0.02641
	Diameter	m	0.02456
Test Data Location	Raw Data File Name		2023-07-19_08-48-22 System-2-CELL-3 IG-BH06-PS002-HC25r.csv
	Date & Time		2023-07-20 08:34:11
	Start Row		607
	End Row		5400
Test Conditions	Avg Cell Temp	C	39.62
	Avg Confining Pressure	kPa	24408
	Pre Pulse Avg Pore Pressure	kPa	8647
	Pulse Pressure	kPa	486
	Effective Stress	kPa	15761
	Post Pulse Avg Pore Pressure	kPa	8647
Pore Fluid & Conditions	Type		Water
	Salt	ppm	0
	Density	kg/m3	996.08
	Viscosity	kg.s/m	6.585E-04
	Compressibility	1/Pa	4.36E-10
Solution	Test System		System 2 - CELL 3
Brace	Nominal Decay Time	s	4793
	Brace Permeability	m2	2.93E-20
Hsieh	Permeability	m2	2.93E-20
	Specific Storage	1/m	8.17E-08
	Permeability	nD	29.7
	Hydraulic Conductivity	m/s	4.35E-13
	Pearson Coeff	()	0.9998890

IG_BH06_PS002_HC25r Eff Stress:15.76 MPa, HC=4.35e-13 m/s, SS=8.17e-8 1/m

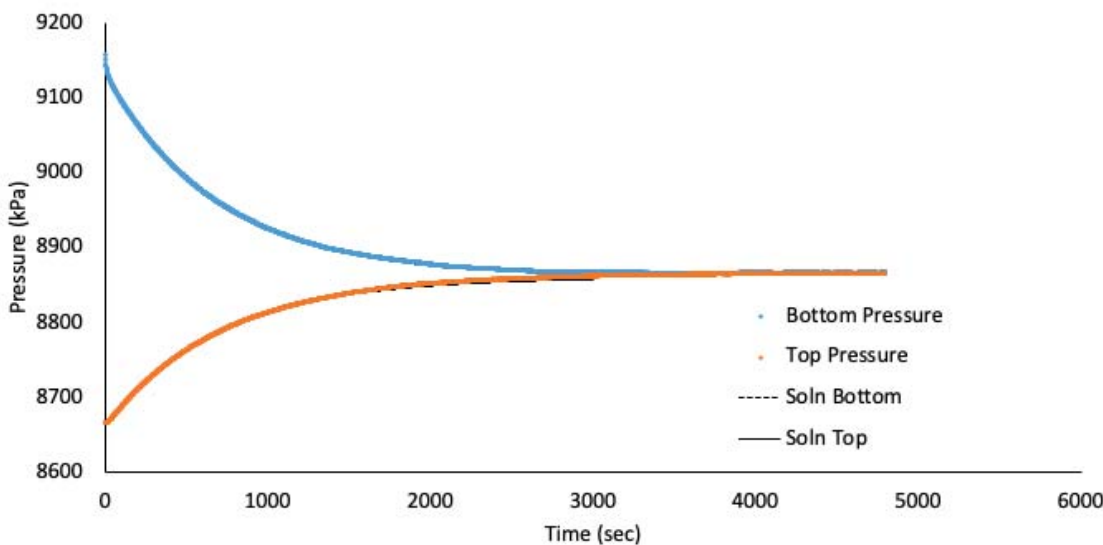


Figure 142 IG_BH06_PS002_HC25r: Effective Confining Stress = 15.76 MPa

	Sample Name		IG_BH06_PS002
	Specimen Name		IG_BH06_PS002_HC25r
	Specimen Top Depth		565.48
	Specimen Bottom Depth		565.505
	Test No		ES3
	Test Name		IG_BH06_PS002_HC25r_ES3
	Operator		Stephen Talman/ Francy Guerrero
Dimensions	Length	mm	26.410
	Diameter	mm	24.560
	Length	m	0.02641
	Diameter	m	0.02456
Test Data Location	Raw Data File Name		2023-07-19_08-48-22 System-2-CELL-3 IG-BH06-PS002-HC25r.csv
	Date & Time		2023-07-21 08:00:46
	Start Row		554
	End Row		6950
Test Conditions	Avg Cell Temp	C	39.68
	Avg Confining Pressure	kPa	29353
	Pre Pulse Avg Pore Pressure	kPa	8643
	Pulse Pressure	kPa	479
	Effective Stress	kPa	20709
	Post Pulse Avg Pore Pressure	kPa	8643
Pore Fluid & Conditions	Type		Water
	Salt	ppm	0
	Density	kg/m3	996.05
	Viscosity	kg.s/m	6.578E-04
	Compressibility	1/Pa	4.36E-10
Solution	Test System		System 2 - CELL 3
Brace	Nominal Decay Time	s	6396
	Brace Permeability	m2	1.61E-20
Hsieh	Permeability	m2	1.65E-20
	Specific Storage	1/m	7.00E-08
	Permeability	nD	16.8
	Hydraulic Conductivity	m/s	2.46E-13
	Pearson Coeff	()	0.9997375

IG_BH06_PS002_HC25r Eff Stress:20.71 MPa, HC=9.46e-14 m/s, SS=4.73e-9 1/m

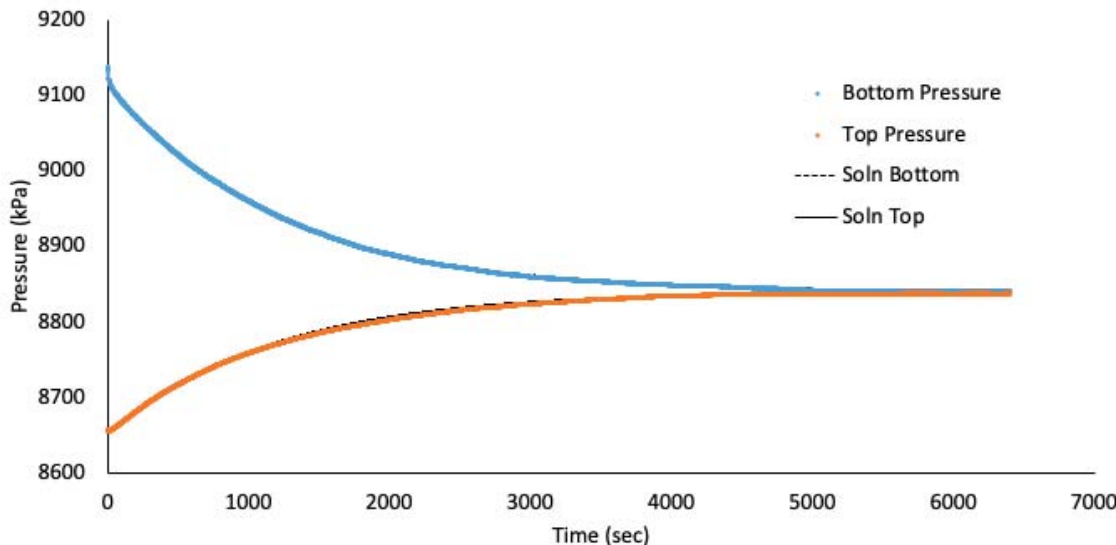


Figure 143 IG_BH06_PS002_HC25r: Effective Confining Stress = 20.71 MPa

	Sample Name		IG_BH06_PS002
	Specimen Name		IG_BH06_PS002_HC61a
	Specimen Top Depth		565.48
	Specimen Bottom Depth		565.542
	Test No		ES1
	Test Name		9009.61779537768_ES1
	Operator		Stephen Talman/ Francy Guerrero
Dimensions	Length	mm	61.860
	Diameter	mm	61.120
	Length	m	0.06186
	Diameter	m	0.06112
Test Data Location	Raw Data File Name		2023-07-19_08-48-04 System-2-CELL-2 IG-BH06-PS002-HC61a.csv
	Date & Time		2023-07-19 08:48:04
	Start Row		16006
	End Row		18950
Test Conditions	Avg Cell Temp	C	39.86
	Avg Confining Pressure	kPa	19710
	Pre Pulse Avg Pore Pressure	kPa	8828
	Pulse Pressure	kPa	502
	Effective Stress	kPa	10881
	Post Pulse Avg Pore Pressure	kPa	8828
Pore Fluid & Conditions	Type		Water
	Salt	ppm	0
	Density	kg/m3	996.07
	Viscosity	kg.s/m	6.556E-04
	Compressibility	1/Pa	4.36E-10
Solution	Test System		System 2 - CELL 2
Brace	Nominal Decay Time	s	2944
	Brace Permeability	m2	3.35E-20
Hsieh	Permeability	m2	3.52E-20
	Specific Storage	1/m	7.95E-08
	Permeability	nD	35.6
	Hydraulic Conductivity	m/s	5.24E-13
	Pearson Coeff	()	0.9994665

IG_BH06_PS002_HC61a Eff Stress:10.88 MPa, HC=5.24e-13 m/s, SS=7.95e-8 1/m

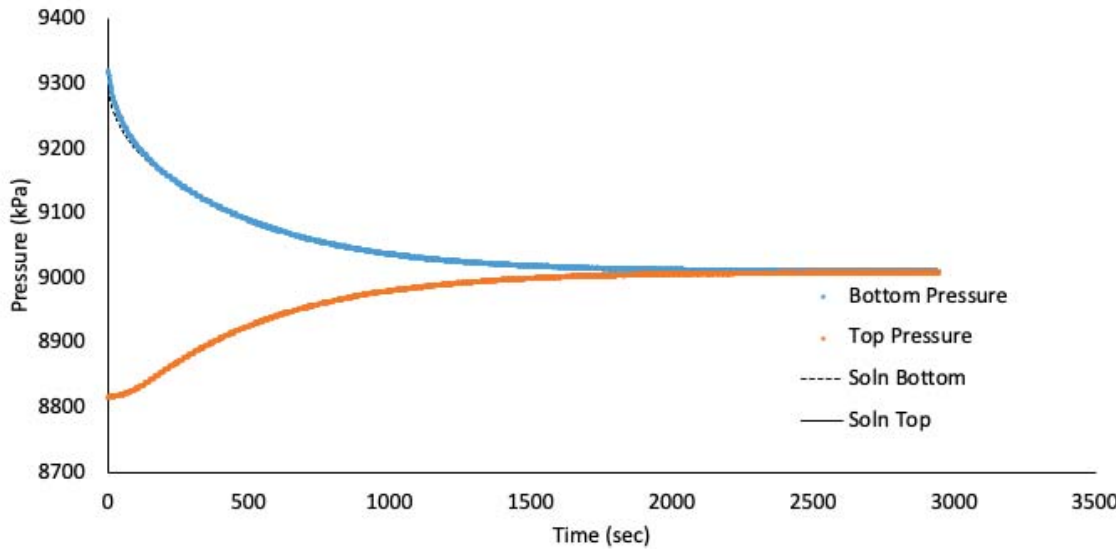


Figure 144 IG_BH06_PS002_HC61a: Effective Confining Stress = 10.88 MPa

	Sample Name		IG_BH06_PS002
	Specimen Name		IG_BH06_PS002_HC61a
	Specimen Top Depth		565.48
	Specimen Bottom Depth		565.542
	Test No		ES2
	Test Name		8831.79235612514_ES2
	Operator		Stephen Talman/ Francy Guerrero
Dimensions	Length	mm	61.860
	Diameter	mm	61.120
	Length	m	0.06186
	Diameter	m	0.06112
Test Data Location	Raw Data File Name		2023-07-19_08-48-04 System-2-CELL-2 IG-BH06-PS002-HC61a.csv
	Date & Time		2023-07-20 08:33:49
	Start Row		635
	End Row		5500
Test Conditions	Avg Cell Temp	C	39.83
	Avg Confining Pressure	kPa	24712
	Pre Pulse Avg Pore Pressure	kPa	8682
	Pulse Pressure	kPa	488
	Effective Stress	kPa	16030
	Post Pulse Avg Pore Pressure	kPa	8682
Pore Fluid & Conditions	Type		Water
	Salt	ppm	0
	Density	kg/m3	996.01
	Viscosity	kg.s/m	6.559E-04
	Compressibility	1/Pa	4.36E-10
Solution	Test System		System 2 - CELL 2
Brace	Nominal Decay Time	s	4865
	Brace Permeability	m2	9.26E-21
Hsieh	Permeability	m2	9.45E-21
	Specific Storage	1/m	2.90E-08
	Permeability	nD	9.6
	Hydraulic Conductivity	m/s	1.41E-13
	Pearson Coeff	()	0.9997966

IG_BH06_PS002_HC61a Eff Stress:16.03 MPa, HC=1.41e-13 m/s, SS=2.90e-8 1/m

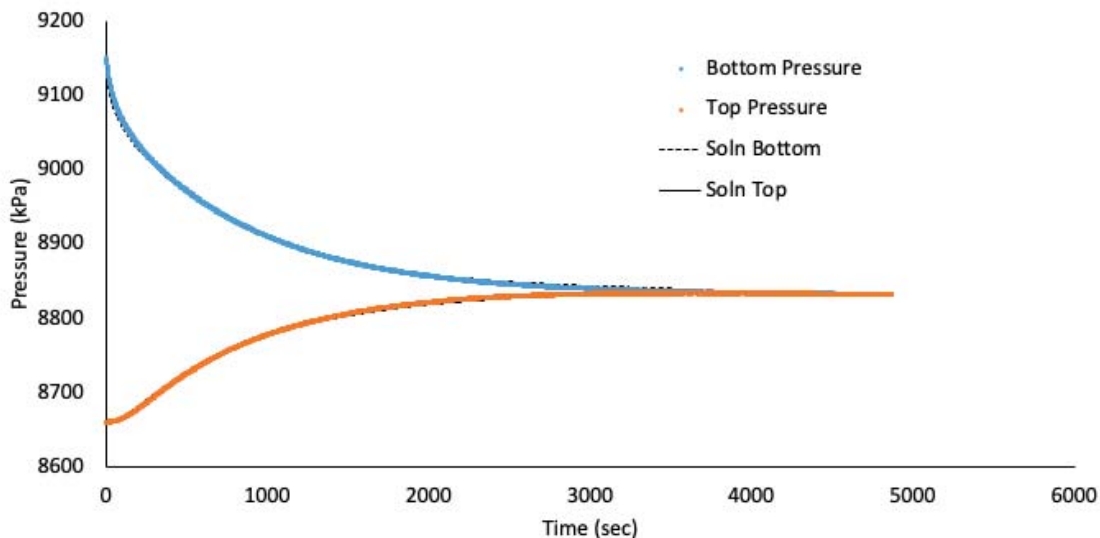


Figure 145 IG_BH06_PS002_HC61a: Effective Confining Stress = 16.03 MPa

	Sample Name		IG_BH06_PS002
	Specimen Name		IG_BH06_PS002_HC61a
	Specimen Top Depth		565.48
	Specimen Bottom Depth		565.542
	Test No		ES3
	Test Name		8832.63694192457_ES3
	Operator		Stephen Talman/ Francy Guerrero
Dimensions	Length	mm	61.860
	Diameter	mm	61.120
	Length	m	0.06186
	Diameter	m	0.06112
Test Data Location	Raw Data File Name		2023-07-21_08-00-30 System-2-CELL-2 IG-BH06-PS002-HC61a.csv
	Date & Time		2023-07-21 08:00:30
	Start Row		577
	End Row		7010
Test Conditions	Avg Cell Temp	C	39.87
	Avg Confining Pressure	kPa	29715
	Pre Pulse Avg Pore Pressure	kPa	8669
	Pulse Pressure	kPa	501
	Effective Stress	kPa	21046
	Post Pulse Avg Pore Pressure	kPa	8669
Pore Fluid & Conditions	Type		Water
	Salt	ppm	0
	Density	kg/m3	995.99
	Viscosity	kg.s/m	6.554E-04
	Compressibility	1/Pa	4.36E-10
Solution	Test System		System 2 - CELL 2
Brace	Nominal Decay Time	s	6433
	Brace Permeability	m2	1.22E-20
Hsieh	Permeability	m2	1.30E-20
	Specific Storage	1/m	4.75E-08
	Permeability	nD	13.2
	Hydraulic Conductivity	m/s	1.94E-13
	Pearson Coeff	()	0.9995930

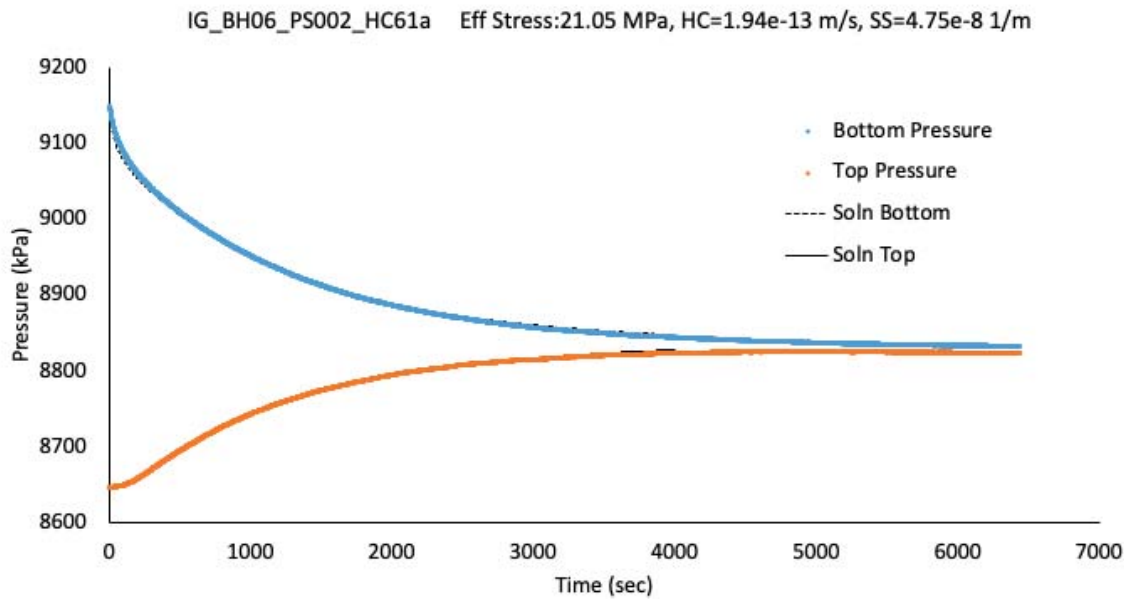


Figure 146 IG_BH06_PS002_HC61a: Effective Confining Stress = 21.05 MPa

	Sample Name		IG_BH06_PS003
	Specimen Name		IG_BH06_PS003_HC25a
	Specimen Top Depth		668.95
	Specimen Bottom Depth		668.990
	Test No		ES1
	Test Name		IG_BH06_PS003_HC25a_ES1
	Operator		Stephen Talman/ Francy Guerrero
Dimensions	Length	mm	25.010
	Diameter	mm	25.270
	Length	m	0.02501
	Diameter	m	0.02527
Test Data Location	Raw Data File Name		2023-08-03_07-43-13 System-2-CELL-1 IG-BH06-PS003-HC25a.csv
	Date & Time		2023-08-03 07:43:13
	Start Row		9418
	End Row		10220
Test Conditions	Avg Cell Temp	C	39.84
	Avg Confining Pressure	kPa	21575
	Pre Pulse Avg Pore Pressure	kPa	9118
	Pulse Pressure	kPa	478
	Effective Stress	kPa	12457
	Post Pulse Avg Pore Pressure	kPa	9118
Pore Fluid & Conditions	Type		Water
	Salt	ppm	0
	Density	kg/m3	996.19
	Viscosity	kg.s/m	6.559E-04
	Compressibility	1/Pa	4.36E-10
Solution	Test System		System 2 - CELL 1
Brace	Nominal Decay Time	s	802
	Brace Permeability	m2	8.42E-20
Hsieh	Permeability	m2	8.84E-20
	Specific Storage	1/m	6.57E-08
	Permeability	nD	89.6
	Hydraulic Conductivity	m/s	1.32E-12
	Pearson Coeff	()	0.9993868

IG_BH06_PS003_HC25a Eff Stress:12.46 MPa, HC=1.32e-12 m/s, SS=6.57e-8 1/m

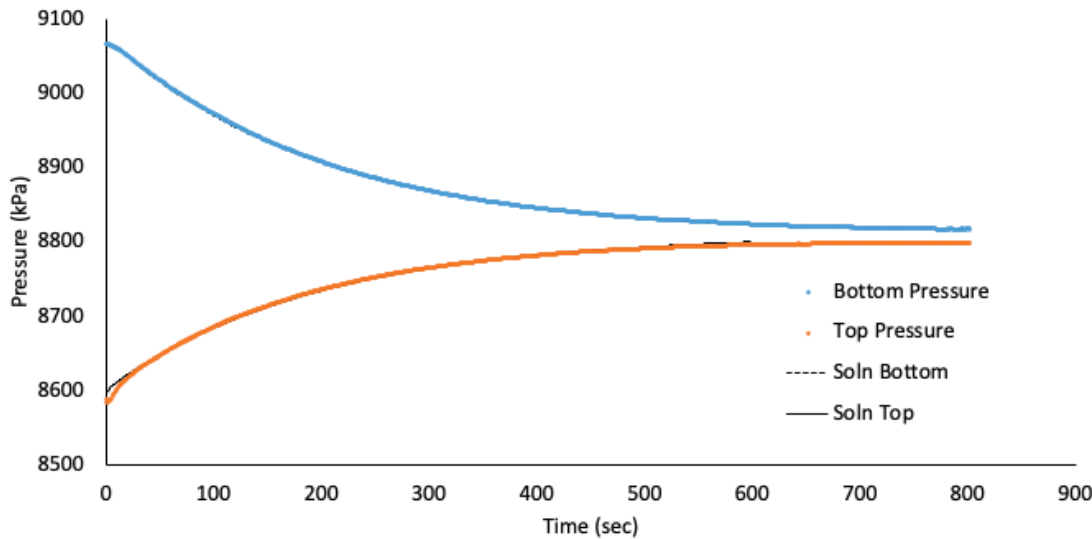


Figure 147 IG_BH06_PS003_HC25a: Effective Confining Stress = 12.46 MPa

	Sample Name		IG_BH06_PS003
	Specimen Name		IG_BH06_PS003_HC25a
	Specimen Top Depth		668.95
	Specimen Bottom Depth		668.990
	Test No		ES2
	Test Name		IG_BH06_PS003_HC25a_ES2
	Operator		Stephen Talman/ Francy Guerrero
Dimensions	Length	mm	25.010
	Diameter	mm	25.270
	Length	m	0.02501
	Diameter	m	0.02527
Test Data Location	Raw Data File Name		2023-08-03_07-43-13 System-2-CELL-1 IG-BH06-PS003-HC25a.csv
	Date & Time		2023-08-04 09:23:38
	Start Row		347
	End Row		3200
Test Conditions	Avg Cell Temp	C	39.85
	Avg Confining Pressure	kPa	26551
	Pre Pulse Avg Pore Pressure	kPa	8912
	Pulse Pressure	kPa	455
	Effective Stress	kPa	17639
	Post Pulse Avg Pore Pressure	kPa	8912
Pore Fluid & Conditions	Type		Water
	Salt	ppm	0
	Density	kg/m3	996.1
	Viscosity	kg.s/m	6.557E-04
	Compressibility	1/Pa	4.36E-10
Solution	Test System		System 2 - CELL 1
Brace	Nominal Decay Time	s	2853
	Brace Permeability	m2	3.71E-20
Hsieh	Permeability	m2	3.89E-20
	Specific Storage	1/m	1.79E-08
	Permeability	nD	39.4
	Hydraulic Conductivity	m/s	5.80E-13
	Pearson Coeff	()	0.9995840

IG_BH06_PS003_HC25a Eff Stress:17.64 MPa, HC=5.80e-13 m/s, SS=1.79e-8 1/m

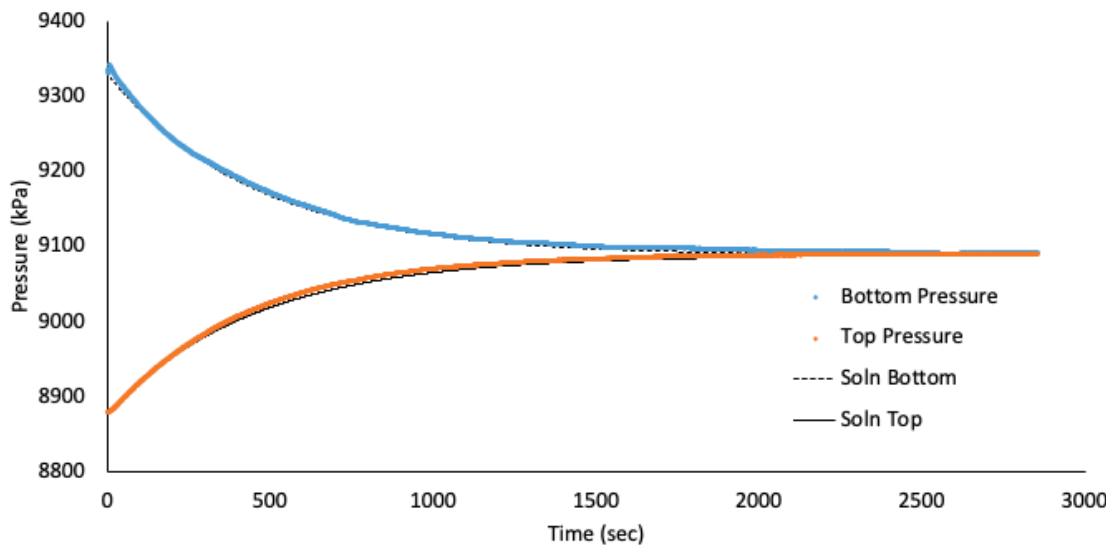


Figure 148 IG_BH06_PS003_HC25a: Effective Confining Stress = 17.64 MPa

	Sample Name		IG_BH06_PS003
	Specimen Name		IG_BH06_PS003_HC25a
	Specimen Top Depth		668.95
	Specimen Bottom Depth		668.990
	Test No		ES3
	Test Name		IG_BH06_PS003_HC25a_ES3
	Operator		Stephen Talman/ Francy Guerrero
Dimensions	Length	mm	25.010
	Diameter	mm	25.270
	Length	m	0.02501
	Diameter	m	0.02527
Test Data Location	Raw Data File Name		2023-08-03_07-43-13 System-2-CELL-1 IG-BH06-PS003-HC25a.csv
	Date & Time		2023-08-04 14:31:31
	Start Row		1942
	End Row		7500
Test Conditions	Avg Cell Temp	C	39.91
	Avg Confining Pressure	kPa	31527
	Pre Pulse Avg Pore Pressure	kPa	9297
	Pulse Pressure	kPa	-531
	Effective Stress	kPa	22231
	Post Pulse Avg Pore Pressure	kPa	9297
Pore Fluid & Conditions	Type		Water
	Salt	ppm	0
	Density	kg/m3	996.25
	Viscosity	kg.s/m	6.550E-04
	Compressibility	1/Pa	4.36E-10
Solution	Test System		System 2 - CELL 1
Brace	Nominal Decay Time	s	5558
	Brace Permeability	m2	2.52E-20
Hsieh	Permeability	m2	2.65E-20
	Specific Storage	1/m	1.19E-07
	Permeability	nD	26.8
	Hydraulic Conductivity	m/s	3.95E-13
	Pearson Coeff	()	0.9984687

IG_BH06_PS003_HC25a Eff Stress:22.23 MPa, HC=3.95e-13 m/s, SS=1.19e-7 1/m

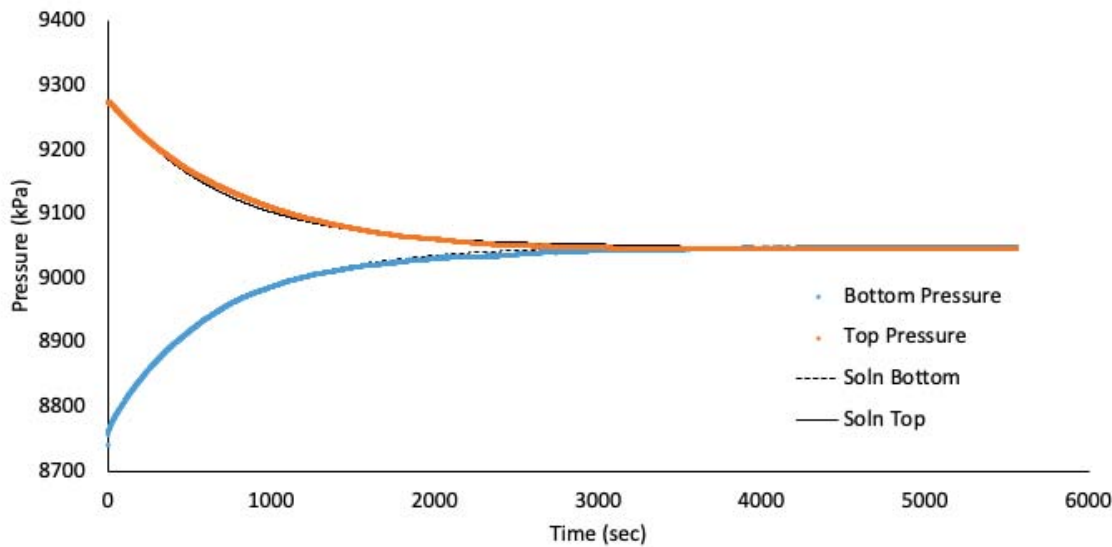


Figure 149 IG_BH06_PS003_HC25a: Effective Confining Stress = 22.23 MPa

	Sample Name		IG_BH06_PS003
	Specimen Name		IG_BH06_PS003_HC25r
	Specimen Top Depth		668.955
	Specimen Bottom Depth		668.990
	Test No		ES1
	Test Name		IG_BH06_PS003_HC25r_ES1
	Operator		Stephen Talman/ Francy Guerrero
Dimensions	Length	mm	24.360
	Diameter	mm	24.630
	Length	m	0.02436
	Diameter	m	0.02463
Test Data Location	Raw Data File Name		2023-08-03_07-43-49 System-2-CELL-3 IG-BH06-PS003-HC25r.csv
	Date & Time		2023-08-03 07:43:49
	Start Row		1734
	End Row		4000
Test Conditions	Avg Cell Temp	C	39.60
	Avg Confining Pressure	kPa	21407
	Pre Pulse Avg Pore Pressure	kPa	9061
	Pulse Pressure	kPa	-499
	Effective Stress	kPa	12346
	Post Pulse Avg Pore Pressure	kPa	9061
Pore Fluid & Conditions	Type		Water
	Salt	ppm	0
	Density	kg/m3	996.26
	Viscosity	kg.s/m	6.588E-04
	Compressibility	1/Pa	4.36E-10
Solution	Test System		System 2 - CELL 3
Brace	Nominal Decay Time	s	2266
	Brace Permeability	m2	7.17E-20
Hsieh	Permeability	m2	7.39E-20
	Specific Storage	1/m	7.54E-08
	Permeability	nD	74.8
	Hydraulic Conductivity	m/s	1.10E-12
	Pearson Coeff	()	0.9998298

IG_BH06_PS003_HC25r Eff Stress:12.35 MPa, HC=1.10e-12 m/s, SS=7.54e-8 1/m

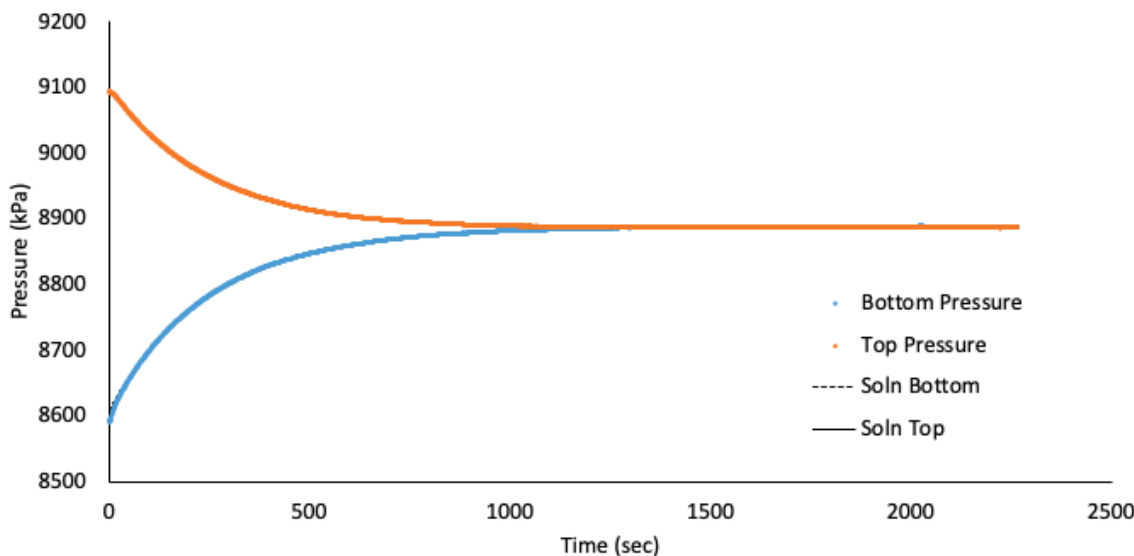


Figure 150 IG_BH06_PS003_HC25r: Effective Confining Stress = 12.35 MPa

	Sample Name		IG_BH06_PS003
	Specimen Name		IG_BH06_PS003_HC25r
	Specimen Top Depth		668.955
	Specimen Bottom Depth		668.990
	Test No		ES2
	Test Name		9087.35323727601_ES2
	Operator		Stephen Talman/ Francy Guerrero
Dimensions	Length	mm	24.360
	Diameter	mm	24.630
	Length	m	0.02436
	Diameter	m	0.02463
Test Data Location	Raw Data File Name		2023-08-03_07-43-49 System-2-CELL-3 IG-BH06-PS003-HC25r.csv
	Date & Time		2023-08-04 09:22:24
	Start Row		410
	End Row		5000
Test Conditions	Avg Cell Temp	C	39.67
	Avg Confining Pressure	kPa	26350
	Pre Pulse Avg Pore Pressure	kPa	8852
	Pulse Pressure	kPa	496
	Effective Stress	kPa	17499
	Post Pulse Avg Pore Pressure	kPa	8852
Pore Fluid & Conditions	Type		Water
	Salt	ppm	0
	Density	kg/m3	996.15
	Viscosity	kg.s/m	6.579E-04
	Compressibility	1/Pa	4.36E-10
Solution	Test System		System 2 - CELL 3
Brace	Nominal Decay Time	s	4590
	Brace Permeability	m2	3.47E-20
Hsieh	Permeability	m2	3.71E-20
	Specific Storage	1/m	8.06E-08
	Permeability	nD	37.6
	Hydraulic Conductivity	m/s	5.51E-13
	Pearson Coeff	()	0.9998959

IG_BH06_PS003_HC25r Eff Stress:17.5 MPa, HC=5.51e-13 m/s, SS=8.06e-8 1/m

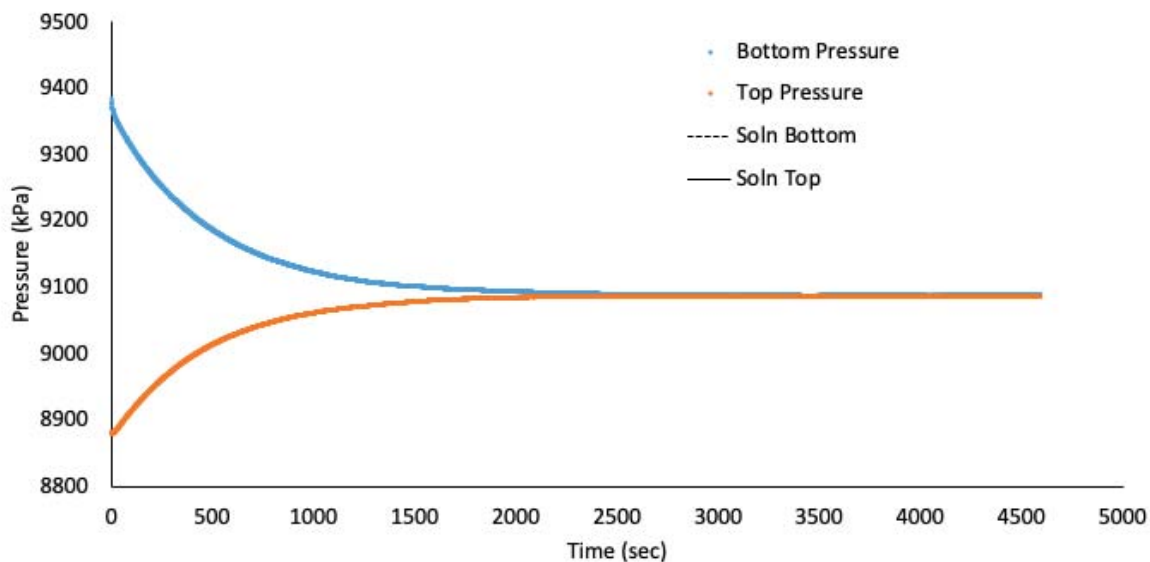


Figure 151 IG_BH06_PS003_HC25r: Effective Confining Stress = 17.5 MPa

	Sample Name		IG_BH06_PS003
	Specimen Name		IG_BH06_PS003_HC25r
	Specimen Top Depth		668.955
	Specimen Bottom Depth		668.990
	Test No		ES3
	Test Name		8986.87516517146_ES3
	Operator		Stephen Talman/ Francy Guerrero
Dimensions	Length	mm	24.360
	Diameter	mm	24.630
	Length	m	0.02436
	Diameter	m	0.02463
Test Data Location	Raw Data File Name		2023-08-03_07-43-49 System-2-CELL-3 IG-BH06-PS003-HC25r.csv
	Date & Time		2023-08-04 14:32:15
	Start Row		13723
	End Row		22000
Test Conditions	Avg Cell Temp	C	39.71
	Avg Confining Pressure	kPa	31297
	Pre Pulse Avg Pore Pressure	kPa	9297
	Pulse Pressure	kPa	590
	Effective Stress	kPa	21999
	Post Pulse Avg Pore Pressure	kPa	9297
Pore Fluid & Conditions	Type		Water
	Salt	ppm	0
	Density	kg/m3	996.32
	Viscosity	kg.s/m	6.575E-04
	Compressibility	1/Pa	4.36E-10
Solution	Test System		System 2 - CELL 3
Brace	Nominal Decay Time	s	8277
	Brace Permeability	m2	2.33E-20
Hsieh	Permeability	m2	2.44E-20
	Specific Storage	1/m	1.18E-07
	Permeability	nD	24.7
	Hydraulic Conductivity	m/s	3.63E-13
	Pearson Coeff	()	0.9891492

IG_BH06_PS003_HC25r Eff Stress:22 MPa, HC=3.63e-13 m/s, SS=1.18e-7 1/m

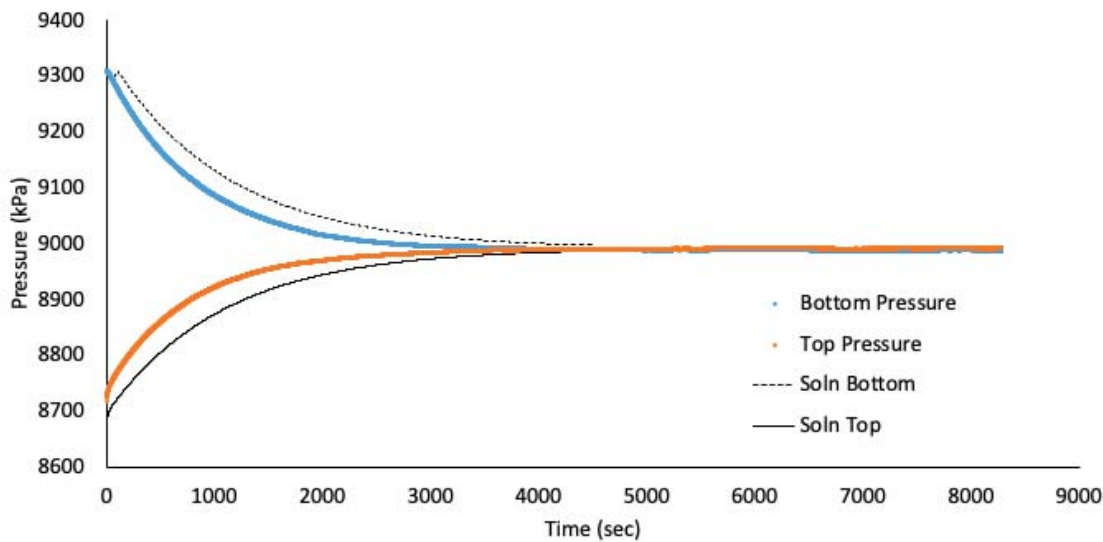


Figure 152 IG_BH06_PS003_HC25r: Effective Confining Stress = 22.0 MPa

	Sample Name		IG_BH06_PS003
	Specimen Name		IG_BH06_PS003_HC61a
	Specimen Top Depth		668.99
	Specimen Bottom Depth		669.052
	Test No		ES1
	Test Name		8927.81395427501_ES1
	Operator		Stephen Talman/ Francy Guerrero
Dimensions	Length	mm	62.150
	Diameter	mm	61.040
	Length	m	0.06215
	Diameter	m	0.06104
Test Data Location	Raw Data File Name		2023-08-03_07-43-32 System-2-CELL-2 IG-BH06-PS003-HC61a.csv
	Date & Time		2023-08-03 07:43:32
	Start Row		1760
	End Row		4300
Test Conditions	Avg Cell Temp	C	39.81
	Avg Confining Pressure	kPa	21677
	Pre Pulse Avg Pore Pressure	kPa	9098
	Pulse Pressure	kPa	-496
	Effective Stress	kPa	12579
	Post Pulse Avg Pore Pressure	kPa	9098
Pore Fluid & Conditions	Type		Water
	Salt	ppm	0
	Density	kg/m3	996.2
	Viscosity	kg.s/m	6.562E-04
	Compressibility	1/Pa	4.36E-10
Solution	Test System		System 2 - CELL 2
Brace	Nominal Decay Time	s	2540
	Brace Permeability	m2	5.37E-20
Hsieh	Permeability	m2	6.45E-20
	Specific Storage	1/m	9.27E-08
	Permeability	nD	65.4
	Hydraulic Conductivity	m/s	9.61E-13
	Pearson Coeff	()	0.9993009

IG_BH06_PS003_HC61a Eff Stress:12.58 MPa, HC=9.61e-13 m/s, SS=9.27e-8 1/m

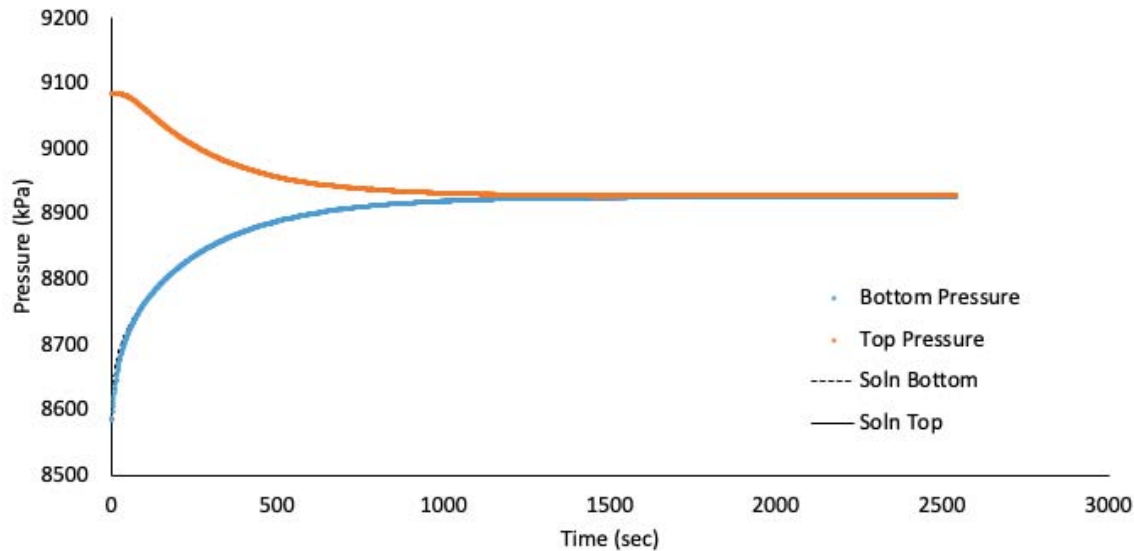


Figure 153 IG_BH06_PS003_HC61a: Effective Confining Stress = 12.58 MPa

	Sample Name		IG_BH06_PS003
	Specimen Name		IG_BH06_PS003_HC61a
	Specimen Top Depth		668.99
	Specimen Bottom Depth		669.052
	Test No		ES2
	Test Name		9053.81036373531_ES2
	Operator		Stephen Talman/ Francy Guerrero
Dimensions	Length	mm	62.150
	Diameter	mm	61.040
	Length	m	0.06215
	Diameter	m	0.06104
Test Data Location	Raw Data File Name		2023-08-03_07-43-32 System-2-CELL-2 IG-BH06-PS003-HC61a.csv
	Date & Time		2023-08-04 09:23:02
	Start Row		378
	End Row		5000
Test Conditions	Avg Cell Temp	C	39.86
	Avg Confining Pressure	kPa	26678
	Pre Pulse Avg Pore Pressure	kPa	8889
	Pulse Pressure	kPa	510
	Effective Stress	kPa	17789
	Post Pulse Avg Pore Pressure	kPa	8889
Pore Fluid & Conditions	Type		Water
	Salt	ppm	0
	Density	kg/m3	996.09
	Viscosity	kg.s/m	6.556E-04
	Compressibility	1/Pa	4.36E-10
Solution	Test System		System 2 - CELL 2
Brace	Nominal Decay Time	s	4622
	Brace Permeability	m2	3.37E-20
Hsieh	Permeability	m2	3.71E-20
	Specific Storage	1/m	7.08E-08
	Permeability	nD	37.6
	Hydraulic Conductivity	m/s	5.53E-13
	Pearson Coeff	()	0.9998061

IG_BH06_PS003_HC61a Eff Stress:17.79 MPa, HC=5.53e-13 m/s, SS=7.08e-8 1/m

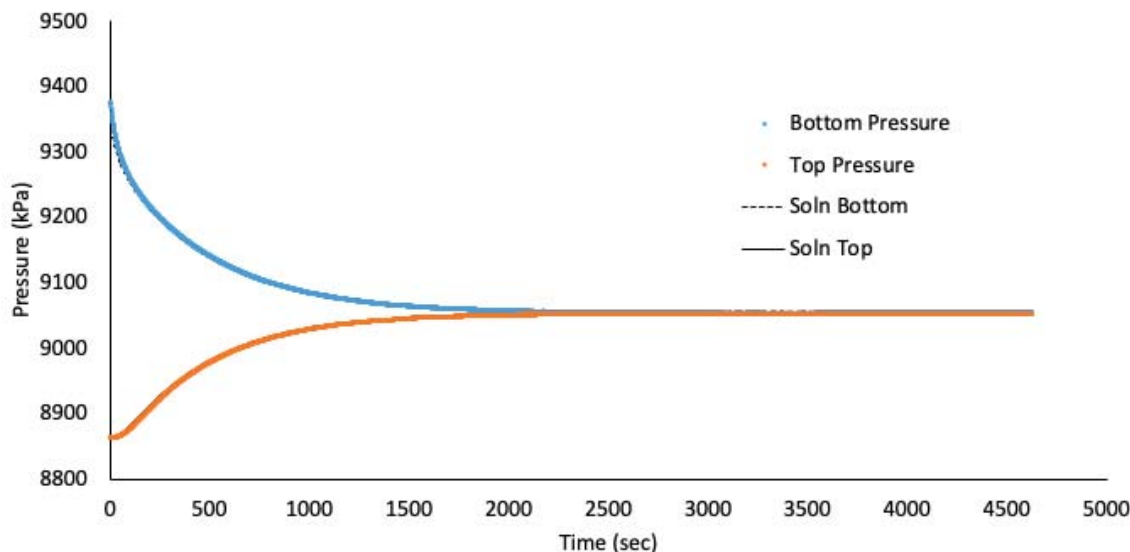


Figure 154 IG_BH06_PS003_HC61a: Effective Confining Stress = 17.79 MPa

	Sample Name		IG_BH06_PS003
	Specimen Name		IG_BH06_PS003_HC61a
	Specimen Top Depth		668.99
	Specimen Bottom Depth		669.052
	Test No		ES3
	Test Name		9079.86228469847_ES3
	Operator		Stephen Talman/ Francy Guerrero
Dimensions	Length	mm	62.150
	Diameter	mm	61.040
	Length	m	0.06215
	Diameter	m	0.06104
Test Data Location	Raw Data File Name		2023-08-03_07-43-32 System-2-CELL-2 IG-BH06-PS003-HC61a.csv
	Date & Time		2023-08-04 14:31:52
	Start Row		663
	End Row		6300
Test Conditions	Avg Cell Temp	C	39.89
	Avg Confining Pressure	kPa	31678
	Pre Pulse Avg Pore Pressure	kPa	9279
	Pulse Pressure	kPa	-503
	Effective Stress	kPa	22399
Pore Fluid & Conditions	Post Pulse Avg Pore Pressure	kPa	9279
	Type		Water
	Salt	ppm	0
	Density	kg/m3	996.25
	Viscosity	kg.s/m	6.553E-04
Solution	Compressibility	1/Pa	4.36E-10
	Test System		System 2 - CELL 2
Brace	Nominal Decay Time	s	5637
	Brace Permeability	m2	2.15E-20
Hsieh	Permeability	m2	2.58E-20
	Specific Storage	1/m	7.15E-08
	Permeability	nD	26.1
	Hydraulic Conductivity	m/s	3.84E-13
	Pearson Coeff	()	0.9997833

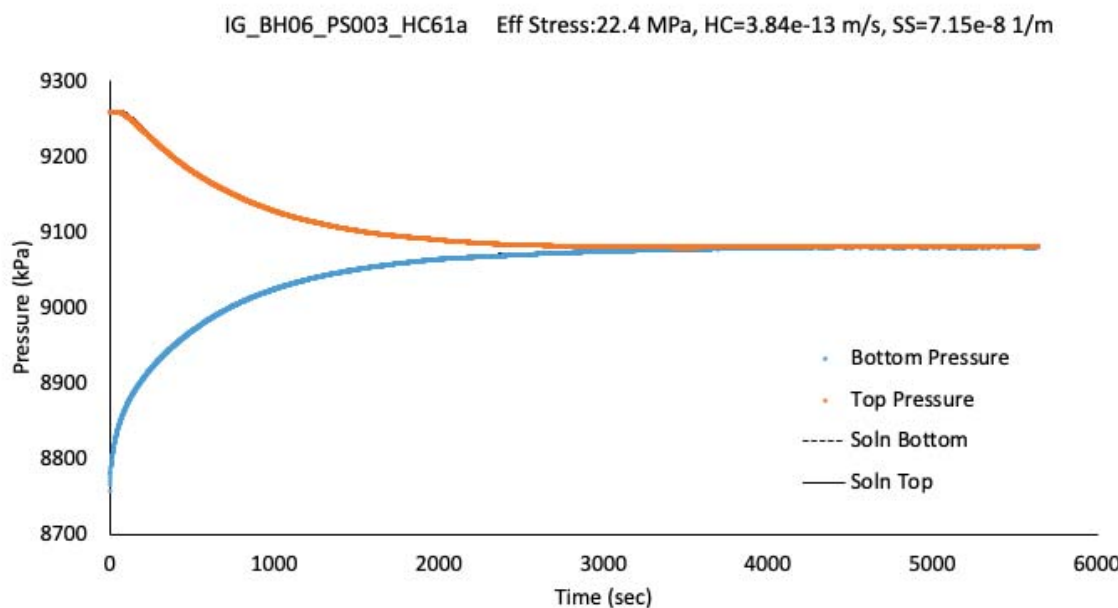


Figure 155 IG_BH06_PS003_HC61a: Effective Confining Stress = 22.40 MPa

	Sample Name		IG_BH06_PS004
	Specimen Name		IG_BH06_PS004_HC25a
	Specimen Top Depth		731.83
	Specimen Bottom Depth		731.870
	Test No		ES1
	Test Name		IG_BH06_PS004_HC25a_ES1
	Operator		0
Dimensions	Length	mm	25.800
	Diameter	mm	25.030
	Length	m	0.0258
	Diameter	m	0.02503
Test Data Location	Raw Data File Name		2023-08-03_08-40-08 System-3-Cell-3 IG-BH06-PS004-HC25a.csv
	Date & Time		2023-08-03 08:40:08
	Start Row		12325
	End Row		18305
Test Conditions	Avg Cell Temp	C	39.82
	Avg Confining Pressure	kPa	22897
	Pre Pulse Avg Pore Pressure	kPa	9572
	Pulse Pressure	kPa	504
	Effective Stress	kPa	13325
	Post Pulse Avg Pore Pressure	kPa	9572
Pore Fluid & Conditions	Type		Water
	Salt	ppm	0
	Density	kg/m3	996.4
	Viscosity	kg.s/m	6.562E-04
	Compressibility	1/Pa	4.36E-10
Solution	Test System		System 3 - Cell 3
Brace	Nominal Decay Time	s	5980
	Brace Permeability	m2	1.14E-20
Hsieh	Permeability	m2	1.16E-20
	Specific Storage	1/m	3.24E-08
	Permeability	nD	11.8
	Hydraulic Conductivity	m/s	1.73E-13
	Pearson Coeff	()	0.9995407

IG_BH06_PS004_HC25a Eff Stress:13.33 MPa, HC=1.73e-13 m/s, SS=3.24e-8 1/m

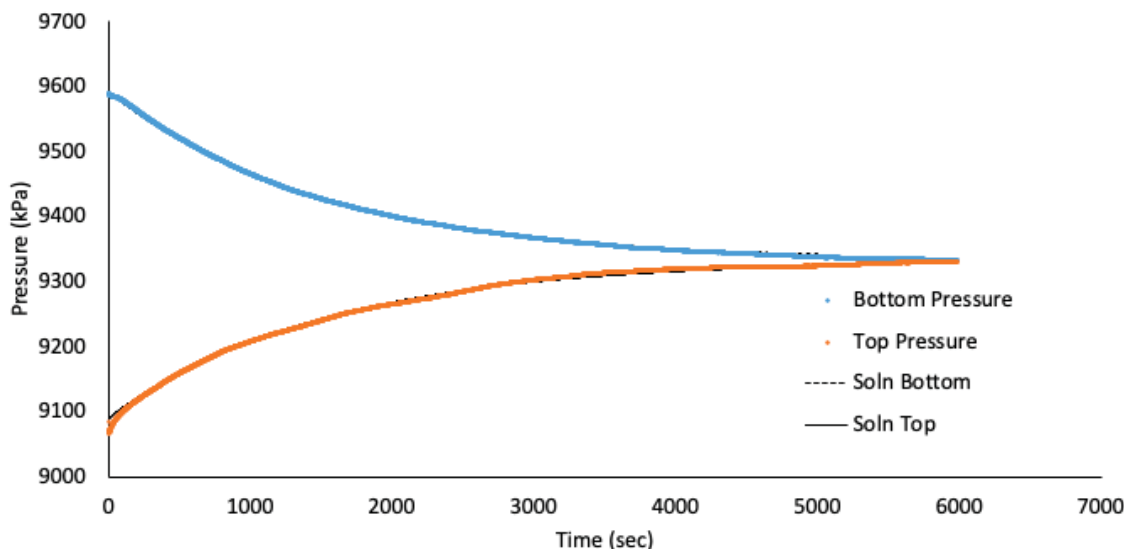


Figure 156 IG_BH06_PS004_HC25a: Effective Confining Stress = 13.33 MPa

	Sample Name		IG_BH06_PS004
	Specimen Name		IG_BH06_PS004_HC25a
	Specimen Top Depth		731.83
	Specimen Bottom Depth		731.870
	Test No		ES2
	Test Name		IG_BH06_PS004_HC25a_ES2
	Operator		0
Dimensions	Length	mm	25.800
	Diameter	mm	25.030
	Length	m	0.0258
	Diameter	m	0.02503
Test Data Location	Raw Data File Name		2023-08-03_08-40-08 System-3-Cell-3 IG-BH06-PS004-HC25a.csv
	Date & Time		2023-08-04 08:56:32
	Start Row		12289
	End Row		19530
Test Conditions	Avg Cell Temp	C	39.84
	Avg Confining Pressure	kPa	27886
	Pre Pulse Avg Pore Pressure	kPa	9456
	Pulse Pressure	kPa	529
	Effective Stress	kPa	18430
	Post Pulse Avg Pore Pressure	kPa	9456
Pore Fluid & Conditions	Type		Water
	Salt	ppm	0
	Density	kg/m3	996.34
	Viscosity	kg.s/m	6.557E-04
	Compressibility	1/Pa	4.36E-10
Solution	Test System		System 3 - Cell 3
Brace	Nominal Decay Time	s	7241
	Brace Permeability	m2	4.23E-21
Hsieh	Permeability	m2	4.66E-21
	Specific Storage	1/m	7.05E-09
	Permeability	nD	4.7
	Hydraulic Conductivity	m/s	6.94E-14
	Pearson Coeff	()	0.9994131

IG_BH06_PS004_HC25a Eff Stress:18.43 MPa, HC=6.94e-14 m/s, SS=7.05e-9 1/m

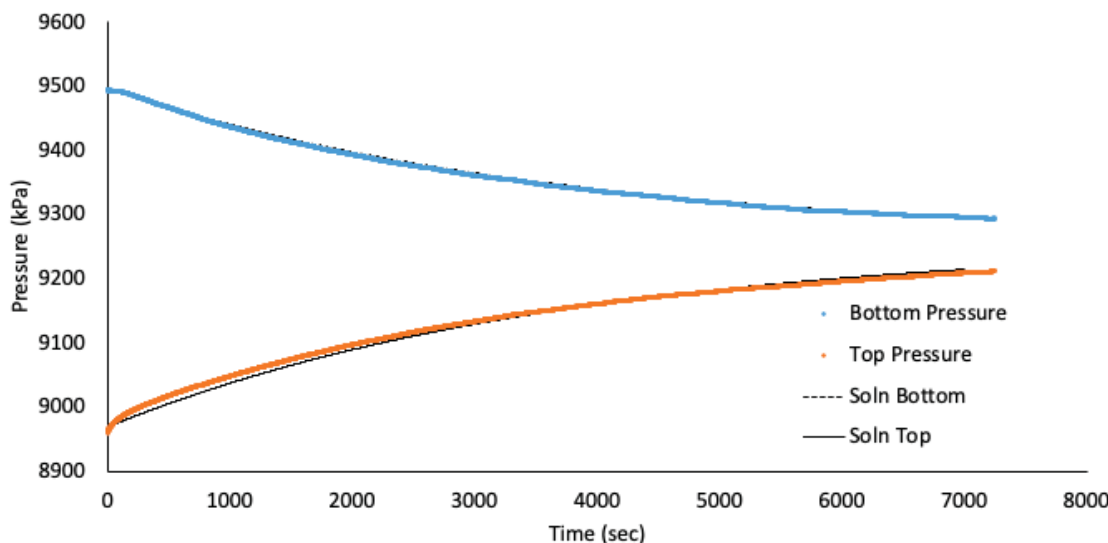


Figure 157 IG_BH06_PS004_HC25a: Effective Confining Stress = 18.43 MPa

	Sample Name		IG_BH06_PS004
	Specimen Name		IG_BH06_PS004_HC25a
	Specimen Top Depth		731.83
	Specimen Bottom Depth		731.870
	Test No		ES3
	Test Name		IG_BH06_PS004_HC25a_ES3
	Operator		0
Dimensions	Length	mm	25.800
	Diameter	mm	25.030
	Length	m	0.0258
	Diameter	m	0.02503
Test Data Location	Raw Data File Name		2023-08-03_08-40-08 System-3-Cell-3 IG-BH06-PS004-HC25a.csv
	Date & Time		2023-08-04 14:25:38
	Start Row		3184
	End Row		37500
Test Conditions	Avg Cell Temp	C	39.87
	Avg Confining Pressure	kPa	32869
	Pre Pulse Avg Pore Pressure	kPa	9359
	Pulse Pressure	kPa	-590
	Effective Stress	kPa	23510
Pore Fluid & Conditions	Post Pulse Avg Pore Pressure	kPa	9359
	Type		Water
	Salt	ppm	0
	Density	kg/m3	996.29
	Viscosity	kg.s/m	6.555E-04
Solution	Compressibility	1/Pa	4.36E-10
	Test System		System 3 - Cell 3
Brace	Nominal Decay Time	s	34316
	Brace Permeability	m2	2.60E-21
Hsieh	Permeability	m2	2.60E-21
	Specific Storage	1/m	1.04E-07
	Permeability	nD	2.6
	Hydraulic Conductivity	m/s	3.88E-14
	Pearson Coeff	()	0.9982782

IG_BH06_PS004_HC25a Eff Stress:23.51 MPa, HC=3.88e-14 m/s, SS=1.04e-7 1/m

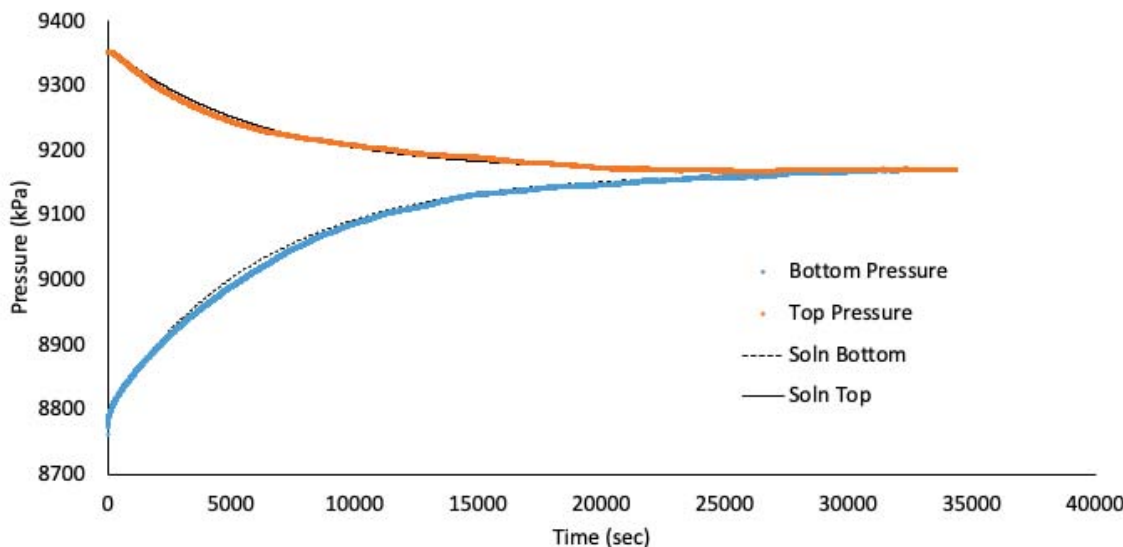


Figure 158 IG_BH06_PS004_HC25a: Effective Confining Stress = 23.51 MPa

	Sample Name		IG_BH06_PS004
	Specimen Name		IG_BH06_PS004_HC25r
	Specimen Top Depth		731.835
	Specimen Bottom Depth		731.870
	Test No		ES1
	Test Name		9370.1111784_ES1
	Operator		0
Dimensions	Length	mm	25.170
	Diameter	mm	24.580
	Length	m	0.02517
	Diameter	m	0.02458
Test Data Location	Raw Data File Name		2023-08-03_08-42-04 System-3-Cell-1 IG-BH06-PS004-HC25r.csv
	Date & Time		2023-08-03 08:42:04
	Start Row		1938
	End Row		6480
Test Conditions	Avg Cell Temp	C	40.36
	Avg Confining Pressure	kPa	22947
	Pre Pulse Avg Pore Pressure	kPa	9595
	Pulse Pressure	kPa	-494
	Effective Stress	kPa	13351
	Post Pulse Avg Pore Pressure	kPa	9595
Pore Fluid & Conditions	Type		Water
	Salt	ppm	0
	Density	kg/m3	996.2
	Viscosity	kg.s/m	6.496E-04
	Compressibility	1/Pa	4.36E-10
Solution	Test System		System 3 - Cell 1
Brace	Nominal Decay Time	s	4542
	Brace Permeability	m2	1.43E-20
Hsieh	Permeability	m2	1.43E-20
	Specific Storage	1/m	1.52E-07
	Permeability	nD	14.5
	Hydraulic Conductivity	m/s	2.15E-13
	Pearson Coeff	()	0.9997893

IG_BH06_PS004_HC25r Eff Stress:13.35 MPa, HC=2.15e-13 m/s, SS=1.52e-7 1/m

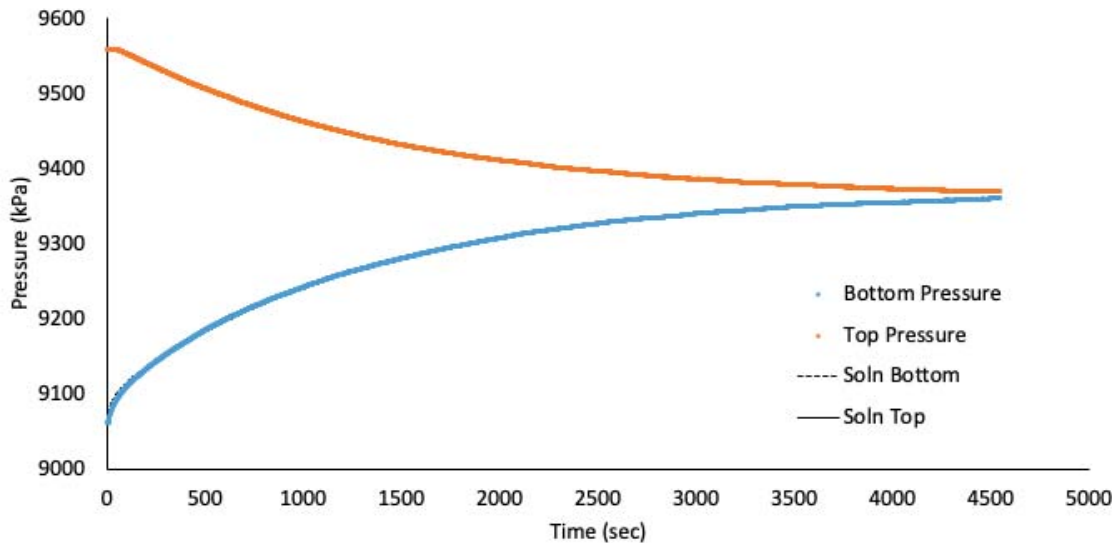


Figure 159 IG_BH06_PS004_HC25r: Effective Confining Stress = 13.35 MPa

	Sample Name		IG_BH06_PS004
	Specimen Name		IG_BH06_PS004_HC25r
	Specimen Top Depth		731.835
	Specimen Bottom Depth		731.870
	Test No		ES2
	Test Name		9386.556162_ES2
	Operator		0
Dimensions	Length	mm	25.170
	Diameter	mm	24.580
	Length	m	0.02517
	Diameter	m	0.02458
Test Data Location	Raw Data File Name		2023-08-03_08-42-04 System-3-Cell-1 IG-BH06-PS004-HC25r.csv
	Date & Time		2023-08-04 08:55:37
	Start Row		963
	End Row		6640
Test Conditions	Avg Cell Temp	C	40.32
	Avg Confining Pressure	kPa	27948
	Pre Pulse Avg Pore Pressure	kPa	9581
	Pulse Pressure	kPa	-475
	Effective Stress	kPa	18367
	Post Pulse Avg Pore Pressure	kPa	9581
Pore Fluid & Conditions	Type		Water
	Salt	ppm	0
	Density	kg/m3	996.21
	Viscosity	kg.s/m	6.501E-04
	Compressibility	1/Pa	4.36E-10
Solution	Test System		System 3 - Cell 1
Brace	Nominal Decay Time	s	5677
	Brace Permeability	m2	8.06E-21
Hsieh	Permeability	m2	8.06E-21
	Specific Storage	1/m	1.37E-07
	Permeability	nD	8.2
	Hydraulic Conductivity	m/s	1.21E-13
	Pearson Coeff	()	0.9996234

IG_BH06_PS004_HC25r Eff Stress:18.37 MPa, HC=1.21e-13 m/s, SS=1.37e-7 1/m

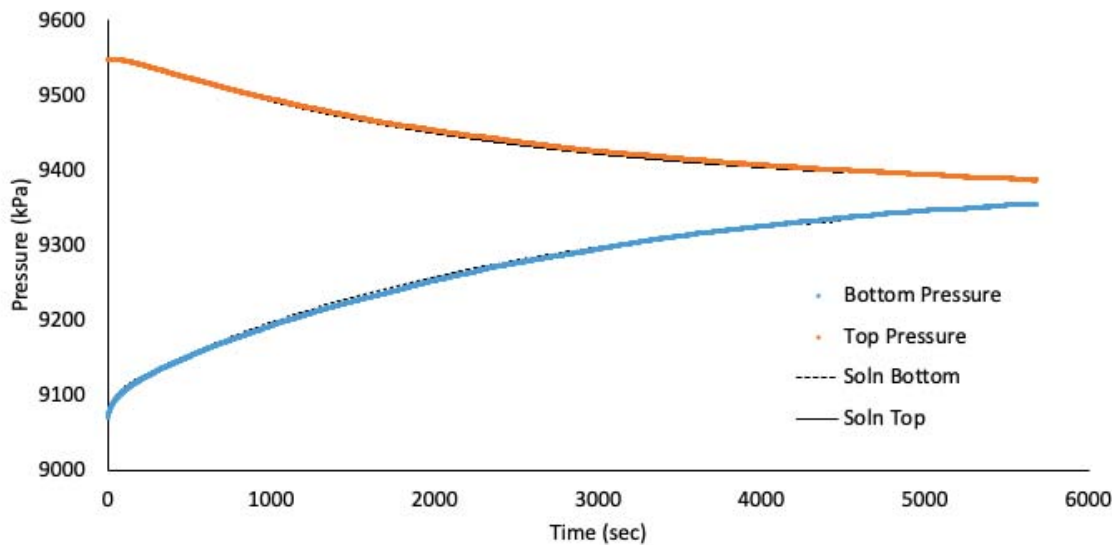


Figure 160 IG_BH06_PS004_HC25r: Effective Confining Stress = 18.37 MPa

	Sample Name		IG_BH06_PS004
	Specimen Name		IG_BH06_PS004_HC25r
	Specimen Top Depth		731.835
	Specimen Bottom Depth		731.870
	Test No		ES3
	Test Name		8958.43320266667_ES3
	Operator		0
Dimensions	Length	mm	25.170
	Diameter	mm	24.580
	Length	m	0.02517
	Diameter	m	0.02458
Test Data Location	Raw Data File Name		2023-08-03_08-42-04 System-3-Cell-1 IG-BH06-PS004-HC25r.csv
	Date & Time		2023-08-04 14:24:47
	Start Row		1321
	End Row		17640
Test Conditions	Avg Cell Temp	C	40.35
	Avg Confining Pressure	kPa	32935
	Pre Pulse Avg Pore Pressure	kPa	9229
	Pulse Pressure	kPa	544
	Effective Stress	kPa	23706
	Post Pulse Avg Pore Pressure	kPa	9229
Pore Fluid & Conditions	Type		Water
	Salt	ppm	0
	Density	kg/m3	996.05
	Viscosity	kg.s/m	6.497E-04
	Compressibility	1/Pa	4.36E-10
Solution	Test System		System 3 - Cell 1
Brace	Nominal Decay Time	s	16319
	Brace Permeability	m2	3.04E-21
Hsieh	Permeability	m2	3.35E-21
	Specific Storage	1/m	9.13E-08
	Permeability	nD	3.4
	Hydraulic Conductivity	m/s	5.03E-14
	Pearson Coeff	()	0.9994252

IG_BH06_PS004_HC25r Eff Stress:23.71 MPa, HC=5.03e-14 m/s, SS=9.13e-8 1/m

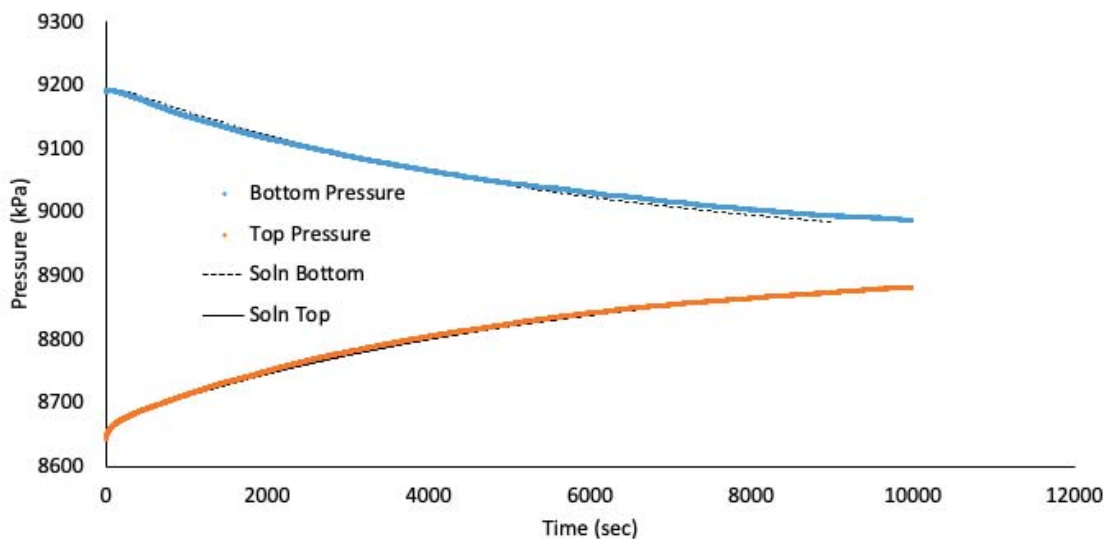


Figure 161 IG_BH06_PS004_HC25r: Effective Confining Stress = 23.71 MPa

	Sample Name		IG_BH06_PS004
	Specimen Name		IG_BH06_PS004_HC61a
	Specimen Top Depth		731.87
	Specimen Bottom Depth		731.932
	Test No		ES1
	Test Name		9455.000246_ES1
	Operator		0
Dimensions	Length	mm	61.890
	Diameter	mm	60.830
	Length	m	0.06189
	Diameter	m	0.06083
Test Data Location	Raw Data File Name		2023-08-03_08-41-05 System-3-Cell-2 IG-BH06-PS004-HC61a.csv
	Date & Time		2023-08-03 08:41:05
	Start Row		1991
	End Row		6530
Test Conditions	Avg Cell Temp	C	40.10
	Avg Confining Pressure	kPa	22939
	Pre Pulse Avg Pore Pressure	kPa	9583
	Pulse Pressure	kPa	-507
	Effective Stress	kPa	13355
Pore Fluid & Conditions	Post Pulse Avg Pore Pressure	kPa	9583
	Type		Water
	Salt	ppm	0
	Density	kg/m3	996.3
	Viscosity	kg.s/m	6.528E-04
Solution	Compressibility	1/Pa	4.36E-10
	Test System		System 3 - Cell 2
Brace	Nominal Decay Time	s	4539
	Brace Permeability	m2	1.72E-20
Hsieh	Permeability	m2	1.75E-20
	Specific Storage	1/m	1.15E-07
	Permeability	nD	17.8
	Hydraulic Conductivity	m/s	2.63E-13
	Pearson Coeff	()	0.9999109

IG_BH06_PS004_HC61a Eff Stress:13.36 MPa, HC=2.63e-13 m/s, SS=1.15e-7 1/m

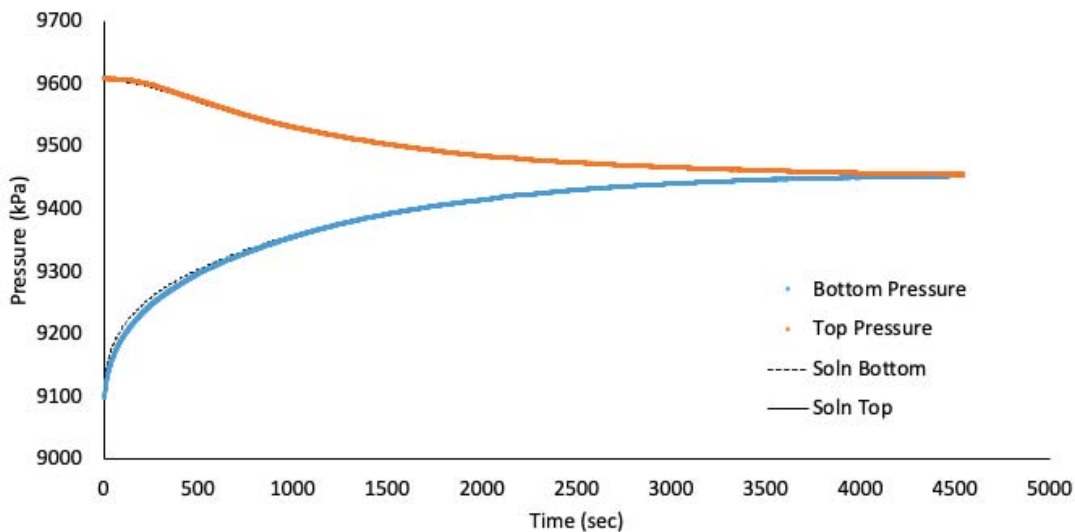


Figure 162 IG_BH06_PS004_HC61a: Effective Confining Stress = 13.36 MPa

	Sample Name		IG_BH06_PS004
	Specimen Name		IG_BH06_PS004_HC61a
	Specimen Top Depth		731.87
	Specimen Bottom Depth		731.932
	Test No		ES2
	Test Name		9446.326341_ES2
	Operator		0
Dimensions	Length	mm	61.890
	Diameter	mm	60.830
	Length	m	0.06189
	Diameter	m	0.06083
Test Data Location	Raw Data File Name		2023-08-03_08-41-05 System-3-Cell-2 IG-BH06-PS004-HC61a.csv
	Date & Time		2023-08-04 08:55:58
	Start Row		934
	End Row		6615
Test Conditions	Avg Cell Temp	C	40.12
	Avg Confining Pressure	kPa	27937
	Pre Pulse Avg Pore Pressure	kPa	9575
	Pulse Pressure	kPa	-503
	Effective Stress	kPa	18362
	Post Pulse Avg Pore Pressure	kPa	9575
Pore Fluid & Conditions	Type		Water
	Salt	ppm	0
	Density	kg/m3	996.28
	Viscosity	kg.s/m	6.525E-04
	Compressibility	1/Pa	4.36E-10
Solution	Test System		System 3 - Cell 2
Brace	Nominal Decay Time	s	5681
	Brace Permeability	m2	1.03E-20
Hsieh	Permeability	m2	8.76E-21
	Specific Storage	1/m	9.00E-08
	Permeability	nD	8.9
	Hydraulic Conductivity	m/s	1.31E-13
	Pearson Coeff	()	0.9998183

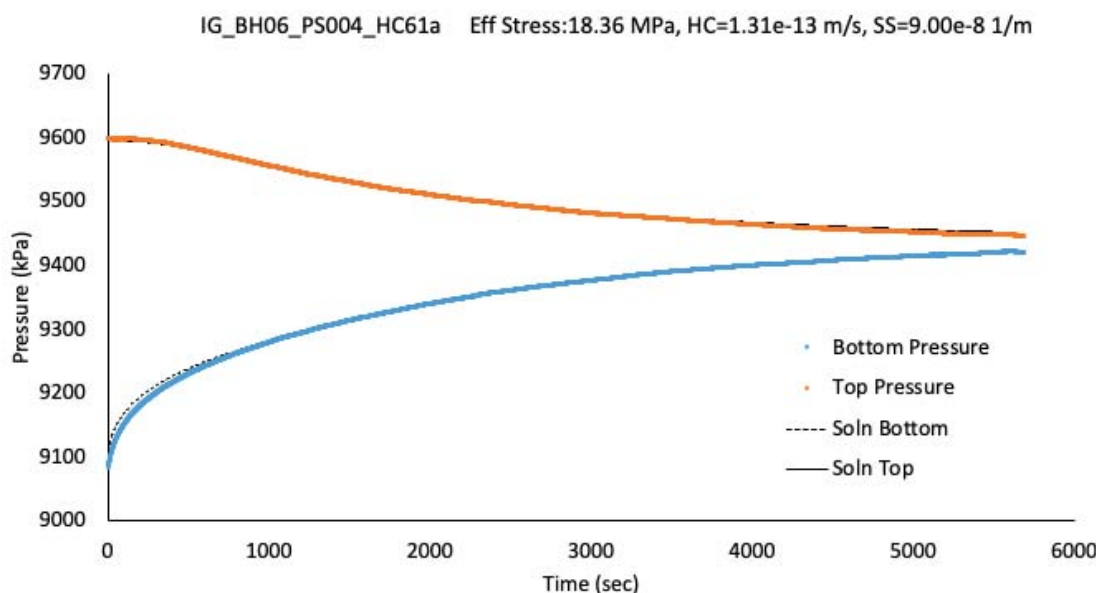


Figure 163 IG_BH06_PS004_HC61a: Effective Confining Stress = 18.36 MPa

	Sample Name		IG_BH06_PS004
	Specimen Name		IG_BH06_PS004_HC61a
	Specimen Top Depth		731.87
	Specimen Bottom Depth		731.932
	Test No		ES3
	Test Name		9074.23253833333_ES3
	Operator		0
Dimensions	Length	mm	61.890
	Diameter	mm	60.830
	Length	m	0.06189
	Diameter	m	0.06083
Test Data Location	Raw Data File Name		2023-08-03_08-41-05 System-3-Cell-2 IG-BH06-PS004-HC61a.csv
	Date & Time		2023-08-04 14:25:19
	Start Row		4574
	End Row		19775
Test Conditions	Avg Cell Temp	C	40.13
	Avg Confining Pressure	kPa	32921
	Pre Pulse Avg Pore Pressure	kPa	9215
	Pulse Pressure	kPa	546
	Effective Stress	kPa	23707
	Post Pulse Avg Pore Pressure	kPa	9215
Pore Fluid & Conditions	Type		Water
	Salt	ppm	0
	Density	kg/m3	996.13
	Viscosity	kg.s/m	6.523E-04
	Compressibility	1/Pa	4.36E-10
Solution	Test System		System 3 - Cell 2
Brace	Nominal Decay Time	s	15201
	Brace Permeability	m2	3.43E-21
Hsieh	Permeability	m2	3.78E-21
	Specific Storage	1/m	8.31E-08
	Permeability	nD	3.8
	Hydraulic Conductivity	m/s	5.66E-14
	Pearson Coeff	()	0.9990092

IG_BH06_PS004_HC61a Eff Stress:23.71 MPa, HC=5.66e-14 m/s, SS=8.31e-8 1/m

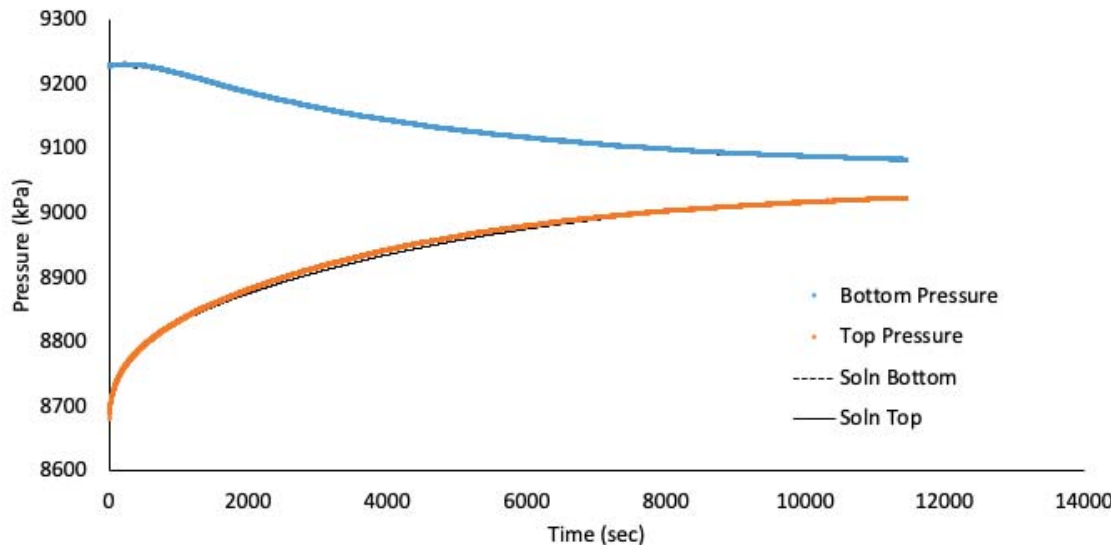


Figure 164 IG_BH06_PS004_HC61a: Effective Confining Stress = 23.71 MPa

Sample ID	IG_BH06_PS004			
Specimen Full Name	IG_BH06_PS004_SSG61a			
Top Depth (m)	731.932			
Bottom Depth (m)	731.994			
Test ID	SSG	ESL	ESM	ESH
Test Name	Steady State N2 Permeability			
Operator 1	A. Sanchez			
Operator 2				
Dimensions	Length mm Diameter mm	61.98		
	Length m Diameter m	0.06		
Test Data Location	Raw Data File Name	rawData_ESL	rawData_ESM	rawData_ESH
	Start Date & Time	2023-03-13		
	End Date & Time	2023-03-22		
Average Test Conditions and Pore Fluids Conditions	Cell Temp C Fluid Type Gas Density kg/m3 Viscosity cP Effective Stress MPa	33.1 Nitrogen 94.1 0.0198 13.9	33.0 Nitrogen 88.8 0.0197 18.9	33.1 Nitrogen 88.7 0.0197 23.9
Results	kapp	m2	3.67E-19	1.14E-19
				1.47E-20

NOTES:

ESL Effective stress - low test condition
 ESM Effective stress - medium test condition
 ESH Effective stress - high test condition
 kapp Apparent gas permeability

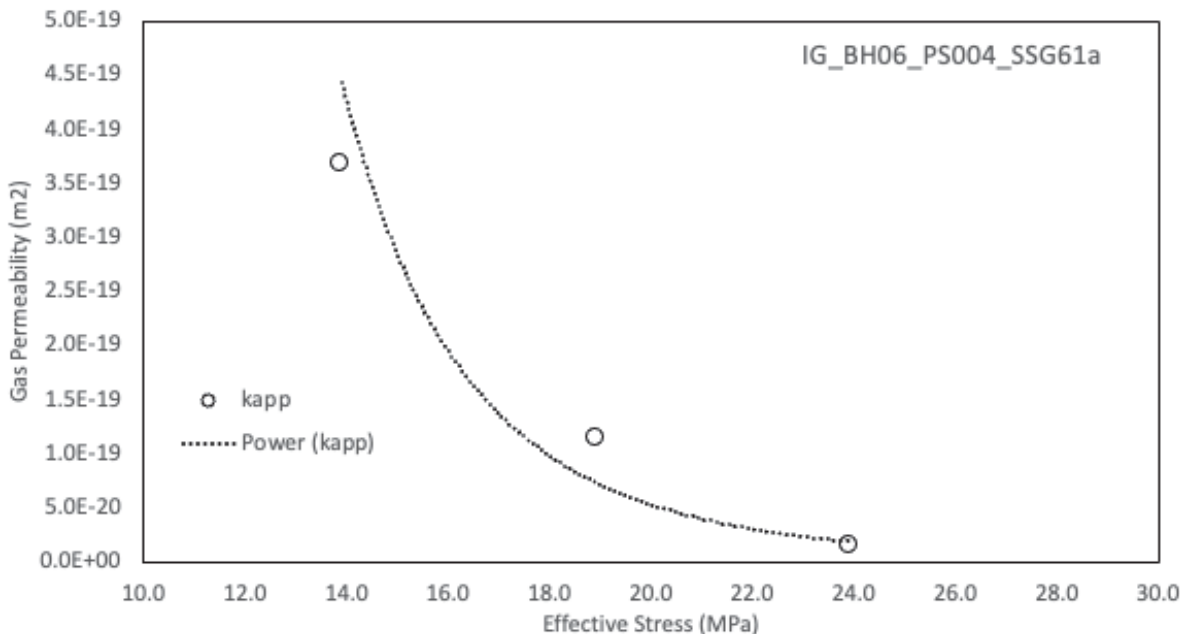


Figure 165 IG_BH06_PS004_SSG61a: Effective Confining Stresses of 13.0 MPa, 18.9 MPa and 23.9 MPa.

	Sample Name		IG_BH06_PS006
	Specimen Name		IG_BH06_PS006_HC25a
	Specimen Top Depth		833.52
	Specimen Bottom Depth		833.570
	Test No		ES1
	Test Name		IG_BH06_PS006_HC25a_ES1
	Operator		Stephen Talman/ Francy Guerrero
Dimensions	Length	mm	25.680
	Diameter	mm	25.340
	Length	m	0.02568
	Diameter	m	0.02534
Test Data Location	Raw Data File Name		2023-09-12_08-26-33 System-3-Cell-1 IG-BH06-PS006-HC25a.csv
	Date & Time		2023-09-12 08:26:33
	Start Row		2110
	End Row		4000
Test Conditions	Avg Cell Temp	C	40.33
	Avg Confining Pressure	kPa	24860
	Pre Pulse Avg Pore Pressure	kPa	8777
	Pulse Pressure	kPa	-739
	Effective Stress	kPa	16083
	Post Pulse Avg Pore Pressure	kPa	8777
Pore Fluid & Conditions	Type		Water
	Salt	ppm	0
	Density	kg/m3	995.86
	Viscosity	kg.s/m	6.499E-04
	Compressibility	1/Pa	4.36E-10
Solution	Test System		System 3 - Cell 1
Brace	Nominal Decay Time	s	1890
	Brace Permeability	m2	1.80E-19
Hsieh	Permeability	m2	2.53E-19
	Specific Storage	1/m	6.08E-08
	Permeability	nD	255.9
	Hydraulic Conductivity	m/s	3.80E-12
	Pearson Coeff	()	0.9998924

IG_BH06_PS006_HC25a Eff Stress:16.08 MPa, HC=3.80e-12 m/s, SS=6.08e-8 1/m

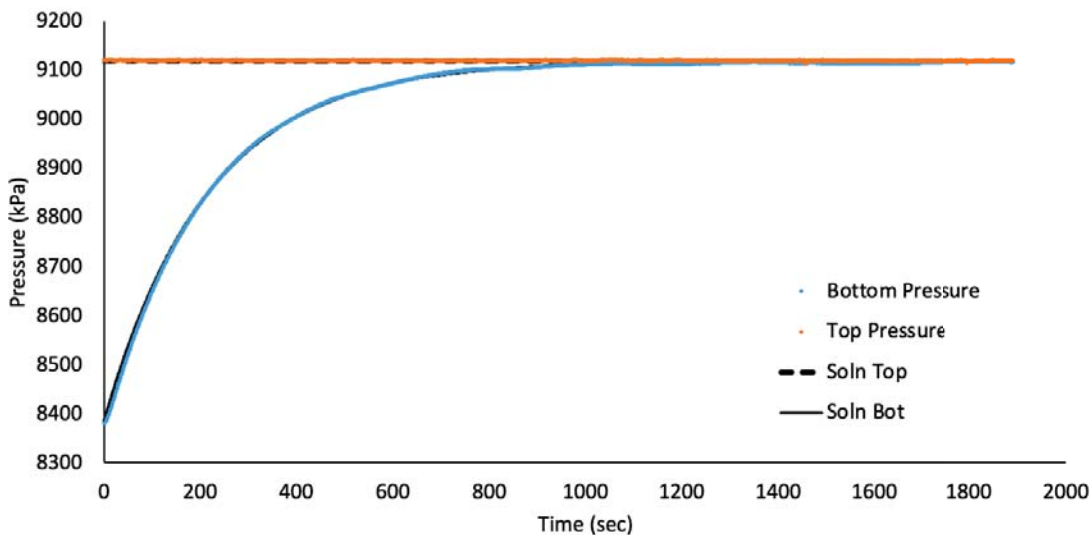


Figure 166 IG_BH06_PS006_HC25a: Effective Confining Stress = 16.08 MPa

	Sample Name		IG_BH06_PS006
	Specimen Name		IG_BH06_PS006_HC25a
	Specimen Top Depth		833.52
	Specimen Bottom Depth		833.570
	Test No		ES2
	Test Name		IG_BH06_PS006_HC25a_ES2
	Operator		Stephen Talman/ Francy Guerrero
Dimensions	Length	mm	25.680
	Diameter	mm	25.340
	Length	m	0.02568
	Diameter	m	0.02534
Test Data Location	Raw Data File Name		2023-09-12_08-26-33 System-3-Cell-1 IG-BH06-PS006-HC25a.csv
	Date & Time		2023-09-12 13:22:00
	Start Row		289
	End Row		4000
Test Conditions	Avg Cell Temp	C	40.34
	Avg Confining Pressure	kPa	29863
	Pre Pulse Avg Pore Pressure	kPa	8798
	Pulse Pressure	kPa	586
	Effective Stress	kPa	21066
	Post Pulse Avg Pore Pressure	kPa	8798
Pore Fluid & Conditions	Type		Water
	Salt	ppm	0
	Density	kg/m3	995.87
	Viscosity	kg.s/m	6.498E-04
	Compressibility	1/Pa	4.36E-10
Solution	Test System		System 3 - Cell 1
Brace	Nominal Decay Time	s	3711
	Brace Permeability	m2	6.41E-20
Hsieh	Permeability	m2	8.98E-20
	Specific Storage	1/m	6.08E-08
	Permeability	nD	91.0
	Hydraulic Conductivity	m/s	1.35E-12
	Pearson Coeff	()	0.9999771

IG_BH06_PS006_HC25a Eff Stress:21.07 MPa, HC=1.35e-12 m/s, SS=6.08e-8 1/m

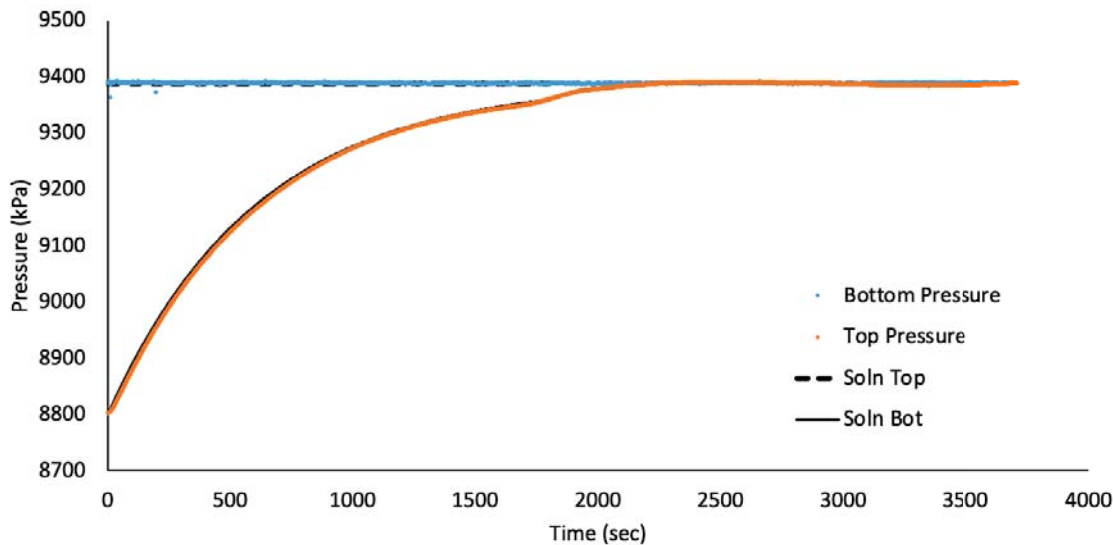


Figure 167 IG_BH06_PS006_HC25a: Effective Confining Stress = 21.07 MPa

	Sample Name		IG_BH06_PS006
	Specimen Name		IG_BH06_PS006_HC25a
	Specimen Top Depth		833.52
	Specimen Bottom Depth		833.570
	Test No		ES3
	Test Name		IG_BH06_PS006_HC25a_ES3
	Operator		Stephen Talman/ Francy Guerrero
Dimensions	Length	mm	25.680
	Diameter	mm	25.340
	Length	m	0.02568
	Diameter	m	0.02534
Test Data Location	Raw Data File Name		2023-09-12_08-26-33 System-3-Cell-1 IG-BH06-PS006-HC25a.csv
	Date & Time		2023-09-15 08:39:55
	Start Row		561
	End Row		8000
Test Conditions	Avg Cell Temp	C	40.34
	Avg Confining Pressure	kPa	34853
	Pre Pulse Avg Pore Pressure	kPa	8728
	Pulse Pressure	kPa	705
	Effective Stress	kPa	26124
	Post Pulse Avg Pore Pressure	kPa	8728
Pore Fluid & Conditions	Type		Water
	Salt	ppm	0
	Density	kg/m3	995.87
	Viscosity	kg.s/m	6.498E-04
	Compressibility	1/Pa	4.36E-10
Solution	Test System		System 3 - Cell 1
Brace	Nominal Decay Time	s	7439
	Brace Permeability	m2	2.81E-20
Hsieh	Permeability	m2	3.93E-20
	Specific Storage	1/m	3.65E-08
	Permeability	nD	39.8
	Hydraulic Conductivity	m/s	5.91E-13
	Pearson Coeff	()	0.9999498

IG_BH06_PS006_HC25a Eff Stress:26.12 MPa, HC=5.91e-13 m/s, SS=3.65e-8 1/m

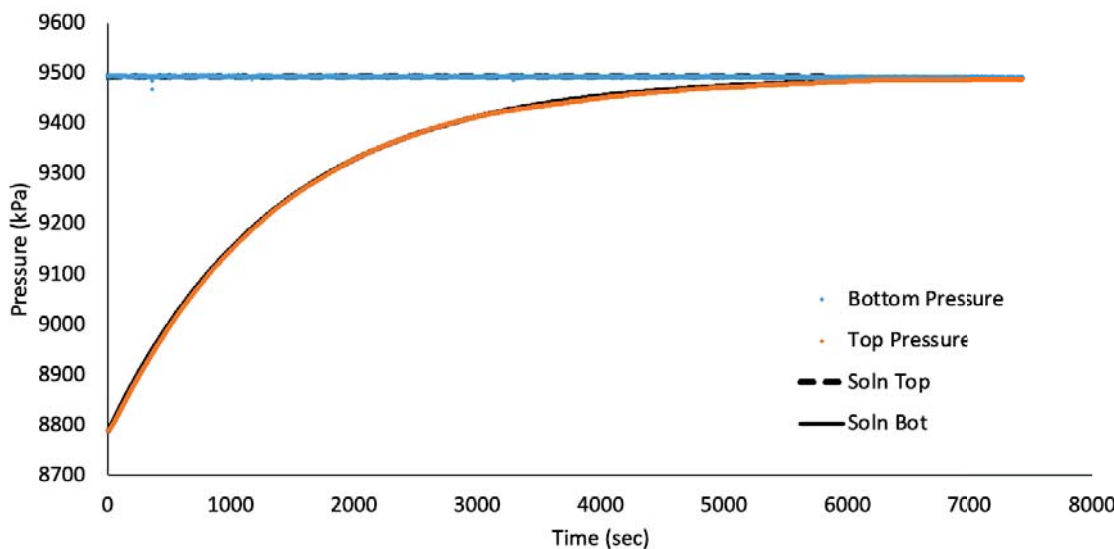


Figure 168 IG_BH06_PS006_HC25a: Effective Confining Stress = 26.12 MPa

	Sample Name		IG_BH06_PS006
	Specimen Name		IG_BH06_PS006_HC25r
	Specimen Top Depth		833.535
	Specimen Bottom Depth		833.570
	Test No		ES1
	Test Name		8818.8972047093_ES1
	Operator		Stephen Talman/ Francy Guerrero
Dimensions	Length	mm	24.500
	Diameter	mm	24.600
	Length	m	0.0245
	Diameter	m	0.0246
Test Data Location	Raw Data File Name		2023-09-12_08-27-23 System-3-Cell-3 IG-BH06-PS006-HC25r.csv
	Date & Time		2023-09-12 08:27:23
	Start Row		2049
	End Row		4000
Test Conditions	Avg Cell Temp	C	39.74
	Avg Confining Pressure	kPa	24807
	Pre Pulse Avg Pore Pressure	kPa	8625
	Pulse Pressure	kPa	504
	Effective Stress	kPa	16181
	Post Pulse Avg Pore Pressure	kPa	8625
Pore Fluid & Conditions	Type		Water
	Salt	ppm	0
	Density	kg/m3	996.03
	Viscosity	kg.s/m	6.570E-04
	Compressibility	1/Pa	4.36E-10
Solution	System and Cell		System 3 - Cell 3
Brace	Nominal Decay Time	s	1951
	Brace Permeability	m2	9.62E-20
Hsieh	Permeability	m2	1.04E-19
	Specific Storage	1/m	1.04E-07
	Permeability	nD	105.3
	Hydraulic Conductivity	m/s	1.55E-12
	Pearson Coeff	()	0.9999138

IG_BH06_PS006_HC25r Eff Stress:16.18 MPa, HC=1.55e-12 m/s, SS=1.04e-7 1/m

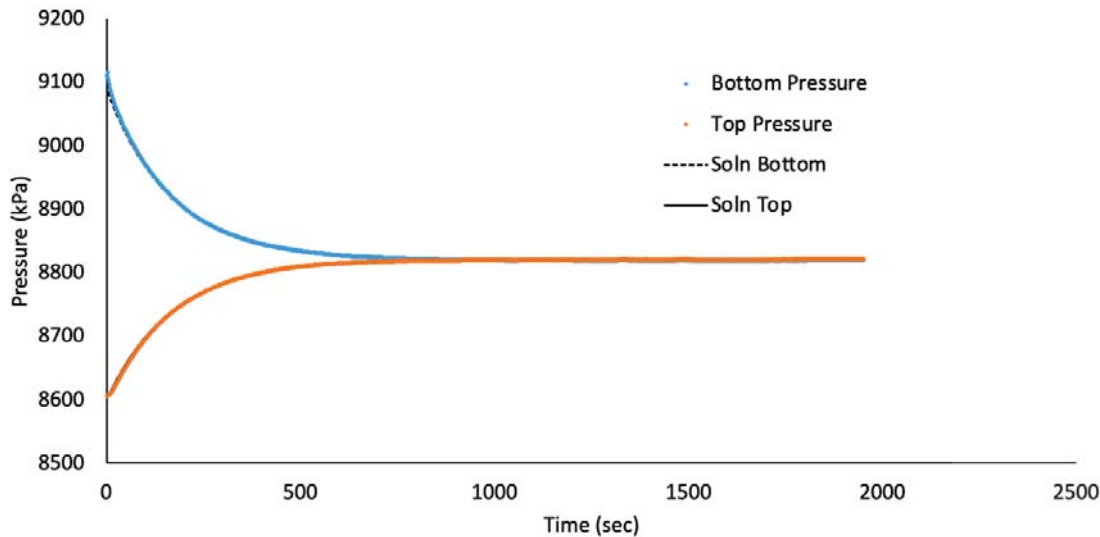


Figure 169 IG_BH06_PS006_HC25r: Effective Confining Stress = 16.18 MPa

	Sample Name		IG_BH06_PS006
	Specimen Name		IG_BH06_PS006_HC25r
	Specimen Top Depth		833.535
	Specimen Bottom Depth		833.570
	Test No		ES2
	Test Name		9010.48313036991_ES2
	Operator		Stephen Talman/ Francy Guerrero
Dimensions	Length	mm	24.500
	Diameter	mm	24.600
	Length	m	0.0245
	Diameter	m	0.0246
Test Data Location	Raw Data File Name		2023-09-12_08-27-23 System-3-Cell-3 IG-BH06-PS006-HC25r.csv
	Date & Time		2023-09-12 13:22:47
	Start Row		810
	End Row		5000
Test Conditions	Avg Cell Temp	C	39.78
	Avg Confining Pressure	kPa	29797
	Pre Pulse Avg Pore Pressure	kPa	8819
	Pulse Pressure	kPa	500
	Effective Stress	kPa	20978
	Post Pulse Avg Pore Pressure	kPa	8819
Pore Fluid & Conditions	Type		Water
	Salt	ppm	0
	Density	kg/m3	996.09
	Viscosity	kg.s/m	6.566E-04
	Compressibility	1/Pa	4.36E-10
Solution	System and Cell		System 3 - Cell 3
Brace	Nominal Decay Time	s	4190
	Brace Permeability	m2	3.69E-20
Hsieh	Permeability	m2	4.06E-20
	Specific Storage	1/m	6.69E-08
	Permeability	nD	41.1
	Hydraulic Conductivity	m/s	6.04E-13
	Pearson Coeff	()	0.9999485

IG_BH06_PS006_HC25r Eff Stress:20.98 MPa, HC=6.04e-13 m/s, SS=6.69e-8 1/m

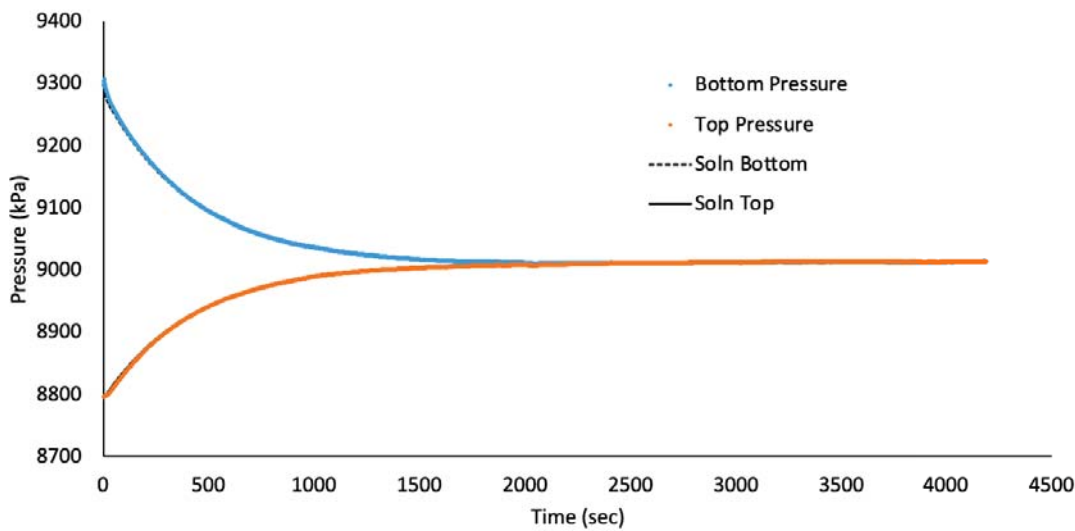


Figure 170 IG_BH06_PS006_HC25r: Effective Confining Stress = 20.98 MPa

	Sample Name		IG_BH06_PS006
	Specimen Name		IG_BH06_PS006_HC25r
	Specimen Top Depth		833.535
	Specimen Bottom Depth		833.570
	Test No		ES3
	Test Name		9005.34747226424_ES3
	Operator		Stephen Talman/ Francy Guerrero
Dimensions	Length	mm	24.500
	Diameter	mm	24.600
	Length	m	0.0245
	Diameter	m	0.0246
Test Data Location	Raw Data File Name		2023-09-12_08-27-23 System-3-Cell-3 IG-BH06-PS006-HC25r.csv
	Date & Time		2023-09-15 08:40:39
	Start Row		512
	End Row		9000
Test Conditions	Avg Cell Temp	C	39.76
	Avg Confining Pressure	kPa	34773
	Pre Pulse Avg Pore Pressure	kPa	8808
	Pulse Pressure	kPa	498
	Effective Stress	kPa	25965
Pore Fluid & Conditions	Post Pulse Avg Pore Pressure	kPa	8808
	Type		Water
	Salt	ppm	0
	Density	kg/m3	996.1
	Viscosity	kg.s/m	6.568E-04
Solution	Compressibility	1/Pa	4.36E-10
	System and Cell		System 3 - Cell 3
Brace	Nominal Decay Time	s	8488
	Brace Permeability	m2	1.44E-20
Hsieh	Permeability	m2	1.59E-20
	Specific Storage	1/m	6.60E-08
	Permeability	nD	16.1
	Hydraulic Conductivity	m/s	2.36E-13
	Pearson Coeff	()	0.9997576

IG_BH06_PS006_HC25r Eff Stress:25.97 MPa, HC=2.36e-13 m/s, SS=6.60e-8 1/m

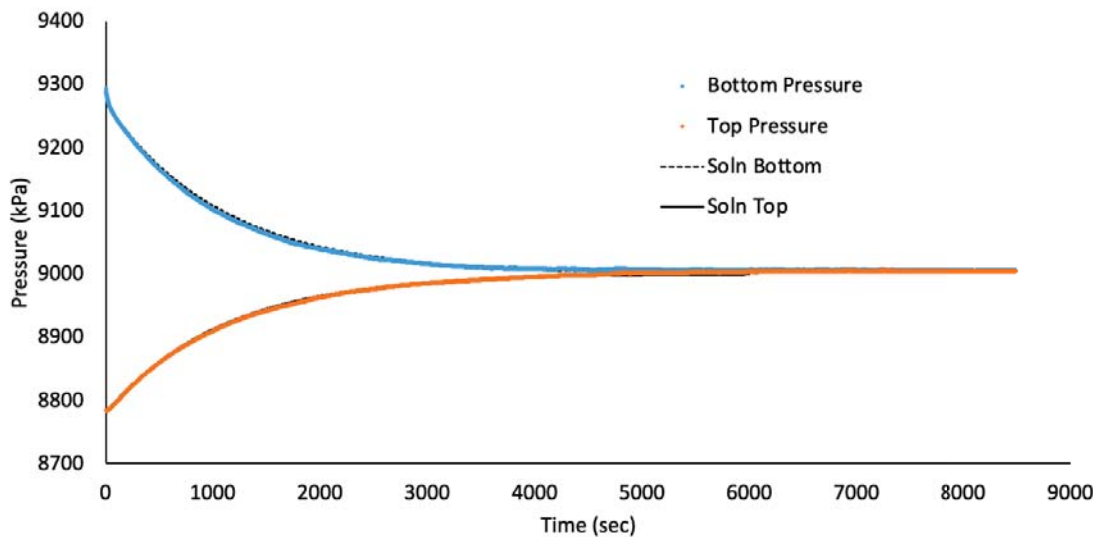


Figure 171 IG_BH06_PS006_HC25r: Effective Confining Stress = 25.97 MPa

Sample ID	IG_BH06_PS006			
Specimen Full Name	IG_BH06_PS006_SSG61a			
Top Depth (m)	833.632			
Bottom Depth (m)	833.694			
Test ID	SSG	ESL	ESM	ESH
Test Name	Steady State N2 Permeability			
Operator 1	A. Sanchez			
Operator 2				
Dimensions	Length	mm	62.08	
	Diameter	mm	61.10	
	Length	m	0.06	
	Diameter	m	0.06	
Test Data Location	Raw Data File Name		rawData_ESL	rawData_ESM
	Start Date & Time	2023-03-29	rawData_ESL	rawData_ESH
	End Date & Time	2023-04-06	rawData_ESM	rawData_ESH
Average Test Conditions and Pore Fluids Conditions	Cell Temp	C	33.0	33.1
	Fluid Type	Gas	Nitrogen	Nitrogen
	Density	kg/m3	88.7	88.7
	Viscosity	cP	0.0197	0.0197
	Effective Stress	MPa	16.8	21.8
Results	kapp	m2	4.30E-19	1.26E-19
				3.84E-20

NOTES:

- ESL Effective stress - low test condition
 ESM Effective stress - medium test condition
 ESH Effective stress - high test condition
 kapp Apparent gas permeability

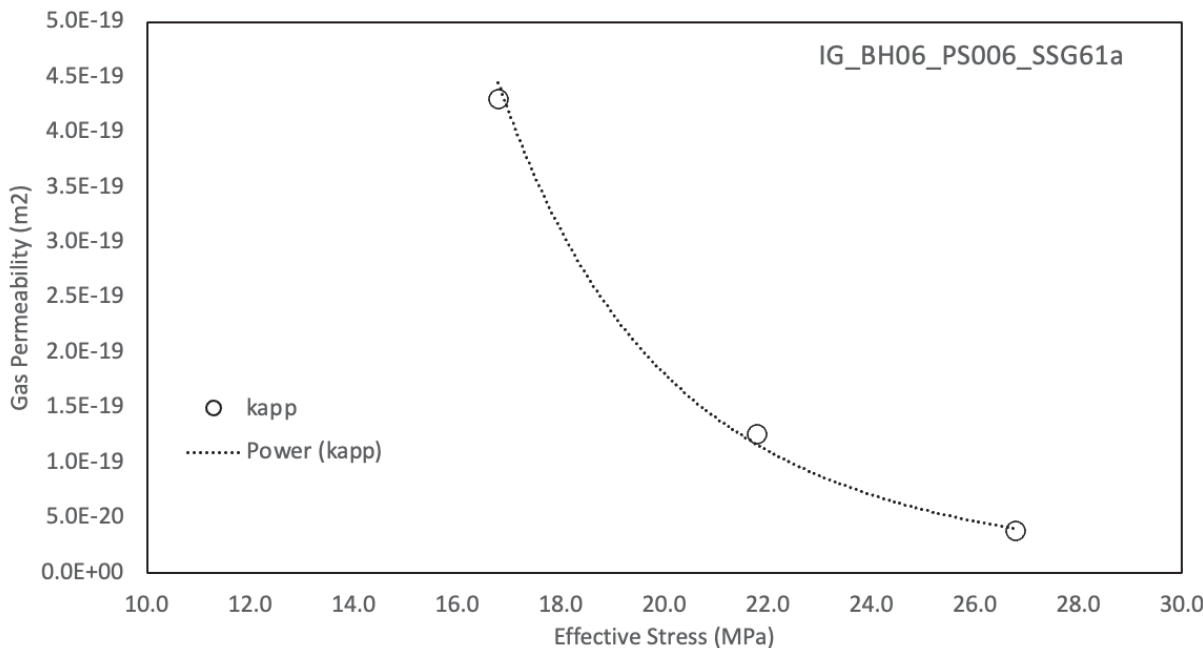


Figure 172 IG_BH06_PS006_SSG61a: Effective Confining Stresses of 16.8 MPa, 21.8 MPa and 26.8 MPa.

	Sample Name		IG_BH06_PS007
	Specimen Name		IG_BH06_PS007_HC25a
	Specimen Top Depth		933.405
	Specimen Bottom Depth		933.44
	Test No		ES1
	Test Name		IG_BH06_PS007_HC25a_ES1
	Operator		Stephen Talman/ Francy Guerrero
Dimensions	Length	mm	25.950
	Diameter	mm	25.330
	Length	m	0.02595
	Diameter	m	0.02533
Test Data Location	Raw Data File Name		2023-08-22_13-17-30 System-2-CELL-1 IG-BH06-PS007-HC25a.csv
	Date & Time		2023-08-24 07:46:10
	Start Row		471
	End Row		1500
Test Conditions	Avg Cell Temp	C	39.86
	Avg Confining Pressure	kPa	26591
	Pre Pulse Avg Pore Pressure	kPa	8894
	Pulse Pressure	kPa	507
	Effective Stress	kPa	17696
	Post Pulse Avg Pore Pressure	kPa	8894
Pore Fluid & Conditions	Type		Water
	Salt	ppm	0
	Density	kg/m3	996.09
	Viscosity	kg.s/m	6.556E-04
	Compressibility	1/Pa	4.36E-10
Solution	System and Cell		System 2 - CELL 1
Brace	Nominal Decay Time	s	1029
	Brace Permeability	m2	1.74E-19
Hsieh	Permeability	m2	1.81E-19
	Specific Storage	1/m	1.42E-07
	Permeability	nD	183.2
	Hydraulic Conductivity	m/s	2.70E-12
	Pearson Coeff	()	#DIV/0!

IG_BH06_PS007_HC25a Eff Stress:17.7 MPa, HC=2.70e-12 m/s, SS=1.42e-7 1/m

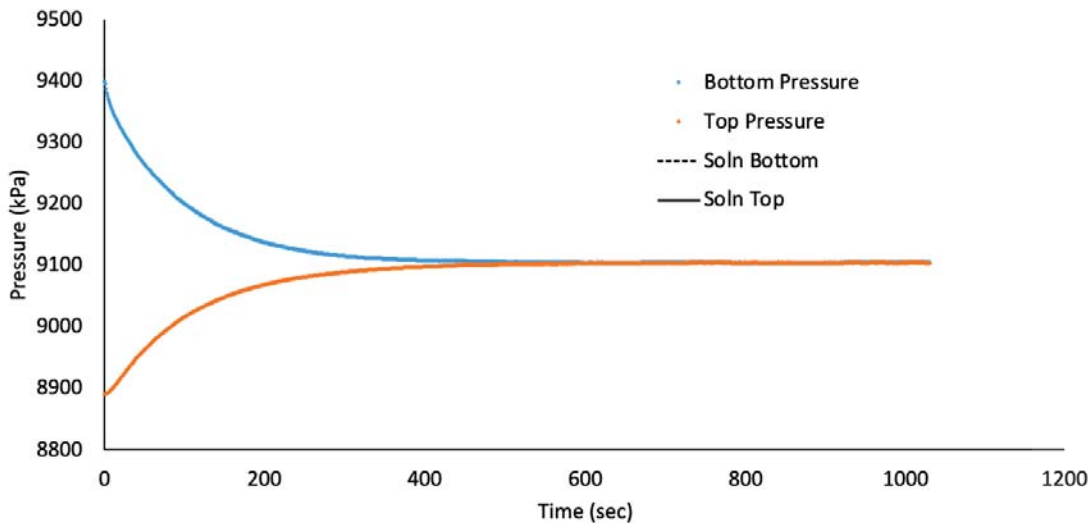


Figure 173 IG_BH06_PS007_HC25a: Effective Confining Stress = 17.70 MPa

	Sample Name		IG_BH06_PS007
	Specimen Name		IG_BH06_PS007_HC25a
	Specimen Top Depth		933.4
	Specimen Bottom Depth		933.440
	Test No		ES2
	Test Name		IG_BH06_PS007_HC25a_ES2
	Operator		Stephen Talman/ Francy Guerrero
Dimensions	Length	mm	25.950
	Diameter	mm	25.330
	Length	m	0.02595
	Diameter	m	0.02533
Test Data Location	Raw Data File Name		2023-08-22_13-17-30 System-2-CELL-1 IG-BH06-PS007-HC25a.csv
	Date & Time		2023-08-27 22:55:15
	Start Row		156
	End Row		3000
Test Conditions	Avg Cell Temp	C	39.79
	Avg Confining Pressure	kPa	31566
	Pre Pulse Avg Pore Pressure	kPa	9307
	Pulse Pressure	kPa	-525
	Effective Stress	kPa	22259
Pore Fluid & Conditions	Post Pulse Avg Pore Pressure	kPa	9307
	Type		Water
	Salt	ppm	0
	Density	kg/m3	996.3
	Viscosity	kg.s/m	6.565E-04
Solution	Compressibility	1/Pa	4.36E-10
	System and Cell		System 2 - CELL 1
Brace	Nominal Decay Time	s	2844
	Brace Permeability	m2	7.84E-20
Hsieh	Permeability	m2	8.15E-20
	Specific Storage	1/m	1.37E-07
	Permeability	nD	82.6
	Hydraulic Conductivity	m/s	1.21E-12
	Pearson Coeff	()	0.9999210

IG_BH06_PS007_HC25a Eff Stress:22.26 MPa, HC=1.21e-12 m/s, SS=1.37e-7 1/m

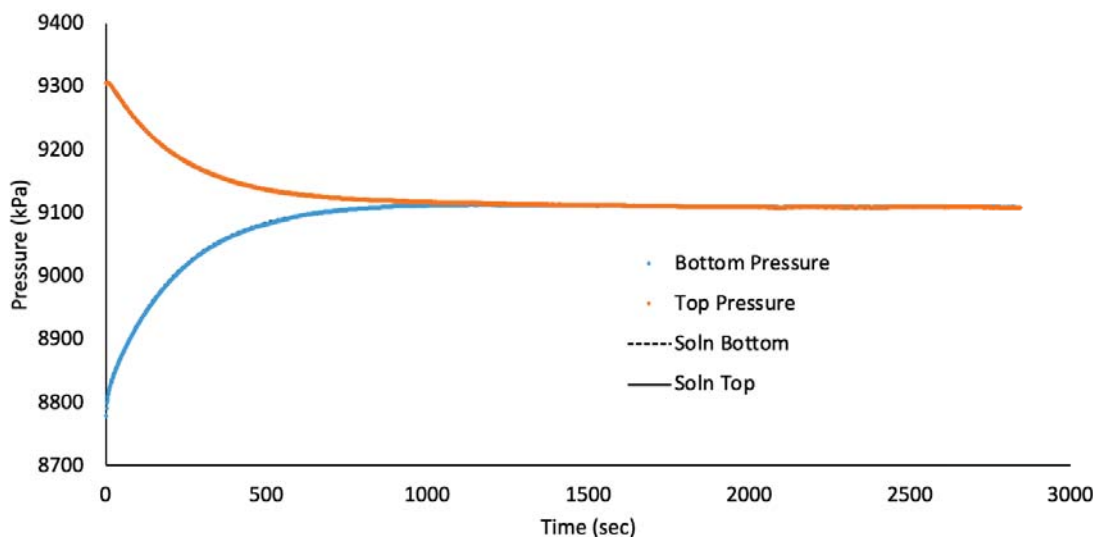


Figure 174 IG_BH06_PS007_HC25a: Effective Confining Stress = 22.26 MPa

	Sample Name		IG_BH06_PS007
	Specimen Name		IG_BH06_PS007_HC25a
	Specimen Top Depth		933.4
	Specimen Bottom Depth		933.440
	Test No		ES3
	Test Name		IG_BH06_PS007_HC25a_ES3
	Operator		Stephen Talman/ Francy Guerrero
Dimensions	Length	mm	25.950
	Diameter	mm	25.330
	Length	m	0.02595
	Diameter	m	0.02533
Test Data Location	Raw Data File Name		2023-08-22_13-17-30 System-2-CELL-1 IG-BH06-PS007-HC25a.csv
	Date & Time		2023-08-28 13:23:41
	Start Row		1610
	End Row		7000
Test Conditions	Avg Cell Temp	C	39.86
	Avg Confining Pressure	kPa	36538
	Pre Pulse Avg Pore Pressure	kPa	9279
	Pulse Pressure	kPa	-483
	Effective Stress	kPa	27259
	Post Pulse Avg Pore Pressure	kPa	9279
Pore Fluid & Conditions	Type		Water
	Salt	ppm	0
	Density	kg/m3	996.26
	Viscosity	kg.s/m	6.556E-04
	Compressibility	1/Pa	4.36E-10
Solution	System and Cell		System 2 - CELL 1
Brace	Nominal Decay Time	s	5390
	Brace Permeability	m2	2.96E-20
Hsieh	Permeability	m2	3.25E-20
	Specific Storage	1/m	1.78E-07
	Permeability	nD	33.0
	Hydraulic Conductivity	m/s	4.85E-13
	Pearson Coeff	()	0.9978406

IG_BH06_PS007_HC25a Eff Stress:27.26 MPa, HC=4.85e-13 m/s, SS=1.78e-7 1/m

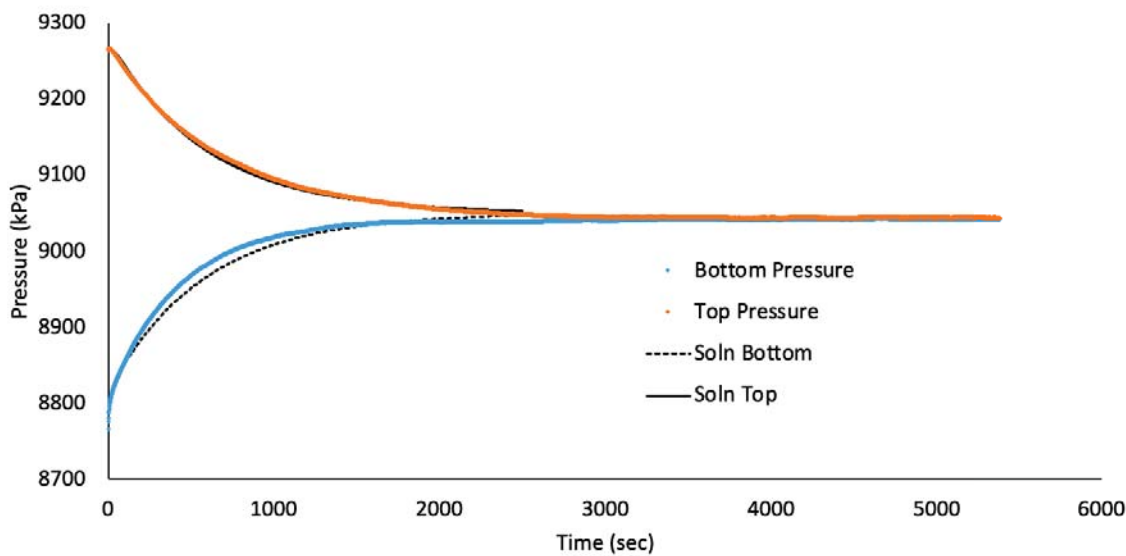


Figure 175 IG_BH06_PS007_HC25a: Effective Confining Stress = 27.26 MPa

	Sample Name		IG_BH06_PS007
	Specimen Name		IG_BH06_PS007_HC25r
	Specimen Top Depth		933.405
	Specimen Bottom Depth		933.440
	Test No		ES1
	Test Name		9082.67222561108_ES1
	Operator		Stephen Talman/ Francy Guerrero
Dimensions	Length	mm	25.120
	Diameter	mm	25.260
	Length	m	0.02512
	Diameter	m	0.02526
Test Data Location	Raw Data File Name		2023-08-22_13-17-44 System-2-CELL-3 IG-BH06-PS007-HC25r.csv
	Date & Time		2023-08-24 07:46:56
	Start Row		2446
	End Row		3500
Test Conditions	Avg Cell Temp	C	39.63
	Avg Confining Pressure	kPa	26391
	Pre Pulse Avg Pore Pressure	kPa	8865
	Pulse Pressure	kPa	500
	Effective Stress	kPa	17526
Pore Fluid & Conditions	Post Pulse Avg Pore Pressure	kPa	8865
	Type		Water
	Salt	ppm	0
	Density	kg/m3	996.17
	Viscosity	kg.s/m	6.584E-04
Solution	Compressibility	1/Pa	4.36E-10
	System and Cell		System 2 - CELL 3
Brace	Nominal Decay Time	s	1054
	Brace Permeability	m2	1.93E-19
Hsieh	Permeability	m2	1.93E-19
	Specific Storage	1/m	1.41E-07
	Permeability	nD	195.8
	Hydraulic Conductivity	m/s	2.87E-12
	Pearson Coeff	()	0.9999518

IG_BH06_PS007_HC25r Eff Stress:17.53 MPa, HC=2.87e-12 m/s, SS=1.41e-7 1/m

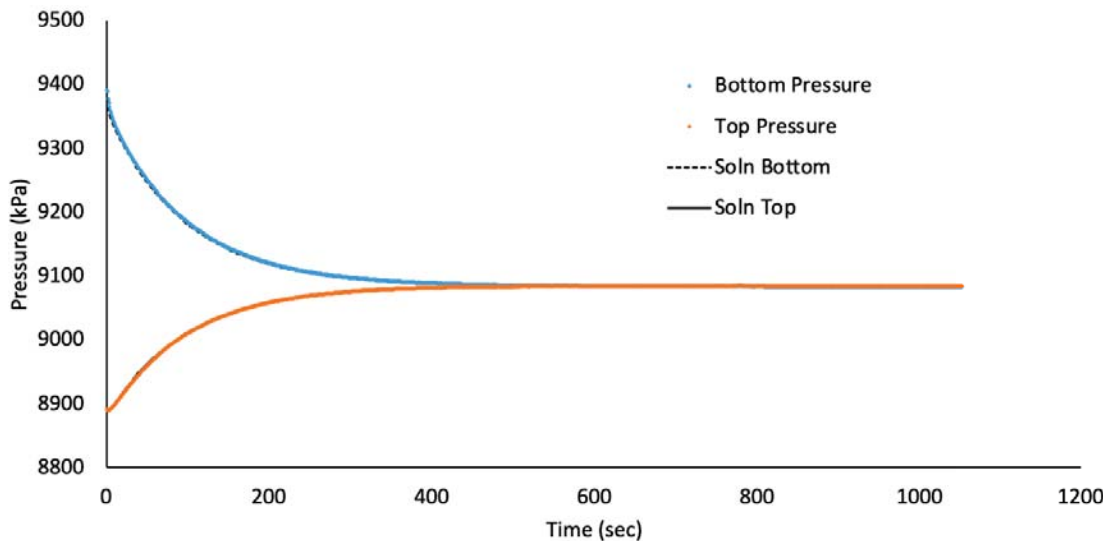


Figure 176 IG_BH06_PS007_HC25r: Effective Confining Stress = 17.53 MPa

	Sample Name		IG_BH06_PS007
	Specimen Name		IG_BH06_PS007_HC25r
	Specimen Top Depth		933.405
	Specimen Bottom Depth		933.440
	Test No		ES2
	Test Name		9112.42655387278_ES2
	Operator		Stephen Talman/ Francy Guerrero
Dimensions	Length	mm	25.120
	Diameter	mm	25.260
	Length	m	0.02512
	Diameter	m	0.02526
Test Data Location	Raw Data File Name		2023-08-22_13-17-44 System-2-CELL-3 IG-BH06-PS007-HC25r.csv
	Date & Time		2023-08-27 22:55:10
	Start Row		5389
	End Row		8000
Test Conditions	Avg Cell Temp	C	39.61
	Avg Confining Pressure	kPa	31334
	Pre Pulse Avg Pore Pressure	kPa	9296
	Pulse Pressure	kPa	-539
	Effective Stress	kPa	22039
	Post Pulse Avg Pore Pressure	kPa	9296
Pore Fluid & Conditions	Type		Water
	Salt	ppm	0
	Density	kg/m3	996.36
	Viscosity	kg.s/m	6.587E-04
	Compressibility	1/Pa	4.36E-10
Solution	System and Cell		System 2 - CELL 3
Brace	Nominal Decay Time	s	2611
	Brace Permeability	m2	7.91E-20
Hsieh	Permeability	m2	8.30E-20
	Specific Storage	1/m	6.13E-08
	Permeability	nD	84.1
	Hydraulic Conductivity	m/s	1.23E-12
	Pearson Coeff	()	0.9998572

IG_BH06_PS007_HC25r Eff Stress:22.04 MPa, HC=1.23e-12 m/s, SS=6.13e-8 1/m

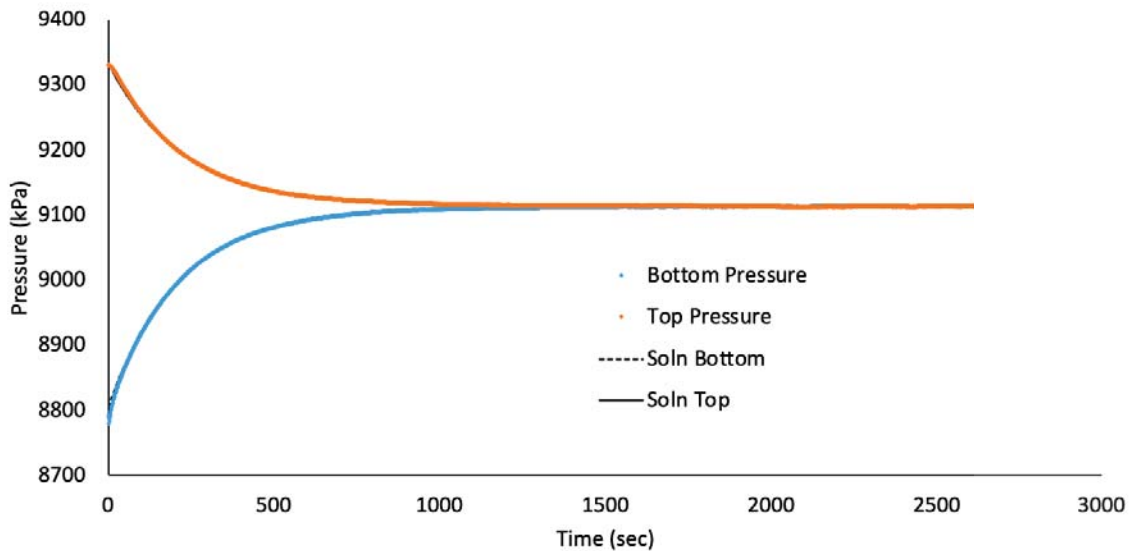


Figure 177 IG_BH06_PS007_HC25r: Effective Confining Stress = 22.04 MPa

	Sample Name		IG_BH06_PS007
	Specimen Name		IG_BH06_PS007_HC25r
	Specimen Top Depth		933.405
	Specimen Bottom Depth		933.440
	Test No		ES3
	Test Name		9098.40378830452_ES3
	Operator		Stephen Talman/ Francy Guerrero
Dimensions	Length	mm	25.120
	Diameter	mm	25.260
	Length	m	0.02512
	Diameter	m	0.02526
Test Data Location	Raw Data File Name		2023-08-22_13-17-44 System-2-CELL-3 IG-BH06-PS007-HC25r.csv
	Date & Time		2023-08-28 13:24:26
	Start Row		1234
	End Row		5000
Test Conditions	Avg Cell Temp	C	39.69
	Avg Confining Pressure	kPa	36275
	Pre Pulse Avg Pore Pressure	kPa	9230
	Pulse Pressure	kPa	-453
	Effective Stress	kPa	27045
	Post Pulse Avg Pore Pressure	kPa	9230
Pore Fluid & Conditions	Type		Water
	Salt	ppm	0
	Density	kg/m3	996.3
	Viscosity	kg.s/m	6.577E-04
	Compressibility	1/Pa	4.36E-10
Solution	System and Cell		System 2 - CELL 3
Brace	Nominal Decay Time	s	3766
	Brace Permeability	m2	3.86E-20
Hsieh	Permeability	m2	3.86E-20
	Specific Storage	1/m	1.13E-07
	Permeability	nD	39.1
	Hydraulic Conductivity	m/s	5.74E-13
	Pearson Coeff	()	0.9998829

IG_BH06_PS007_HC25r Eff Stress:27.05 MPa, HC=5.74e-13 m/s, SS=1.13e-7 1/m

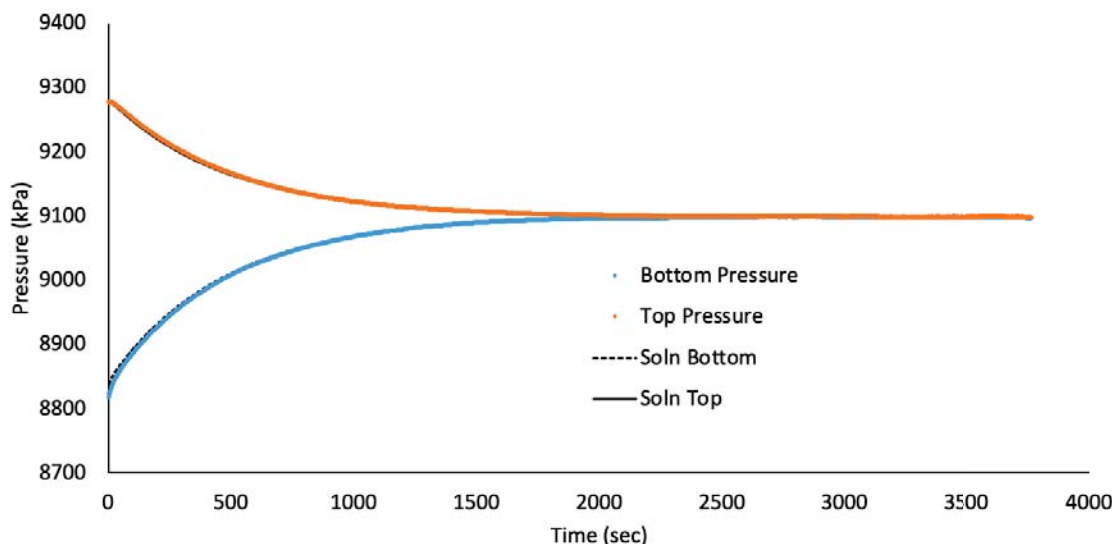


Figure 178 IG_BH06_PS007_HC25r: Effective Confining Stress = 27.05 MPa

	Sample Name		IG_BH06_PS007
	Specimen Name		IG_BH06_PS007_HC61a
	Specimen Top Depth		933.44
	Specimen Bottom Depth		933.502
	Test No		ES1
	Test Name		9046.07049412591_ES1
	Operator		Stephen Talman/ Francy Guerrero
Dimensions	Length	mm	62.050
	Diameter	mm	61.140
	Length	m	0.06205
	Diameter	m	0.06114
Test Data Location	Raw Data File Name		2023-08-22_13-17-15 System-2-CELL-2 IG-BH06-PS007-HC61a.csv
	Date & Time		2023-08-24 07:46:34
	Start Row		60
	End Row		1600
Test Conditions	Avg Cell Temp	C	39.83
	Avg Confining Pressure	kPa	26717
	Pre Pulse Avg Pore Pressure	kPa	8893
	Pulse Pressure	kPa	490
	Effective Stress	kPa	17824
	Post Pulse Avg Pore Pressure	kPa	8893
Pore Fluid & Conditions	Type		Water
	Salt	ppm	0
	Density	kg/m3	996.1
	Viscosity	kg.s/m	6.560E-04
	Compressibility	1/Pa	4.36E-10
Solution	Test System		System 2 - CELL 2
Brace	Nominal Decay Time	s	1540
	Brace Permeability	m2	8.40E-20
Hsieh	Permeability	m2	9.24E-20
	Specific Storage	1/m	1.26E-07
	Permeability	nD	93.6
	Hydraulic Conductivity	m/s	1.38E-12
	Pearson Coeff	()	0.9980735

IG_BH06_PS007_HC61a Eff Stress:17.82 MPa, HC=1.38e-12 m/s, SS=1.26e-7 1/m

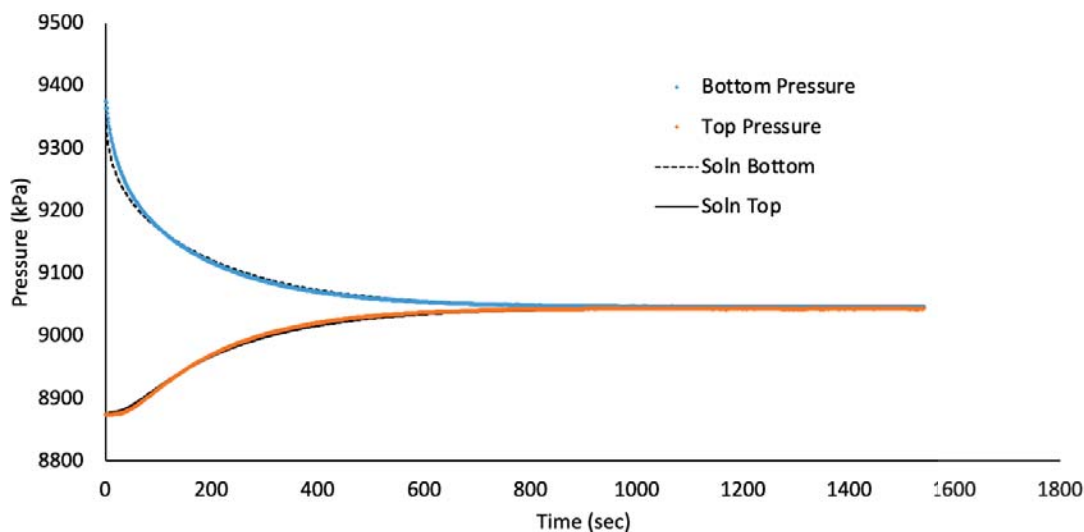


Figure 179 IG_BH06_PS007_HC61a: Effective Confining Stress = 17.82 MPa